UNIVERSITY OF CAPE TOWN

IYUNIVESITHI YASEKAPA • UNIVERSITEIT VAN KAAPSTAD

Environmental influences on tuna movement patterns in the Indian Ocean

Author: Beenesh Anand MOTAH

Student ID: MTHBEE001

Dissertation presented for the degree of

Doctor of Philosophy

in the department of Oceanography

Faculty of Science

University of Cape Town

South Africa

Date: January 2017

UNIVERSITY OF CAPE TOWN

IYUNIVESITHI YASEKAPA • UNIVERSITEIT VAN KAAPSTAD

Supervisors:

Dr. Francis Marsac

IRD (Institut de Recherche pour le Developpement),

ICEMASA – UMR 248 Marbec,

Avenue Jean Monnet CS 30171,

34203 Sète Cedex,

France.

Emeritus Professor, Dr. John Field

Ma-Re Institute,

R.W James Building,

University Avenue,

University of Cape Town,

Rondebosch, 7701,

Republic of South Africa.

Dr. Daniel Gaertner

IRD (Institut de Recherche pour le Developpement),

ICEMASA – UMR 248 Marbec,

Avenue Jean Monnet CS 30171,

34203 Sète Cedex,

France.

Declaration

The present work has been originally written by me, with the full support of my supervisors: Prof. John Field (UCT), Dr. Daniel Gaertner (IRD) and Dr. Francis Marsac (IRD/UCT) from the Department of Oceanography, University of Cape Town (South-Africa) and Institute of Research for Development (IRD), UMR MARBEC, Sete, France. Important contributions on the approach used in this study are clearly acknowledged by referencing it within the text.

University of Cape Town, March 29, 2017

Signature

Signed by candidate

Signature Removed

Acknowledgements

I wish to express my heartfelt gratitude to all the people who have supported me in this long journey through direct contribution to my research study or who have encouraged me. First, my special thanks goes to my supervisors Dr. Daniel Gaertner, Prof. John Field and Dr. Francis Marsac for their valuable guidance and help. Along with them, I wish also to thank Dr. Jean-Pierre Hallier. The Institut de recherche pour le développement (IRD) and the University of Cape Town supported my research work. This study would not have been possible without the financial support of the International Centre for Education, Marine and Atmospheric Sciences over Africa (ICEMASA) and I am deeply grateful. The Indian Ocean Tuna Commission (IOTC) have granted me access to the Regional Tuna Tagging Programme in the Indian Ocean (RTTP-IO) dataset and I wish also to thank the following persons for their advice and help: A. Fonteneau and J. Million.

Gaëlle Mathias, Arnaud Grüss, Louis Du Buisson, Liliana Pascuali, Philipppe Verley and Amande Monin Justin are people whom I got the opportunity to meet during my study provided much encouragement and lots of great moments shared together. Along the way, I had the pleasure to meet the family of a few of them who have been the most welcoming.

Raymon Roman and Christo Whittle my office mates, very supportive and great to work with. I wish to thank Emlyn Balarin, Claire Khai, Pavs Pillay for their support and kindness. Dr. Dawit Yemane and Jerome Guiet are thanked for their help when I got stuck.

During my two years in South Africa, I was really lucky to share my time with Louis, Philipppe and Christo. I would like to express my deep gratitude to Christo and his family (Tracy, Engela, Peter and many more) who made me feel at home. My thanks also goes to Anjali Callicharan for her help. I wish to thank Lara for her support and being here for me.

Finally, I wish to express my deep respect and gratitude to my Mother and Father for always being here and making me who I am, without forgetting my Brother and his wife, my cousins and our relatives. Special thanks to my friends in Mauritius at home and office.

Abstract

The Indian Ocean Tuna Commission conducted a small-scale tagging programme (2002-2009) and also a large-scale tagging programme: the Regional Tuna Tagging Programme of the Indian Ocean (RTTP-IO, 2005-2009). Both tagging programmes known as the Indian Ocean Tuna Tagging Project (IOTTP), targeted three main species of tuna commercially exploited in the Indian Ocean: bigeye (*Thunnus obesus*), skipjack (*Katsuwonus pelamis*) and yellowfin (*Thunnus albacares*). The two programmes tagged 219,149 tuna and 34,294 recaptures were reported to the commission. This study focused on tuna behaviour in the Indian Ocean looking at seasonal impacts, inter-annual variability in relation to ocean environment, survival estimates, movement patterns, size-groups and school-type: Free Schools (FS) and Fish Aggregating Devices (FADs). Using a multivariate approach, it was found that the years 2005 to 2007 were most abundant in recoveries of skipjack adults (77.45%) while yellowfin adults were mainly abundant during 2008 to 2011. It also showed that year and zone were significant factors influencing local abundance in tuna. The Kaplan-Meier survival curves enabled estimates on the longevity of the three species to be made. It was estimated that the cohorts (99%) vanished at 12, 5.8 and 10 years for bigeye, skipjack and yellowfin, respectively. The years 2006 (cold-productive phase) and 2007 (warm-chlorophyll depleted phase) showed tuna movement patterns changing with an El Niño event and primary productivity. Tuna tagged in the Tanzanian region, showed that those under FADs moved pre-dominantly towards the Somalian and Seychelles waters, while those in FS moved to the Seychelles and Mozambique waters. General Additive Model (GAM) analyses showed that the area bounded by 5^oN-5^oS and 45^o-55^oE was the main tag recovery regions for tuna under FADs. While in FS, the core recovery region was observed to be from 0^oN-10^oS and 50^o-60^oE. Recoveries were distributed in the temperature range 25-29 ^{o}C. Modelling tuna movement and drift related to ocean surface currents and swimming speed, a closer match between simulated and actual recovery positions were obtained for large tuna (particularly free schools) in comparison to small tuna associated with FADs.

Contents

List of Figures

List of Tables

List of Acronyms and Abbreviations

AOI	Area of Interest
Chl-a	Chorophyll 'a' concentration
CPUE	Catch per unit effort
DSL	Deep Scattering Layer
EACC	East African Coast Current
ECDF	Empirical Cumulative Distribution Function
EEZ	Exclusive Economic Zone
EU	European Union
FAD	Fish Aggregating Devices
FS	Free School
GAM	Generalized Additive Models
GW	Great Whirl
IOD	Indian Ocean Dipole
IOTC	Indian Ocean Tuna Commission
IOTTP	Indian Ocean Tuna Tagging Project
JC	Java Current
MLE	Maximum Likelihood Estimate
MSY	Maximum Sustainable Yield
LHS	Left Hand Side
NEM	North East Monsoon
NEMC	North-East Madagascar Current
NMC	North-East Monsoon Current
PS	Purse Seine

RHS	Right Hand Side
RTTP-IO	Regional Tuna Tagging Programme of the Indian Ocean
SEC	South Equatorial Current
SECC	South Equatorial Counter Current
SEMC	South-East Madagascar Current
SG	Southern Gyre
SMC	South-West Monsoon Current
SST	Sea Surface Temperature
SWM	South West Monsoon
WICC	West Indian Coast Current

Chapter 1

Introduction and overview

1.1 Introduction

This chapter reviews the literature on the oceanography of the Indian Ocean, tuna fisheries, tuna behaviour and habitats, with emphasis on the oceanic parameters that influence tuna dynamics and fisheries as the basis for this research study. Tuna are known to be highly migratory species covering large distances in relatively short time intervals (Fonteneau et al., 2008). Climatic variations and exploitation rates heavily impact the abundance of fisheries, altering migration patterns (Walther et al., 2002). In order to ensure sustainable tuna stocks, it is crucial to understand movement of tuna in relation to the ocean processes. This study is based on the dataset generated through the tuna tagging project (the IOTTP, described in Chapter: 2) by the Indian Ocean Tuna Commission (IOTC). The objective was to analyse tuna movements in relation to the oceanographic conditions as well as, their recapture with regard to seasons, year, size of the tagged fish, fish school-type and tagging/recapture regions.

Tuna form a resource mostly distributed in the temperate and tropical oceans; the tuna industry has grown over the decades to become one of the major industries with huge amounts of revenues for both developing and developed countries. Over the years, tuna fisheries have moved from artisanal/traditional fishing to industrialised fishing methods driven by purse seine and longline vessels. Besides being a source of protein for coastal developing countries, tuna gained high value with the advent of the canning industry, tuna market and sashimi market. Canned tuna

started as a low profit industry but the demand and market increased rapidly by the 1960s; the net weight caught is estimated to be 1 million tons by early 2000s (Miyake et al., 2010). Moreover, fresh tuna consumption has become a lucrative business with prices far higher than canned tuna. The sashimi market is mainly concentrated in Japan but has now expanded worldwide. These three main types of market have been driving the tuna industry with large investments in coastal developing countries, globally representing more than 85 countries (FAO, 2013).

Early tuna fisheries exploitations started in the Pacific and east Atlantic (Africa) in the 1950s, with the global catch around 0.6 million tonnes (1950) to almost 6.6 million tonnes (2010) annually, representing a value-at-landing of USD 10 billion (FAO, 2013). In the Indian Ocean, stock levels are closely monitored under the IOTC by conducting annual meetings to evaluate stock levels and formulate measures to ensure that the exploitation is maintained within sustainable levels.

The Indian Ocean Tuna Commission is an intergovernmental organisation responsible for the management of tuna in the Indian Ocean. It promotes cooperation for biological and environmental research that serves the objectives of its mandate. The outcomes on tuna stock status, science-based management recommendations, and updated results on biology and environment are compiled every year by its Scientific Committee. In this respect, the Indian Ocean Tuna Commission recommended that multi-disciplinary approaches linking ocean physics to the biology, to be developed. These parameters would eventually be used for ecological models, to assess the impact of deployment of a large number of Fish Aggregating Devices (FADs) on tuna schools in contrast to free schools (FS), and evaluate survival and mortality rates due to fishing and natural causes, migration and growth.

1.2 Key questions addressed

It is recognised that most of the purse seine tuna catches around the world are made under FADs (60-70%), with FS contributing to the remainder of the catch. The issue lies in the fact that the large number of FADs in the ocean, could significantly impact tuna behaviour by altering their movement, feeding and reproduction patterns, and ultimately stock distribution (Marsac et al., 2000; Hallier and Gaertner, 2008). With

the growing concern about the tuna stocks and fishing practices, research focusing on growth rates, movement patterns, tuna habitat as a whole and factors limiting their abundance are key issues for stock assessment. It is well recognised that a huge effort is still required in terms of research and modelling to capitalise on the Regional Tuna Tagging Programme of the Indian Ocean (RTTP-IO) data collected (Marsac et al., 2014).

The goal of this study is to use tuna tag and release data collected through the RTTP-IO and the small-scale tagging programme to better understand the dynamics of the three main tuna species (skipjack, yellowfin and bigeye) exploited in the Indian Ocean, in relation to their environment. The following key questions were addressed:

- Can one detect tuna assemblages (groups) based on size, year, school and seasonal factors?
- What are the survival rates of the tagged and recaptured tuna?
- How is tuna distribution impacted by the seasons, ocean parameters, school-type and size-class after release?
- How are recapture zones populated with respect to above factors?
- How do ocean currents impact the overall movements of tuna?

1.3 General characteristics of the Indian Ocean

The Indian Ocean is the only ocean which is land-bound on its northern limit; it is also the smallest ocean. The northern part of the Indian Ocean is closed by the Asian continent extending on the eastern side, and is partially bounded by Indonesia to about latitude 10°S. The south-eastern part of the Indian Ocean is partially bounded by the Australian continent (Fig. 1.1). On the western side, it is bounded by the African continent and the Arabian Peninsula. A unique feature of the Indian Ocean is that it has only one large scale gyre compared to the Pacific and Atlantic Oceans, both having two gyre systems. Three distinct synoptic circulations systems can be demarcated: a seasonal changing monsoon gyre in the northern hemisphere, a southern hemispheric subtropical anticyclonic gyre and Antarctic waters with the

Circumpolar current (Wyrtki, 1973*a*). The latitudinal extent of the Indian Ocean is from 30°N-70°S and longitudinally, from 20°-146.5°E (IHO, 1953). The deepest bathymetric zone in the Indian Ocean is more than 7000m deep and is situated in the NW Australian Basin and the average depth of the ocean is around 5000m.

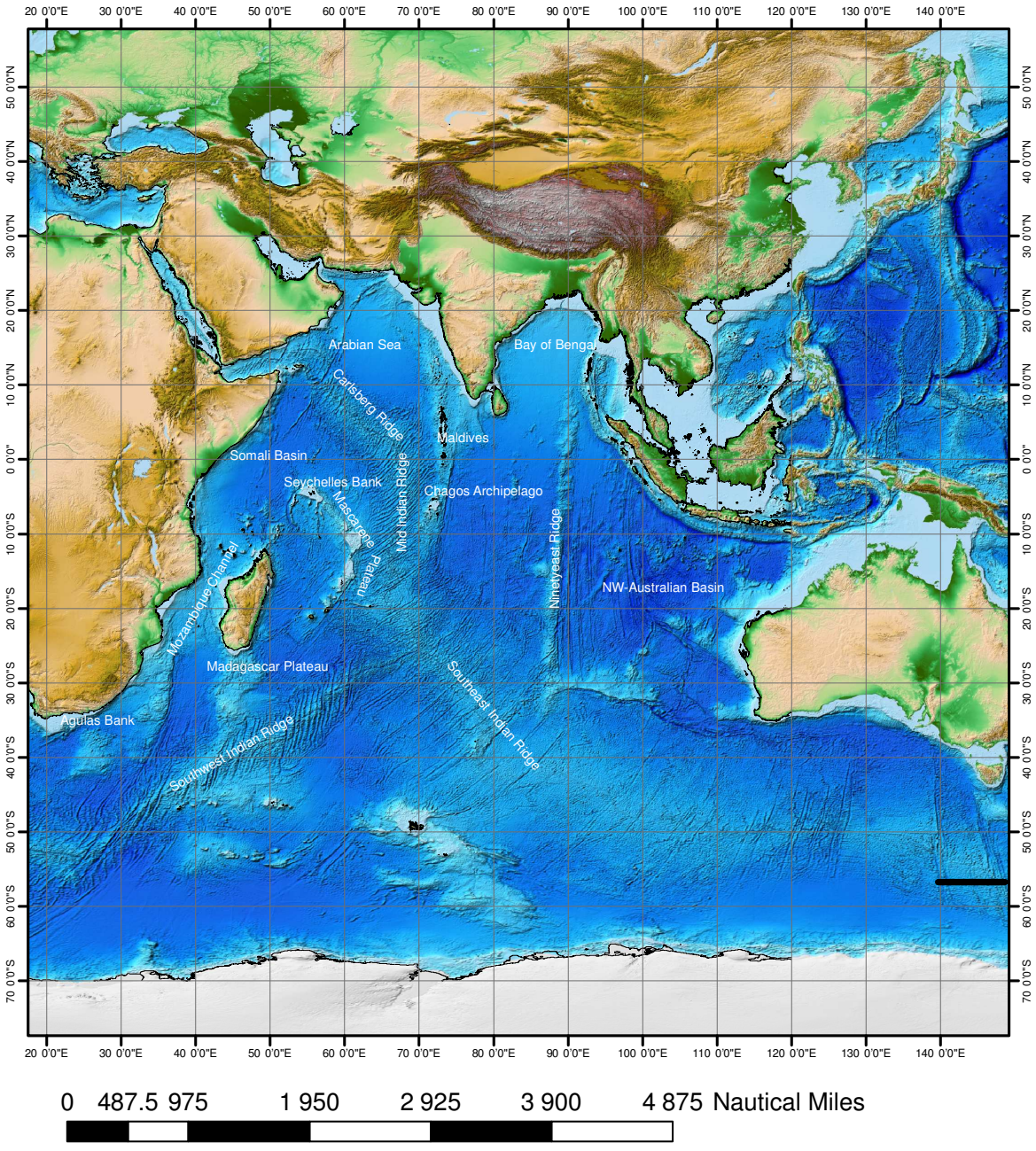

Figure 1.1: Indian Ocean submerged features and bathymetry (ETOPO2v2, 2006).

1.3.1 Indian Ocean Monsoon

The seasonal monsoon cycle alters the circulation, hydrological and biological properties of the Indian Ocean. The Indian Ocean water circulation is a wind driven current system different from the Pacific and Atlantic Ocean. The land mass in the northern part of the Indian Ocean, limits the ocean up to about 25^{o}N. Due to this land mass, differential atmospheric pressure changes take place between the continent and ocean, that induce a seasonal variation of winds in that region. The heat energy exchange cycle on land (heating and cooling) goes faster than that of the ocean, thus creating this differential atmospheric pressure pattern. During boreal summer (Jun-Sep), the continent is a low pressure centre while high pressure are distributed south of equator, causing wind to blow from the south to north (from high to low pressure centres) with heavy rains on the Indian continent. In boreal winter, the pattern is reversed, with high pressure on high grounds of the Indian continent and low pressure in the south equatorial region. Then, winds blow from the north to the south (from the north-east north of the equator, and from the north-west south of the equator), a season also called the North-East monsoon (Dec - Mar). Hence, the seasonal monsoon cycle is triggered by the changes in wind directions of more than 90^o from summer to winter and this seasonal change in wind patterns causes changes in the ocean currents system (Ramage, 1969). However, it should be noted that south of 10^{o}S, the south-east trades persist throughout the year. There are two inter-monsoons between the winter and summer monsoons, in April-May and October–November when the winds are westerly along the equator.

1.3.2 Indian Ocean circulation

Schott and McCreary (2001) gave a schematic (Fig. 1.2) of the Indian Ocean current patterns during the (northern) summer and winter monsoons. The ocean current transport is expressed in Sverdrup units (SV, 1 Sv = 10 ^{6}m^{3}s^{-1}) appearing in red (Fig. 1.2). Here the focus is laid on the current system affecting the West Indian Ocean. The South Equatorial Current (SEC) is driven by the South-East trade winds and forms the northern limb of the subtropical gyre. It extends to the west of the Indian Ocean and splits when it reaches the coast of Madagascar, into the North-East Madagascar Current (NEMC) and South-East Madagascar Current (SEMC). The

SEMC flows along the coast and goes into a retroflection system, partly feeding the Agulhas current (through the South Mozambique Channel, to the West) and partly circulating back in the southern subtropical gyre with eddy formations moving to the east. The NEMC passes by the northern tip of Madagascar flowing across the North Mozambique Channel to the East African Coast, where it splits between a south branch feeding the North Mozambique Channel circulation, and a northern branch forming the East African Coast Current (EACC). This pattern of currents does not change dramatically over the seasons. The currents that are described in the next paragraphs do exhibit seasonal changes.

During the boreal summer monsoon, the SEC and the EACC strengthen and form the north flowing Somali Current which triggers the Somalian upwelling. Because of the Coriolis force and its location in the northern hemisphere, the current deflects to the right and forms three local gyring systems: the Southern Gyre (SG) between 0^o – 4^oN, the Great Whirl (GW) between 5^oN – 10^oN and ultimately, the Socota Eddy (SE). The Southwest Monsoon Current (SMC) flows north of the equator in the eastward direction. In the Arabian Sea, the anticyclonic circulation with strong currents creates upwelling along the coasts of the Arabian Peninsula and India. During the boreal winter monsoon, the wind system reversal causes the Somali current to flow southwards. The EACC meets up with the Somali Current (SC), to supply the South Equatorial Counter Current (SECC) which flows eastward towards the Indonesian coast to feed in the South Java Current (JC). The North-East Monsoon Current (NMC) flows in a north westerly direction from south of Sri Lanka, and thereby feeds the West Indian Coast Current (WICC) in the Arabian Sea. During the two inter-monsoons, a westerly jet (Wyrtki jet) develops along the equator.

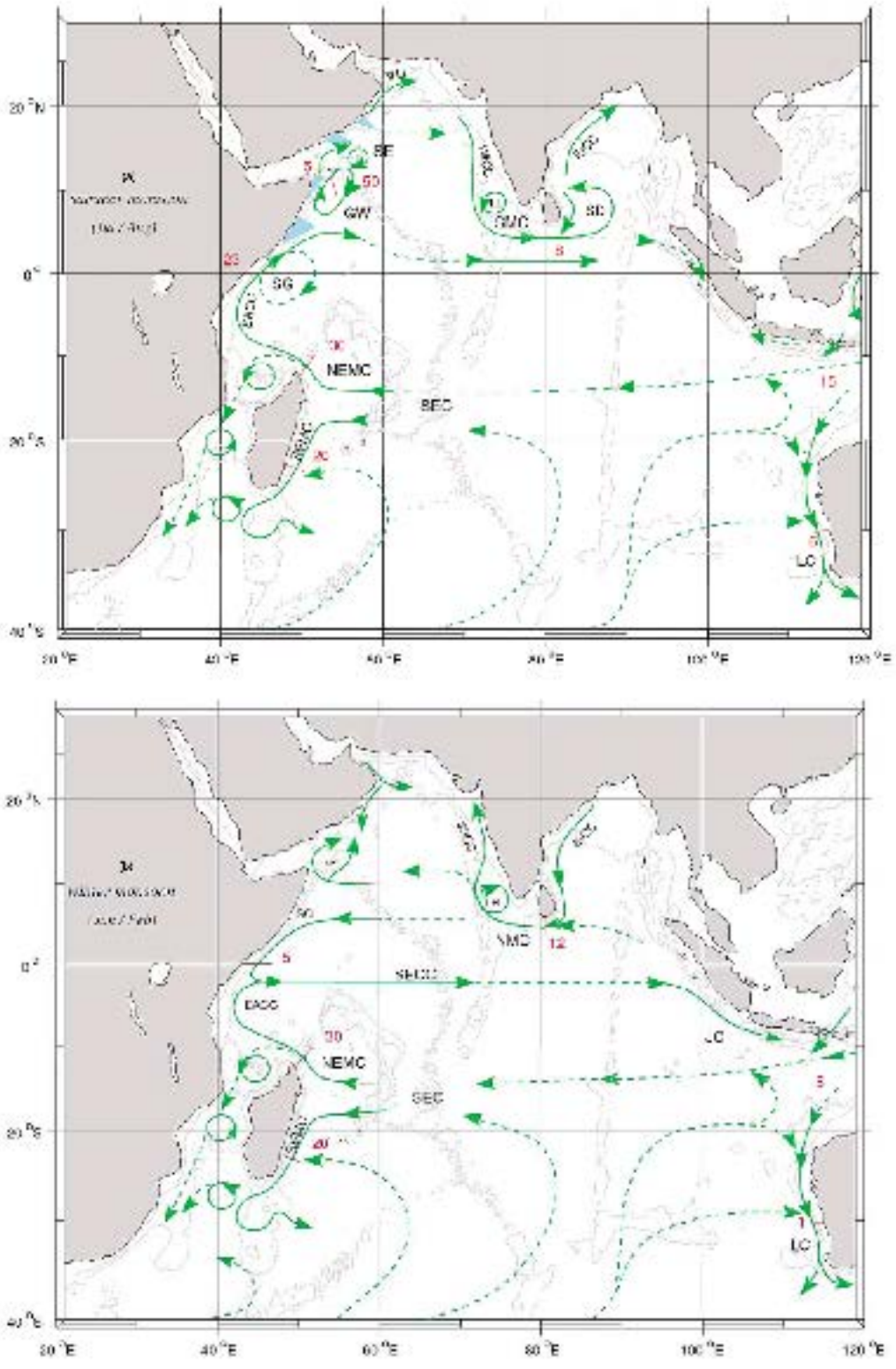

Figure 1.2: Schematic of surface water circulation in the Indian Ocean, (a) Summer Monsoon, (b) Winter Monsoon (Schott and McCreary, 2001).

1.3.3 Hydrological and biogeochemical properties of the Indian Ocean

The salinity concentrations in the east and west of the northern hemisphere of the Indian Ocean are different. The Arabian Sea (West) shows high surface salinity while the Bay of Bengal (East) decreases from about 34 to 31 parts per thousand (ppt). High salinity in the Arabian Sea is due to the dominance of evaporation over precipitation, whereas the low salinity in Bay of Bengal is a consequence of high precipitation and intense river run-off especially during the SW-monsoon. Wyrtki (1973*b*) described the Indian Equatorial Water found below the surface layer north of 10^{o}S. The salinity of this water mass is relatively uniform 34.9 -35.5 ppt. Warren (1981*b*) observed that below the mixed layer 50-100m deep, temperature decreases rapidly with depth in the thermocline, down to 5 ^{o}C at 1000m depth. Salinity along the surface mixed layer is low when compared to the layer where density gradient is greatest (pycnocline). The south Indian Ocean waters generally have a low salinity at lower latitudes. There are two reasons accounting for this: first, water incoming in the Indian Ocean between Indonesian Islands from the Pacific, and second, due to localize precipitation from evaporation. The low salinity spreads southward with fluctuations of the SEC.

The photic zone of the ocean ranging at about 200m depth in extreme cases, constitutes most of the particulate matter coming from surface layer due to photosynthetic action of phytoplankton. In turn, the phytoplankton are grazed by zooplankton which at the same time act as nutrient and waste producers, developing a whole chain of organisms feeding and decomposing around it. Therefore, the surface layer recycles a large part of the organic matter while only a small portion of this particulate matter sinks down to the bottom of the ocean. These constitute the principal chemical elements of organic matter: oxygen, hydrogen, carbon, nitrogen and phosphorus. The surface layer of the ocean is usually the most saturated with dissolved oxygen in the water coming mainly from the atmosphere and the photosynthetic action of phytoplankton. The south Indian Ocean has a low oxygen and high nutrient concentration in the photic zone which is linked to weak maxima in silica and phosphate (Wyrtki, 1971; Warren, 1981*a*). Phosphate, nitrate and silicate have a low concentration in the upper 100m but increases in deep waters.

These nutrients have low concentrations in the upper part of water column because they are used by the phytoplankton and the increase in concentration with depth because of decaying of materials sinking down the water column. The upper layers of the Indian Ocean (10^oN-40^oS) are generally low in phosphate, less than 1 μg/kg (Wyrtki, 1971). This concentration further increases between 1000-2000m, up to 2 μg/kg. Silicate concentration values from 10^oN-25^oS in the upper 200m are low. In deeper layers, the concentration of silicate increases to more than 120 μg/kg.

1.3.4 Ocean upwelling

Upwelling systems have been widely investigated worldwide, from physical to biological perspectives (Bain, 1982; Fréon, 1983; Lutjeharms and Machu, 2000; Marsac et al., 2014). Usually, coastal upwelling is induced by the wind blowing at the sea surface along a coast in a particular direction, applying a force to the surface of the water coupled with Coriolis effect (deviation as a result of earth's rotation) and Ekman transport, causing water to move to the left or right (left: southern and right: northern, hemisphere) of the wind's direction. This causes the surface water to move away from the coast thereby pulling nutrient rich cold water to the surface. This results in nutrient and phytoplankton enrichment and consequently attracting a rich diversity of marine species from small to large predators. Coastal upwellings can extend more than 10km offshore and many hundreds of km alongshore alongshore (Bain, 1982). There are other known sources of upwelling caused by deviation of water currents offshore of islands, ridges and sea mounts. The Somalia upwelling, is one the strongest upwelling systems in the world observed on a large scale and extremely valuable for tuna fisheries (Marsac et al., 2014).

Somalian waters form a very dynamic region affected by monsoons, where there is reversal of the entire surface current pattern (Schott and McCreary, 2001). In summer the thermocline deepens. However, along shore winds cause upwelling northward on the Somalian coast (Stéquert and Marsac, 1989; Le Gall and Bergès, 1989; Schott and Fischer, 2000). At the beginning of the SW monsoon, upwelling along the coast can be observed clearly but at the onset of the October inter-monsoon period, the upwelling disappears, although traces of upwelling can be observed in the north. The Seychelles region is also affected by monsoon seasons, and upwelling

occurs on the south-eastern part of Mahé bank towards the end of the NE monsoon, when the strong south equatorial counter current flows (Stéquert and Marsac, 1989). During the SW monsoon, upwelling events occur off Saya De Malha Banks. In this region, divergence and convergence of surface water currents form an integral part of the hydrology (Stéquert and Marsac, 1989).

1.4 El Niño/Southern Oscillation and Indian Ocean Dipole

The Pacific Ocean is subjected to inter-annual oscillation in the atmospheric pressure of the southern hemisphere. This oscillation is characterised by cyclic warm and cold phase of sea surface temperature of the tropical Pacific Ocean, with the warm phase commonly called El Niño and the cold phase La Niña. This coupled alternating warm and cold temperature is known as the El Niño/Southern Oscillation (ENSO). ENSO plays an important role in influencing the depth of the thermocline. In normal conditions, the wind blowing from the east to west of the Pacific maintains pool of warm water on the western tropical side creating air convection going back to the east. Hence, the thermocline rises to the surface on the eastern side of the Pacific rich in nutrient and enhancing productivity. During the El Niño phase in the Pacific, the wind has reduced strength causing the anomalously warm waters to move to the east and high pressure on the east side pushes the thermocline further down the water column, resulting in less nutrient rich cold water in the euphotic zone (Wyrtki, 1975). The inverse situation occurs during the La Niña phase. There is a low-pressure gradient and wind moves the surface water mass from the east to west, causing the thermocline to move closer to the surface with more nutrient-rich cold waters in the east.

Similar to the ENSO events in the Pacific, the Indian Ocean has inter-annual climatic variability known as the Indian Ocean Dipole (IOD) (Saji et al., 1999; Webster et al., 1999). The positive phase is characterised by surface temperatures significantly lower than the average off Sumatra and high sea surface temperatures in the western Indian Ocean altering wind and precipitation patterns. This causes deepening of the thermocline reaching about down to 30m (Marsac, 2008; Marsac

et al., 2014). Saji et al. (1999) in their study concluded that the ENSO in the Pacific and IOD in Indian Ocean are independent of each other. The IOD event was found to be heavily dependent on monsoonal circulation having strong effects on the climate variability of the Indian Ocean affecting the rainfall regime on the east African Coast. Although there is no clear indication how these two phenomena are linked, it was noticed that during an El Niño event and positive IOD events (2007); satellite derived chlorophyll-a (Chl-a) series were anomalously low. The years 2001-2006 were marked by a shallow thermocline and positive Chl-a anomalies resulting in high CPUEs of yellowfin in the Indian Ocean (IOTC, 2010).

1.5 Tuna fisheries

1.5.1 Global tuna fisheries

In the Pacific Ocean, the tuna catch represents 70% of the entire world's tuna catch or amounting to 3.3 million tonnes, with skipjack tuna being the most exploited. Figure 1.3 shows that catch levels in the Indian Ocean exceeded those of the Atlantic Ocean during the mid-nineteen eighties. The industrial exploitation of tuna started in the early 1950's (Miyabe and Nakano, 2004), with catches less than 50 000 tonnes per species in the Indian Ocean. In 1968, the Food and Agriculture organization (FAO) of the United Nations held their first session of the Indian Ocean Fishery Commission (IOFC) to look into measures for management of the Indian Ocean fisheries. Most of the delegates expressed the need for assistance in developing fisheries management in the region (FAO, 1968). It was recognised that the need for statistics in the Indian Ocean fisheries was a matter of prime importance. During the meeting, participants also expressed the need to increase exploitation of fisheries, as at that time it was estimated to be under exploited in the Indian Ocean.

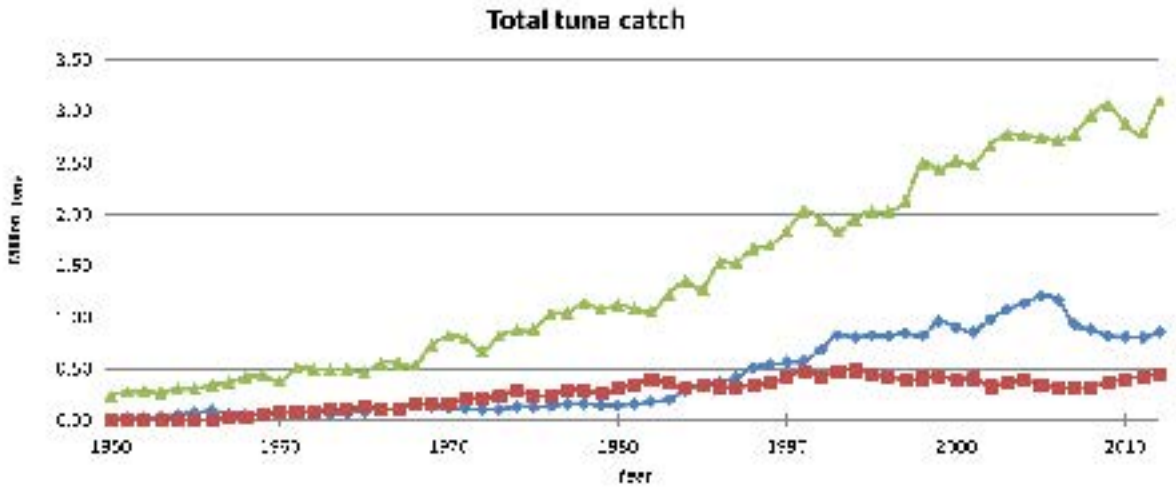

Figure 1.3: Catch levels of the world tuna catches in the Atlantic (red line), Indian (blue line) and Pacific (green line) Ocean, 1950-2012.

1.5.2 Indian Ocean tuna fisheries

After the recommendations of the IOFC, the tuna fishery went through a gradual growth. It should be mentioned that stocks of yellowfin and albacore were acknowledged to be heavily fished in the north-western part of Indian Ocean, which was actually a wrong perception due to the poor quality and many gaps in the available data. Within ten years, the exploitation rate increased slowly until 1980 where it started to increase significantly due to the introduction of purse seine fisheries. The catch trend increased until historically high records in 2005 and 2006, then declined and remained stable at lower levels, due to several combined causes: a plausible overfishing during the previous 4 years, less favourable habitat conditions due to the 2007 El Niño, and negative impacts of the Somalian piracy. National and international bodies came to the consensus that proper management and conservation measures enforced by legal policies were required for the sustainable exploitation of this valuable resource. The Indian Ocean Tuna Commission was adopted for establishment by the FAO council in November 1993. By the year 1996, the agreement was in effect and by March 1997, it was operational after adoption of Financial Regulations and Rules of Procedure. The Commission, in its endeavour to promote cooperation among stakeholders related to the Indian Ocean fisheries resources and sustainable development and management of fisheries stock have been monitoring and gather-

ing information on the state of tuna stocks in the Indian Ocean. Gaps in terms of biological knowledge, stock structure, fisheries indicators and behavioural response to ocean environment variability were clear areas where attention needed to be focused. In 2000, the scientists participating to the IOTC Working Party on Tagging (WPT) proposed a large scale tagging programme to gather information to define the objectives and deliverables of such programme aiming at dramatically reducing uncertainties in the assessment of the three major tuna species, skipjack, yellowfin and bigeye (IOTC, 2000*b*). The programme was called the Regional Tuna Tagging Programme-Indian Ocean (RTTP-IO). It embraced a large scope of objectives, from information on natural and fishing mortality, growth rate, stock structure, influences of school fishing practices to oceanic processes affecting movement and exploitation. The programme will be further discussed in Chapter 2.

1.6 Tuna habitats

1.6.1 Swimming depths

Information on the vertical distribution of tuna is important for research and fishing operations. For research, it provides useful information on their physiology, modes of feeding, reproduction, and behaviour. While in fishing operations, knowing their depths helps in terms of catchability of the species. It is noteworthy that the term catchability refers to the relationship between the abundance of the species and efficiency of fishing gear (Arreguín-Sánchez, 1996). For instance, in the Indian Ocean, the optimal depth of bigeye tuna was estimated to be 160-240 m (IOTC, 2008*b*) but it can even go further down to 300 m (IOTC, 2013, 2014). As for the case of yellowfin, swimming to depths of more than 1000 m shown through archival tagging is thought to be feeding on meso-pelagic prey (IOTC, 2014). Longline catch data supports the idea that their distribution is throughout the entire tropical Indian Ocean.

Schaefer et al. (2007) described four types of diving behaviour for tuna in terms of temperature and depth recorded:

1. the first type characterised by spending most of the time in depths less than 50 m (night-time) and 100 m (daytime),

2. a second type similar to the first for night-time but during daytime diving ranged from 50-300 m where tuna made dives about ten times during daytime to depths greater than 150 m,

3. a third type of diving was exhibited by a few large yellowfin, with dives more than 1000m, lasting 1.2 hours and withstanding low temperatures. The recorded ambient water temperature during those dives was around 4.5 °C. The temperature preceding these dives was recorded to be 28.4 °C,

4. the last type is described as surface-oriented behaviour activities occurring both during day and night time. These authors suggested that the second type of diving behaviour may be in response to hunting mode targeting prey in the Deep Scattering Layer (DSL), while type three diving behaviour is suggested as being associated with food searching or bathymetric exploration or escaping predators and potentially avoiding detection.

1.6.2 Water temperature and dissolved oxygen

Isotherms and eddies are considered to be important features providing favourable conditions for attracting tuna schools (Hynd, 1969; Marsac and Blanc, 1998; Maury et al., 2007; Tewkai and Marsac, 2010). Most of the catches were made near thermal fronts. A number of authors have tried to come up with a temperature range for tuna (Zagaglia et al., 2004; Schaefer et al., 2007; Fonteneau, 2008). For instance, Fonteneau (2008) stated that the temperature range for tropical tuna in the Indian Ocean on a yearly average to be between 25 - 29 °C although these are not the extreme conditions. In the IOTC report (IOTC, 2013, 2014), surface temperature greater than 24 °C is associated with favourable conditions for tuna in the Indian Ocean. It is suggested that the sea surface temperatures between 29 - 30 °C correspond to high frequencies of yellowfin tuna catches (IOTC, 2010).

Dissolved oxygen concentration is another important factor delimiting depths which tuna can reach. Skipjack have been reported to survive dissolved oxygen levels as low as 2.8 $ml.l^{-1}$ and yellowfin down to levels of 1.4 $ml.l^{-1}$ (Sund et al., 1981). Furthermore, at depth of 100 m, the vertical distribution of bigeye tuna is considerably reduced with oxygen levels lower than 1 $ml.l^{-1}$. Table 1.1 shows oxygen

tolerance of the three species for two fork lengths, 50 cm and 75 cm respectively.

Table 1.1: Estimated oxygen tolerance level (Sharp and Dizon, 1978).

Species	Fork length (cm)	Estimated lower oxygen tolerance, 10 min levels (ml O_2/l H_2O)
Katsuwonus pelamis (skipjack)	50	2·45
	75	2·89
Thunnus albacares (yellowfin)	50	1·49
	75	2·32
T. obesus (bigeye)	50	0·52
	75	0·65

However, Cayré and Marsac (1993) found that the thermocline and oxycline are key factors determining vertical swimming behaviour rather than absolute temperature and oxygen levels. The authors compared the diurnal vertical behaviour of yellowfin tuna observed from sonic tagging experiments in the western Indian Ocean (Comoros archipelago) with the vertical profiles of temperature and dissolved oxygen concentration. They established that the rate of change or gradient of oxygen level and temperature is more of a restricting factor than absolute values of dissolved oxygen level and temperature. The oxycline depth was found to be strongly related to concentrations of 3.6 - 4.2 $ml.O_2.l^{-1}$ in the tropical western Indian Ocean. Considering the whole Indian Ocean, it was found that the oxycline depth positions corresponded to 4.2 - 4.3 $ml.O_2.l^{-1}$ concentrations.

1.6.3 Effect of upwelling on tuna distribution

Among numerous oceanic processes, upwelling is of particular importance for tuna. Upwelling pulls nutrient rich waters from the deep ocean to the surface; consequently, the formation of micronekton communities feeding there attract tuna. The number of days or weeks that it takes for a significant tuna school to feed on such ocean event is not clearly known. Different authors have suggested different time lapses based on their observations and geographic location. Mansor et al. (2001) used SST distribution charts to identify thermal boundaries and upwelling zones. They found that for an upwelling zone to become an effective fish catch area, it took a few weeks. They used chlorophyll imagery and carried out acoustic survey recordings which showed a good correlation with fish density in their study region. Nonetheless,

they argued that further studies are required to determine the time needed for a fish community to aggregate. Sund et al. (1981) stated that from observations made, it took three months for the abundance of yellowfin tuna to become important after an upwelling and further argues that, the lag time being due to the time taken for micronekton biomass to built-up and also for temperatures to be warm enough for tuna.

It is known that monsoon winds trigger coastal upwelling and small scale upwelling; the short periods of time have significant effects in terms of ocean primary productivity (Stéquert and Marsac, 1989). Small scale upwellings refers to a scale of 10km, while coastal upwelling has been have described with respect to locations such as Northwest Africa, the Southern Benguela region and the Somali coast on a scale of 100s of km along the coast. Convergence zones are other oceanic features attracting tuna. They delineate current boundaries between warm and cold waters and provide regions of high biological activity supporting a diversity of organisms from phytoplankton to large predators. They tend to have an aggregative effect due to accumulation of drifting debris.

1.6.4 Warm water masses

Lehodey et al. (1997) have shown that zonal displacement of warm water masses triggers spatial shifts in skipjack populations. The authors tried to test the hypothesis of correlating relative skipjack abundance observations at the 29 °C SST isotherm and the Southern Oscillation Index (SOI). Usually, warm water pools as argued by Lehodey et al. (1997) in their study, are characteristic of low productivity and are unlikely to attract tuna. Although the western Pacific was warm, tuna schools were formed. They suggested that this may be explained by planktonic communities attracting tuna from the Pacific equatorial upwelling and being transported by the south equatorial current towards the west. One interesting observation noted by Sund et al. (1981) was that, yellowfin tuna gather mostly at the warm side of frontal boundaries. In addition to this, sea mounts and banks are said to be areas where tuna tend to be more abundant as these areas show upwelling properties. The western Pacific warm pool is the location where the highest tuna catches occur although this region is characterised low primary productivity (Lehodey et al.,

1997). They calculated the longitudinal centre of gravity of CPUEs and found it to be correlated with the 29 °C SST isotherm with amplitudes to be of almost the same order suggesting a phase lag of two months between ENSO zonal displacement and skipjack distribution.

1.7 Purse seine fishing and tuna school-type associations

1.7.1 Purse seine fishing

A number of fishing practices are currently used to exploit tuna resources throughout the world. Those techniques developed over the years aim at increasing tuna catch but are not necessarily efficient and sustainable. The fishing practices have varied impacts on the environment and on the stock levels. The following are the main fishing practices in commercial fisheries:

- purse seine net,
- trawl net,
- gillnet,
- longline,
- pole and line,
- trolling.

The recoveries for the IOTTP programme were mainly reported by purse seine fishing vessels. For this reason, the following description relates to purse seine fishing only. Purse seine fishing method is used to catch fish schools (group of fish swimming together) of species such as mackerels, tuna and sardines; usually near the surface. After spotting a school of tuna, purse seiners deploy a long strip of net (the breadth can go down to 300m deep and length up to 2km) around the school of fish. Once the starting point of the net is reached, the bottom of the net is then closed 'pursed' with the fish school trapped in the middle and the school of tuna are pulled on the fishing vessel (FAO, 2016; Stéquert and Marsac, 1989).

1.7.2 Tuna school-types

Tuna school-types or fish school associations are classified in two main categories: Free School (FS) or Fish Aggregating Devices (FADs). Free school or free swimming school are usually applied to fish swimming freely in a group, moving from one location to another; in search of forage-rich areas. Free schools may consist of a mix of size groups (juveniles, pre-adults and adults) of tuna as well as species (Romanov, 2002). Fish have been observed to aggregate around floating objects in the oceans. Fish Aggregating Devices (also termed as associated schools) consist of both natural logs or drifting objects and rafts manmade to attract tuna. Initially, catches were targeted under natural logs but then with growing fishing fleets, the deployment of artificial drifting FADs was increased to raise catch levels (Marsac et al., 2000). In their study, Marsac et al. (2000) suggest the potential consequences of FAD fishing are that it tends to attract mostly juveniles, alter the natural pathways of tuna, increase fish natural morality and reduce growth rates.

The expansion of FAD fishing began in the early 1990s and had a marked effect on catch per unit effort (CPUE). The FADs CPUE increased after that for a certain period of time but later decreased (Fonteneau et al., 2000). Marsac et al. (2000) postulated that FADs might have significant impacts on the natural displacement and feeding patterns of tuna (the so-called "ecological trap hypothesis"). Moreover, the effect of FADs was more likely to be on juvenile tuna, consequently increasing their vulnerability to larger predators such as large tuna, sharks and billfishes. In the Indian Ocean, the number of drifting FADs deployed by purse seine vessels has increased dramatically over the past 10 years and may reach around 10,000 FADs; monitored in 2013 (for the EU and Seychelles purse seine fleets only) (IOTC, 2014). Seventy percent of catches was reported to be made in association with FADs by the tropical tuna purse seine fisheries (Fonteneau, 2008). Figure 1.4 depicts the distribution of FAD-Associated Schools and FS in the Indian Ocean by purse seine. It can be observed that the north-western part is mostly associated schools compared to regions below the equator on the central eastern part. Moreover, the Mozambique Channel can be observed to have an equal share of Associated and Free schools.

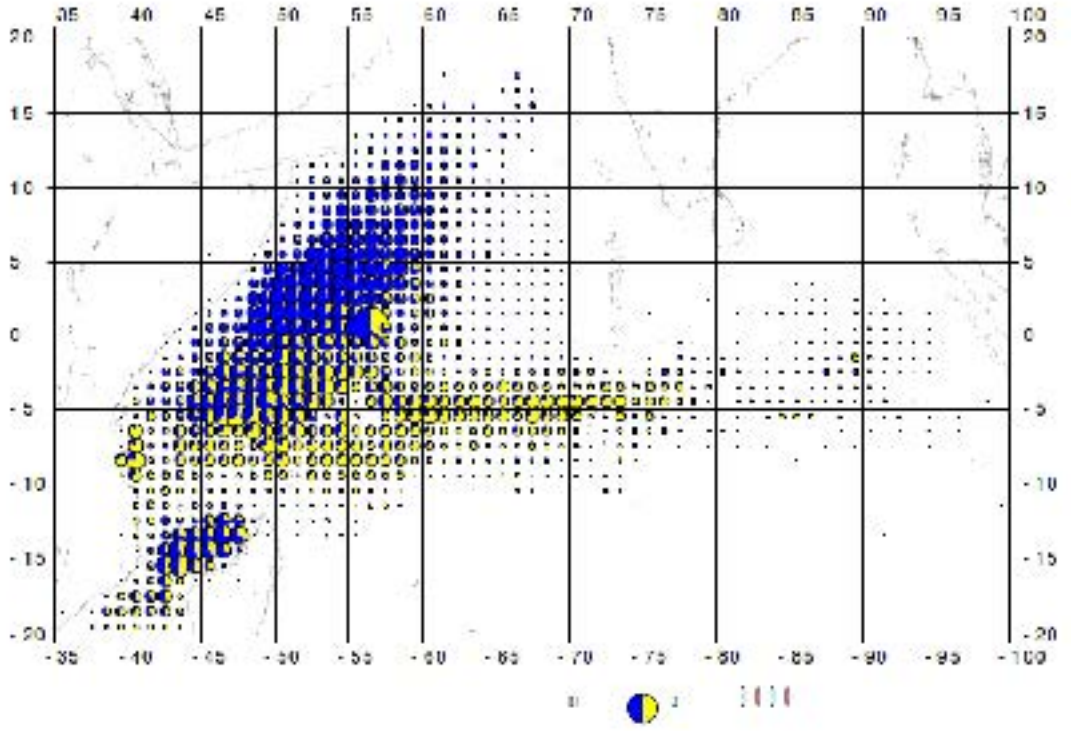

Figure 1.4: Spatial distribution of purse seine tuna catches (all species combined) by school type (average 1991-2007). The area of the circle indicates the amount of catch (reference circle = 3000 tons) and the pie indicates the relative proportion of catch by school type (blue = FAD-Associated Schools and yellow = Free Schools).

Hallier and Gaertner (2008), studied the effects of FADs on the biology and the ecology of tuna in the Indian and Atlantic Oceans. The authors analysed four indicators under the two fishing modes FS and FADs, namely:

- stomach fullness of tuna,
- plumpness of tuna,
- individual growth rates of tuna,
- migratory direction and displacement rates.

The study showed that, 87% of skipjacks caught as FS had food in their stomachs (stomach fullness measured as a presence or absence of food in stomach) compared

to 26% of those taken under FADs. Similar, trends were observed for yellowfin and bigeye tuna. In addition, Sund et al. (1981) suggested that free swimming tuna schools can be expected to leave areas deficient in nutrients to graze on food richer areas. For the plumpness of tuna, model relationship was constructed between thorax girth and fork length on a log scale, and the fishing mode, location and observer. The results showed that tuna caught under FADs had a high probability of being thinner (Fig. 1.5) than those caught as FS.

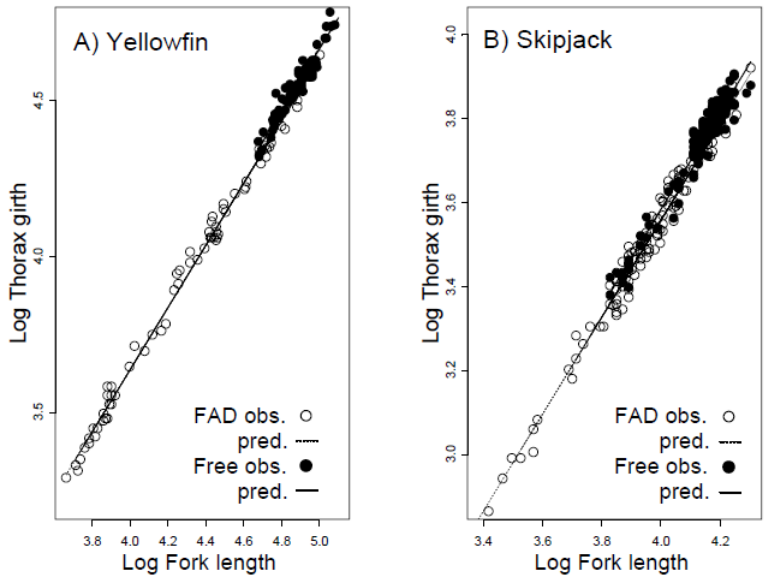

Figure 1.5: Relationship of observed fork length and thorax girth of yellowfin (A) and skipjack (B) (Hallier and Gaertner, 2008).

From the study of Hallier and Gaertner (2008), it was evident that the calculated growth rates of tuna under FADs were less than those in FS by 0.03 cm per day. It should be noted that, tuna caught under FADs were found to cover longer distances and faster (median value of 13.19 nautical miles per day (nmi.d^{-1}) compared to 2.882 nmi.d^{-1} for FS. Sund et al. (1981) suggested the following reasons as to why tuna and other pelagic fish are attracted by FADs:

- shelter from predators and where some species (other than tuna) may spawn,
- attracts large fish preying on small ones,
- as a food reserve, where fish feeding on algae and decaying materials from the floating structure,

- provides shade and also making zooplankton more visible to fish,
- floating objects are cleaning stations.

On the other hand, it was also argued that natural FADs (drifting wood logs, coconut branches and large whales) drift with ocean current to convergence zones which are highly nutrient rich, hence encouraging the accumulation of tuna (Hall et al., 1992; Hallier and Gaertner, 2008). Kingsford (1999) investigated the utility of FADs and factors influencing fish association with FADs. The downside of FADs would be that fish aggregation can make them potentially vulnerable, alter migration routes, affect the natural state of usual sites where spawning or recruitment may be occurring and not the least, it is a redistribution of natural fish stocks from a holistic view. The positive points would be the increase in fish catch within an area, recruitment in a particular area and attracting fish to areas which were less likely habitats.

1.8 Modelling

Tuna tagging and tracking have been key in modelling tuna behaviour with respect to the environment, in order to understand their vulnerability to changing environmental conditions. Vulnerability is related to the probability of encountering fish by the fishing gear while catchability is related to abundance of fish and to fishing effort. Changes in environmental conditions affect both vulnerability and catchability. Modelling is one of the means of assessing the impact of environmental conditions on vulnerability of fish. Temperature and oxygen have been identified as key parameters affecting tropical tuna. To this end, in the Indian Ocean, Cayré and Marsac (1993) have applied a sonic tagging system to track yellowfin tuna in the Indian Ocean. The study was to correlate the vertical movements of yellowfin tuna in terms of the oxygen gradient and consequently to predict the depth of maximum probability of the presence of yellowfin tuna. The methodology they applied was to delimit layers with respect to gradients in temperature and oxygen with depth. Zainuddin et al. (2008) have used a combination of Generalized Additive Models (GAMs) and Generalized Linear Models (GLMs) to identify relationships between tuna catch and ocean parameters. They studied the relationship of fishing grounds with respect to oceanographic conditions to predict probabilities of finding tuna

habitat. Their models were able to predict spatial patterns of tuna habitat and were found to be in agreement with observed data. In the present study, the use of the GAMs was considered to be useful for predicting environmental impacts on tagged tunas.

1.9 Thesis outline

Chapter One provides the basis of the study, which includes the objectives, scientific background and reasons for carrying out this research. It gives a broad overview of the several pertinent issues dealing with tuna fisheries with emphasis on the Indian Ocean. The thesis consists of eight chapters where the five questions addressed earlier are further elaborated. The second chapter focuses on the Indian Ocean Tuna Tagging Project (IOTTP) dataset used for analysis to reach the objectives of the research. It also describes the parameters collected through the IOTTP programme and other complementary data which was used. Furthermore, Chapter 2 gives the data processing methodology used through subsequent chapters in addition to chapter-specific methodologies applied. Chapter 3 presents a multi-variate approach to study tuna and the ocean environment. It looks into the seasonal changes, annual effect interaction with tuna species and their size-class. The fourth chapter deals with survival and recovery estimates of tuna based on the tagging and recovery. Three different models have been studied in order to come up with an estimate with survival and recovery. It should be mentioned that the approach used in Chapters 3 and 4 have not been tested before in the context of this dataset. The fifth chapter investigates the movement pattern of tuna with respect to their tagging locations and where the tuna move to geographically. As we know SST and chlorophyll are important factors affecting tuna displacement, Chapter 5 looks into how these parameters shape their movement in addition to the season and year effects while taking into considering the school type and size-class. Chapter 6 has a similar approach to Chapter 5, but it looks into the source regions of tuna populating a particular zone. The seventh chapter tries to understand how surface ocean currents influence tuna displacement. Different scenarios of movement have been simulated to better understand how ocean surface currents affect tuna migrations.

Finally, the last chapter (8), gives an overall summary of the main conclusions and pertinent matters this study has raised.

Chapter 2

Indian Ocean Tuna Tagging Programme-IOTTP, Indian Ocean monsoon and data standardisation

2.1 Indian Ocean Tuna Tagging Programme-IOTTP

2.1.1 Rationale to develop a tuna tagging programme

By the end of the 1990's, the tuna fishing industry was well developed with over 800,000 t (total stock) of tropical tuna (Marsac et al., 2014). The lack of more detailed data did not allow proper estimates of stock to be carried out, although studies by the IOTC were already showing that some stocks were near over-exploitation. The fact that the Indian Ocean has a rapidly growing tuna catch with respect to skipjack tuna (*Katsuwonus pelamis*), yellowfin tuna (*Thunnus albacares*) and bigeye tuna (*Thunnus obesus*), caused the IOTC to conduct a large scale tagging programme (hereafter: the RTTP-IO) to gather information on biological, physical and environmental parameters in relation to these species. Multiple studies discussed the use of Catch Per Unit Effort (CPUE) to tuna stocks in the world's ocean (Fonteneau et al. (2008); Lezama-Ochoa et al. (2010); Hazin et al. (2012), among others), underlining the fact that CPUE series barely represent biomass trends and that direct methods need to be considered to improve the diagnostic. This classical method of tagging to study fish populations allows the observation of movement

patterns and migration, and also the vertical movements of tuna in the water column. Furthermore, it provides crucial information on growth rates with respect to age/size, sex and habitats; estimates on fishing mortality compared natural mortality and finally, in the calculation of estimates of stock levels. In the year 2000, the scientific community and country representatives approved the tagging programme in the Indian Ocean with the following objectives (Marsac et al., 2014):

- to estimate parameters important for model evaluation of stocks, fishing and natural mortality,
- to provide biological information necessary for base models such as growth rare and age validation of tuna,
- to determine stock structures and movements of tropical tuna,
- to estimate exploitation rates and vulnerability difference by fishing gear and zone,
- to evaluate the influence of features causing fish aggregation, submarine mounts especially FADs,
- to allow estimates of rate of interactions between fishing grounds,
- to determine the influence of ocean parameters and bathymetry on tuna movements and exploitation in the Indian Ocean.

2.1.2 Tagging operations

The RTTP-IO survey started in May 2005 and ended in September 2007, targeting specific regions of the Indian Ocean. This large-scale tagging programme was conducted to ultimately improve the population parameters for the assessment of three tuna stocks that are heavily exploited in the Indian ocean: skipjack tuna (*Katsuwonus pelamis*), yellowfin tuna (*Thunnus albacares*) and Bigeye tuna (*Thunnus obesus*) (Hallier, 2008). Along with the large-scale tagging programme (RTTP-IO), small-scale tagging operations were also conducted focusing on the north-central and eastern parts of the Indian Ocean. The tagging platforms and strategy of the small tagging, differed substantially from the large scale programme and have been

partially utilised depending on the hypothesis investigated. It should also be noted that small-scale tagging operations were undertaken covering eastern Indian Ocean funded by Japan (Hallier, 2008). The RTTP-IO along with the small-tagging operations were termed as the Indian Ocean Tuna Tagging Project (IOTTP). Therefore, for the whole IOTTP a total of 36,000 bigeyes, 66,547 yellowfins and 115,718 skipjacks were tagged, representing 16.4%, 30.4% and 52.9% of the whole number of tuna tagged in the Indian Ocean, respectively.

2.1.2.1 Tagging vessels

In the RTTP-IO, tuna were caught and tagged from two pole and line vessels which were hired by the programme. Normally, the pole and line technique uses live bait fish thrown around the boat to attract tuna. The hooks are barb-less (to facilitate unhooking of tuna on the deck) and no bait is attached to the hook. Bait is normally caught inshore, in bays, before going to sea for tuna fishing. During fishing events, the fishing vessels spray water jets around to mask the fishers and, combined with the bait around the boat, creates frenzy among tuna which bite at the hooks. The peculiarity of the RTTP-IO tagging events off Tanzania is that no bait was used, and saved time and therefore maximised tuna fishing time at sea. This technique took advantage of the aggregation of tuna for several weeks under the vessel, forming a pool of tuna which were tagged and released. More than 122,000 tuna were tagged using this technique. A minor fraction of tuna tagged by this technique (6 to 10% on average) were recaptured by the tagging vessel (Marsac et al., 2014).

2.1.2.2 Tag types

Four types of tags were used in the RTTP-IO, namely: dart tags, electronic archival, pop-up and sonic tags. A dart tag constitutes a plastic strip with a pointed barbed end, usually fixed on the back of the tuna; this is mainly to evaluate changes at recovery from data recorded at tagging. The electronic archival tags are electronic devices surgically inserted in the abdomen of the tuna collecting depth and temperature information. Pop-up tags are attached on the back of large tunas, they basically give information on location, depth and temperature at which tuna have been swimming. Pop-up tags detach themselves from the fish after a determined

period and transmits the data through satellite. Sonic tags are radio transmitting devices inserted in the abdomen of tuna that transmit information when tuna are within the range of a receiving station. This type of tag is mainly used to assess the residency time of tuna in FAD-associated schools (Hallier, 2008; Marsac et al., 2014). The electronic tags were in very limited number (290, 0.2% of total). The dataset analysed in this study consisted of only dart tags (also known as "spaghetti" tags) which are plastic darts inserted in the dorsal muscle of the fish, behind the second dorsal fin, using a tag applicator (see Fig. 2.1 and 2.2). These low-cost tags are designed to be implanted on large numbers of fish of various sizes and species, and can provide valuable information on growth, movements, natural mortality and stock abundance. Of the 168,163 fish tagged during the RTTP-IO, 167,698 (99.7%) had dart tags implanted. Usually, only one tag is implanted on the fish and this refers to "standard tagging". However, in order to estimate the shedding rate (i.e. the loss of tags for various reasons), double tagging was also performed on a fraction of the tagged fish. Another minor group of fish received a second tag (with a different colour) to indicate that they had been subject to oxy-tetracycline (OTC) injection that marks the otolith increment on the day of tagging (and is later used for purposes of evaluating growth). The number of tags deployed, by tag type and species, is summarized in Table 2.1. Incomplete or doubtful information occurred on some fish and tags, they are referred to as "unknown" in Table 2.1 and will not be used in the study.

Figure 2.1: Dart tags implanted on tuna. The middle tuna was subject to double tagging, with one tag on each side of the 2^{nd} dorsal fin.

Figure 2.2: A tuna tagging operation on board the pole and line vessel chartered by the RTTP-IO. Applicators with tags inserted and ready for implant are arranged in a rack (in the background). The fish is tagged on a soft cradle and set back at sea within a few seconds. In the meantime, the species, length of the fish and its condition are taped on a digital recorder. The tagging data of the day are entered in the database in the evening (in addition to ancillary information) by replaying the digital recorder.

Table 2.1: Number of tags deployed by type and tuna species during the RTTP-IO.

	Dart tags				Electronic tags (IAT, PAT, ST)	Unknown tag	Total no of tags by species
	Standard tagging	Double tagging	OTC treated	Total			
Skipjack	67 205	9 626	1 500	**78 331**	0	0	**78 331**
Yellowfin	41 762	10 683	2 019	**54 464**	223	2	**54 689**
Bigeye	24 526	7 517	2 443	**34 486**	67	14	**34 567**
Unknown species	365	30	22	**417**	0	159	**576**
Total by tag type	133 858	27 856	5 984	**167 698**	290	175	**168 163**
% of total tags	79.6	16.6	3.6	**99.7**	0.2	0.1	100.0
% of dart tags	79.8	16.6	3.6	100.0			

2.1.2.3 Tagging locations

The main tagging location was the region of Tanzania (79% of all tags deployed). The remainder was distributed in the Seychelles (13%), in the North Mozambique Channel (3%), in the Arabian Sea (2%) and in international waters (3%) (Fig. 2.3). It should be highlighted that tagging was conducted in off-peak fishing periods where possible. This was done purposely to allow sufficient mixing of tagged tuna within the wild population before being caught by the fleets. The figures 2.4-2.6 represent the tagging densities of each species and their recoveries as of September 2011.

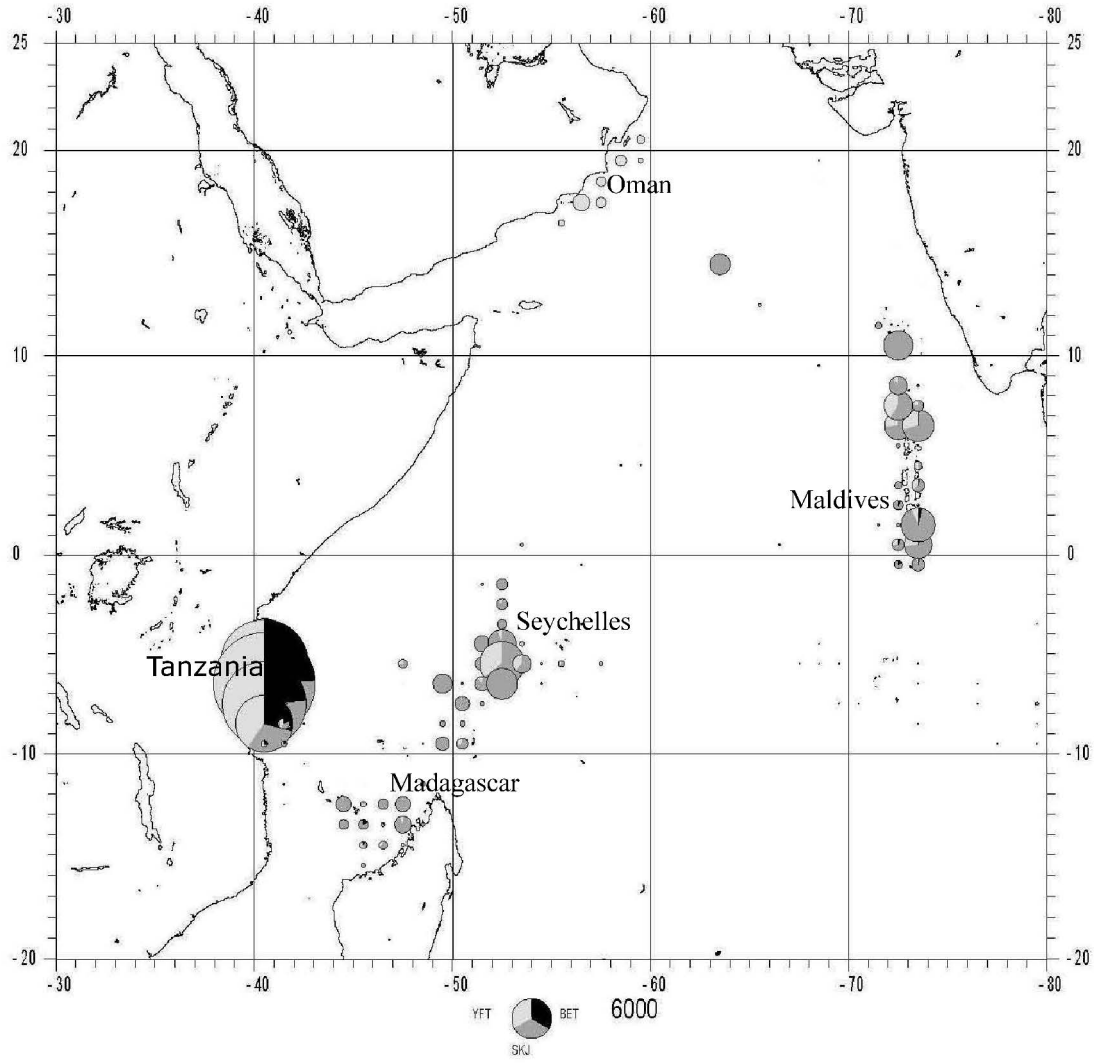

Figure 2.3: Geographic distribution of the RTTP-IO tagging operations. YFT: Yellowfin tuna, SKJ: skipjack, BET: Bigeye tuna.

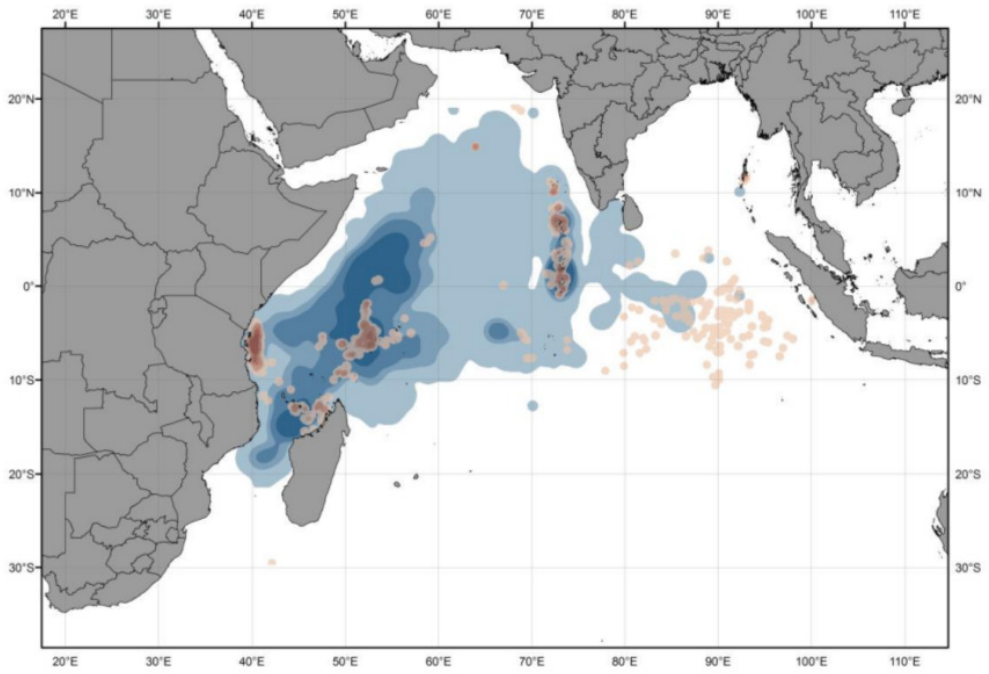

Figure 2.4: Densities of releases (in red) and recoveries (in blue) of skipjack tuna. Data as of September 2011 (IOTC, 2011).

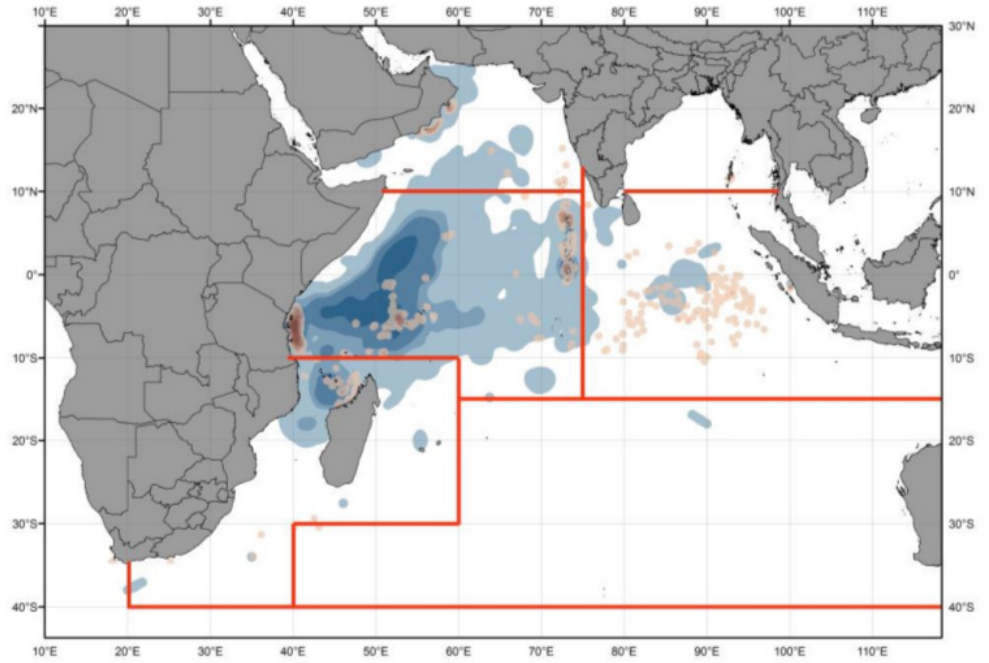

Figure 2.5: Densities of releases (in red) and recoveries (in blue) of Yellowfin tuna. Data as of September 2011 (IOTC, 2011).

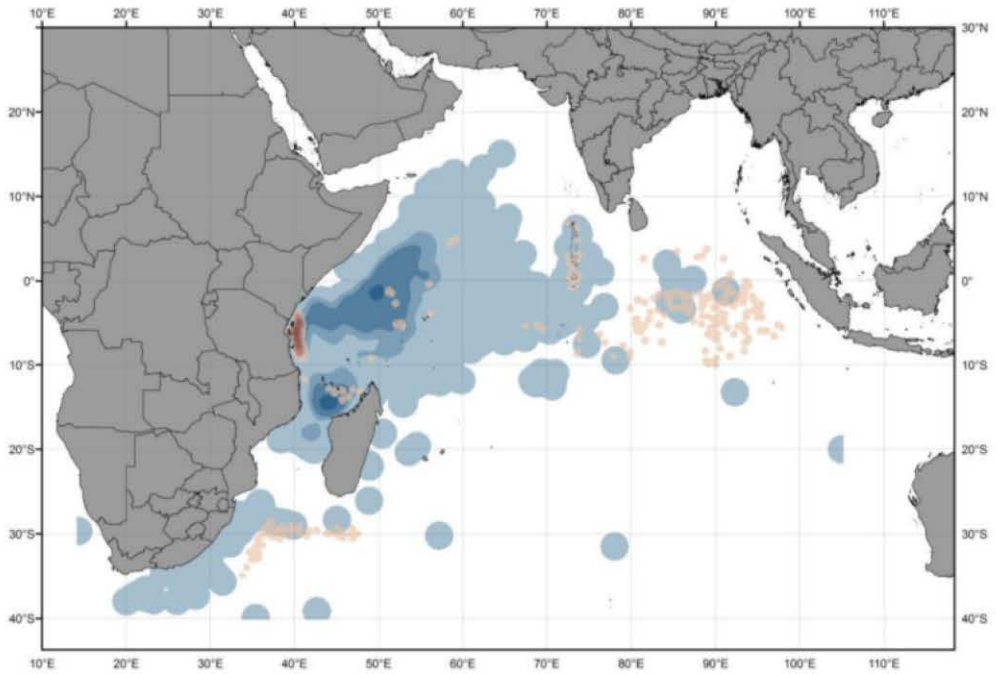

Figure 2.6: Densities of releases (in red) and recoveries (in blue) of bigeye tuna.Data as of September 2011 (IOTC, 2011).

2.1.2.4 Species tagged

Catches of tuna in the Indian Ocean (Fig. 2.7) are given species wise from the year 1950 to 2013. Catch levels start to rise suddenly in early 1980s with record catches in 2006 before decreasing. Exploitation of yellowfin tuna follows closely skipjack catches, while bigeye catches remain considerably less.

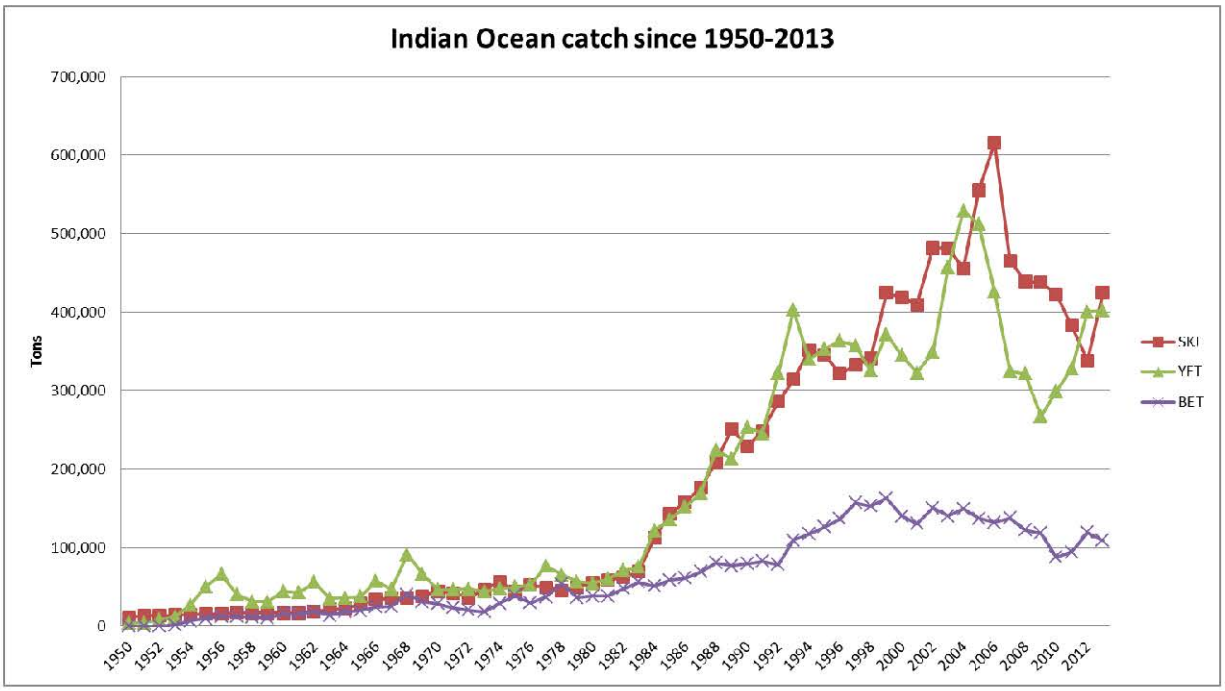

Figure 2.7: Indian Ocean tuna catches by species, IOTC. BET: Bigeye, SKJ: Skipjack and YFT:Yellowfin.

Skipjack Tuna

The skipjack tuna (*Katsuwonus pelamis*, Fig. 2.8), is known to be an epipelagic species, spending most of its time near the surface in open sea associated with convergence zones, where cold and warm fronts encounter each other. Skipjack tuna catches started gradually in the 1950s, with 50,000 t in the mid-1970s, exploited mainly by pole-and-line and gillnet fishing vessels. The arrival of Purse Seine (PS) fishery in the Indian Ocean increased catch levels dramatically. In 2006 the annual catch was over 600,000 t but catches have declined recently, with the lowest catch levels recorded since 1998 in 2012, around 315,000 t (IOTC, 2013, 2014). The reported percentage catch by PS in the past recent years were over 90% in the Indian Ocean (IOTC, 2014).

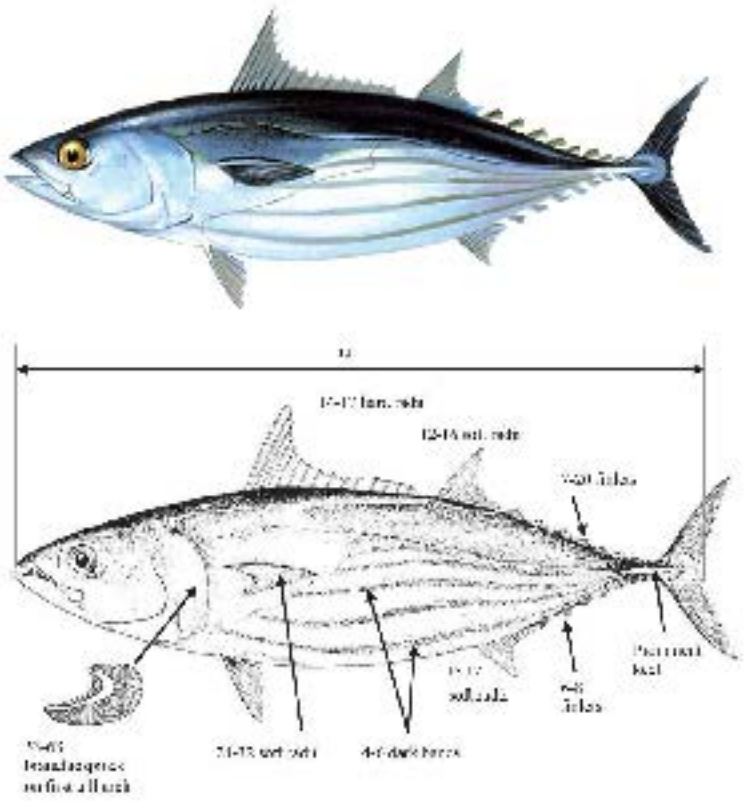

Figure 2.8: Characteristics of adult skipjack tuna (*Katsuwonus pelamis*) (ICCAT (2009)).

The skipjack stock in 2014 was assessed to be currently 'not overfished' (IOTC, 2014). Skipjack catch levels by purse seiners have been increasing since 1980s as a consequence of the development of the FAD fishing. However, the gradual rise in catch levels peaked in 2007 and was followed by a sharp decline. Until 2007 the major part of the catch was from the Western Indian Ocean but in 2008-2011 piracy along the Somalian coast caused a shift in fishing activity from these waters.

Skipjack tuna have a small size at maturity with a short life cycle but a high productivity which therefore, makes them less prone to overfishing. The maturity size of skipjack is described to be 41 and 43 cm for females and males respectively (IOTC, 2013). Skipjack tuna can spawn throughout the year in the inter-equatorial waters of the Indian Ocean depending on favourable conditions. They are generally associated with other juveniles of bigeye and yellowfin tuna. They are known to be large scale migratory species, covering large distance in short periods of time. In

the Indian Ocean the average distance between tagging and recovery positions was estimated to be around 640 nautical miles (nmi) (IOTC, 2011).

Yellowfin tuna

Yellowfin tuna (*Thunnus albacares*, Fig. 2.9) is both an epipelagic and mesopelagic species (ICCAT (2009)). From 2004 to 2009, the estimate of total and spawning stock in the Indian Ocean showed a decrease which was attributed to high catch levels from 2003 to 2006. In 2010, the reduction in catch levels improved slightly the stock. Fish landings of yellowfin rose from 300,000 t in 2010, to 327,490 and 368,663 tonnes in the following two consecutive years. Recent stock assessment in 2012 indicates that the stock is 'not overfished' and not subject to overfishing (IOTC, 2014). Recruitment, was estimated to be lower than the time series average and consequently the catches have been set at lower levels than the Maximum Sustainable Yield (MSY) to keep the stock level sustainable. It should be emphasized that artisanal fisheries represent a considerable share in the Indian Ocean, up to 20 - 30% of the total catch but the feedback from artisanal fisheries is poor in some regions.

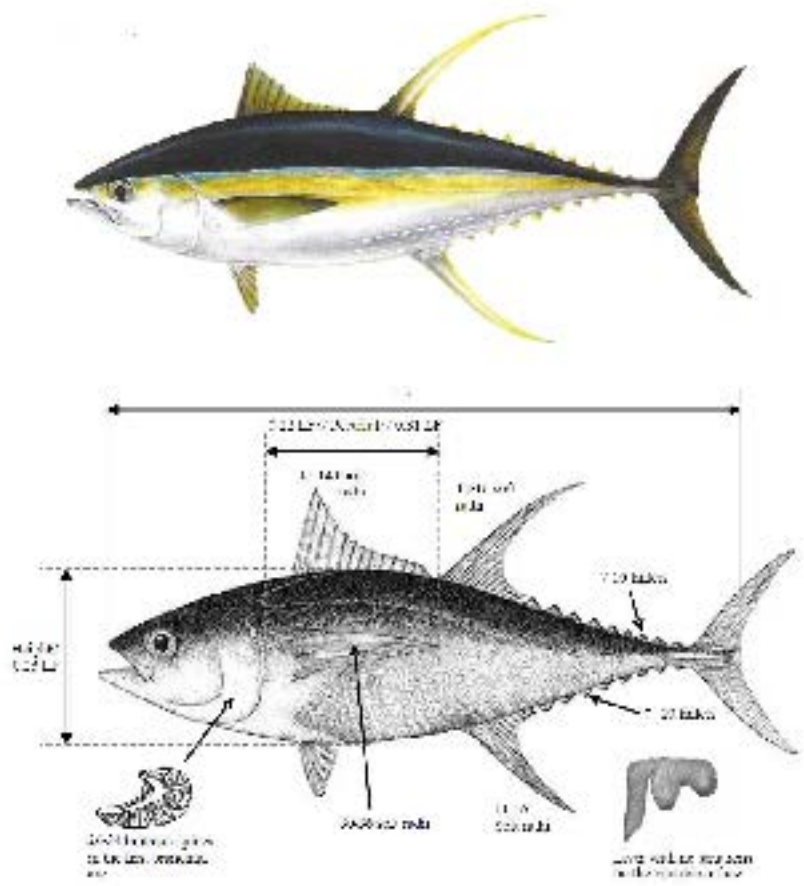

Figure 2.9: Characteristics of adult yellowfin tuna (*Thunnus albacares*) (ICCAT (2009)).

It is commonly acknowledged that FADs tend to attract more small size tuna (91% of the catches reported to be under 10 kg), although there are a few large individuals of yellowfin and bigeye (Ménard et al., 2000b; IOTC, 2013). A considerable number of small yellowfin are caught under FADs along with skipjack and juvenile bigeye while big yellowfin tuna are caught in free swimming schools (IOTC, 2014). In the Indian Ocean, the IOTC (2014) report established the maturity size to be 100 cm for both males and females. Spawning grounds have been identified in equatorial waters (0° - 10° S) from December to March but main spawning areas are found in the west of the Indian Ocean (IOTC, 2013). There are other known spawning locations off Sri Lanka, the Mozambique Channel and off the Australian coast in the west.

Bigeye Tuna

The bigeye tuna (*Thunnus obesus*, Fig. 2.10), is both an epipelagic and mesopelagic species. Currently, bigeye is mainly exploited by industrial longline vessels (70%) followed by purse seine (19%) and then other fisheries (11%). Stock assessment of bigeye was estimated to be stable compared to the previous years with fish mortality below that for maximum sustainable yield (MSY). The average catch over the 2008-2012 period was estimated to be below the MSY, approximately 107,600 t. The IOTC (2014) estimated that bigeye tuna are 'not overfished' and are not prone to overfishing based on the stock evaluation in 2013. The report pointed out that under the current fishing pattern, there is a low probability of reducing the stock level below spawning biomass over the next 10 years. Nonetheless, it also highlighted the need for continued monitoring and data collection to reduce uncertainties. The purse seine catch in weight consists of a large majority of juvenile taken under FADs (70-80%), the remaining being taken as Free School (FS). Recently (2011-2012), the purse seine catch of bigeye on associated schools have dramatically declined (10,400 t in 2012 compared to an average of 19,000 t for 2003-2009). Purse seiners have started to operate substantially on FADs in the early 1990s so that the average weight of total catch (all gears) declined. The overall biomass of bigeye in all fisheries has declined since 1950 (IOTC, 2013).

Tropical and temperate waters are the preferred habitats of bigeye, generally found in deep and cooler waters as compared to yellowfin and skipjack. In terms of movement, bigeye tuna are seen to migrate further than yellowfin as observed from tag and recapture data (ICCAT, 2009). The average distance covered by this species in the Indian Ocean from tag release to recapture data is 657 nmi and maturity in terms of size of bigeye tuna is estimated to be 100 cm for both males and females (IOTC, 2014). Observations made with respect to size category of tuna in FS and FAD associated schools show that the latter are typically made up small or young tuna whilst FS have a more diverse size range.

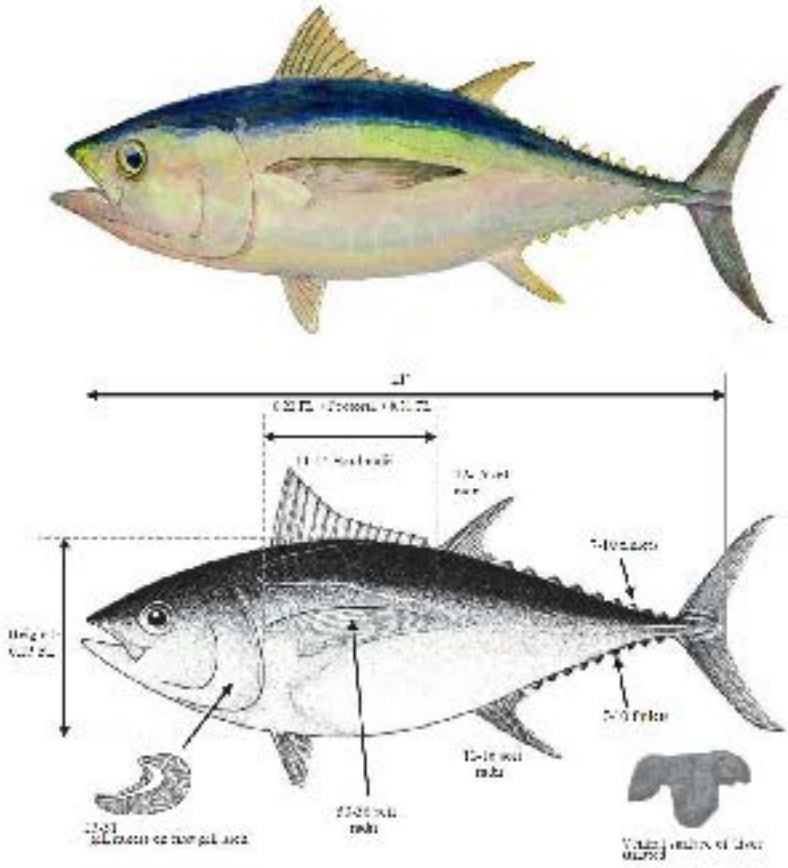

Figure 2.10: Characteristics of adult bigeye tuna (*Thunnus obesus*) (ICCAT, 2009).

Bigeye spawning areas are known to be along eddy rims, local sea mounts and frontal interactions, with the temperature range being higher than 24 °C and usually in equatorial zones. Pereira (2005) reported that for 86.9% of bigeye catches, SST values were between 16 - 20 °C. The spawning season of bigeye tuna in the Indian Ocean is normally from December to January but in the East of Indian Ocean spawning also occurs during June (IOTC, 2013).

2.1.2.5 Size of tuna tagged

The ideal situation would have been to tag the range of size categories from small tuna to large ones. Unfortunately, small tuna of 20 - 40 cm were not captured for tagging. About 1010 yellowfins above 110 cm were tagged along the Oman region, while 99% of them were in the range of 40 - 118 cm (Marsac et al., 2014). Size ranges among bigeye tuna were of 40 - 90 cm, representing 99% of the bigeye tagged and finally, for skipjacks, 40 - 68 cm, also representing 99%.

Recoveries of tuna with less than one month of liberty were discarded as the time-at-liberty does not allow sufficient mixing with the untagged population. The recoveries were subset by species, size categories (based on the fork length, FL) and school-type. Three size categories were attributed to bigeye and yellowfin to depict three life stages (juveniles, pre-adults and adults) whereas two size categories (for juveniles and adults) were used for skipjack. Limits in size categories adopted for the three species are given in table 2.2.

Table 2.2: Size-class of Indian Ocean tropical tuna adopted for the purpose of the study. Skipjack tuna being relatively small in size a pre-adult stage is not applicable (N/A) (Hassani and Stequert, 1991; Cayré and Farrugio, 1986; Praulai, 2004).

Species	Juvenile (Fl/cm)	Pre-adult (Fl/cm)	Adult (Fl/cm)
Bigeye	< 70	70 – 100	> 100
Skipjack	< 45	N/A	≥45
Yellowfin	< 65	65 – 100	> 100

2.1.2.6 Recoveries

The number of recoveries and the quality of the information associated with those recoveries are key in the success of a tagging program. The distribution of recoveries by species and gear of recapture from the RTTP-IO is shown in Table 2.3. The overall recovery rate for the 3 species (skipjack, yellowfin and bigeye) is 16.7%, which is quite satisfactory for such a large area. The recovery rate by species (as listed above) is respectively 16.1%, 17.9% and 16.2%. Purse seine catches contribute to the bulk of recoveries (94.4%). The recovery rate is very low for longline fleets although many longliners operate in the Indian Ocean, but this may reflect the low reporting rate (possibly intentional) rather than the real fraction of longline-caught

tuna.

Table 2.3: Recoveries of the RTTP-IO tags by gear and species.

	PS	PL	LL	GL	HL	TL	OT	UN	Total	%
Skipjack	12 091	386	5	68	36	48		10	**12 644**	45.2
Yellowfin	9 116	250	89	151	94	49	1	17	**9 767**	34.9
Bigeye	5 217	90	257	4	18	5			**5 591**	20.0
Unknown	4		3						**7**	0.0
Total by gear	**26 428**	**726**	**354**	**223**	**148**	**102**	**1**	**27**	28 002	100.0
%	94.4	2.6	1.3	0.8	0.5	0.4	0.0	0.1		

PS : purse seine ; PL : pole and line; LL : longline; GL : gillnet ; HL : hand line; TL : troll line; OT : other: UN : unclassified

The best recovery data comes from fish detected at sea, during the fishing operation, as a precise date and position can be associated with the recapture (Fig. 2.11). In some instances, tagged tuna are recovered during unloading or trans-shipment. On purse seiners, knowing the well of origin, it is possible to assign a date range and approximate location as the mechanical engineer keeps record of the storage wells for specific sets and day. Finally, the worst case is a tag detected in a cargo ship or at a cannery abroad, as no date and/or precise location can be assigned to the recovery.

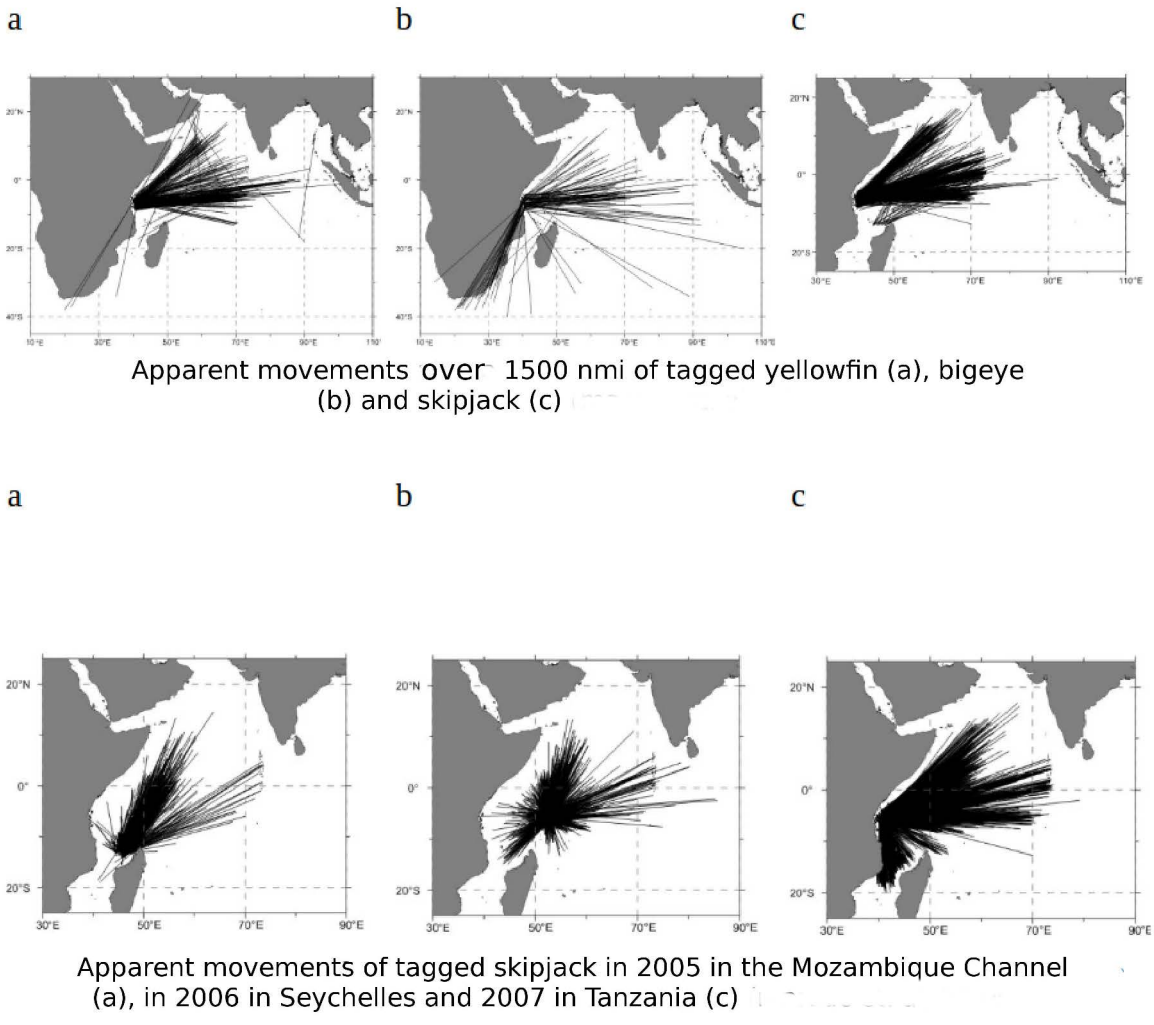

Figure 2.11: Geographic distribution of the RTTP-IO (Marsac et al., 2014).

2.1.2.7 Summary of the data archiving system

Tag-release and environmental data collected at sea were quality-controlled and archived in an Access database. When recaptures were returned to the IOTC, the record corresponding to each returned tag was completed with the information associated with the recovery data. The database comprises a rich diversity of information to answer several questions related to tuna. The programme consisted of two main phase: the tagging activity and recovery, which can be seen in the database. There are several fields of parameters recorded as a result of the tagging activity and consequently, recovery (Fig. 2.12). Here, a summary of the fields recorded in the database used for the purpose of the study is presented:

- Tagging and recovery positions.
- Fork length at tagging and recovery.
- Species tagged.
- ID allocated to each fish.
- Reliability of data collected.
- Dates of tagging and recovery.
- Time-at-liberty.
- Gear under which the tuna was caught.
- School type under which tuna were caught.
- Tagging programme under which the tuna was tagged (small scale or large scale).
- Tagging regions

For each of the following chapters different combination of fields were used as not all fields were relevant in each analysis conducted. In most of the cases the data had to be further transformed before they could be incorporated in the software presented below.

Although, the dataset gathered through these tagging programmes brought valuable information which would not be possible otherwise, it should be kept in mind that there are limitations. Among the main constraints: 1) the real trajectory of the tuna during its time-at-liberty cannot be estimated, 2) the success of the programme was dependent of tag returns from the different types of fishing vessels, 3) small tunas (below 40 cm) were not tagged and few large tunas were tagged, 4) the accuracy of recapture locations were not always respected due to transshipment of fish and, finally 5) returns from the east Indian Ocean (mainly operated by longliners) were very low.

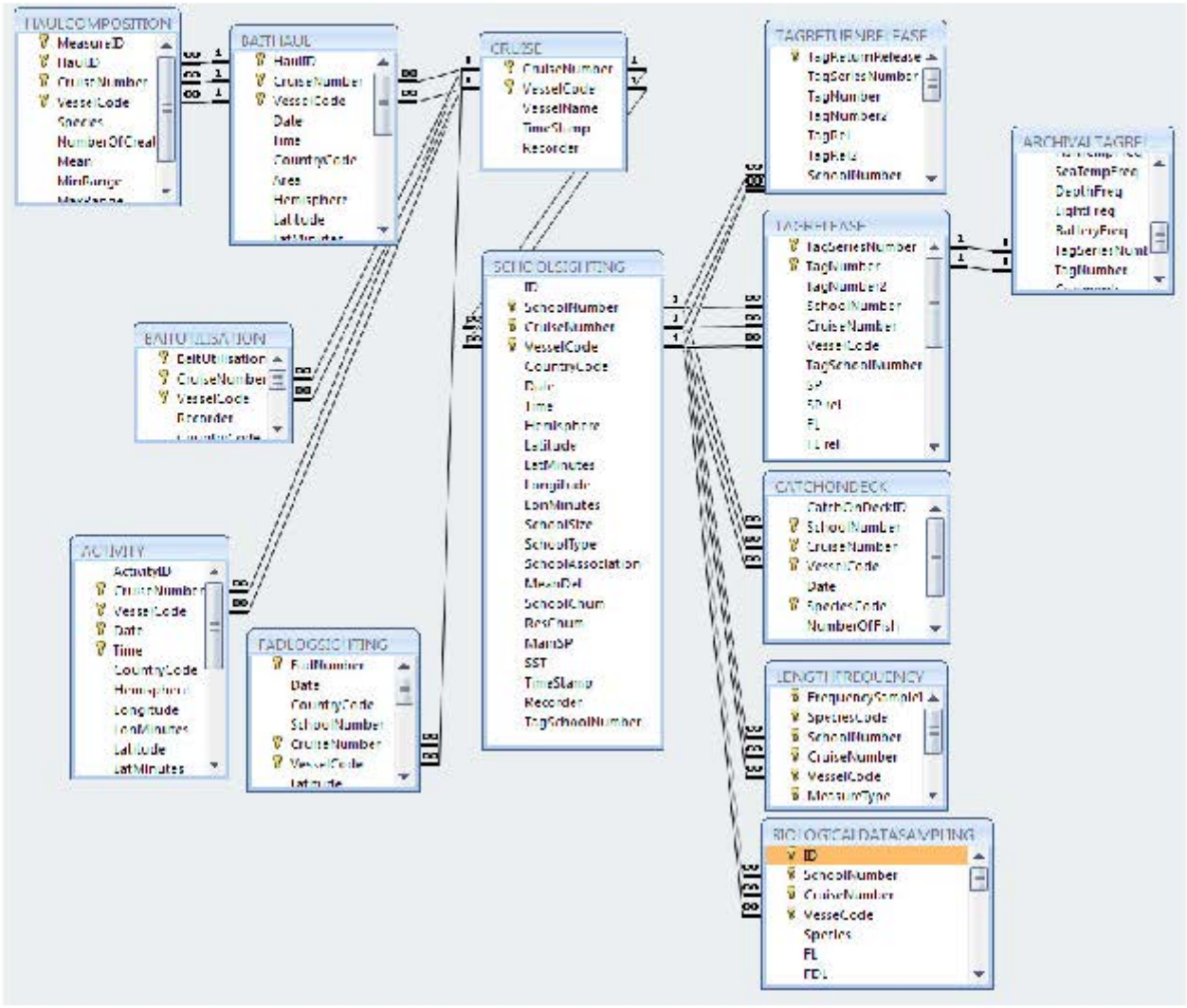

Figure 2.12: RTTP-IO database design (Sugathadasa and Hallier, 2010).

2.2 Indian Ocean Seasonal Spatial Stratification

Several factors can cause ocean spatial stratification which can be physical or biological or both. Mixed layer dynamics, phytoplankton biomass distribution, upwelling, temperature and salinity variations, are among the factors leading to ocean spatial stratification which can be observed at the microscale, mesoscale or macroscale. The distribution of tuna catch is often related to Chl-*a* patterns, both at mesoscale (Fonteneau et al., 2008; Tewkai and Marsac, 2010) and large scale (Marsac, 2008, 2012, 2013). In addition to Chl-*a*, known parameters influencing behaviour and distribution of tuna are sea surface temperature, dissolved oxygen concentration and thermocline depth (Sund et al., 1981; Hynd, 1969; Lehodey et al., 1997; Schae-

fer et al., 2007; Fonteneau, 2008). Forage distribution varies through the year and Marsac (2011) produced seasonal surface spatial stratification zones for the Indian Ocean based on surface Chl-a distribution and thermocline depth. The demarcation of the zones was based on the mean surface distribution of Chl-a from MODIS at 9 km resolution aggregated on the GODAS/NCEP grid (1^o longitude by $1/3^o$ latitude). It was observed that from a mesoscale and large scale point of view, that there is a good correlation between Chl-a distribution and tuna fisheries. It noteworthy that searching for forage is also among the factors driving tuna movement.

The seasonal spatial stratification zonation developed by Marsac (2011) highlights four main seasons:

- the North East (NE) Monsoon from December to March,
- the first Inter-Monsoon (IM1) period from April to May,
- the South West (SW) Monsoon from June to September,
- the second Inter-Monsoon (IM2) from October to November.

Zone between 2° - 10° S is strongly influenced by the South Equatorial Counter-Current during the NE-Monsoon. The Somali Current in this region flows to the south west during the NE monsoon and north east during the SW monsoon along the African coast. Moreover, the thermocline depth (using the 20 °C isothermal depth as a proxy) was used to determine the spatial stratification along with Chl-a. Based on Chl-a distribution and the thermocline depth, spatial zones for each of the seasons were demarcated. For each of the stratified seasons in Fig. 2.13, seasonally stratified zones were demarcated by the letters A to H, note that zone F phases out during the South West Monsoon (SW) and October-November Inter-Monsoon (IM2).

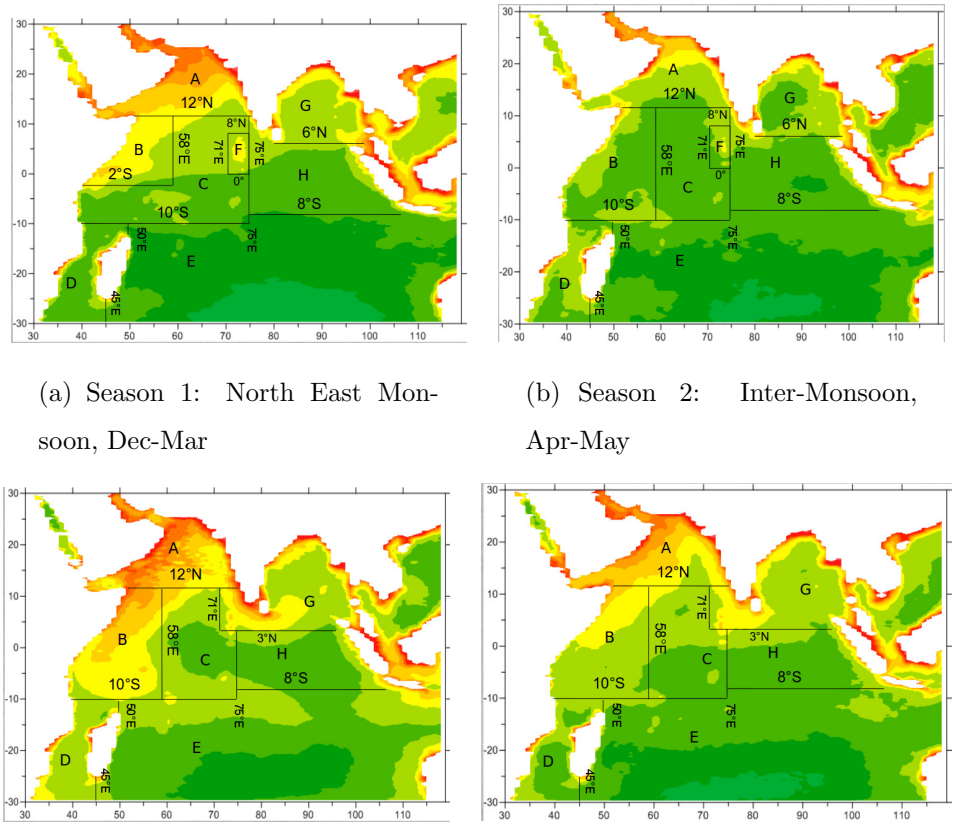

(a) Season 1: North East Monsoon, Dec-Mar

(b) Season 2: Inter-Monsoon, Apr-May

(c) Season 3: South West Monsoon, Jun-Sep

(d) Season 4: Inter-Monsoon, Oct-Nov

Figure 2.13: Surface chlorophyll-a spatial stratification in the Indian Ocean.

2.3 Analysis tools and methodologies

Modelling of ocean parameters related to salinity, temperature, current, etc., has been a useful tool for understanding the dynamics of the ocean. Modelling has a diverse scope of application, models range from simulating the ocean flow, to heat exchange of the ocean/atmosphere to forecasting and hind casting of ocean/atmosphere to energy flow in ecosystems (Guyomard et al., 2004; Maury et al., 2007; Maury, 2010). General Additive Models (GAMs), were used to investigate correlation of ocean parameters with tuna movement. In addition to modelling ocean parameters, survival and recapture or recovery of tuna in the Indian Ocean were also investigated. There are a number of robust models to estimate survival and recovery of animals. In this study three approaches have been applied to investigate tuna survival and recovery in the Indian Ocean (Chapter 4).

The study has been focused on various aspects. The main exploratory themes for analysis were to investigate tuna migration patterns with respect to oceanic parameters, multivariate analysis of tuna distribution and also survival probabilities of tuna in the Indian Ocean. In order to carry out these studies, the following core software packages were used to filter, correct and analyse the datasets:

- MATLAB (MATLAB, 2011),
- R project (R Development Core Team, 2008),
- MARK (White and Burnham, 1999),
- PRIMER v6 (Clarke and Gorley, 2006),
- Microsoft Access (Microsoft, 2010),
- ArcGIS (ESRI, 2009)

For the purpose of analysis several statistical approaches have been used. Among statistical analysis tools, Analysis of Variance (ANOVA) was also used. ANOVA is a procedure for determining whether variation in the response variable arises within or among different population groups (MATLAB, 2011). The ANOVA returns the significance (p-value) and displays the standard ANOVA table and a box plot of the columns. The purpose of one-way ANOVA is to assess whether data from several groups (levels) of a factor differ significantly from have a common mean. Moreover, the box-plots presented in the following chapters have additional keys to describe the data distribution. The central mark of the box-plot is the median, the edges of the box are the 25^{th} and 75^{th} percentiles. Whiskers extend to most extreme data points and outliers are plotted individually. In this case, extreme data points refers to data which fall within the lower and upper limits and the outliers are data smaller than lower or larger than the lower and upper limits respectively, but relevant as they are outlying with the respect to bulk data.

2.4 Standardizing observed tag recoveries

With the aim of accounting for the fishing mode at recapture, either associated schools around fish FADs or FS, the original dataset was reclassified into these two

main groups. For tuna not classified in either of these two groups (which means the actual fishing mode was not recorded), the dominant fishing mode found in the 1°x1° box/month strata (average 1984-2008) was assigned where the recapture was made.

Recapture probabilities are affected by the time and area distribution of fishing effort. These two parameters can heavily influence recapture rates. Hence there is need for a standardised recapture probability so that recoveries are comparable. The major part of recoveries has been done for the purse seine fishery and other gears gave a poor response with regard to their recoveries. Therefore, in this study purse seine recoveries only were used. The actual number of recoveries is a function of the number of fish tagged and the time at liberty during which the fish have been exposed to natural and fishing mortality. But systematic errors are also part of the process, which can be classified into two types:

- type-1 errors: these affect the actual numbers of tags recovered independently of time, that is post tagging mortality, immediate tag shedding and failure to report recovered tags,
- type-2 errors: these affect the return rate of tags over time, that is continuous tag shedding and/or mortality or emigration outside the fishery.

Experiments were conducted during the RTTP-IO to estimate the tag shedding rate (or its inverse, the tag retention rate) and the reporting rate.

2.4.1 Shedding rate

Estimation of the shedding rate has been conducted by double tagging fish. The simple analysis is based on the ratio of double tagged fish which were returned with a single tag to the number of double tags returned (Chapman et al., 1965). The probability of tag being retained was assessed by Gaertner and Hallier (2009) on the RTTP-IO dataset. These authors concluded that a simple constant rate model was sufficient to characterise tag shedding, compared to more complex formulations. The probability of retention π, which varies with time $(_t)$, is the estimated as follows:

$$\pi_t = \alpha e^{-\lambda t} \tag{2.1}$$

The coefficients α and λ refer to type-1 and type-2 shedding rates respectively and are species-dependent. The following values were estimated by Gaertner and Hallier (2009):

Table 2.4: Values of α and λ estimated with bootstrapped confidence interval for constant shedding rate model in the Indian Ocean (Gaertner and Hallier, 2009).

Species	α	λ **(per year)**
skipjack	0.987	0.015
Yellowfin	0.977	0.041
Bigeye	0.996	0.024

The yearly trend coefficient is divided by 12 to represent a monthly λ coefficient which will be used in the study (respectively: 0.00125, 0.00342 and 0.00200 for skipjack, yellowfin and bigeye).

2.4.2 Reporting rate

The reporting rate has been estimated by Hillary and Areso (2008), for only the purse seine fishery operating from Seychelles. Seychelles is by far the major purse seiner landing site in the Indian Ocean (50,938 MT in 2012 (IOTC, 2013)) and 96% of the tags were recovered from the purse seiners. Seeding experiments were conducted, where dead fish were discreetly tagged in the wells. Then, at landing, the number detected by the stevedores was compared to the number actually tagged (which is known in this case) and this provides the basis of the analysis.

Indeed, the reporting rate can vary across the fleets. Longliners should normally have a high reporting rate as catches are handled by individuals. Furthermore, tuna is generally gilled and gutted, increasing the probability that a tag can be detected during the process. Fonteneau (2008) mentioned that, for the same quantities of large yellowfin caught by purse seiners and longliners in the same area, purse seiners have reported 63 times more tags than longliners. This suggests a deliberated non-reporting of tags by the longliners crews. This partly undermines the goals of the RTTP-IO as recoveries of large fish after a long time at liberty would provide very valuable information on growth and mortality rates. It is obvious that the

probability of taking those large fish is declining dramatically as the abundance of the tagged cohorts is substantially reduced 7 years after the first fish were tagged.

After exploring the effects of various factors (species, size, tagger and time), Hillary and Areso (2008) concluded that year and quarter interaction were present but that species and size-specific effects were not likely to influence the estimates of the mean reporting rate (only the precision of these estimates). Moreover, there were no visible systematic differences in the estimate of reporting rate by species, therefore an all-species reporting rate was recommended to work with as it utilizes all of the available data. The model estimates of reporting rates by year-quarter proposed by Hillary and Areso (2008) are as follows:

Table 2.5: Quarterly estimates of reporting rates 2006-2008 (Hillary and Areso, 2008).

Years	Quarter 1	Quarter 2	Quarter 3	Quarter 4
2006	0.61	0.84	0.89	0.91
2007	0.93	0.91	0.91	0.88
2008	0.88	0.91	N/A	N/A

The study comprised recoveries up to mid-2008, but the reporting rate has been very stable since the 3^{rd} quarter of 2006, and it is assumed that this stable level has been maintained throughout the duration of the recoveries. The reporting estimates are discrete values by quarter. In order to obtain continuous monthly estimates for the rest of the study, we fitted a model to the observed reporting rates. The model is defined so that the reporting rate reaches an asymptotic value. The reporting rate β is given by

$$\beta_t = a(1 - \mathrm{e}^{-bt}) \tag{2.2}$$

where t is expressed in months, and the parameter estimates at 95% confidence interval are a = 0.903 and b = 0.556. Parameter estimates, their 95% confidence limits and p values, are as follows:

- a = 0.903, [0.890 – 0.917], p=0.000.
- b = 0.556, [0.495 – 0.617], p=0.000.

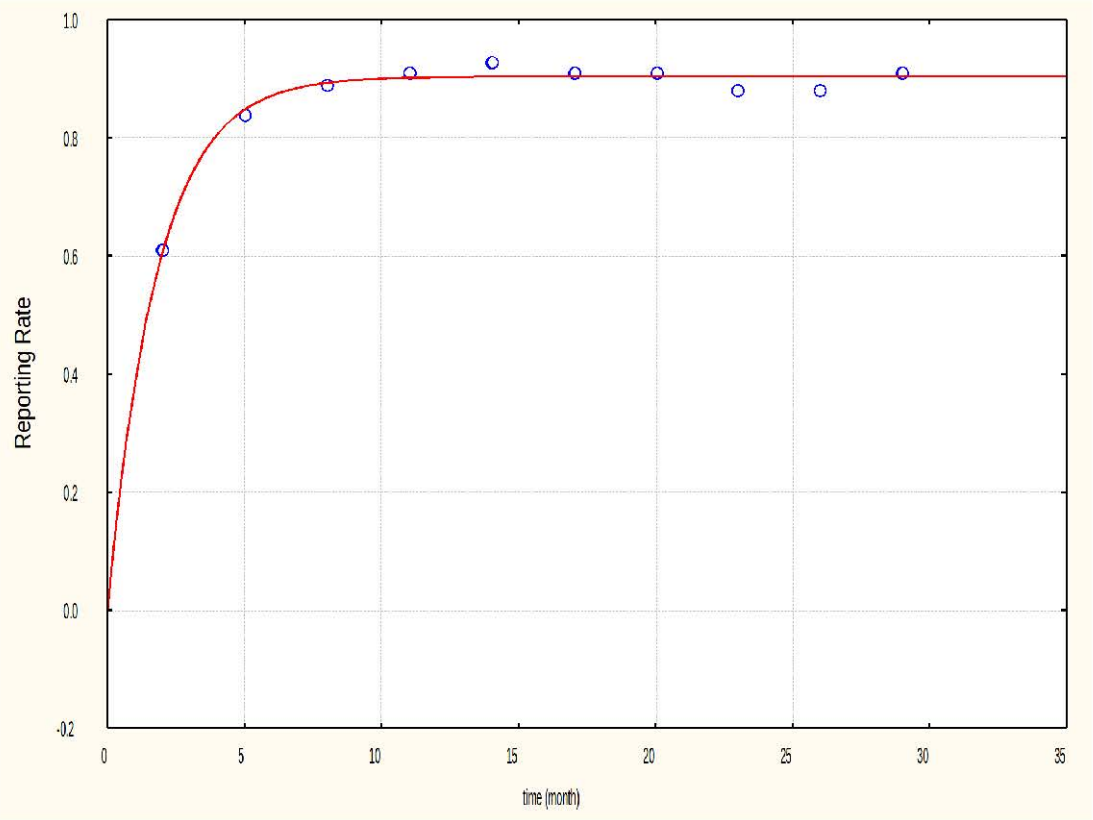

Figure 2.14: Reporting rate against time (months).

The reporting rate estimated here applies to purse seiners. According to the approximation proposed by Fonteneau (2008), for longline recoveries a reporting rate is considered to be 1% of that of purse seiners.

2.4.3 Correction of actual recoveries

To obtain corrected recoveries (R'), we add the fraction of recoveries lost by shedding and those lost by non-reporting to the observed number of recoveries. This calculation is disaggregated by area (1^o grid), time (year-month), fishing mode, species and size group, as follows:

$$R'_{ijklm} = R_{ijklm} + R_{ijklm}(1 - \pi_l) + R_{ijklm}(1 - \beta) \tag{2.3}$$

Where π is the retention rate which varies in time and by species, and β is reporting rate, varies only with time, and i, j, k, l, m denoting respectively area, time, fishing mode, species and size group.

2.4.4 Standardization using catch at size by the fishing fleets

To explore how the spatial distribution of the recaptures may be influenced by the spatial distribution of the fishing intensity, we compare the observed number of recaptures by species and size group and a standardised value. Many studies on recapture rates claim that recaptures should be standardised by the fishing effort exerted in the same strata. However, fishing effort remains problematic since it must be standardised to allow the comparison of the effect of different fishing gears and, in addition there is no evidence that it is linearly related with the number of recoveries. Moreover, fishing strategies should also be taken into consideration, e.g. whether targeting FAD associated or FS schools, as the median size of fish caught is quite different, but this cannot be easily reflected in terms of dedicated fishing effort. In contrast, the catch in number reflects the population from which tagged fish is sampled. Therefore, the following will be used:

- For purse seiners recoveries: extrapolated purse seine catch at size (SKJ, YFT, BET) by 5^o area-year-quarter and type of school to be calculated from the IOTC database. Those figures are based on the French and Spanish size sampling done in Seychelles.

- For longliner recoveries: longline catch at size (YFT, BET) by year, quarter and large area (West and East Indian ocean) produced by the IOTC for the 2011 working party on tropical tunas. Those data are discriminated between fleets (countries). There is no finer level of aggregation as the size sampling coverage of the longline catch is very poor.

- For baitboats, trolling and handline recoveries: relevant catch at size (SKJ, YF, BET) by year, quarter and large area (West and East Indian ocean) for each fleet (country)produced by the IOTC for the 2011 working party on tropical tunas.

The standardisation of recoveries by strata was based on purse seine catch at size by 5^o x 5^o area-year-quarter and school type, for each of the three species (IOTC database, European Union fleet). It was assumed that the proportion of catch by size group for each year-month, fishing mode and species corresponding

to a 5^o grid area could be assigned to all 1^o squares fished within this particular 5^o grid area. The actual catch by size group was then estimated in each 1^o square using the purse seine catch which are available by month, species and fishing modes at this spatial resolution. Applying the approach described by Bayliff (1979), the proportional distribution of tagged fish (P_{ijklm}) was estimated from the corrected recoveries (R'_{ijklm}) weighted by the purse seine catch (C_{ijklm}) and size of the area (A_{ij}):

$$P_{ijk} = \frac{R'_{ijk}/(C_{ijk}/A_{ij})}{\Sigma_{ijk}(R'_{ijk}/(C_{ijk}/A_{ij}))} \tag{2.4}$$

Where *i,j,k,l,m* denote the same factors as in equation 2.3. In this process, the probability of a tag to be recovered is assumed to be linearly related to the catch.

Overall, 7372 strata (combining all subscripts) were produced by this procedure, corresponding to a total of 12544 standardized recoveries (4027 yellowfin, 6295 skipjack, 2222 bigeye). The recoveries corresponding to the first 6 months at liberty originated primarily from the Tanzanian tagging area (83.4%) and then from the Seychelles area (14.7%).

Chapter 3

Factors impacting tuna behaviour: a multivariate approach

3.1 Introduction

Among the major purposes of tuna tag and release operations is to understand processes that influence tuna behaviour and population dynamics. The stage of maturity of tuna and their immediate interactions with their environment are factors influencing their movement patterns and are key issues guiding tuna research efforts. This research is aimed at promoting the sustainable exploitation of the resource. Tuna behaviour and interaction with their immediate environment have been studied (Sund et al. (1981); Praulai (2004); Fonteneau et al. (2008); Lezama-Ochoa et al. (2010); Tewkai and Marsac (2010)), in order to explain factors that affect their behaviour and movement. Usually, variables are studied separately or in pairs to one another but variables in a system are not independent of each other. A change in one parameter can affect several other variables. For instance, physical variables such as temperature (SST) and Chlorophyll-a (Chl-a) distribution may characterise zones influencing the distribution of tuna (Sund et al., 1981; Tewkai and Marsac, 2010).

Multivariate analysis is the use of numerical and statistical methodology to give insight of underlying structures through observation and analysis of a set variables simultaneously. It allows the understanding of how the variables are related to each other and what role they play in the assemblage of species with respect to their

habitat. This concept seemed to be an attractive approach to study tuna and factors affecting their behaviour. The idea was to see whether there are some patterns in the assemblage of species with respect to their size-class and environmental factors affecting their movement or migratory patterns. This approach has been very effective in determining underlying community structures of species in relation to their habitats (Kolasinski et al., 2012; Commins et al., 2013).

In the context of the Regional Tuna Tagging Programme - Indian Ocean (RTTP-IO) and this study, a number of factors have been tested applying this approach. Fundamental questions such as the influence of fish schools or school-type, movement patterns, seasonal spatial stratification and environmental influences were addressed. Environmental impact was assessed with regard to two ocean parameters: SST and Chl-*a*. The SST and Chl-*a* were derived from remotely sensed satellite data. These datasets represent monthly means which were are spatially and temporally retrieved corresponding to the recapture positions of the tuna on a monthly basis. The spatial resolution was 4km. The monthly mean data was used as it contains less missing data and compared to daily data where cloud cover is a problem much of the time.

The Indian Ocean being seasonally affected by the Monsoons, can be demarcated into different provinces of surface chlorophyll (Chl-*a*) distribution (Wiggert et al., 2009). Hence, it is possible to use multivariate analysis as a test case to analyse the movement patterns of the tuna in the context of the seasonal variation of surface Chl-*a*. In this chapter, three species of tuna are analysed with respect to their size-class, recapture year, school-type, seasonal positional zones and school-type. The patterns observed are then related to season, zone, SST and Chl-*a*. The objective is to understand the influence of environmental factors on the tuna behaviour.

3.2 Methodology

3.2.1 Study area and data

A multivariate approach was adopted to understand the interaction of community structure of the three species (bigeye, skipjack and yellowfin) with environmental factors. The RTTP-IO dataset is a very dense database to work with. In this respect, the study was conducted on tuna tagged and released in Tanzania only, as a pilot

study because the RTTP-IO dataset was too large to be analysed in toto. Having chosen the tuna tagged and released from Tanzania, does not limit their spatial distribution. Although the majority of the tag and release exercise was conducted in Tanzanian waters, tuna move fast, covering large distances. The whole Indian Ocean as defined by the International Hydrographic Organization (IHO, 1953) was considered spatially in terms of the stratified zone demarcations.

As a general rule, tuna with a time-at-liberty of more than 30 days were chosen, allowing a good population mix (IOTC, 2008*a*) of tagged tuna with untagged tuna. The dataset was standardised (see Chapter: 2) based on reporting and shedding rates as preliminary data treatment. Tuna species were categorised by size-class, school-type (FAD or FS), recapture seasons and seasonally stratified zones in terms of surface Chl-*a* distribution coupled with the average thermocline (20°C isotherm) and compositionally analysed from 2005 to 2011. The monsoon seasons in the Indian Ocean affect the surface Chl-*a* distribution (Fig. 2.13). Spatial stratification based on the surface distribution of Chl-*a* can be observed over four seasons. The first season: North East Monsoon (NEM) from December to March, the second season: Inter-Monsoon (IM1) from April to May, the third season: South West Monsoon (SWM) from June to September and the last season: Inter-Monsoon (IM2) from October-November. The relationship between the tuna and surface water temperature and Chl-*a* was assessed using the monthly mean Chl-*a* data and Sea Surface Temperature (SST) from Aqua-MODIS with 4km resolution. The satellite Chl-*a* and SST data were retrieved corresponding to the month and geographical location of each individual tuna recaptured. The Chl-*a* data were log transformed to harmonise differences between high and low Chl-*a* values while the SST dataset did not require transformation.

3.2.2 Pre-analysis

The RTTP-IO dataset comprises of several data fields relating to the three species. Information pertaining to geographical positions at tagging and positions of recaptured tuna, fork lengths, dates when tuna were tagged and recaptured, under which school-type they were caught, etc. After removal of a few bad entries in the dataset, it was standardised so that the recaptures reflect the harmonized distribution in

terms of recaptures (see Chapter: 2). As described in chapter 2, the Indian Ocean was stratified into eight zones based on the Chl-*a* distribution. The number of recaptures by season, year, zone and school-type were calculated using MATLAB and classified by species/size-class.

3.2.3 Basis of analysis

In order carry out the analysis, non-parametric multivariate methods in PRIMER v6 (Clarke and Gorley, 2006) with PERMANOVA+ (Anderson et al., 2008) packages were used. Cluster analyses and multidimensional scaling (MDS) ordinations were performed using a Bray and Curtis (1957) similarity matrix. The Bray-Curtis measure of similarity is commonly used for ecological comparisons of species abundances (Bray and Curtis, 1957; Field et al., 1982). Hierarchical agglomerative clustering was carried out on the similarity matrix, to demarcate groups having similar species and size groups. The tuna species and size-class abundances were square root transformed to prevent excessively high values dominating the analysis. The similarity profile test (SIMPROF) is a permutation test of the hypothesis that dendrogram groups do not differ from each other in multivariate structure (Clarke and Gorley, 2006). This approach restrains one from over-interpretation of structures inside groups where they do not exist (Clarke and Gorley, 2006). The ordination (MDS) diagram represents dissimilarities between samples based on species/size classes.

The SIMPER routine was applied to investigate which species by size-class characterised the season, year, zone and school-type. To analyse environmental influence of environmental factors, the BEST (Bio-Env) routine was used. The principle behind this routine is to find a match between multivariate sample patterns of an assemblage and environmental variables associated with those samples (Clarke and Gorley, 2006). It allows one to analyse the extent to which abiotic environmental variables contribute to the biotic behaviour or pattern either singly or in combination. The hypothesis was to test that oceanographic features influence tuna assemblages categorised into eight group depending on the species/size-class (see Chapter: 2).

Analysis of Similarities (ANOSIM) allows investigation of differences between factors and size-class compositions (Bray and Curtis, 1957) of the Bray-Curtis sim-

ilarity matrices of tuna abundance. Differences between depths or dates of the species/stage composition were investigated by analysis of similarities (ANOSIM) of Bray-Curtis similarity matrices of species abundance (Bray and Curtis, 1957; Clarke and Ainsworth, 1993). This analysis measures how alike sampling units are in terms of, e.g. species composition, by calculating average similarities within and between sampling units. In this instance, sampling units constituted discrete samplings of species abundances at different depths and dates.

3.3 Results

Assemblages of tuna species (biotic) abundance were analysed in relation to (abiotic) environmental factors. Based on the tuna recoveries, the data were aggregated with respect to zone (Fig. 2.13), season, school-type and year. Classification of the three species by their size-class gave eight biotic variables; bigeye tuna: juveniles, pre-adults and adults; skipjack tuna: juveniles and adults; and yellowfin tuna: juveniles, pre-adults and adults (Cayré and Farrugio, 1986; Hassani and Stequert, 1991; Praulai, 2004). Figure 3.1 gives an example of the processing tree or structure of one of the datasets used and its statistical analysis performed. The table 3.1 shows a truncated section of the abundance of the variables with respect to the samples.

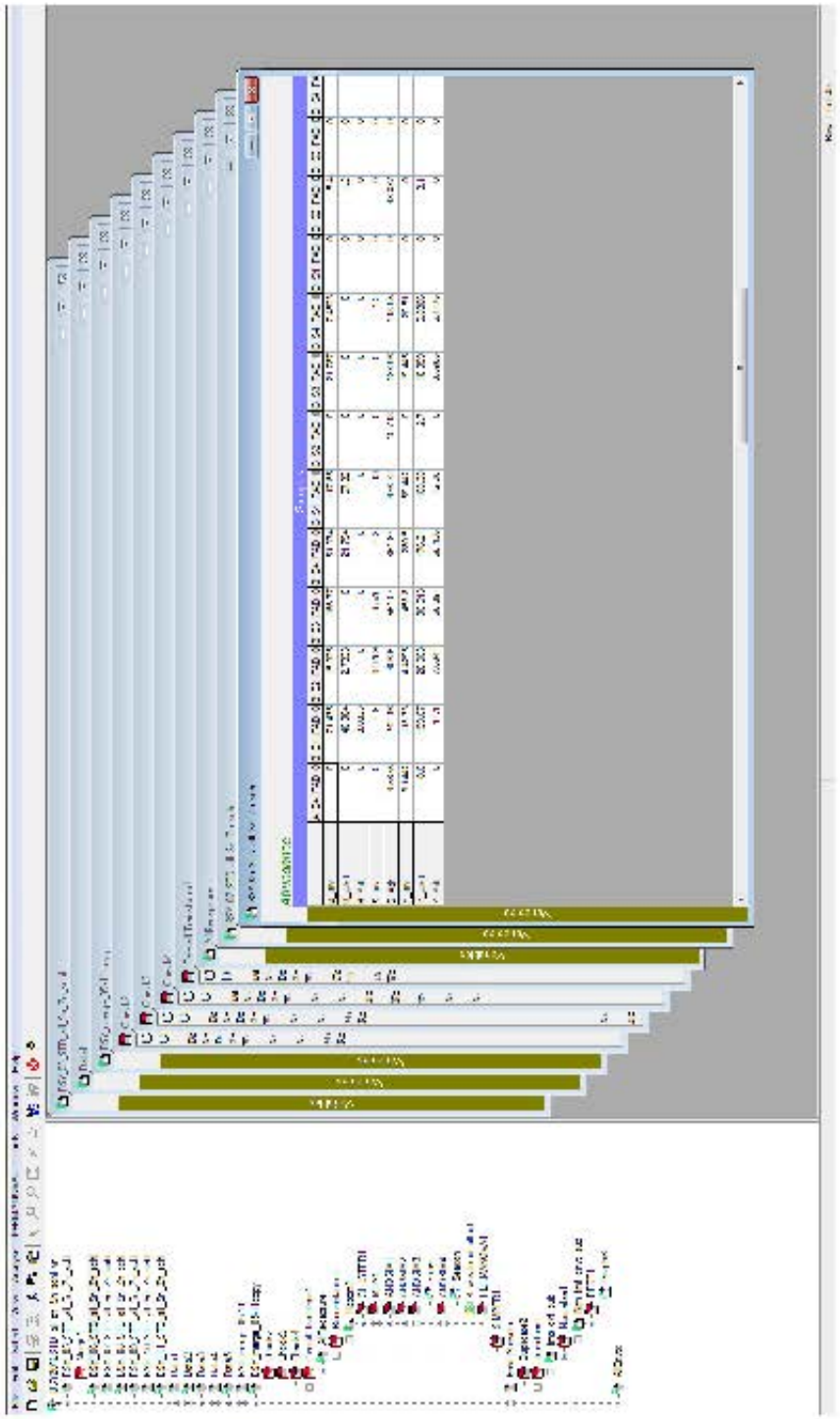

Figure 3.1: Data analysis on PRIMER of standardised tuna species. Where B juv: bigeye juveniles, B pAd: bigeye pre-adults, B Adt: bigeye adults, S juv: skipjack juveniles, S Adt: skipjack adults, Y juv: yellowfin juveniles, Y pAd: yellowfin pre-adults, Y Adt: yellowfin adults and the header in the samples' fields infer to zone, season, school and year of recoveries, e.g. A S4 FAD 06 is zone A, season 4 under FAD for year 2006.

Table 3.1: Sample of raw data loaded in PRIMER for transformation and processing. Where B_juv: bigeye juveniles, B_pAd: bigeye pre-adults, B_Adt: bigeye adults, S_juv: skipjack juveniles, S_Adt: skipjack adults, Y_juv: yellowfin juveniles, Y_pAd: yellowfin pre-adults, Y_Adt: yellowfin adults and the header in the samples' fields infer to zone, season, school and year of recoveries. For instance, A_S4_FAD_06 is zone A, season 4 under FAD for year 2006.

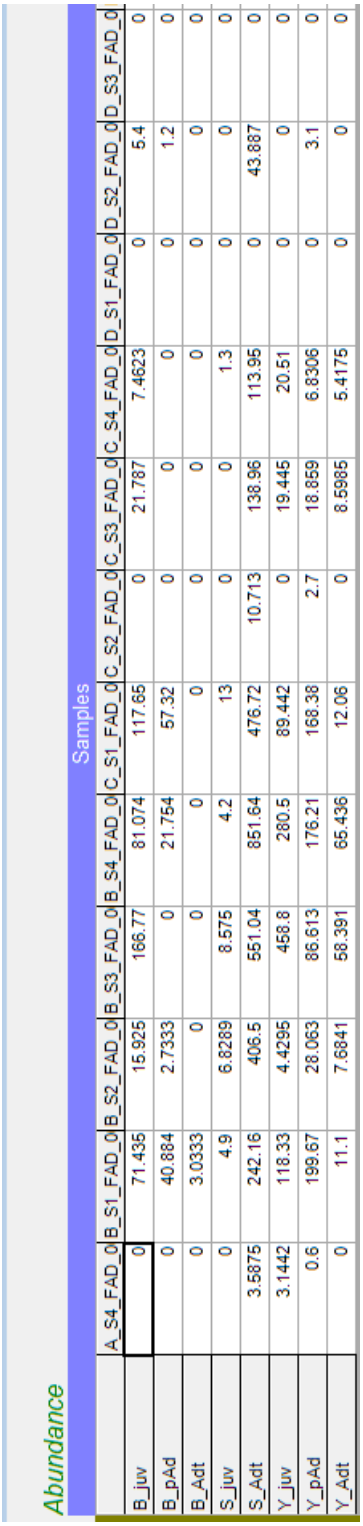

Abundance / Samples	A_S4_FAD_0	B_S1_FAD_0	B_S2_FAD_0	B_S3_FAD_0	B_S4_FAD_0	C_S1_FAD_0	C_S2_FAD_0	C_S3_FAD_0	C_S4_FAD_0	D_S1_FAD_0	D_S2_FAD_0	D_S3_FAD_0
B_juv	0	71.435	15.925	166.77	81.074	117.65	0	21.787	7.4623	0	5.4	0
B_pAd	0	40.884	2.7333	0	21.764	57.32	0	0	0	0	1.2	0
B_Adt	0	3.0333	0	0	0	0	0	0	0	0	0	0
S_juv	0	4.9	6.8289	8.575	4.2	13	0	0	1.3	0	0	0
S_Adt	3.5875	242.16	406.5	551.04	851.64	476.72	10.713	138.96	113.95	0	43.887	0
Y_juv	3.1442	118.33	4.4295	458.8	280.5	89.442	0	19.445	20.51	0	0	0
Y_pAd	0.6	199.67	28.063	86.613	176.21	168.38	2.7	18.859	6.8306	0	3.1	0
Y_Adt	0	11.1	7.6841	58.391	65.436	12.06	0	8.5985	5.4175	0	0	0

The cluster analysis dendrogram (Fig. 3.2) shows evidence of some clustering of the species/size-class abundance data. Although six main groups could be identified from the figure, there is no clear pattern based on the school-type. Figure 3.3 shows the same dendrogram for school-type but characterised by years. Observing the clustering in Fig. 3.3 from left to right, the first assemblage constituting of mostly years 2005 and 2006 showed slight predominance of FAD over FS. This observation applies the similarly to the next assemblage consisting mainly of years 2006, and 2007. Visualising the next diagram for Fig. 3.3 which is made mostly of years 2008-2011, assemblages were chiefly FS. Year 2008 and 2010 show more FS recoveries compared to the year 2011 with prominence towards FAD recoveries.

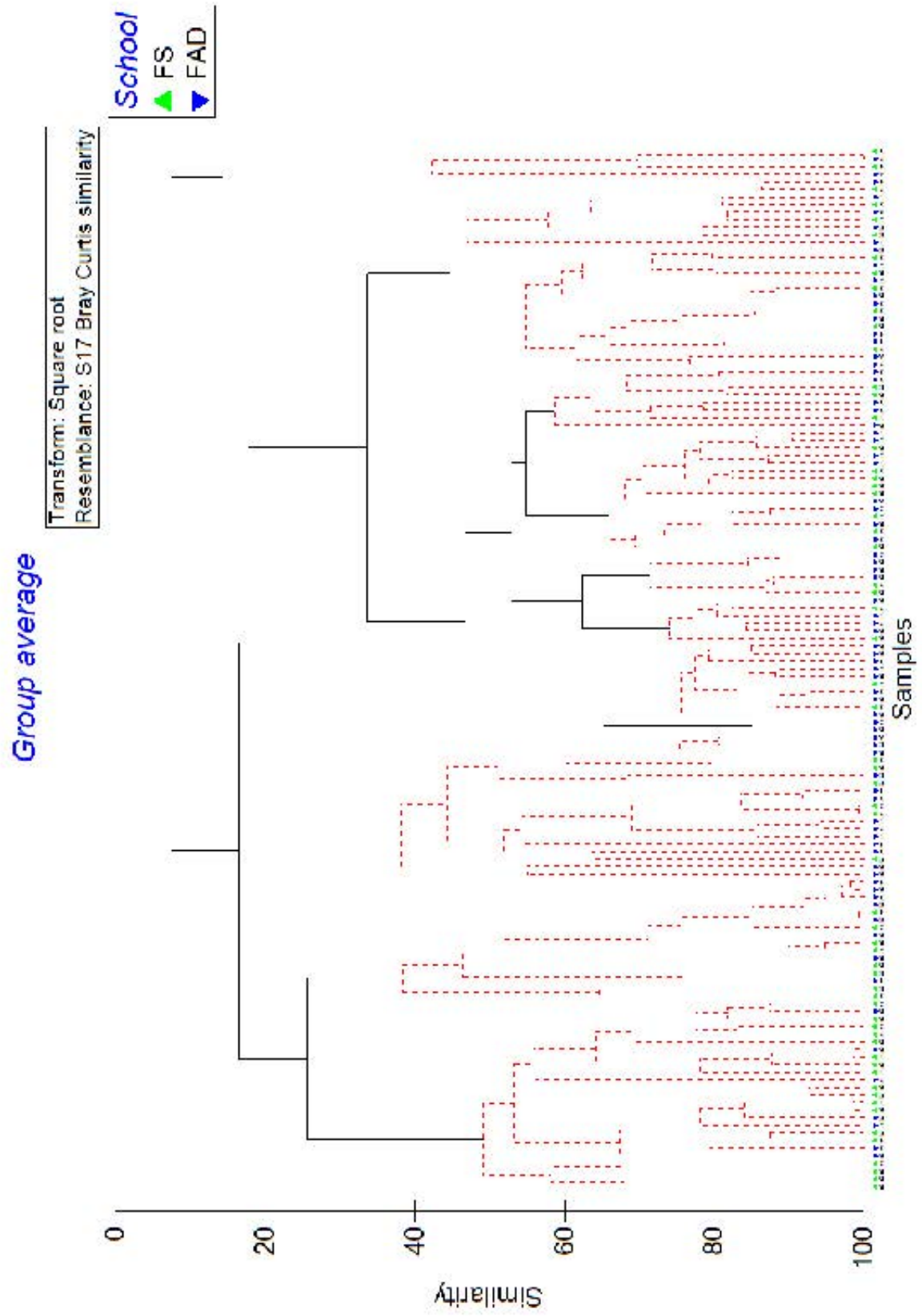

Figure 3.2: Dendrogram of Tuna abundance with respect to school-type and zone. Grouping in red lines are not significantly different (using SIMPROF tests). Black lines show significantly different groups. The bottom labels define the zones of recaptures and green triangle for Free Schools (FS) and blue for Fish Aggregating Devices (FAD).

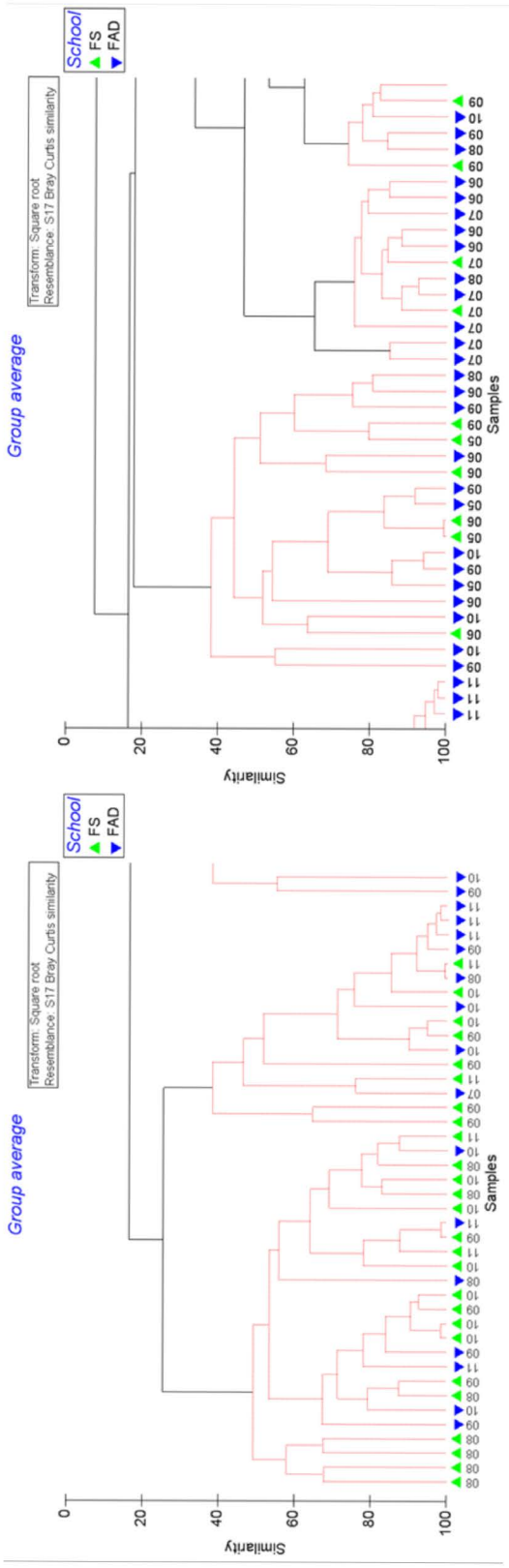

Figure 3.3: Enlarged view of dendrogram of tuna abundance with respect to school-type and year. Grouping in red lines are not significantly different (using SIMPROF tests). Black lines show significantly different groups. The bottom labels define the years of recaptures and green triangle for FS and blue for FAD.

Figures 3.4 to 3.7 show the five clusters identified in the dendrogram (Fig. 3.2 and 3.3) at the 30% level of similarity, encircled, with other factors superimposed using symbols. Four of the five clusters show some overlap. However, the years 2006, 2007 and 2008 cluster together (Fig. 3.4). Viewing the MDS of tuna recapture abundance by year and school (Fig. 3.5), this cluster is comprised of both FS and FAD but mainly recovered in zones B, C and D (Fig. 3.6). The cluster is comprised of all the four seasons (Fig. 5.7). The years 2009, 2010 and 2011 tend to group towards the left side of Fig. 3.4. Figure 3.5 shows no clear pattern with regard to school type, with both FAD and FS intermingled across the clusters. Figure 3.6 again shows no clear pattern of recapture zones, although Zone B recaptures tend to be towards the upper left of the diagram. Figure 3.7 shows little seasonal pattern in the recaptures.

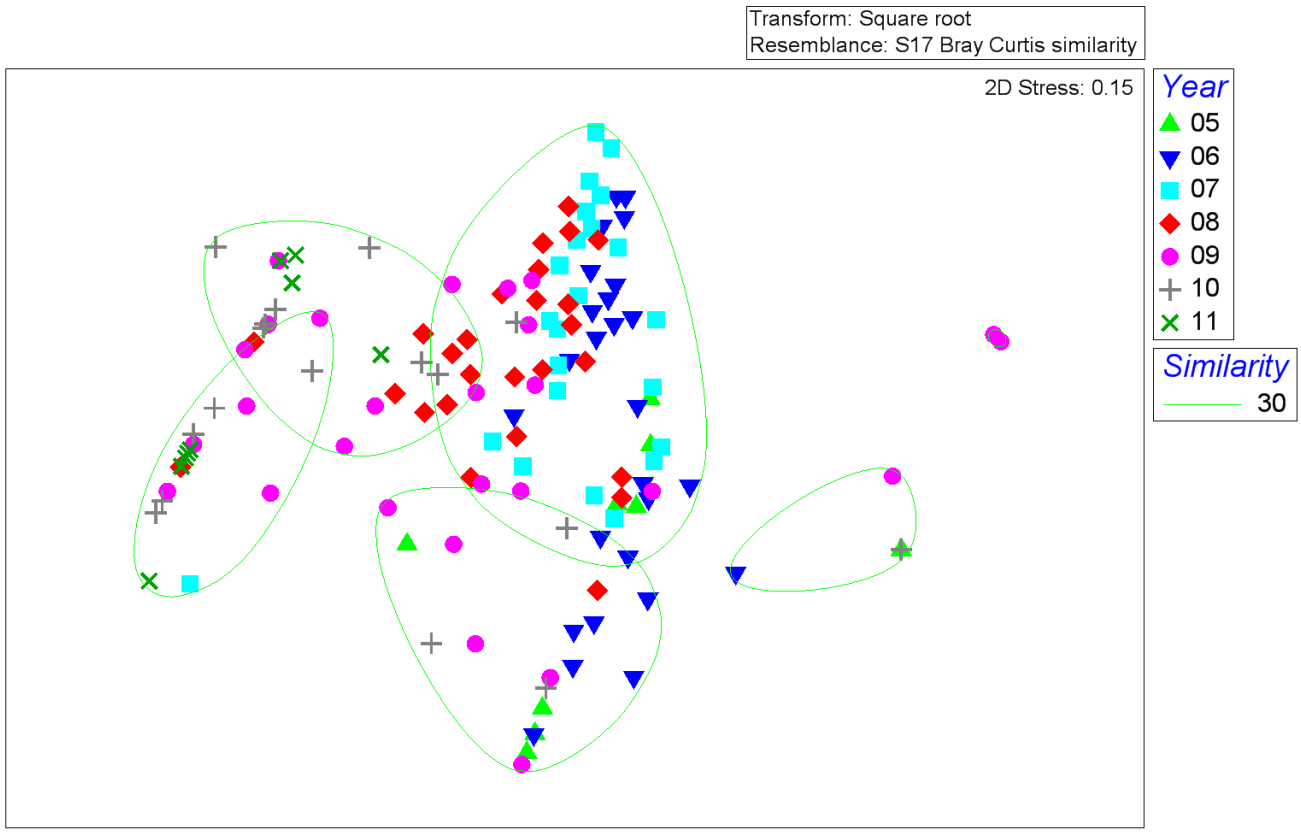

Figure 3.4: Multi-Dimensional Scaling (MDS) of tuna recapture abundances by year.

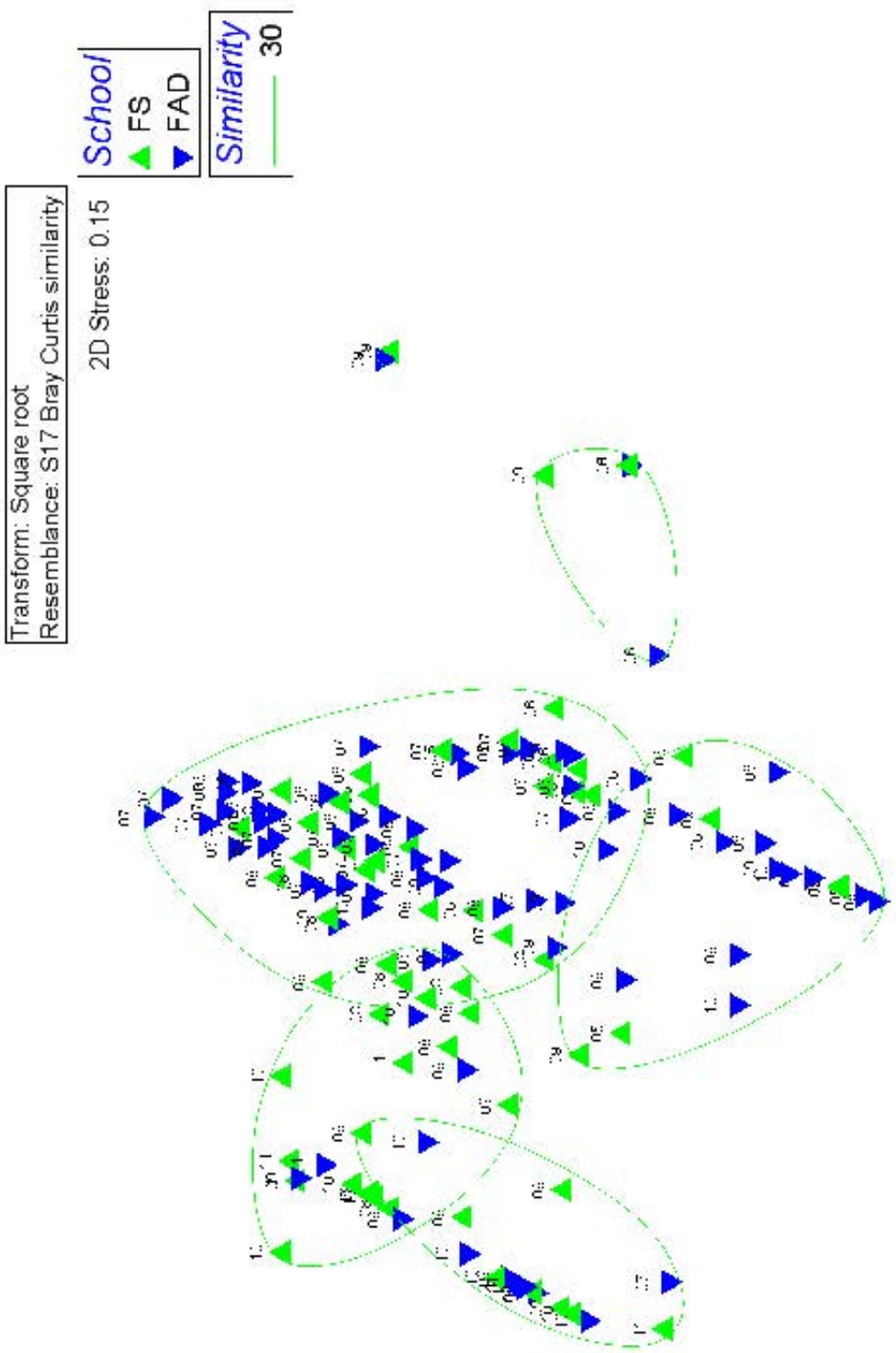

Figure 3.5: Multi-Dimensional Scaling (MDS) of tuna recapture abundances by year and school.

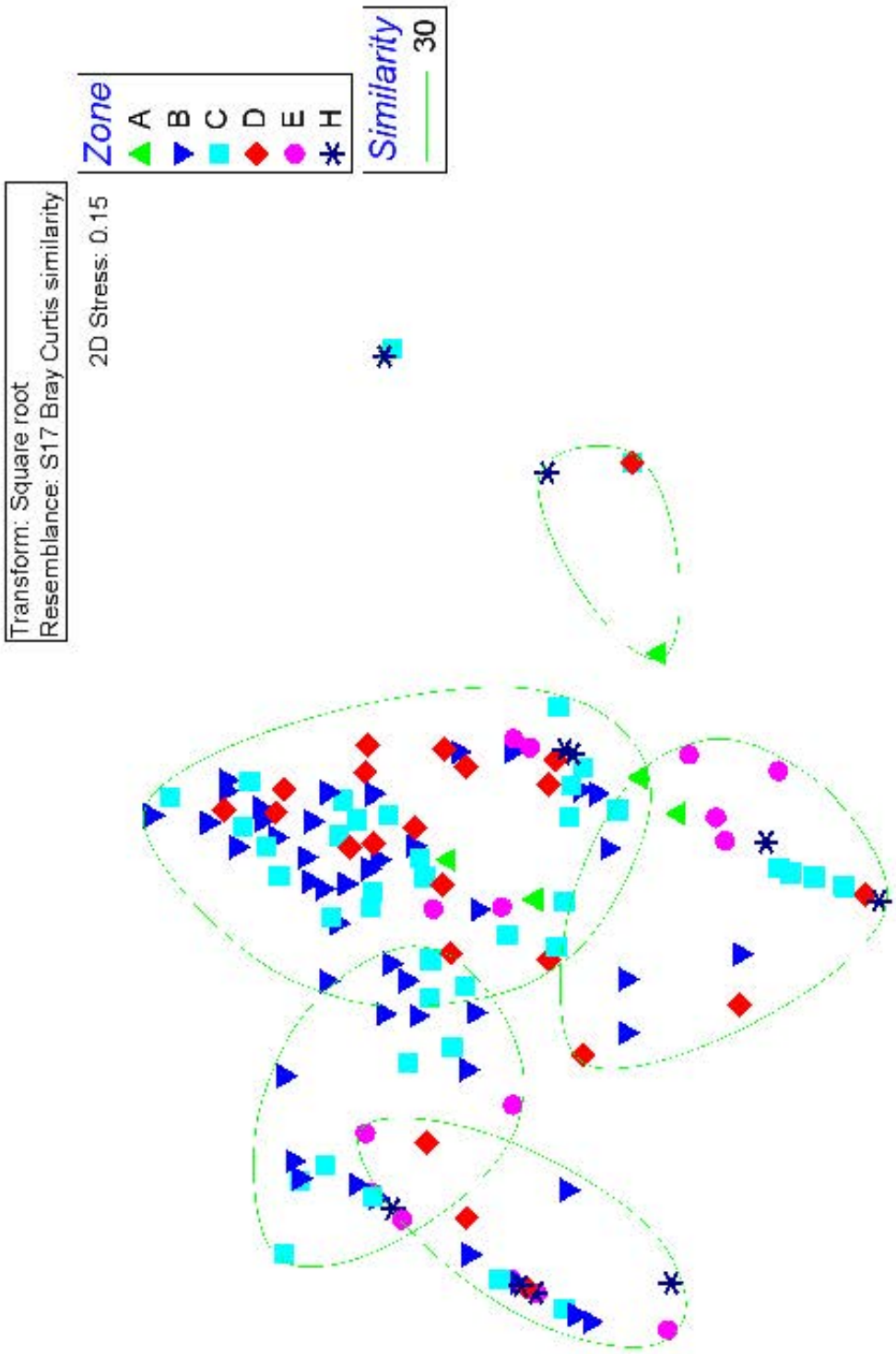

Figure 3.6: Multi-Dimensional Scaling (MDS) of tuna recapture abundances by zone.

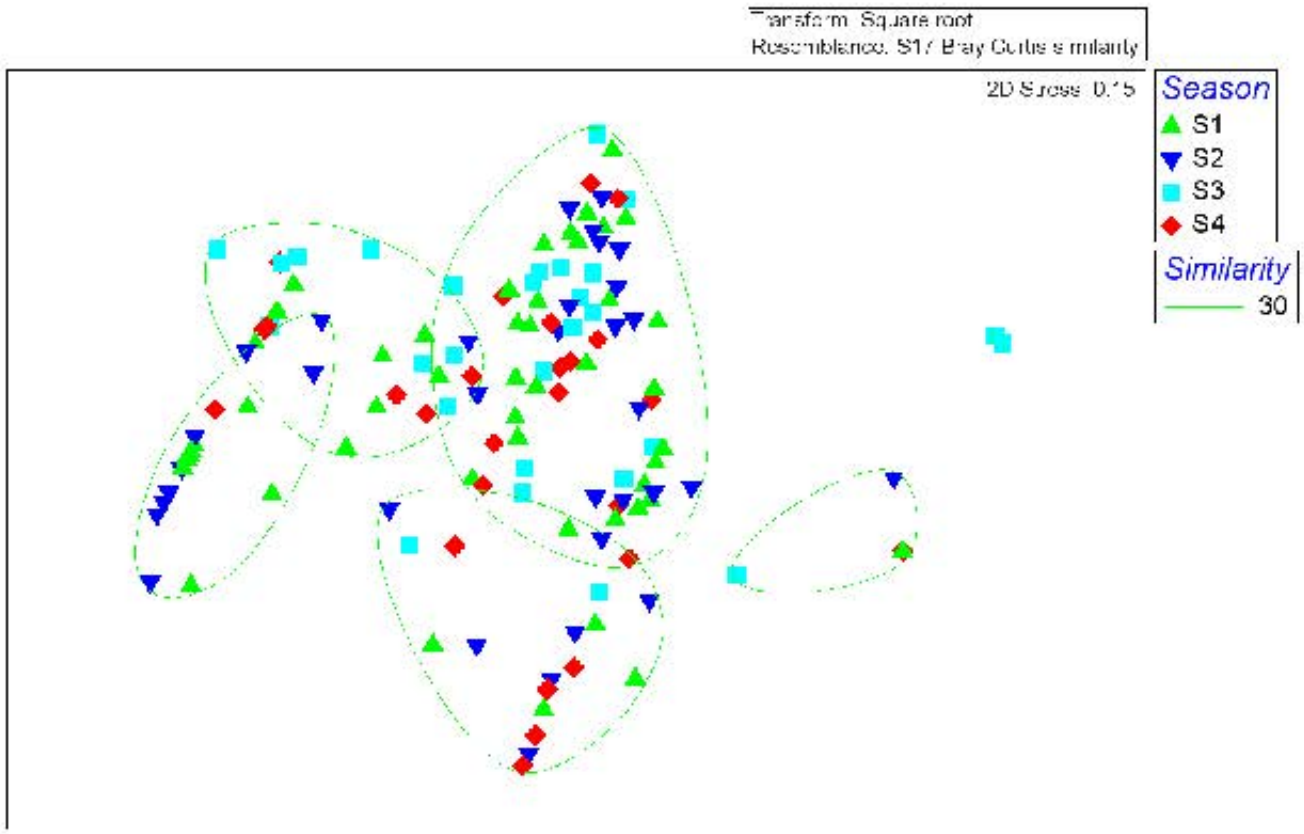

Figure 3.7: Multi-Dimensional Scaling (MDS) of tuna recapture abundances by season, where S1: NEM season, S2: First inter-monsoon season, S3: SWM season and S4: Second inter-monsoon season.

3.3.1 Testing abiotic factors affecting biotic groupings

ANOSIM (Analysis of Similarities) is used to see whether there is a relationship by comparing the Bray-Curtis similarity within classification group to similarity between the groups. The R value varies between zero and one, where zero would imply no relationship and one, a strong relationship. The four factors (year, season, zone and school-type) were analysed through a one-way ANOSIM analysis test shown in Fig. 3.8. The graphs show the distribution of the R-statistic under the null hypothesis that the factor under test has no influence on the multivariate assemblage data. It can immediately be seen that there are significant differences among the years and then zones, while schools are not significant nor are seasons. Table 3.2 shows the test results of R and p values for each of the factors investigated.

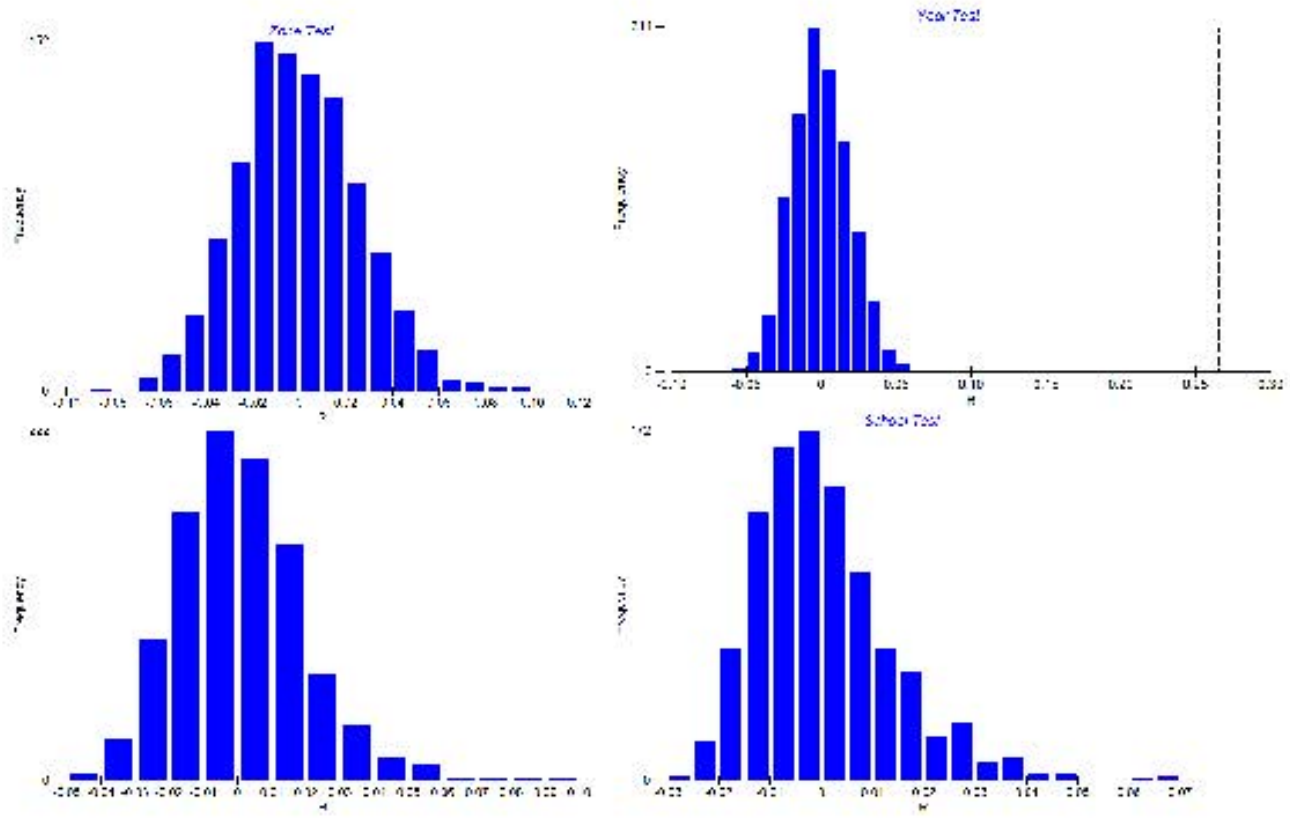

Figure 3.8: Single way ANOSIM test for factors: year, season, zone and school. R value depicted by the pale line on the x-axis on the graphs.

Table 3.2: Single way ANOSIM test results. Number of permutations: 999 (Random sample from a large number).

ANOSIM Year
Sample statistic (Global R): 0.265
Significance level of sample statistic: 0.1%
Number of permuted statistics greater than or equal to Global R: 0
ANOSIM School
Sample statistic (Global R): 0.016
Significance level of sample statistic: 11.4%
Number of permuted statistics greater than or equal to Global R: 113
ANOSIM Zone
Sample statistic (Global R): 0.104
Significance level of sample statistic: 0.1%
Number of permuted statistics greater than or equal to Global R: 0
ANOSIM Season
Sample statistic (Global R): 0.003
Significance level of sample statistic: 42.1%
Number of permuted statistics greater than or equal to Global R: 420

3.3.2 Species/sizes responsible for biotic groupings

The full result of the SIMPER analysis is given in Appendix: B and partially in Table 3.3 which describes the percentage similarities and dissimilarities calculated based on the contribution by species size-class over the years. The ANOSIM results have shown that Year and Zone are the two statistically significant factors. In this section, these two factors are analysed using SIMPER to see which species/sizes have contributed to holding these groups together. Table 3.3 examines the Year groups and Table 3.4 the Zone groups.

Several features can be highlighted from the SIMPER analysis; the main features are highlighted in Table 3.3. From 2005 to 2007, skipjack tuna have mainly contributed to the grouping, with adult skipjacks contributing to 77.45% and the remaining contributions by bigeye and yellowfin juveniles in 2005. The year 2006 showed skipjack adults to 56.37% and a mix of yellowfin adult and juveniles and bigeye juveniles. The share of skipjacks adults was lower (34.76%) in 2007 but still

higher than to the other two species, this is followed by yellowfin pre-adults.

Table 3.3: Simper anaylsis examining Year groups across all Zone group. Where B_juv: bigeye juveniles, B_pAd: bigeye pre-adults, B_Adt: bigeye adults, S_juv: skipjack juveniles, S_Adt: skipjack adults, Y_juv: yellowfin juveniles, Y_pAd: yellowfin pre-adults and Y_Adt: yellowfin adults. For the year 2005: Group 05, year 2006: Group 06, year 2007: Group 07, year 2008: Group 08, year 2009: Group 09, year 2010: Group 10 and year 2011: Group 11.

Group 05					
Average similarity: 38.26					
Species	Av.Abund	Av.Sim	Sim/SD	Contrib%	Cum.%
S_Adt	2.54	29.64	1.2	77.45	77.45
B_juv	0.43	3.08	0.54	8.05	85.5
Y_juv	0.5	2.83	0.29	7.41	92.91
Group 06					
Average similarity: 49.02					
Species	Av.Abund	Av.Sim	Sim/SD	Contrib%	Cum.%
S_Adt	9.09	27.63	1.81	56.37	56.37
Y_pAd	3.23	5.12	1.09	10.44	66.8
B_juv	2.96	4.9	0.9	10	76.81
Y_juv	3.72	4.89	0.66	9.98	86.78
Y_Adt	1.91	4.23	0.99	8.63	95.42
Group 07					
Average similarity: 48.11					
Species	Av.Abund	Av.Sim	Sim/SD	Contrib%	Cum.%
S_Adt	12.66	16.72	1.98	34.76	34.76
Y_pAd	5.85	8.26	1.37	17.17	51.94
B_juv	6.55	6.63	1.47	13.79	65.73
Y_Adt	4.96	6.41	1.08	13.33	79.06
Y_juv	5.47	5.04	1.36	10.47	89.53
B_pAd	3.86	3.9	0.94	8.11	97.64
Group 08					
Average similarity: 48.31					
Species	Av.Abund	Av.Sim	Sim/SD	Contrib%	Cum.%
Y_Adt	5.14	15.5	1.34	32.08	32.08
S_Adt	5.19	12.85	1.57	26.61	58.69
B_juv	3.39	5.61	0.84	11.62	70.31
Y_pAd	2.18	5.1	1	10.56	80.86
B_pAd	2.93	4.53	0.73	9.38	90.24
Group 09					
Average similarity: 30.29					
Species	Av.Abund	Av.Sim	Sim/SD	Contrib%	Cum.%
Y_Adt	2.69	15.61	0.83	51.54	51.54
S_Adt	1.71	5.4	0.61	17.84	69.38
S_juv	0.65	3.3	0.35	10.88	80.26
B_Adt	1.01	2.09	0.41	6.89	87.15
B_pAd	1.1	1.68	0.36	5.56	92.71
Group 10					
Average similarity: 31.91					
Species	Av.Abund	Av.Sim	Sim/SD	Contrib%	Cum.%
Y_Adt	2.49	21.35	0.98	66.89	66.89
B_Adt	1.48	6.82	0.72	21.38	88.27
Y_juv	0.47	2.24	0.27	7.03	95.3
Group 11					
Average similarity: 61.75					
Species	Av.Abund	Av.Sim	Sim/SD	Contrib%	Cum.%
Y_Adt	2.53	49.61	1.78	80.34	80.34
B_Adt	1.43	12.14	0.59	19.66	100

Interestingly in 2008, 2009, 2010 and 2011, yellowfin adults contributed most to similarity of the year groups, 32.08%, 51.54%, 66.98% and 80.34% respectively. These were followed by bigeye adults than skipjacks tuna. Of course, looking at the dissimilarities between the years; skipjack and yellowfin adults contribute to group differences in most cases (Appendix: B).

Comparing the species/size-class contribution in the recapture zones given in Table 3.4 and Appendix B shows that skipjack and yellowfin tuna contribute to abundance at higher percentages than bigeye. Zone A consisted primarily of skipjack adults and yellowfin juveniles (53.50% and 32.68%, respectively) with yellowfin adults contributing a smaller percentage. In zone B, yellowfin and skipjack adults contribute to 32.70% and 28.06% respectively, then there are smaller contribution from pre-adult yellowfin and bigeye juveniles. In zone C, major contributions were from skipjack (38.84%) and yellowfin adults (26.55%). Although in zone D, most of contributions was from skipjack adults (38.84%), bigeye and yellowfin tuna also presented a fair share, 15.48% bigeye juveniles, 15.16% yellowfin adults, 12.91% bigeye pre-adults and 12.36% yellowfin juveniles. Zone E has a high contribution of yellowfin adults (51.04%) followed by skipjack adults (35.95%). Comparing zone E to zone H, an inverse situation was observed, where skipjack juveniles make up to 39.39% to zone H and yellowfin adults 32.42%.

Table 3.4: Simper Anaylsis examining Zone groups across all Year group. Where B_juv: bigeye juveniles, B_pAd: bigeye pre-adults, B_Adt: bigeye adults, S_juv: skipjack juveniles, S_Adt: skipjack adults, Y_juv: yellowfin juveniles, Y_pAd: yellowfin pre-adults and Y_Adt: yellowfin adults. The zones are denoted as follows: Zone A: Group A, Zone B: Group B, Zone C: Group C, Zone D: Group D, Zone E: Group E and Zone H: Group H

Group B					
Average similarity:	45.72				
Species	Av.Abund	Av.Sim	Sim/SD	Contrib%	Cum.%
Y_Adt	5	14.95	0.98	32.7	32.7
S_Adt	7.27	12.83	1.06	28.06	60.76
Y_pAd	3.23	4.61	0.99	10.08	70.84
B_juv	3.31	3.92	0.82	8.58	79.42
B_Adt	1.54	3.48	0.48	7.61	87.03
Y_juv	3.18	2.94	0.63	6.43	93.45
Group C					
Average similarity:	32.72				
Species	Av.Abund	Av.Sim	Sim/SD	Contrib%	Cum.%
S_Adt	5.61	12.71	0.9	38.84	38.84
Y_Adt	3.62	8.69	0.74	26.55	65.39
Y_pAd	2.49	2.99	0.64	9.13	74.52
B_juv	2.24	2.33	0.55	7.13	81.65
B_Adt	1.03	2.16	0.39	6.6	88.25
Y_juv	1.92	1.78	0.41	5.43	93.68
Group D					
Average similarity:	49.27				
Species	Av.Abund	Av.Sim	Sim/SD	Contrib%	Cum.%
S_Adt	6.63	16.22	1.44	32.93	32.93
B_juv	3.82	7.63	0.95	15.48	48.41
Y_Adt	1.77	7.47	0.71	15.16	63.57
B_pAd	1.84	6.36	0.94	12.91	76.49
Y_juv	2.33	6.09	0.62	12.36	88.85
Y_pAd	1.76	4.67	0.98	9.49	98.33
Group E					
Average similarity:	54.14				
Species	Av.Abund	Av.Sim	Sim/SD	Contrib%	Cum.%
Y_Adt	1.22	27.63	1.06	51.04	51.04
S_Adt	1.36	19.46	0.72	35.95	86.98
Y_pAd	0.67	2.28	0.25	4.22	91.2
Group A					
Average similarity:	60.27				
Species	Av.Abund	Av.Sim	Sim/SD	Contrib%	Cum.%
S_Adt	3.84	32.24	2.1	53.5	53.5
Y_juv	1.59	19.69	0.71	32.68	86.18
Y_Adt	0.59	4.31	0.71	7.15	93.33
Group H					
Average similarity:	36.03				
Species	Av.Abund	Av.Sim	Sim/SD	Contrib%	Cum.%
S_juv	0.51	14.19	0.66	39.39	39.39
Y_Adt	0.61	11.68	0.35	32.42	71.81
S_Adt	0.99	4.25	0.5	11.79	83.6
Y_juv	0.26	2.99	0.35	8.31	91.91

The SIMPER analysis for school-type and seasons is shown in Appendix B.2 part two. Recaptures in FS were mostly contributed by yellowfin adults (41.21%) followed by skipjack adults 28.61%, whereas under FAD, skipjack adults contribut-

ing to 43.21% then yellowfin adults 22.73%. The seasons showed contribution to the similarity groups mainly by skipjack adults except for the NEM season (S1) where yellowfin adults were the major input (33.60%). Very small contributions from bigeye tuna are noted in most of the cases.

3.4 Discussion

Cluster analysis shows that the multivariate relationships of species/size class with year, zone, school (FS vs FAD) and season are complex, and it is difficult to see clear patterns in the dendrogram or the multidimensional scaling graphs. However, non-parametric analysis of similarities (analogous to ANOVA) show clearly that there are highly significant differences among years and among zones, whereas school type and season are not significant factors in the multivariate groupings. The SIMPER analysis confirms that skipjack tuna were the most abundant species in catch records by fishing gears. In the years 2008, 2009, 2010 and 2011 the catches consisted of primarily yellowfin adults. One plausible reason would be that most of recaptures for years before 2008 were mainly skipjacks. Hence, recoveries of tagged skipjacks would decline over the years while tags from bigeye and yellowfin tuna would continue to be recovered. Chassot et al. (2012) noted that the fishing effort increased until 2007 and then reduced significantly thereafter. Most of the tag and release done in zone B were skipjack tuna and, SIMPER analysis shows that the percentage contribution of skipjack adults in zone A was high. Yellowfin adults moved to other regions of the Indian Ocean (mostly towards Seychelles) while most skipjack tuna moved to the northern part of the Indian Ocean. Furthermore, most of the recaptured yellowfin that were tagged in Tanzanian waters have shown large scale movement to zones A and H. Zone D seems to be an area where the variety of species and size-class is important compared to the other demarcated zones. The SIMPER analysis also shows that the yellowfin influence is important in zone E, the Mozambique Channel. Fraile et al. (2013) in their study identified the Mozambique Channel as being a potential nursery ground in addition to the Seychelles region (zone C), which was quite distinctive in comparison.

It is not surprising that under FADs most of that catches were contributed by

skipjacks and small species. Marsac et al. (2000) suggested the potential effect of FADs on migration patterns and the size-classes of tuna that agglomerate underneath them; the consequences of FADs such as long periods of association to FADs, shift in natural movement patterns of tuna, and altering growth and mortality of tuna were discussed with plausible reasons for these effects.

The impact of environmental factors on distribution of tuna in the Indian Ocean has been well documented (Hynd, 1969; Sund et al., 1981; Tewkai and Marsac, 2010). Most of the studies showed that links with temperature and biomass distribution influence movement patterns of tuna and other migratory species (Sund et al., 1981). For instance, Fonteneau et al. (2008) stated that purse seiners generally use SST, phytoplankton and altimetry data to locate potential fishing grounds. This information also forms the fundamental basis for analysing trends and modelling the habitats of the marine top predators (Marsac and Blanc, 1998; Maury et al., 2007; Tewkai and Marsac, 2010).

3.5 Conclusions

The ANOSIM analysis reveals that year and zone were significant factors compared to school and season. It is interesting to note that the few variables (only eight categories of tuna size-class) played an important role in demarcation of assemblages. SIMPER analysis shows areas where abundance of species/size-class pre-dominance could be demarcated. This approach requires more diversity of species for a better response. Nonetheless, it did show small particularities in terms of abundance species by size class in relation to four abiotic factors. The multivariate tests show community structures influenced to some extent by annual variability and geographic zone. Seasonal spatial stratification showed that in some regions it enhances the agglomeration of certain species by size-class. The relationships between species and environmental factors such as sea surface temperature and Chl-a will be analysed by more conventional univariate methods in subsequent chapters.

Chapter 4

Estimating survival and recovery probabilities of tuna using tag and release surveys

4.1 Introduction

Understanding population dynamics of tuna is essential for proper stock assessment and its management. Tag and release surveys have often been applied to understand the population dynamics to derive estimates of abundance and mortality. With regard to tagging of commercial fisheries, most of the surveys have been focused on estimating growth rates, movement patterns and stock clusters. Polacheck et al. (2010) noted that mark and recapture experiments have been the main method for studying population dynamics in the wild dating back a century. Their main objective was to study the efficiency of three basic approaches of tagging experiments by conducting single tagging methods: Petersen, tag-attrition and Brownie. The Petersen approach has been mostly used in experimental context where sampling is conducted preceding tagging. In this approach, tag returns bear no uncertainty which is not the case when carrying out fisheries tagging. The tag-attrition approach is based on the possibility of predicting tag returns over time from a single tag release cohort, depending on natural and fishing mortality rates, while the Brownie approach predicts tag returns from each of the tag release cohorts. Polacheck et al. (2010) developed integrated methodologies of these three approaches

combining Petersen/tag-attrition and Petersen/Brownie. It was concluded that a combination of Brownie and Petersen methods was the most suitable approach in terms of range of parameters that could be estimated.

Stock assessment requires an estimate of abundance and fish mortality among other parameters. Most surveys of stock assessment are indirect estimates of fish stocks usually based on commercial fish landings. Polacheck et al. (2010) points out that the mark and recapture approach is key in understanding population dynamics as it gives direct estimates of essential parameters for stock assessment. The RTTP-IO tagging experiment was independent of commercial fishing and data gathered was very pertinent for the purpose of understanding tuna stock dynamics in the Indian Ocean.

Survival rate can be represented by the proportion of species surviving a particular age group in a population over a period. To estimate survival probabilities or rates, a number of statistical tools are available for land based species with a large amount of documentation, but Polacheck et al. (2010) noted that multiple recapture experiments are not commonly applied to commercial fisheries in contrast to land based experiments, where it is possible to conduct multiple tagging. They further argued that most tagging experiments have been conducted without any special consideration of the estimation method to be applied. In their work, they enumerated a number of assumptions to be considered when analysing tag and release surveys. Among the most important ones are: thorough mixing of tagged fish within the wild untagged population, negligible tag loss, survival and recapture rates not being affected the tagging operation. Finally, time-at-liberty can have strong implications so it needs to be recorded accurately, bearing in mind the time scale of the estimation model.

One of the key questions of the RTTP-IO tag and recovery programme was to estimate the survival rates of the three species of tropical tuna (skipjack (*Katsuwonus pelamis*), bigeye (*Thunnus obesus*) and yellowfin tuna (*Thunnus albacares*)) in the Indian Ocean. Survival rates can be defined as the probability that a species of a particular age group will survive to the next age class or time period (White and Burnham, 1999; Pollock et al., 1989). In order to analyse the survival and eventually, the mortality probability of tuna tagged and released through the RTTP-IO

programme and small scale tagging projects, three approaches were adopted: (1) The MARK recovery model (White and Burnham, 1999), (2) Daily survival rate and using (DeMaster and Drevenak, 1988; van der Toorn, 1997), 3) applying the Kaplan-Meier estimate of mortality rates (Pollock et al., 1989). Applying these estimation models in addition to the assumptions highlighted above, it is assumed the population dynamics of the three tuna species are interrelated to one another. This means that they are likely to share the same environment with similar size range and migrate together in their respective swimming schools.

4.2 Methodology

4.2.1 Data

The RTTP-IO tagging operations started in May 2005 and continued until September 2007, whereas the small-scale tagging programme began before the RTTP-IO on a regional basis. Both programmes generated a huge combined dataset, 219,149 tags released and 34,294 returns (tuna recaptured and tag information reported back) for the three species combined. It was logistically not possible to run the whole dataset in all the three models proposed above. Consequently, in order to alleviate this problem depending on the analysis performed, the dataset had to be truncated to manageable sizes for each of the analysis.

The program MARK (White and Burnham, 1999) was used to estimate survival and recapture probabilities of tagged and released tuna in the Indian Ocean. After a number of failed runs during data processing, tuna tagged and released in Tanzania were selected from the dataset as a test case to evaluate how best MARK models fit the dataset. The RTTP-IO formed the major part of the dataset accounting over 80% of the whole dataset merged. In an ideal study, the sampling periods and recovery periods would be designed to occur at regular time intervals and cover the same areas through the sampling period. In the case of a commercial fishery, such optimal sampling methodology could not be applied for practical and logistical reasons. As a consequence, the RTTP-IO tagging frequency showed irregularities in the number of tuna tagged over time (Fig. 4.1).

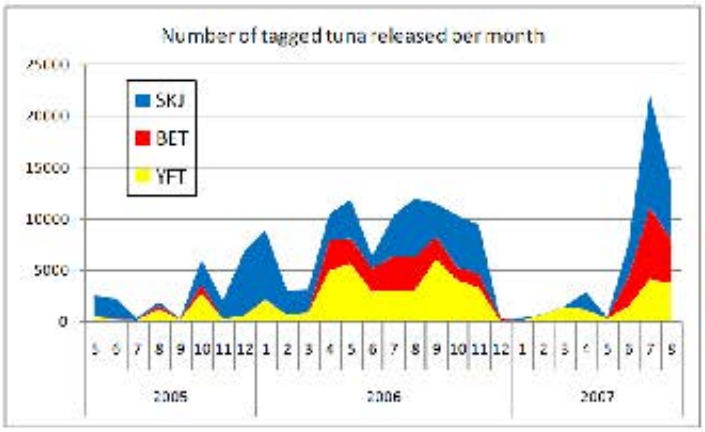

Figure 4.1: Monthly tuna tagging distribution by species from May 2005 to September 2007 (Hallier, 2008). Where SKJ = Skipjack, BET = Bigeye and YFT = Yellowfin.

Success of the RTTP-IO programme was dependent on the degree to which tuna fishing vessels would cooperate in the aftermath of tagging. The RTTP-IO carried out an awareness campaign concerning the tagging programme in countries bordering the Indian Ocean as well as with European and Japanese fleets exploiting Indian Ocean tuna. Theoretically, fishing vessel would report back recovery of tagged tuna to the Indian Ocean Tuna Commission (IOTC) with the necessary information. Although the return rate was high for purse-seine fisheries (nearly 80% of the total recoveries), reporting levels were low for other fishing gears (Table 4.1). The data were analysed from 2005 to 2012 and many recoveries occurred in 2006 and 2007.

Table 4.1: Number of recoveries of tuna by fishing gear and catches (in tonnes) for bigeye, skipjack and yellowfin (Unk = Unknown, NA = Not available). The numbers represent raw data.

Fishing gear	No of recoveries	Percentage recovery	Tuna catches: 2005-2012 (IOTC-2014-SC17)
purseseine	26865	78.34	2475901
Gil net	284	0.83	422532
Hand line	261	0.76	363207
Longline	398	1.16	1206159
Pole line	6289	18.34	971444
Rod & reel	2	0.01	NA
Troll line	121	0.35	157662
Unk	73	0.21	NA
Other	1	0.00	1694926
Total recoveries	34294	100.00	7291831

Carruthers et al. (2014) identified reporting rates as a crucial factor in estimating exploitation rates along with probabilities for natural mortality, tagging mortality and tag shedding. In their paper, they computed the reporting rates for 13 fleets operating in the Indian Ocean based on the RTTP-IO and the small scale tagging programme dataset (Table 4.2). The results showed high reporting rate for the European (EU) purse-seine fleets compared to other fishing vessels exploiting the Indian Ocean. There are several factors given to explain the high reporting rates which included the sensitivity based on categorisation and the publicity campaigns.

Table 4.2: Posterior probability density estimates of tag reporting rate of 13 fleets. Where EU: European, ALL: all countries, ZAF : South Africa, ESP : Spain, CHN: China, JPN: Japan, FRA: France, TWN + SYC: Chinese Taipei and Seychelles, OTH: other flags, PS: Purse-seine, BB : Bait Boat, HAND: Handline, LL: longline, GILL: Gill net, OTH-W/E: All gears operating in western/eastern Indian Ocean (adapted from Carruthers et al. (2014).

Reporting rate %		Mean	SD
Flag	Gear		
EU	PS	93.64	0.58
ALL	BB	25.85	0.50
ALL	HAND	18.78	1.60
ZAF	LL	16.43	4.95
ESP	LL	12.69	4.60
ALL	GILL	12.02	0.88
CHN	LL	7.25	1.27
JPN	LL	4.22	0.56
FRA	LL	3.77	1.38
ALL	OTH-W	3.62	0.25
TWN + SYC	LL	3.49	0.38
OTH	LL	1.94	0.31
ALL	OTH-E	0.01	0.00

4.2.2 Survival estimate approach I: MARK recovery model

The first approach was to explore MARK recovery models, to estimate survival and recovery probabilities of the tagged and released tuna. This was based on two types of parameterization models: (1) Brownie model (Brownie et al., 1985) and (2) Seber (S and r) model (Seber, 1970). Both of the models deal with dead or alive probabilities of open populations, the difference is the fate of the tagged tuna. Unlike several encounters of conventional tagging surveys for birds and mammals, the application of the Brownie model for fish is based on only one tagging and one single recovery event (if recaptured and reported) for each tuna tagged. Only three outcomes can be envisaged: (i) the tagged tuna survives the year, (ii) the

tag is recovered and (iii), it dies from natural mortality or permanently moved to another location (Fig. 4.2). The parameters associated with the 3 outcomes are S the probability of survival, K the tuna is recaptured by fishermen and *(1-S-K)* the probability that it dies from 'natural' causes (Fig. 4.2(a)). In addition, the tag on the recaptured tuna can either be found and reported to the IOTC denoted by λ or, tag was not found/not reported back *(1-λ)*. From the recaptures, the information that can be retrieved from reported recovered tuna is the product $F = K\lambda$ referred as the recovery rate but the individual part of K and λ cannot be resolved directly. In general, the fate schematic reduces to S, F and *1-S-F* (Fig. 4.2(b)).

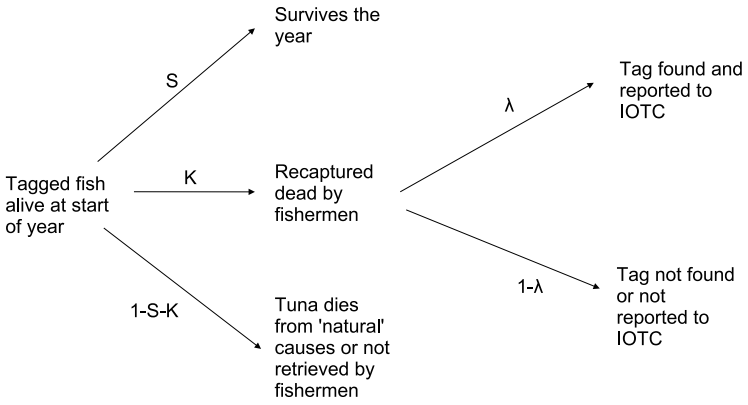

(a) Fate diagram of tuna.

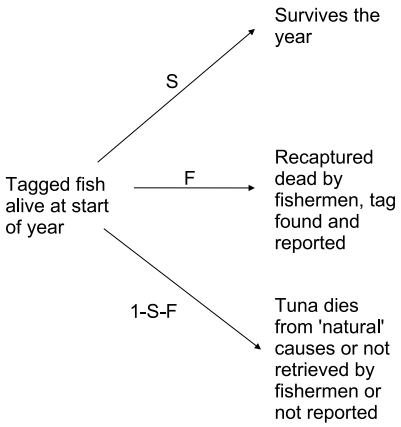

(b) Fate diagram product of tuna.

Figure 4.2: Possible fate diagram of a tagged tuna (Brownie et al., 1985).

Hence, from the survival and recapture parameters, the model structure (Table 4.3) is built over the years assuming that survival, recoveries and reporting are time specific and independent of the year of tagging (Brownie et al., 1985). From the model structure, f is the overall recovery rate and S_1 and f_1 are the respective survival rate and recovery rate for the first year of tagging (tagged or released referred to

as banded in Table 4.3) where l is the number of years over which recoveries are registered and k is the number of years over which tagging was effected.

Table 4.3: Model structure of expected recoveries. Banded = released (Brownie et al., 1985).

Year banded	Number banded	Year of recovery				
		1	2	3	4	$\ell = 5$
1	N_1	$N_1 f_1$	$N_1 S_1 f_2$	$N_1 S_1 S_2 f_3$	$N_1 S_1 S_2 S_3 f_4$	$N_1 S_1 S_2 S_3 S_4 f_5$
2	N_2		$N_2 f_2$	$N_2 S_2 f_3$	$N_2 S_2 S_3 f_4$	$N_2 S_2 S_3 S_4 f_5$
$k = 3$	N_3			$N_3 f_3$	$N_3 S_3 f_4$	$N_3 S_3 S_4 f_5$

In the Seber (S and r) model, the term r is the recovery probability that a dead tuna is reported during the period of tag and recovery (note that recovery or encounter is a simultaneous process, explained below) and the death of tuna not only due to fishing practice only (Fig. 4.3). Equation 4.1 shows the relation of the Seber parameterization to that of Brownie's. The subscript i are the years over which the tag and release period, $i = 1$ for the year one and $i = 2$ for year two and so forth. It is important to distinguish the recovery term r_i is different from the Brownie model recovery probability f_i . The recovery parameter in the Brownie model is the probability that the tuna is fished, retrieved and reported between the tag and release cohorts, where as in the Seber model, death is not necessarily related to tuna being reported. Therefore, a tagged and released tuna either survives (S) or dies in the following way: recovered and reported implying probability *r(1-S)* or dies and not recovered or not reported, implying a probability of *(1-S)(1-r)*.

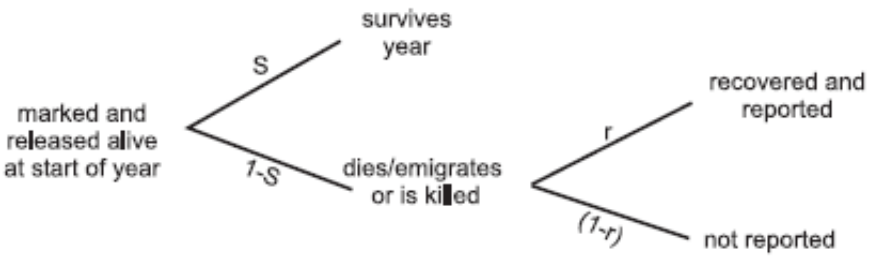

Figure 4.3: Fate diagram based on Seber model.

$$r_i = \frac{f_i}{1 - S_i} \tag{4.1}$$

MARK requires a system of individual encounter history (catch history in this case) which simply says whether the marked individual is alive (L) or dead (D). This would be translated into a series of 1's (alive) and 0's (dead or not spotted again) over time for each tagged individual. As an example an encounter history of 1011000 (i.e., LDLLDDD), would imply: marked and release first time, not spotted second time, spotted third and fourth time and not spotted or dead for the last three time steps. The time steps can be days, months, years or seasons; depending on frequency of the repeated surveys. In the present case, the encounter history for both Brownie and Seber models are in the format of LDLDLDLD, which is a double entry system at each event recording whether the species is live or dead (LD). At the first encounter, the record will show 10 (live = 1, dead = 0). The second encounter will be 10, if species is still alive and the encounter history will be (1010) and if dead, the record will be 01 (live = 0, dead =1) with an encounter history 1001. Therefore, an encounter history of (LDLDLDLD) LD LD LD LD is interpreted as 4 events where tagging and recovery are both carried out, each event is a 'double' recording of live 'L' encounter and dead 'D' encounter. Based on the model structures (Table 4.3) elaborated above, the MARK program needs to reconstitute the cohorts of survival and recapture probabilities over the encounter history. Therefore, each survival probability from the first cohort and subsequent recaptures and so forth, are indexed in a PIM (Parameter Information or index Matrix, Fig. 4.4).

Considering the whole Tanzanian tag and release dataset from the first date of tagging to the last recovery, it was possible to build a catch history on a daily basis for each individual. However, because processing the data on a daily basis was too bulky and impossible to manage in MARK, the time steps were set to 3 months. Thus, an individual tagged on particular date would have a span of 3 months to be recorded as marked or recaptured. It should be noted that, an individual can only have at maximum two 1's in its catch history as it was only marked and recaptured once and not available again for recapture. The data was grouped by school-type in which tuna were caught. Three groups were designated: free schools (FS), fish

aggregating devices (FAD) and unknown (Un). Hence, for the each of the group, the survival (S) and recoveries (f) structure is constructed. The output represents combinations of models where time, group and time/group dependence are evaluated based on time steps on a 3-month basis, 32 occasions and 3 groups.

4.2.3 Survival estimate approach II: daily survival rate

The second approach was to calculate survival rates based on the probability that the tuna alive on day d, survives to day $d+1$ (DeMaster and Drevenak, 1988; van der Toorn, 1997). The Daily Survival Rate (DSR) is given as:

$$DSR = 1 - \frac{\sum_{i=1}^{k} Y_i}{\sum_{i=1}^{k} X_i} \tag{4.2}$$

where k is total number of tuna tagged, Y_i is 1 if tuna was reported over a defined period and 0 if tuna assumed to be still alive and X_i is the time-at-liberty of the tuna i over the defined period of time. Following the daily survival probability, the Annual Survival Rate (ASR) is calculated as:

$$ASR = DSR^{365.25} \tag{4.3}$$

Two main assumptions are considered in this approach (DeMaster and Drevenak, 1988). First, death (i.e., recapture) of individuals are independent of each other implying that the time-at-liberty for each tuna is different and secondly, that there is a constant daily-survival probability. Considering these two assumptions and that a tuna can either survive or be recaptured (dead), therefore each day of time-at-liberty is a binomial event. Hence, the probability of a tuna surviving n days is the daily survival rate to the power of n and probability of death over that time-at-liberty will be binomial too. For this approach, two time periods are defined: one period considering the whole duration of tag and recovery (i.e., the whole RTTP-IO dataset) and a second period, considering only tuna tagged and recovered during 2006 and 2007. Most of the recoveries were made in 2006-2007; this allows comparison with the whole duration of the tag and recovery process.

4.2.4 Survival estimate approach III: Kaplan-Meier estimate

The Kaplan-Meier estimate has been particularly used in the field of medicine to study survival probability of patients treated for illness which may lead to death or recovery. Although, this approach has been primarily applied in medical field, it has been used to study the probability of survival of species through tag and recapture (Marçalo et al., 2010; Capello et al., 2012; Hutchinson et al., 2015). The survival package in R software (Team, 2015) uses a multi-state approach to estimate survival probability among which is the Kaplan-Meier estimate. This methodology is best suited to the present dataset with tuna tagged at the beginning of a time step at the start of the tagging operations and it is either recovered (dead) or not. It is flexible in the sense that it allows new entries to be accommodated after the tagging operation has started (Pollock et al., 1989) and to take into account tuna that were not recovered.

The survival function (S_t) is the probability of a tuna in the population surviving time t from the start of the tagging. Therefore, taking discrete time steps as the tuna is recaptured (death) would give a non-parametric maximum likelihood estimate (MLE) estimator of the S_t. Suppose that the study starts at t_o and the survival probability S_o is equal to 1 at the beginning for a tagged individual, thus, the survival estimate can be calculated based on survival time of each individual from 1 to n (t_1, t_2, t_3 ,..., t_n). Therefore, the Kaplan-Meyer estimate of the survival probability S at time t_i (Eq. 4.4) and the variance (Eq. 4.5) is given by the following formula:

$$S(t_i) = \prod(1 - \frac{d_i}{r_i}) \tag{4.4}$$

$$var(S_t) = (S_t)^2 \sum_{i=1}^{t_i}(\frac{d_i}{r_i(r_i - d_i)}) \tag{4.5}$$

where d_i is the number of individuals recaptured (death) at time t_i and r_i is the number of tagged individuals at risk (i.e., who have not experienced the event). Hence, the probability of surviving t_o to t_1 is estimated by $S(t_1) = 1 - d_1/r_1$. Similarly, the probability of surviving from t_1 to t_2 is $1 - d_2/r_2$ and $S(t_2)$ is the given by $(1 - d_1/r_1)(1 - d_2/r_2)$. For the purpose of this survival analysis, survival curves were analysed based on the time-at-liberty and on two factors: 1) species and 2)

school-type. Note that the survival measured here reflects the effect f, and the total mortality Z, which is the sum of the natural (M) and fishing (F) mortality.

4.3 Results and Discussion

4.3.1 Brownie model

As mentioned above, the data were classified into three categories of school-type or fishing mode: Free School (FS), Fish Aggregating Devices (FAD) and Unknown (Un). The first model run takes into consideration time and group effects for both survival and recapture. After calculating the survival and recapture estimates of the first model, the subsequent models are fitted by altering the time and group effects thereby testing the time dependent and independent models and likewise testing for group effects (Tab. 4.4).

The Brownie parameterization fits the first model with full time dependence considering group effect for survival and recapture (*S(g*t)f(t)PIM*) where S: survival estimate (rate), g: group effect, t:time, f: recovery or recapture estimate (rate), and PIM, the parameter index matrix. Based on the first model analysis, different candidate sub-models are fitted to be compared with one another. The table presents the combination of models and the effect for which it was computed (first column in table). For example, the model *S(g*t)F(.)PIM* means that survival probability estimate was considered with the time dependent group effect (fishing mode), while in the probability estimate of recovery, the group effect was not considered and time was constant. Likewise, a number of interactions were tested for each model computed. The model names are described by (i) the corrected Akaike's Information Criterion (AICc), (ii) Delta AICc (the difference in the value of the AICc from the model with the lowest AICc), (iii) the number of estimated parameters, and (iv) the model deviance. The relevance of these factors is that they help to evaluate the different candidate models and to choose the best one to fit the data. Hence, the AIC is a criterion indicates that the most parsimonious model: the model with the lowest number of parameters catering for variation in the dataset.

The best among the candidate models is therefore described by the lowest AICc value. The corrected AICc was introduced because the AIC itself may not be very

effective when there are too many parameters compared to the sample size. To account for differences in sample sizes, a sample bias adjustment was taken into account hence the corrected AICc (Cooch and White, 2006). Given that there are several candidate models, standardisation is required to compare the models which have close AICc values. Akaikie weights give an approximate likelihood between close AIC models. The 'Model likelihood' given in the table, is not the likelihood value used to calculate the AIC but is the AICc weights of the model of interest divided by the best model. Hence, the model with highest weight denotes the best model.

Table 4.4: Results of generated models, Brownie parameterization shown to 2 decimal places, S is the survival probability, f is the recovery rate and PIM is the parameter index matrix. The letters g and t imply group and time dependent parameters respectively. The dot (.) implies that it was considered to be constant for the effect tested. Models have been ranked from best to worst according to the Akaike weights. Note the (F) in the model was calculated arbitrarily in MARK.

Model	AICc	Delta AICc	AICc Weight	Model Likelihood	Par
{S(g*t) f(g*t) PIM}	17130.64	0.00	0.50	1.00	6.00
{S(t)F(t)}	17130.64	0.00	0.50	1.00	6.00
{S(t) f(g*t) PIM}	17257.04	126.41	0.00	0.00	69.00
{S(g*t) f(t) PIM}	21874.38	4743.70	0.00	0.00	4.00
{S(g*t) f(g) PIM}	23595.17	6464.50	0.00	0.00	6.00
{S(g*t) f(.) PIM}	29856.47	12725.00	0.00	0.00	4.00
{S(t) f(g) PIM}	38893.92	21763.00	0.00	0.00	7.00
{S(t) f(t) PIM}	48170.89	31040.00	0.00	0.00	11.00
{S(g) f(t) PIM}	48188.92	31058.00	0.00	0.00	20.00
{S(t) f(.) PIM}	63015.59	45884.00	0.00	0.00	8.00
{S(g) f(.) PIM}	71141.25	54010.00	0.00	0.00	2.00

The best models were *S(g*t)f(g*t)PIM* and *S(t)F(t)*. Overall it means those two models (very small difference between models: 0.001) explains best the variation in the data. Appendix A.1 gives the parameter estimates for the survival S and recovery f for the first model *S(g*t)f(t)PIM*. The survival estimates and recapture or recovery probabilities were estimated over the 93 intervals on a 3 months' basis, where the survival and recapture are recorded for each individual during the period analysed. This corresponds to parameters 1 to 93 for survival parameters and 94 to 188 for recovery probabilities, respectively. It should be borne in mind that there are 32 occasions and 3 groups considered on a 3 months' basis. Therefore, the

actual time span over which the model runs is 8 years. Hence, if the first interval: parameter 1, first group (Fig. 4.4) is considered all the tuna that were recorded will be accounted for this event. Of course, a tuna tagged in subsequent events, will have a catch history record of 00 (live:0 , dead:0) at the first interval until it is tagged (10) and subsequently recaptured (01) after a series of intervals of 00's (this can be interpreted as the time-at-liberty).

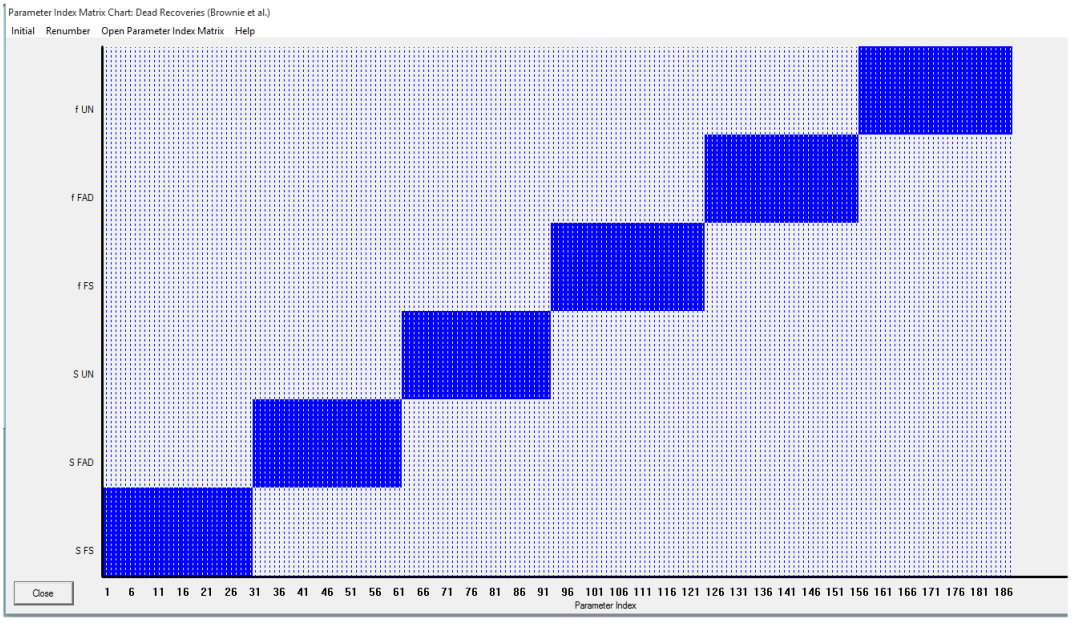

Figure 4.4: Parameter Index Matrix (PIM) for tuna tagged in Tanzanian waters under the Brownie parameterization. The x axis represents the 189 parameters for the 32 encounter occasions of the 3 groups on the double recording system for survival (S) and recovery (f).

Figure 4.5 shows the variation of the survival probabilities for the period of study. The survival estimates quickly rise to 1 and stabilises to that level with a few dips. Since Brownie parameterization takes into account the catch history of all the recorded tuna and it evaluates the survival and recapture from the first interval and subsequent intervals until the last interval, the estimate is likely to rise to 1 as there were more taggings than reported recaptures. The model therefore assumes that tuna survived the years. Similarly, Fig. 4.6 gives the estimates for the recovery probabilities staying at one and later dropping to 0.5 on average. The Brownie

model shows survival probability stabilising at one as a result of recoveries not being sufficiently large over the intervals. Taking into account that the reportings of tuna were low compared to the number tagged, the models estimates tuna surviving for years as the time-at-liberty of reported tuna was long. If there had been regular reporting, the model would have given a realistic estimate of the survival rate declining with time. As a result of irregular reporting and few recoveries, the model's estimate of the confidence intervals varies, in a few instances with large variability (1-0) and at other instances, very little variability barely visible in the figure. As estimates of recovery probability and output from the Seber model are presented further below (Fig. 4.6), it is noticed that the estimates of the confidence interval improves.

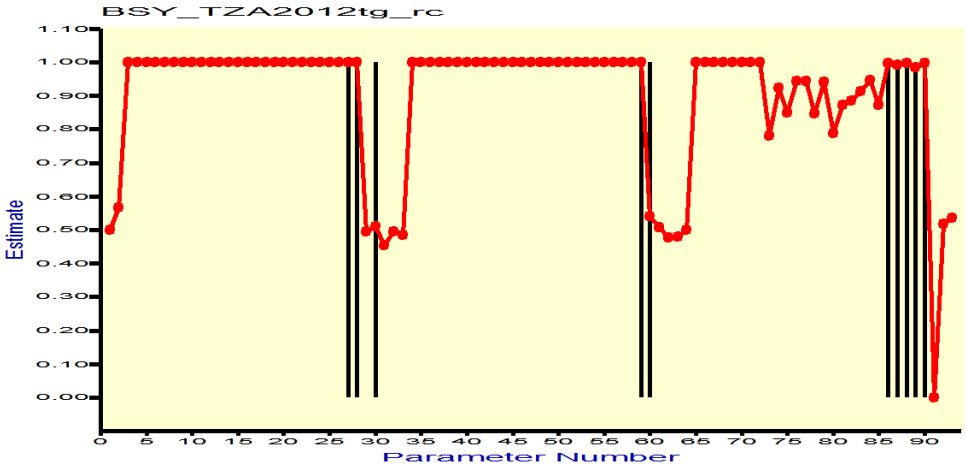

Figure 4.5: Estimated survival probability (S) in red and corresponding 95% confidence interval in black for tuna tagged in Tanzanian waters under Brownie parameterization. The x axis represents the 93 time intervals for S over 32 occasions for 3 groups. For most of the points, the confidence interval is too small to be visible, while it covers the whole range (0 to 1) in other sections of the series.

Estimated survival probability (S) in red and corresponding 95% confidence interval in black for tuna tagged in Tanzanian waters under Brownie parameterization. The x axis represents the 93 time intervals for S over 32 occasions for 3 groups. For most of the points, the confidence interval is too small to be visible, while it covers the whole range (0 to 1) in other sections of the series.

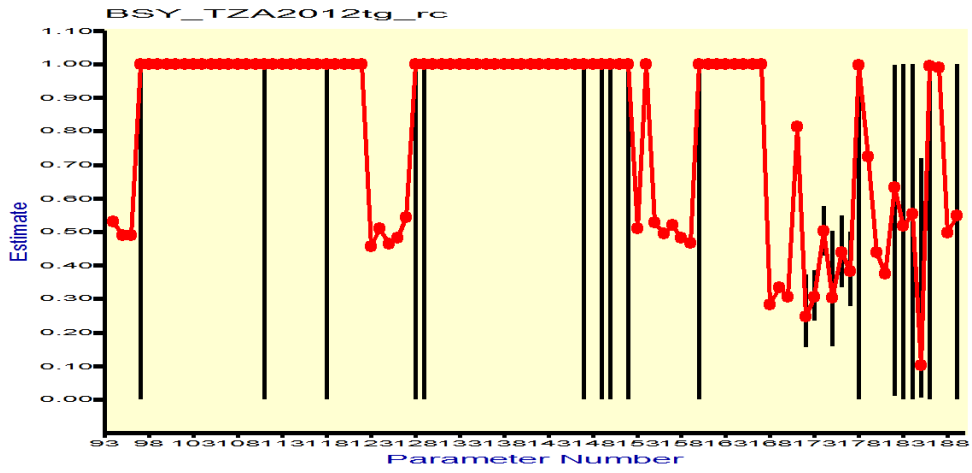

Figure 4.6: Estimated recovery (f) probability in red and corresponding 95% confidence interval in black for tuna tagged in Tanzanian waters under Brownie parameterization. The x axis represents the 93 time intervals for f over 32 occasions for 3 groups. For most of the points, the confidence interval is too small to be visible, while it covers the whole range (0 to 1) in other sections of the series.

4.3.2 Seber model

From the result runs, of the Seber (S and r) models (Table 4.5), the model *S(t)r(.)PIM* best explains the variation in the data with the lowest AICc value, survival estimates were time dependent and the recovery estimates were constant as opposed to a fully time-dependent model *S(t)r(t)PIM*.

Table 4.5: Results of generated models, Seber parameterization.

Model	AICc	Delta AICc	AICc Weight	Model Likelihood	Par
{S(t) r(.) PIM}	10477.789	0.00	1.00	1.00	28.00
{S{t}f{t}	10529.781	51.99	0.00	0.00	53.00
{S(t) r(t) PIM}	10529.781	51.99	0.00	0.00	53.00
{S(.) r(.) PIM}	11720.818	1243.00	0.00	0.00	2.00
{S(.) r(t) PIM}	11771.534	1293.70	0.00	0.00	27.00

Figure 4.7 shows the survival estimate the first model. The survival estimates correspond to parameters 1 to 32 and recovery probabilities (time independent) corresponding to parameter number 33. Detailed information is given in Appendix A.2, specifically, the parameter estimates for the survival *(s)* and recovery *(r)* for

the first model *S(t)r(.)PIM* using the Seber parameterization. The Seber *(S and r)* model showed a high survival probability with a decreasing trend over time compared to the Brownie parameterization. Considering the recoveries, the estimates with a time dependent recovery do not fit the data in the Seber parameterization. The Seber model works under the assumption that recaptured individuals are reported within the set tag and recovery periods, while in the RTTP-IO project, reporting by fishing gears went beyond the tag and recovery period.

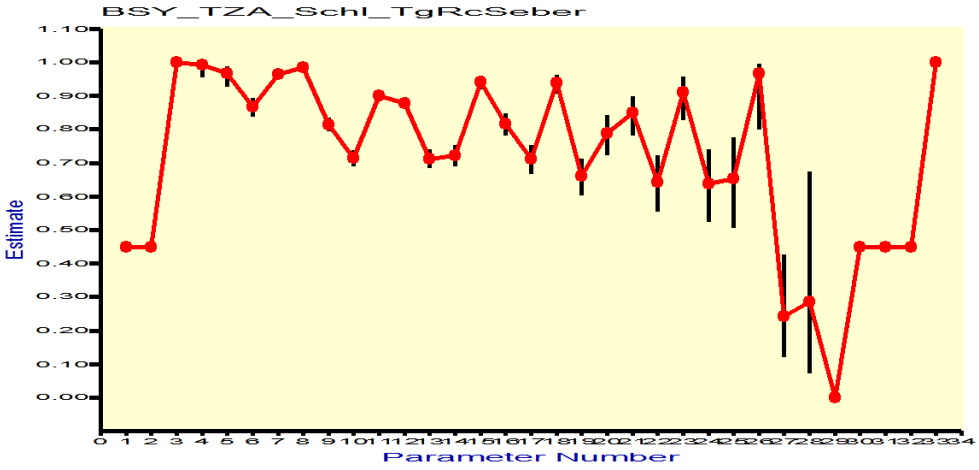

Figure 4.7: Estimated recovery probability in red and corresponding 95% confidence interval in black for tuna tagged in Tanzanian waters, Seber parameterization.

4.3.3 Daily survival rate

The daily survival probability was near 0.99 (at 2. d.p) for 2006, 2007 and all the years in the dataset (Table 4.6). Considering the ASR, the calculated probabilities showed small variations between the years and through all the years combined.

Table 4.6: Estimated daily (DSR) and annual survival (ASR) probabilities.

	2006	**2007**	**All years**
DSR	0.99	0.99	0.99
ASR	0.82	0.84	0.97

The daily approach for survival probabilities resulted in high values, almost 1

calculated on daily basis and the annual survival probabilities were still strong, over 0.8. The reporting period were limited to 365.25 days for 2006 and 2007 while the for all the years combined, it was calculated from the first tagging date to the last recovery date of the dataset (i.e, from 23^{rd} March 2002 to 28^{th} May 2012). A plausible explanation for the high values is that the number of recoveries was not high enough for a proper survival estimate. Another point is that the lapse of time between tag-release and the recovery was irregular.

4.3.4 Survival estimate: Kaplan-Meier estimate

Survival curves of the three species are shown in Fig. 4.8 for comparison. The x-axis gives the time-at-liberty and the y-axis gives the survival probability. It can be observed that among the three species, bigeye has highest survival probability, followed by yellowfin and finally skipjack. In order to compare the curves statistically, a log rank test was carried out which shows that the survival curves were significantly different for the three species (p-value = 0.00 (2 d.p.) with log rank test, bigeye, skipjack, yellowfin, refer below, Table 4.7).

Table 4.7: Time-at-liberty and species log rank test. p-value = 0.00 (2 d.p.)

	N	Observed	Expected	(O-E)^2/E	(O-E)^2/V
Bigeye	283	283	468	73.1	112.8
Skipjack	507	507	211	414.7	529.7
Yellowfin	657	657	768	16	34.5
Chisq= 555 on 2 degrees of freedom, p= 0					

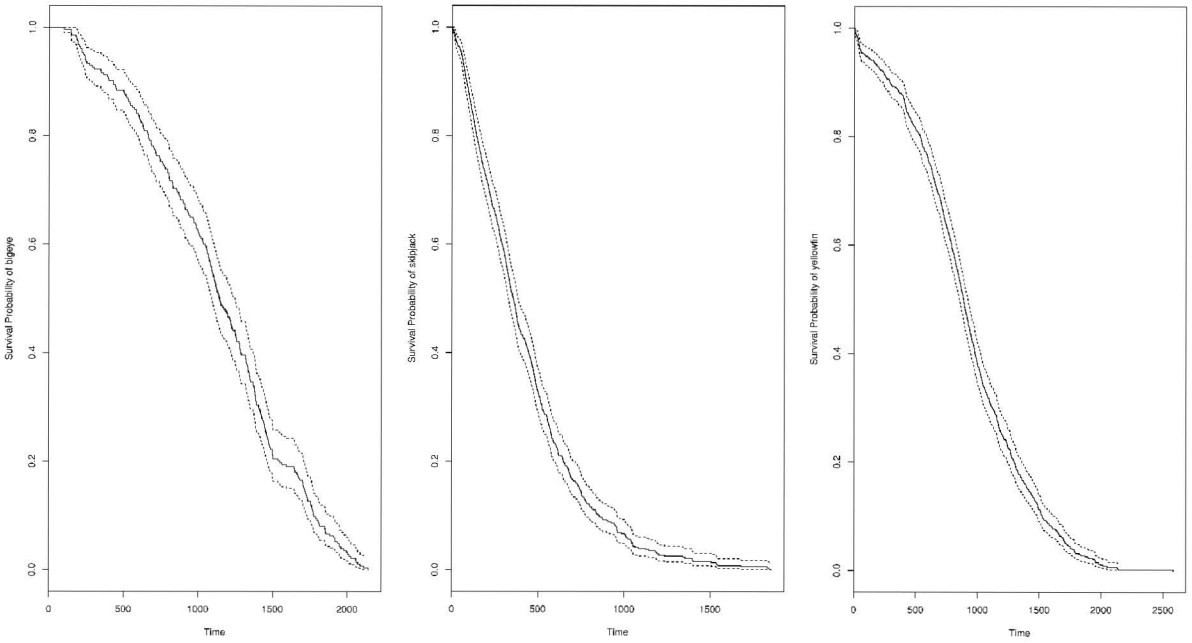

Figure 4.8: Survival curves of bigeye, skipjack and yellow. Time = time-at-liberty (days). Dotted lines: 95% confidence interval.

Similar analyses were carried out to estimate the survival probability with respect to school-type. The data were categorised by the FADs and FS (see output of log rank test below, Table 4.8). From Fig. 4.9, FS tuna show a higher survival probability than tuna which were associated with FAD. The log rank test show that the survival curves are significantly different for the two school-type (p-value = 0, with log rank test).

The estimates of longevity of tropical tuna found in the literature are 11 years for bigeye (Solovieff, 1970), 9 years for yellowfin (a single reference cited in Fishbase: Altman et al. (1962)) and 7 years for skipjack (IOTC, 2014). The longevity estimates based on the RTTP-IO and inferred from the Kaplan-Meier method allows revisiting those values.

The total mortality rate (Z) per year estimated from the survival curves are 0.4 for bigeye, 0.5 for yellowfin and 0.8 for skipjack. Using those rates, the 99% of the cohorts vanishes at 11.5, 9.2 and 5.7 years respectively. However, this can be refined by applying the shedding rates by species presented in Chapter 2 that allow correcting the population size at time intervals (as shedding rates introduce

an apparent mortality). Thus, the estimated Z values are lower (decrease of 5%, 8% and 1.8% for the three species, respectively) and consequently, the ages where 99% of the cohort vanishes are slightly older: 12 years for bigeye, 10 years for yellowfin and 5.8 years for skipjack. We consider that these estimates are more reliable than those presented above, because they concern specifically Indian Ocean tuna and are calculated from a direct method (tag-recovery experiment).

Table 4.8: Time-at-liberty and school log rank test.

	N	Observed	Expected	(O-E)^2/E	(O-E)^2/V
School: FAD	344	344	241	43.6	72
School: FS	299	299	402	26.2	72
Chisq= 72 on 1 degrees of freedom, p= 0					

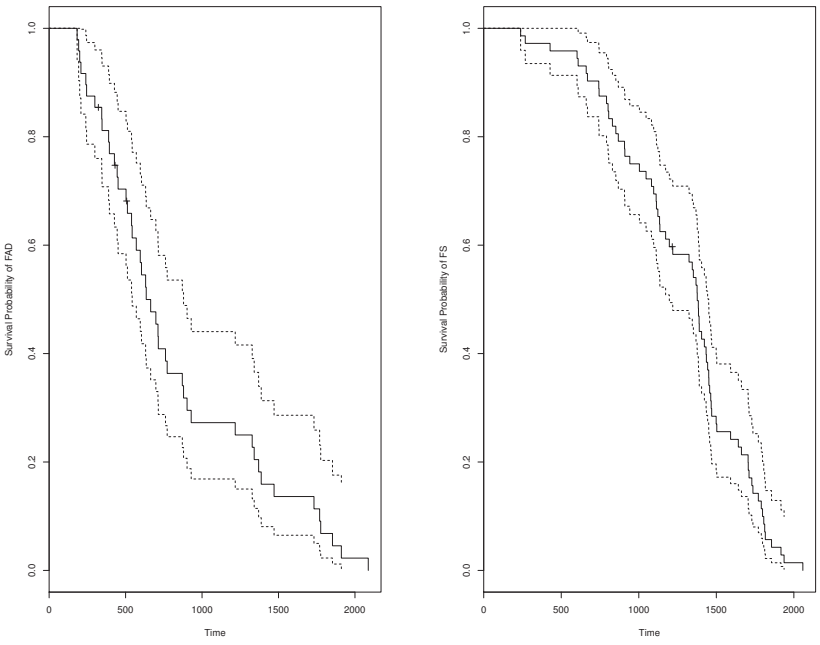

(a) (b)

Figure 4.9: Survival curves under tuna school-type (a: FAD and b: FS). Dotted lines: 95% confidence interval.

4.4 Conclusions

Several uncertainties occur because of a multitude of factors such as unreported recoveries, incomplete mixing, unpredictable movement patterns affecting catch, etc. Most of tag and release surveys were conducted on several occasions with multiple release occasions. In the context of the RTTP-IO programme, the dataset constituted only one tagging and recapture event. The advantage of having multiple releases is that it increases the reliability of the model to fit the dataset. Polacheck et al. (2010) stated that too many fisheries do not give enough attention to the statistical properties of the catch estimates. Taking into account the model structure of expected recoveries, k and l are expected to be on a regular basis. In this context, regular tagging and recovery intervals could not be observed as they varied over time. Also in the particular case that, $k < l$, recoveries hypothetically might continue beyond the tag and recovery period. The non-uniform time period both in the marking and recovery process certainly makes it difficult to have a proper estimate of the probabilities of survival and recovery. This test case showed the difficulties and limitations of the approaches adopted to compute survival and recovery estimates. This also highlights that proper estimates requires a consistent sampling process. The first two approaches adopted (MARK recovery model and the Daily survival rate), have not proven to be efficient in addressing the main questions of survival and recovery probability related to tuna mark and recapture in the RTTP-IO context.

Using the Kaplan-Meier estimate approach has given a better understanding of the survival probability. Numerous studies have discussed the effect of FADs and FS on tuna behaviour. It is clear that tuna swimming under free schools have a higher survival probability than those under fish aggregating devices. On the other hand, detectability of FAD is higher than a free school and tuna under FAD are generally juveniles which affects the survival estimate assuming that juveniles have a higher natural mortality. The analysis also showed that vulnerability of the three species is different. This indicates that tuna exploitation under FADs impacts the abundance of tuna more than those in FS. This study, using the Kaplan-Meier method, has provided improved estimates of the mortality rates and lifespans of the three tuna species in the Indian Ocean. The total mortality rates (Z) estimated

from the survival curves are: 0.4 per year for bigeye, 0.5 per year for yellowfin and 0.8 per year for skipjack; while revised lifespans are: 12 years for bigeye, 10 years for yellowfin and 5.8 years for skipjack.

Chapter 5

Environmental influences on tuna movement patterns in the Indian Ocean

5.1 Introduction

Commercial catches of Indian Ocean tuna started in the late 1950's with the development of longliner fishing activity and have been growing ever since. From 1962 to 1978 stock levels in the Indian Ocean for Albacore, bigeye, yellowfin and skipjack were not of much concern (Riggs, 1981). Since the early 1980's, tuna catch levels increased rapidly and since 1989, the yearly tuna catch levels have been higher than the Atlantic Ocean (Miyabe and Nakano, 2004). By the 1990's, the tuna fishing industry was well established with over 800000 tonnes of tropical tuna catches IOTC (2014).

The exploitation of the Indian Ocean tuna resource spans from the Indian Ocean bordering countries to Europeans, Japanese and Taiwanese fleets with considerable catch (IOTC, 2000*a*). The Indian Ocean Tuna Commission (IOTC) in its endeavour to promote cooperation among stakeholders related to the Indian Ocean fisheries resources and sustainable development and management of fisheries stock (IOTC, 1996) raised concerns on the stock levels in the Indian Ocean, expressing a pressing need to ensure sustainable tuna exploitation. In order to achieve this goal, information on stock levels and fluctuations of the habitats of tuna are of prime

importance. Although fishery indicators related to catch levels can reasonably be computed, gaps were found with regard to biological data, stock structures and behavioural responses to ocean environmental variation hampering stock assessment estimates.

Tagging has been widely used for similar goals, mostly for terrestrial species. This tuna tagging programme was a challenge and it eventually achieved more tagging than was initially planned. In the year 2005, the Regional Tuna Tagging Programme in the Indian Ocean (RTTP-IO) was launched, funded by the EU at the request of the IOTC scientific community. The survey targeted three species of tropical tuna: yellowfin tuna (*Thunnus albacares*), bigeye (*Thunnus obesus*) and skipjack (*Katsuwonus pelamis*) in the western Indian Ocean (Hallier, 2008). The RTTP-IO started in May 2005 and lasted till the end of August 2007. Tagging consisted of three types of tagging devices namely, dart tags, electronic archival tags and electronic pop-up tags (Marsac et al., 2014). The key question addressed in this chapter is: does inter-annual variability of environmental factors affect the spatial dynamics of tuna? The approach adopted was to analyse the spatial movement patterns of tuna in relation to the oceanographic environment.

5.2 Methodology and Data

5.2.1 Tag-recovery dataset

The tag-recovery dataset used in this study was limited to conventional tagging with dart tags (known as "spaghetti" tags) released and recovered within the framework of the RTTP-IO for the three species of tropical tuna (Hallier, 2006). The field parameters relevant to the investigation were date, location, species, size, school type, gear of recapture, and time-at-liberty. For this study, we only considered standardised tags which were recaptured by purse seiners, knowing that 96% of all recaptures were made by this gear. Selecting a single gear ensures robustness in the standardisation process of the recoveries. Furthermore, in order to minimise the probability of seasonal movements with fish returning to their tagging location, fish with time at liberty greater than six months were not considered. A filter was applied based on the time-at-liberty (time between tagging and recovery), keeping

only recoveries ranging from 31 to 180 days after tagging as suggested by Hallier and Million (2009).

5.2.2 Tuna movement in the Indian Ocean

Apparent tuna movements were analysed with respect to tuna tagging and recapture positions and maps showing displacement patterns were produced on the WGS-84 (World Geodetic System: 1984) coordinate system with Mercator projection. The apparent distance covered by fishing modes for the three species were calculated using the Vincenty's formula (Vincenty, 1975). Vincenty's formula allows the computation of distance between two geographical coordinates in terms of latitude and longitude on the earth's surface based on an accurate WGS-84 ellipsoidal earth model. It should be noted that the accuracy concerning tuna tagging is not a significant factor as the latitudes and longitudes have been reported to the nearest minute. The units of apparent distance covered by tuna were calculated in nautical miles (nmi, note in the figures the nautical miles have been denoted by M).

5.2.3 Angular displacement of tuna

In order to evaluate the preferred direction and movement of tuna, the whole dataset was filtered using an ArcGIS platform to categorize them: 1) by region tuna were tagged, 2) by fish school they were caught, 3) by size category and 4) by fork length. After selecting tuna based on the four criteria described, the data was exported to MATLAB for angular analysis. It should be noted that all lengths measurements at tagging were in fork length, hence for angular displacement analysis the following criteria were used:

- fork length size category,
- fork length reliability with assigned value as '1', implying properly measured,
- by fishing mode at recapture (free swimming school or fish aggregating devices),
- and finally tagging region.

5.2.4 Angular movement and displacements

In order to analyse migration patterns of tagged tuna in the Indian Ocean, angular movements were calculated from tagging positions along with apparent distance covered (hereafter termed 'distance'). The angular movement (azimuth angles) and distance moved in nautical miles were computed based on Vincenty's formula (Vincenty, 1975) for each tuna species using their tagging and recovery positions. The angle represents the direction with respect to north, taken by a tuna from its initial tag and release position relative to its final recovery position, in order to assess migratory patterns. Rose plots were plotted with respect to tagging season and region, species, size category and school-type. Angular sectors were defined to assess the general direction of the movements undertaken from two main tagging locations, Tanzania and Seychelles (Fig. 5.1). For instance, tuna tagged in Tanzanian waters and moved towards the Somali basin (angles 40-65°), and angles 65-110° represented those moving towards Seychelles. Fish tagged in Seychelles could move towards four sectors: East Seychelles from 45-210°, Mozambique Channel from 210-240°, Tanzania from 240-300° and Somali Basin in the remaining angles.

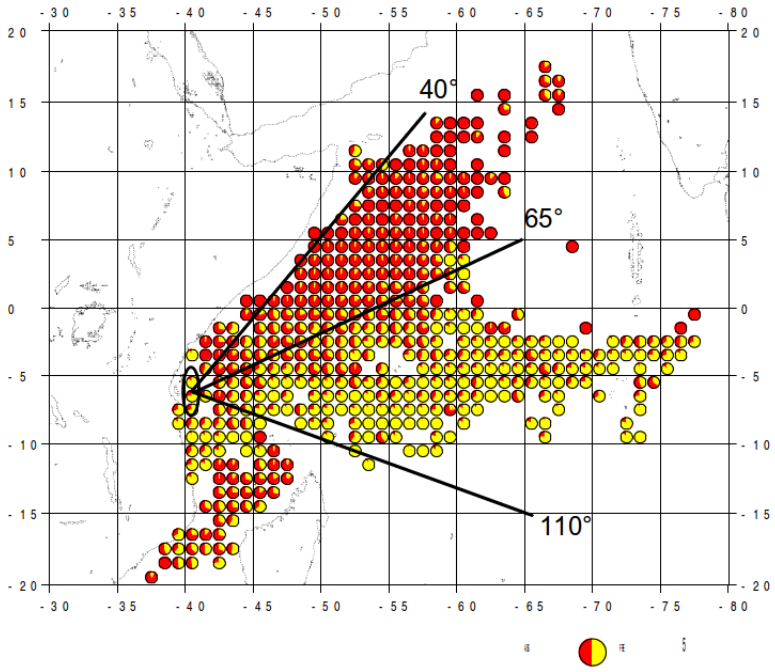

(a) Angular sectors demarcated from tagging location near Tanzanian region.

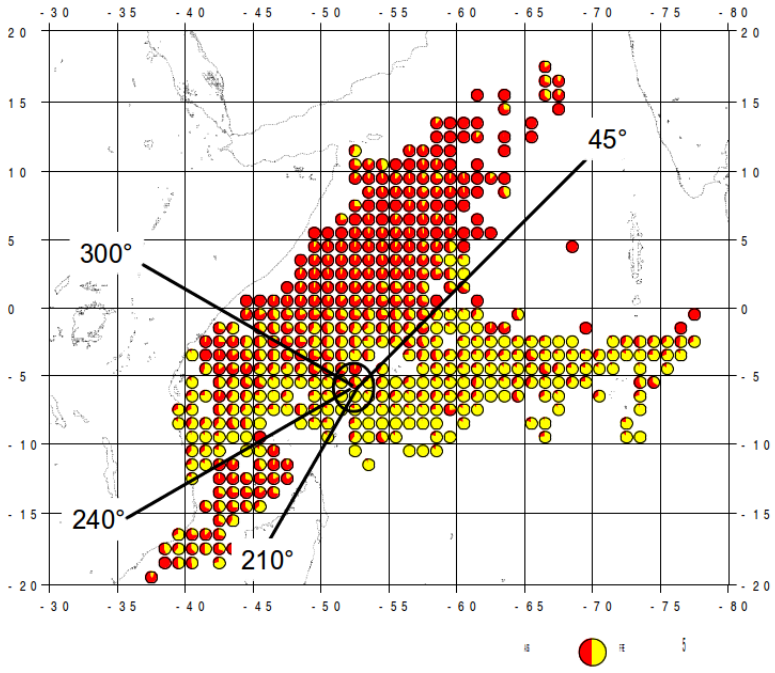

(b) Angular sectors demarcated from tagging location near Seychelles region.

Figure 5.1: Angular sectors demarcated by tagging locations. Red portions of circles represent FAD percentage catch and yellow portion represent FS percentage catch.

5.2.5 Environmental data

Two sources of ocean environmental data were used. The first source is based on circulation model outputs (Global Ocean Data Assimilation System [GODAS] of the US National Center for Environmental Prediction [NCEP]) from which sea surface temperature (SST) and surface currents were extracted, at a resolution of 1^o longitude, $1/3^o$ latitude and month. The second source was based on satellite observations (MODIS) from which surface chlorophyll data (Chl-a) was extracted, at a 9km-month resolution (Level-3). In order to have all data sets available along the same grid, Chl-a data was aggregated on a 1^o x $1/3^o$ month GODAS grid by averaging all non-cloud pixels. Empirical Orthogonal Function (EOF) analysis provides a space and time perspective to time series data (Bjornsson and Venegas, 1997). EOF calculates eigenvector and eigenvalue of covariance or correlation matrix computed from a time series data. EOF analysis was applied to study the spatial and temporal variability of SST and Chl-a in the western Indian Ocean. Hovmöller diagrams are another useful method to describe a variable spatially as a function of time (Hovmöller, 1949).

5.2.6 Modelling distance travelled

Distance travelled was modelled as a function of SST and Chl-a using Generalized Additive Models (GAMs). GAMs provide a non-parametric generalization of multiple linear regressions that is not restricted to specific functional relationships (e.g. linearity) or underlying statistical distributions (e.g. normality) of data (Hastie and Tibshirani, 1990; Swartzman et al., 1992).

GAMs take into account liner and generalized linear models while incorporating smoothing functions of informative variables. Smoothness is determined from either of the following, 1) the parameter that directly controls the smoothness of the curve, or 2) estimated predictive accuracy (Maindonald, 2010). Thus, GAMs are effective in examining environmental and stock relationships that are unlikely to be monotonic, linear, or parametric (Maravelias and Reid, 1997).

With GAMs, the dependent or response variable is modelled as the additive sum of unspecified covariate or predictor variables, with scatter-plot smooths replacing the least-squares estimates used in multiple linear regression (Hastie and Tibshirani,

1990). GAM takes the following general form whereby the mean response (μ) is related to the predictor variables (X1,...,Xp) by the following relationship:

$$g(\mu) = \alpha + \sum_{j=1}^{p} f_j(X_j) \tag{5.1}$$

where g(μ) is the link function defining the relationship between the response and the additive predictor, α is the intercept term, and f_j is the unspecified smooth function. For modelling distance travelled, a Gaussian distribution was assumed.

5.3 Analysis and results

5.3.1 Inter-annual variability patterns of SST and Chl-*a*

EOF analysis of the West Indian Ocean (WIO) for SST and Chl-*a* explained 28.7% and 20.5% of variance respectively. The space and time EOF plots show an intensively dynamic system in the WIO, (Fig. 5.2). The greatest inter-annual variability of SST in the WIO is found off the Somali coast (in relation with the upwelling) and along the Seychelles-Chagos Thermocline Ridge (SCTR) located along 10° S. In recent years, the strongest negative coefficients occurred in March-August 2002, May-September 2004, February-May 2008 and December 2010 - May 2011, denoting negative SST anomalies in the above-mentioned areas. Occurrences of positive coefficients (warmer temperature) were during November 2002 - February 2003, November 2006 - September 2007 (in relation to a Niño event), February 2009 - July 2010 and September - December 2011. In the north equatorial region, east of 60° E, there is very little inter-annual variability of SST.

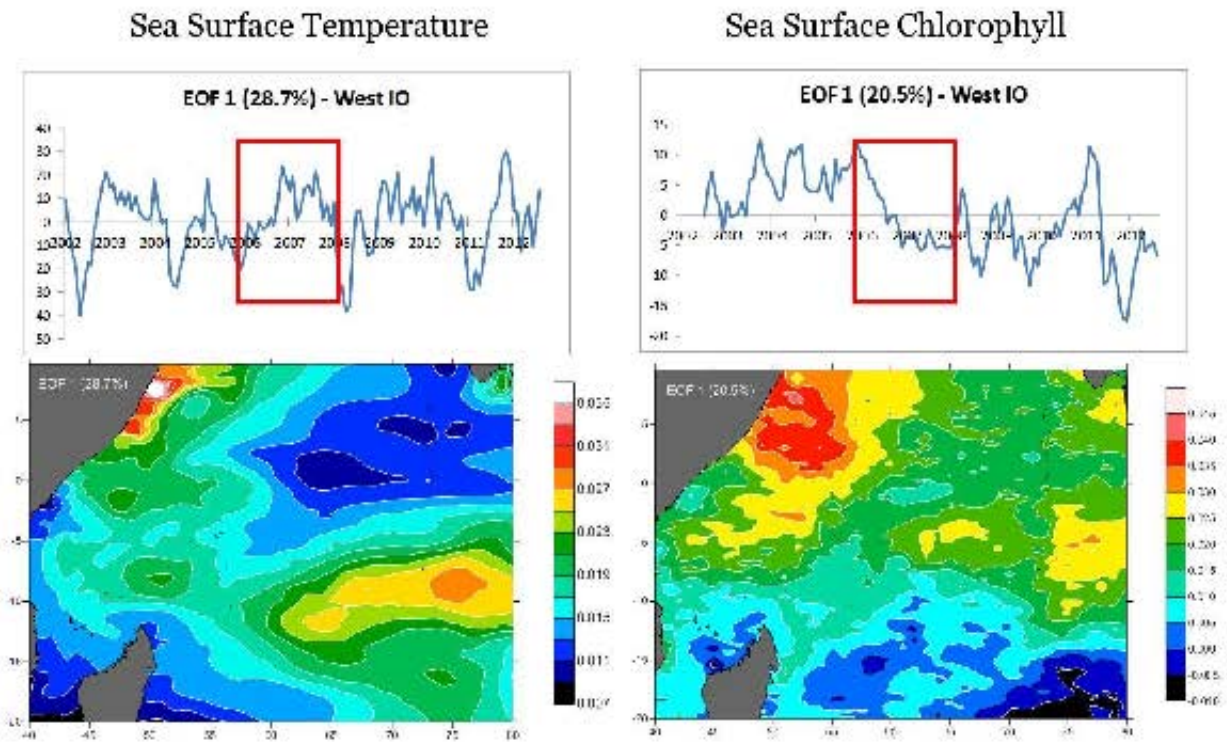

Figure 5.2: EOF variability of SST (R.H.S) and Chl-a (L.H.S) in the western Indian Ocean. SST and Chl-a variability explained 28.7% and 20.5% of variability. The red box denotes the Niño event.

The greatest inter-annual variability of Chl-a takes place in the Somali basin. A meridional gradient is noticeable, with higher variability in the north of the SCTR (10°S) compared to the South. Two distinct phases are displayed in the time series: a positive phase from 2002 to 2006, and a rapid shift to a negative phase from 2007 onwards. The shift towards low Chl-a from 2006 to 2007 was fuelled by the 2007 El Niño causing warm SST anomalies in the WIO. After 2007, the only positive and significant coefficient was observed in early 2011, in relation with La Niña event, characterized by a positive Chl-a anomaly that developed in the East basin and propagated westwards.

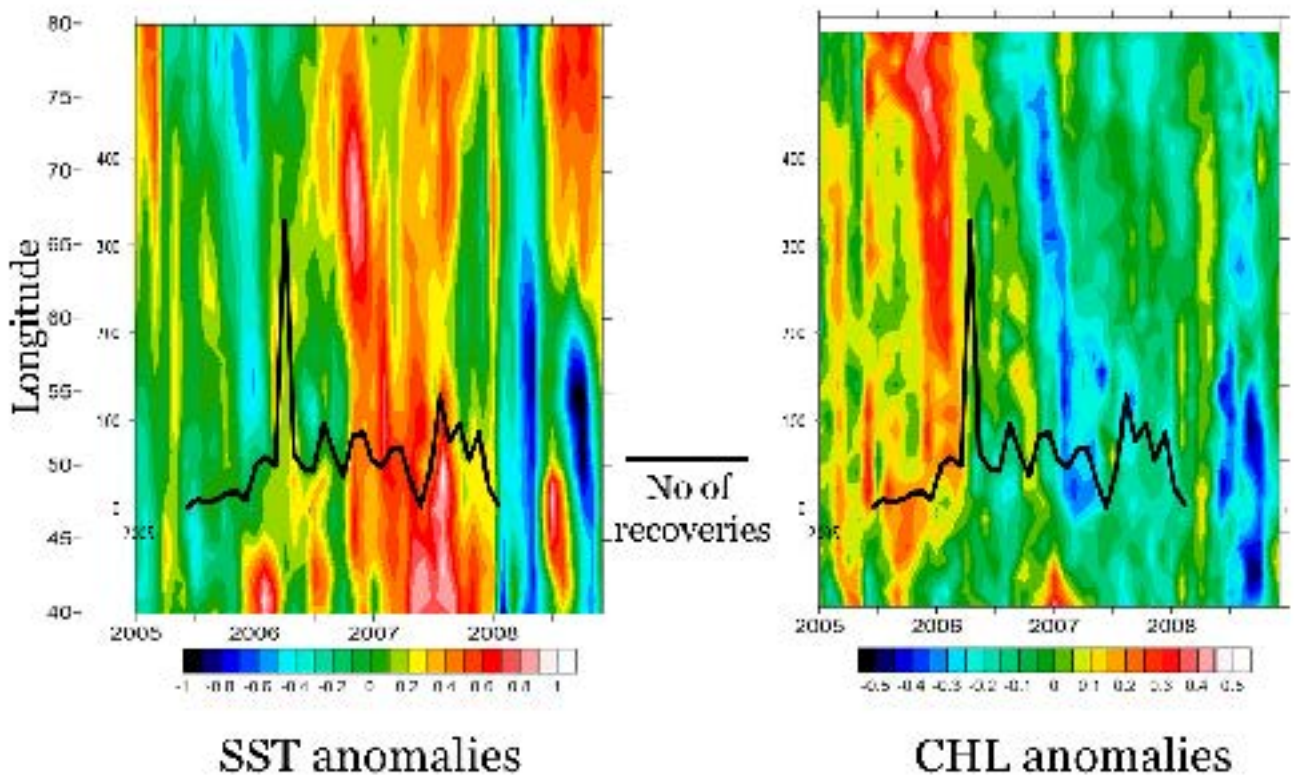

Figure 5.3: Hovmöller plots of SST and Chl-*a* anomalies in the western Indian Ocean. Black line denotes number of tuna tag recoveries.

The major part of the tagging programme was conducted during the shifting ENSO phase shown in the red boxes in Fig. 5.2, characterized by a temperature increase at the start of the tagging period and a dramatic decline of Chl-*a*. The time-longitude Hovmöller plot represented in Fig. 5.3 outlines two distinct regimes as suggested by the EOFs: i) a cool and Chl-*a* enhanced regime before mid-2006, and ii) a warm and Chl-*a* depleted regime from mid-2006 onwards. Recoveries made over the same time period and defined spatial region were superposed. High number of recoveries can be observed to correspond with cold SST and high Chl-*a* anomalies and there is a drastic drop in recoveries around mid-2007 but the recoveries pick-up again although it is a warm and low productivity phase.

5.3.2 Distance travelled by species and school mode

On average for both those individuals caught under FAD and those caught as FS the distance travelled in 2006 was shorter that in 2007 (Fig. 5.4). However, the

mean distance travelled for individuals caught under FADs or as FS (averaged across species) depends on the year. For instance, individuals caught under FADs travelled further compared to those caught in FS in 2007 and the converse holds true for 2006. Table 5.1 shows that the mean distances travelled by the three species were shorter in 2006 than in 2007. During 2007, yellowfin and skipjack tuna could be observed to cover longer mean distances than bigeye tuna.

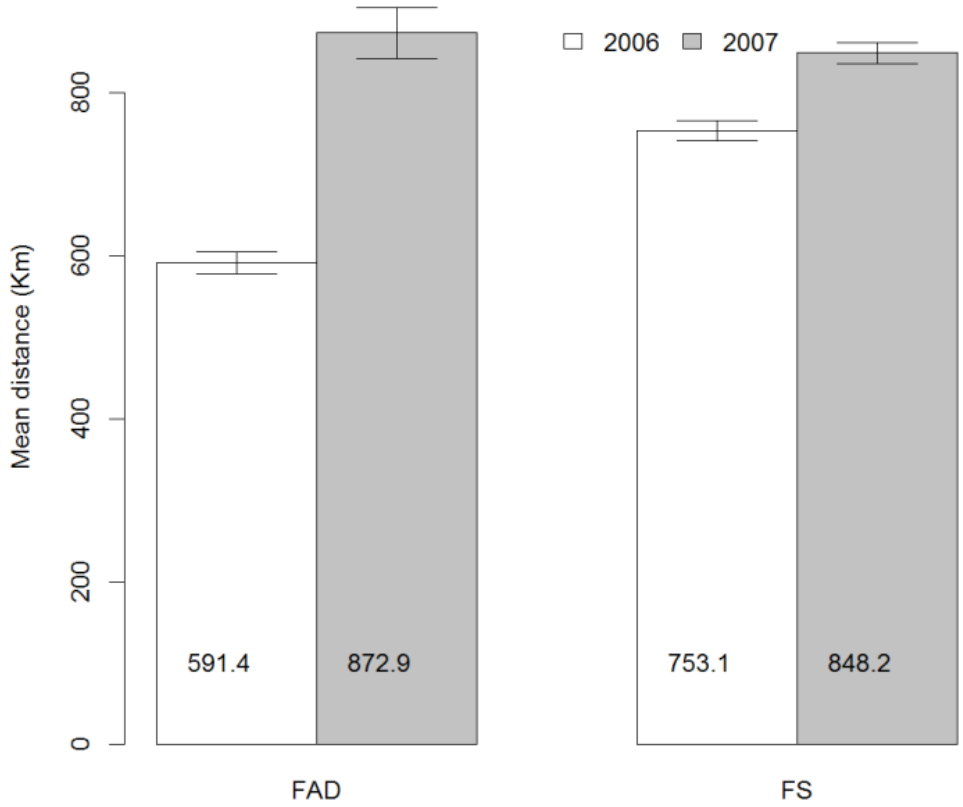

Figure 5.4: Mean distances travelled by all 3 species tuna caught under FADs and FS (± standard errors).

Table 5.1: Mean distance travelled by the three species for the year 2006 and 2007. Numbers at bottom of the bars show mean values

	Year	Species	Distance(Km)
1	2006	Bigeye	679.56
2	2007	Bigeye	740.33
3	2006	Skipjack	636.13
4	2007	Skipjack	907.88
5	2006	Yellowfin	755.02
6	2007	Yellowfin	873.27

5.3.3 Angular movements of tuna

Considering the Tanzanian tagging region and recoveries for 2006 and 2007 under FADs, juvenile bigeye tuna showed movement to the south east from Tanzania, as compared to yellowfin and skipjack for the same size-class (Fig. 5.5(a)). For yellowfin and skipjack juveniles, more than 50% moved in the north east direction with an angle of 50^o from azimuth, with apparent distances of ranging between 1000 - 1200 nmi while others ranged between 800 -1000 nmi or shorter distances (Fig. 5.5(b) and 5.5(c)). It should be noted that large distances of 1400 - 1600 nmi were covered by a small percentage of juvenile skipjacks. When the directional movements of tuna under FADs and FS are compared, it can be observed the spread of the angular direction is much narrower under FADs than for FS tuna (Fig. 5.6).

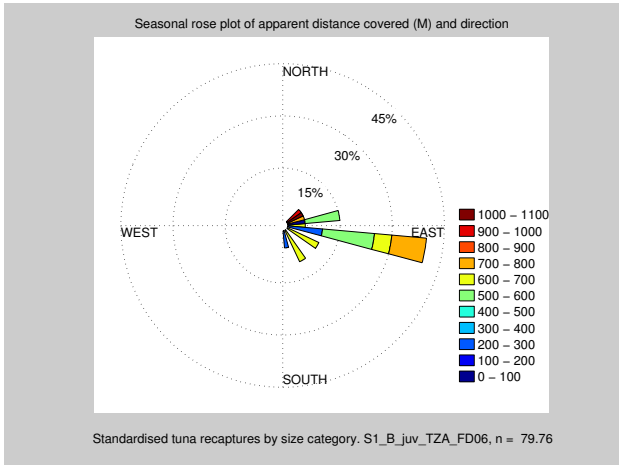

(a) Juvenile bigeye, tagged in season 1, 2006.

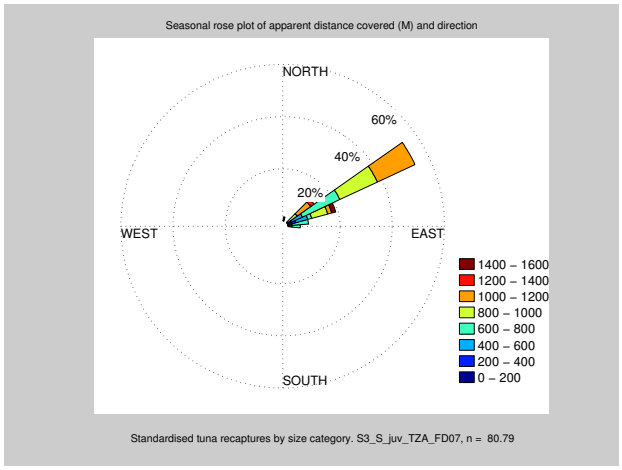

(b) Juvenile skipjack, tagged in season 3, 2007.

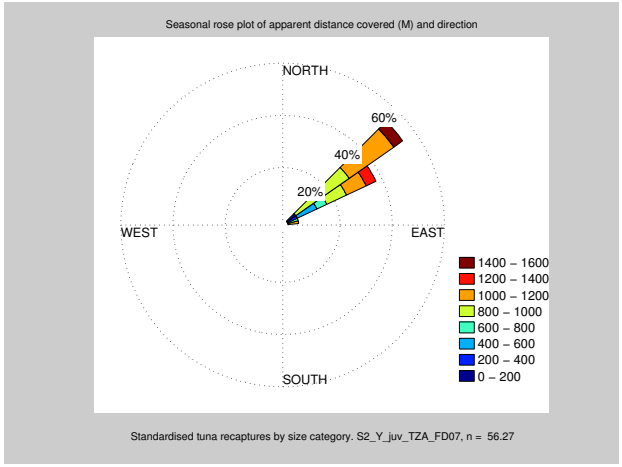

(c) Juvenile yellowfin, tagged in season 2, 2007.

Figure 5.5: Tuna tagged in the Tanzanian region and recaptured under FADs. The letter 'n' denotes the number of standardised recaptures. Each of the stripe represents the direction in percentage taken by the tuna after being released and the colour code is apparent distance (nmi = M) range covered

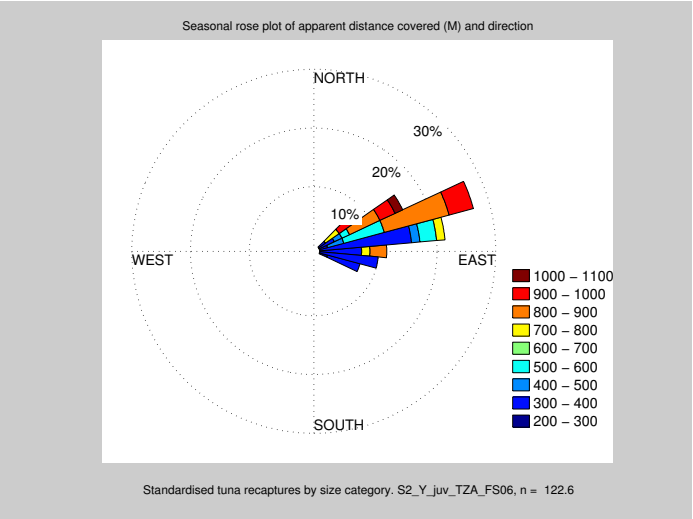

(a) Juvenile yellowfin, tagged in season 2, 2006.

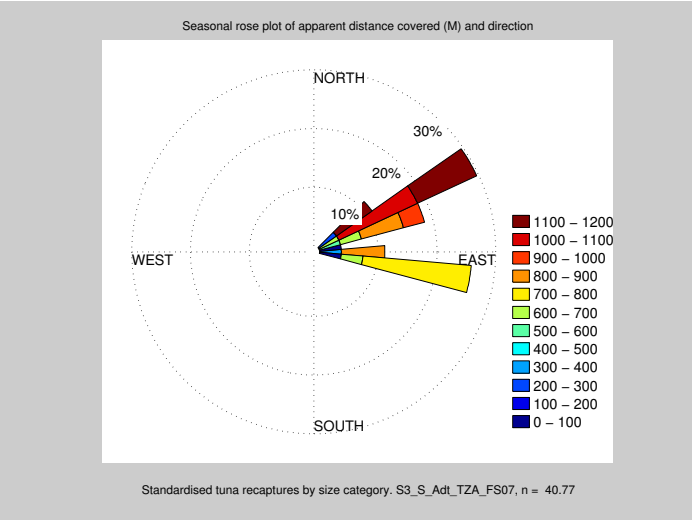

(b) Adult skipjack, bigeye, tagged in season 3, 2007.

Figure 5.6: Rose diagram of Tuna tagged in the Tanzanian region and recaptured in FS. The letter 'n' denotes the number of standardised recaptures. Each of the stripes represent the direction in percentage taken by the tuna after being released and the colour code is apparent distance (nmi = M) range covered.

Angular movements by species, seasons, year, school, size class and tagging region are summarized in Fig. 5.7. Figure 5.7(a) depicts the angular pattern of tuna tagged near Tanzania over the seasons. Tagging conducted in NEM (Dec-Mar) and IM2 (Oct-Nov) seasons, movements were towards the Seychelles for tuna caught under FAD. While for the IM1 (Apr-May) and SWM (Jun-Sep) seasons tagging, movement were directed to the north towards Somalia. For tuna caught in FS, it can be

observed that for the NEM and IM2 seasons, the movements shifted towards the Mozambique Channel although a few still moved in the direction of the Seychelles. During the IM1 and SWM seasons, tuna movements were primarily directed towards the Seychelles.

The seasonal movement of tuna tagged in the Seychelles shows a different pattern (Fig. 5.7(b)). FAD caught tuna are seen to move around Seychelles in the third season. While tuna tagged during the NEM and IM1 seasons, spread in all directions except towards the Somalian waters. Looking at FS recaptured tuna, a wider angular spread is observed.

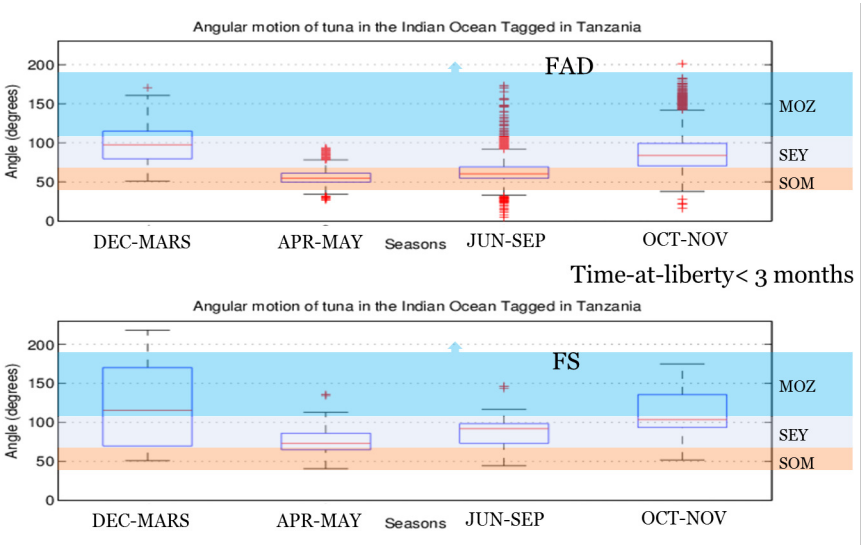

(a) Seasonal angular movement for tuna caught under FADs and FS, Tanzania

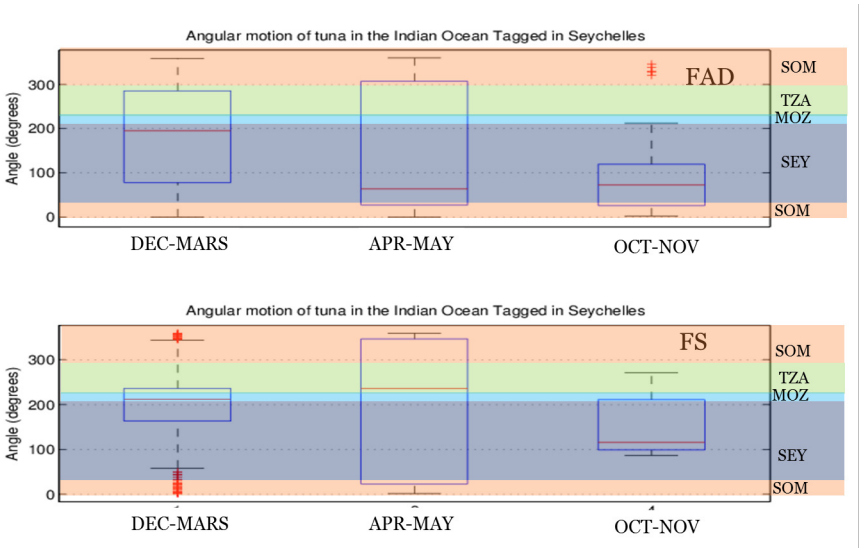

(b) Seasonal angular movement for tuna caught under FADs and FS, Seychelles

Figure 5.7: Seasonal angular pattern of tuna tagged in the Tanzanian and Seychelles' region recaptured under FAD and FS. Central mark of the box-plot is the median, the edges of the box are the 25^{th} and 75^{th} percentiles. Whiskers extend to most extreme data points and outliers are plotted individually.

Angular movements in relation to the size classes of the three species were plotted for Tanzania and Seychelles (Fig. 5.8 (a) and (b), respectively). The obvious feature is that there is no difference species wise or by size class, with respect to the direction headed whether in FS or FAD; all head in same direction Fig. 5.8(a) for tuna tagged

in Tanzanian waters. In FS tuna headed towards the Seychelles and by contrast, under FADs, they moved towards Somalia.

A different scenario is observed for tuna tagged in the Seychelles region. Interestingly, on FADs juvenile skipjack and juvenile bigeye have similarities with predominant directions towards Tanzania and Somalia whereas pre-adult and adult bigeye generally headed in the Seychelles direction (Fig. 5.6(b)). In FS mode, adult skipjack and pre-adult bigeye have similar movement patterns towards Tanzania and Somalia whereas bigeye adults and juvenile skipjacks headed towards the Mozambique and Seychelles region. Table 5.2 gives generalized movement patterns of tuna tagged in Tanzania and Seychelles.

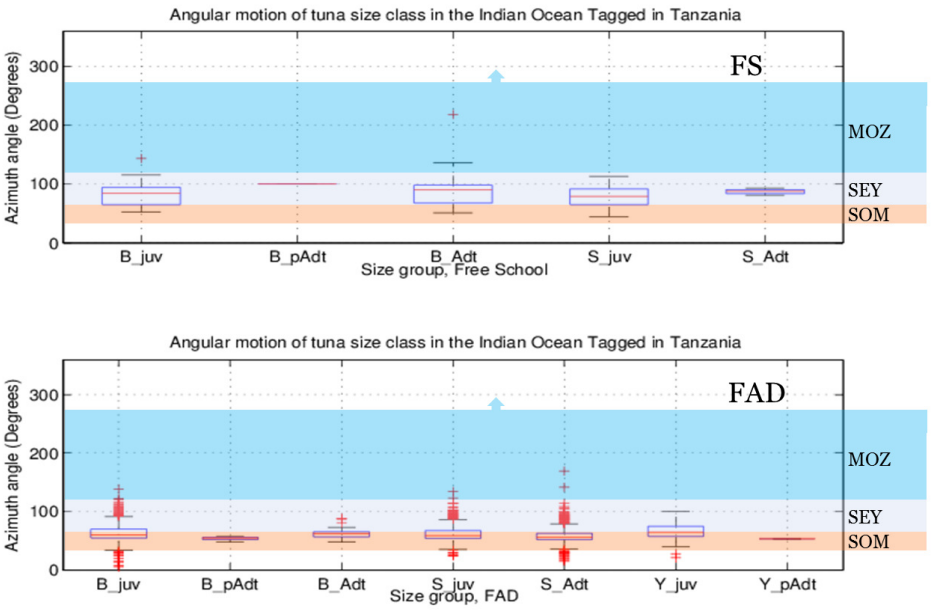

(a) Angular movement and species/size-class for tuna caught under FADs and FS, Tanzania

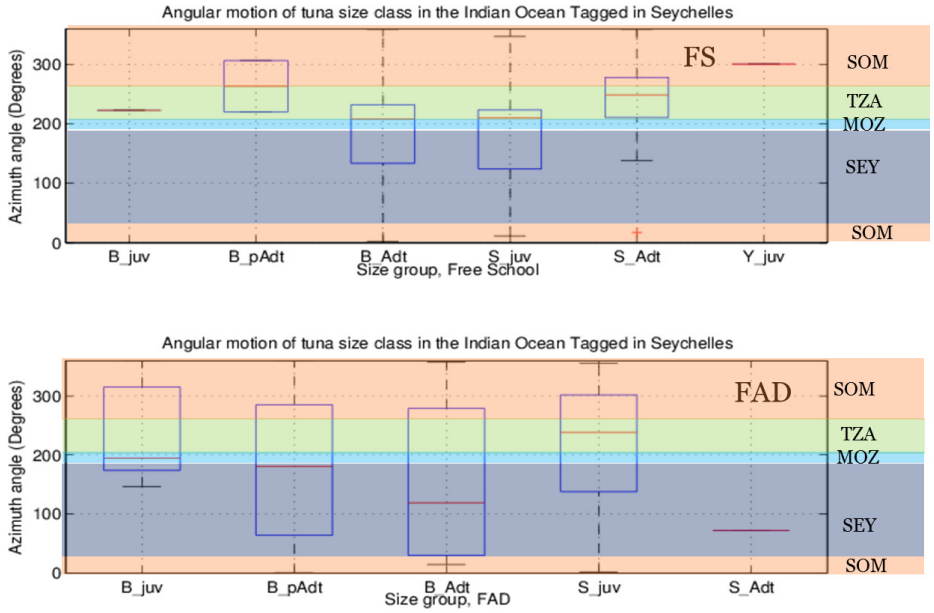

(b) Angular movement and species/size-class for tuna caught under FADs and FS, Seychelles

Figure 5.8: Angular movement pattern of Tuna tagged in the Tanzanian(a) and Seychelles(b) region recaptured under FADs and FS, with respect to species/size-class. Central mark of the box-plot is the median, the edges of the box are the 25^{th} and 75^{th} percentiles. Whiskers extend to most extreme data points and outliers are plotted individually.

Table 5.2: Summary of angular movements of tuna tagged in Tanzania and Seychelles. BET: bigeye tuna, SKJ: skipjack tuna

- Fish tagged in Tanzania

	FAD	FREE
Dominant directions :	Somalia Seychelles	Seychelles Mozambique
Species/size grouping :	All species together, towards Somalia	All species together, towards Seychelles

- Fish tagged in Seychelles

	FAD	FREE
Dominant directions :	SEY	Can concern all areas
Species/size grouping :	PreAds &Ads BET Juv. SKJ and BET	Ad BET & Juv SKJ PreAd BET&Ad SKJ

5.3.4 SST variability and Chl-*a* regimes

The comparison of percentage transfer of tuna within the 180 days of time-at-liberty for the years 2006 and 2007 is presented in Table 5.3. The major result concerns the fact that during the cold 2006 phase transfer rates in zones C and D were observed to be relatively low for tuna tagged in Tanzanian waters in contrast to 2007 when tuna shifted to zones C and D with large distances covered in this short lapse of time from their tagging location.

Table 5.3: Percentage transfer rates of tuna from tagging regions into spatially stratified zones (figure below the table) for the years 2006 and 2007. Where MOZ: Mozambique, TZA: Tanzania, SYC: Seychelles and OMN: Oman. The bold black boxes represent regions where tagging was conducted and the recovery zones corresponding to those tagging regions. The bold italic numbers boxes highlight cells where percentage transfer rates from one tagging region to another zone have been significant.

2006	Percentage proportion of transfer for tuna with 180 days of Time-at-liberty.					
	A	B	C	D	E	H
MOZ	0	0	0	0	0	0
TZA	0.71	51.73	***18.96***	0.24	0.02	0.01
SYC	0	10.16	16.82	0.66	0.44	0
OMN	0	0.12	0	0.14	0	0

2007	Percentage proportion of transfer for tuna with 180 days of Time-at-liberty.					
	A	B	C	D	E	H
MOZ	0.02	0.08	0.05	0.02	0	0
TZA	0.5	57.57	***34.19***	***5.24***	0.39	0.02
SYC	0	0.2	1.56	0.15	0	0
OMN	0	0	0	0	0	0

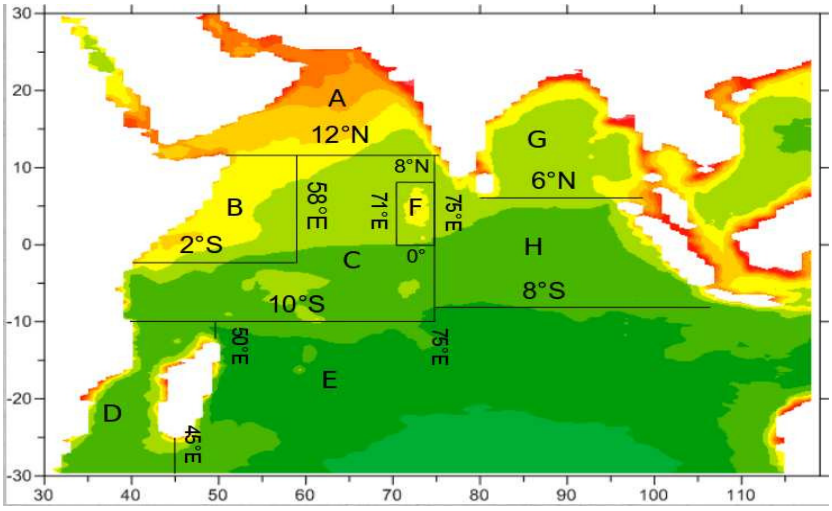

Movement plots of SST and Chl-*a* anomalies are shown in Fig. 5.9(a). The month of April 2006 corresponds to IM2 season and that of January 2007, corresponds to the NEM season. The year 2006 had a low SST anomaly and a high productivity phase, tuna movement were observed not to be as widespread as in the warm phase of January 2007, even though it is a low productivity phase when looking at the chlorophyll-a anomalies. Analysis in terms of distribution of recoveries over the cold and warm phases showed that the recovery densities are spread out at the start of warm phase, December 2006 (Fig. 5.9(b)). By the end of December 2007, the distribution density of recoveries is found to be closer to the edge of the

fronts with reduced widespread.

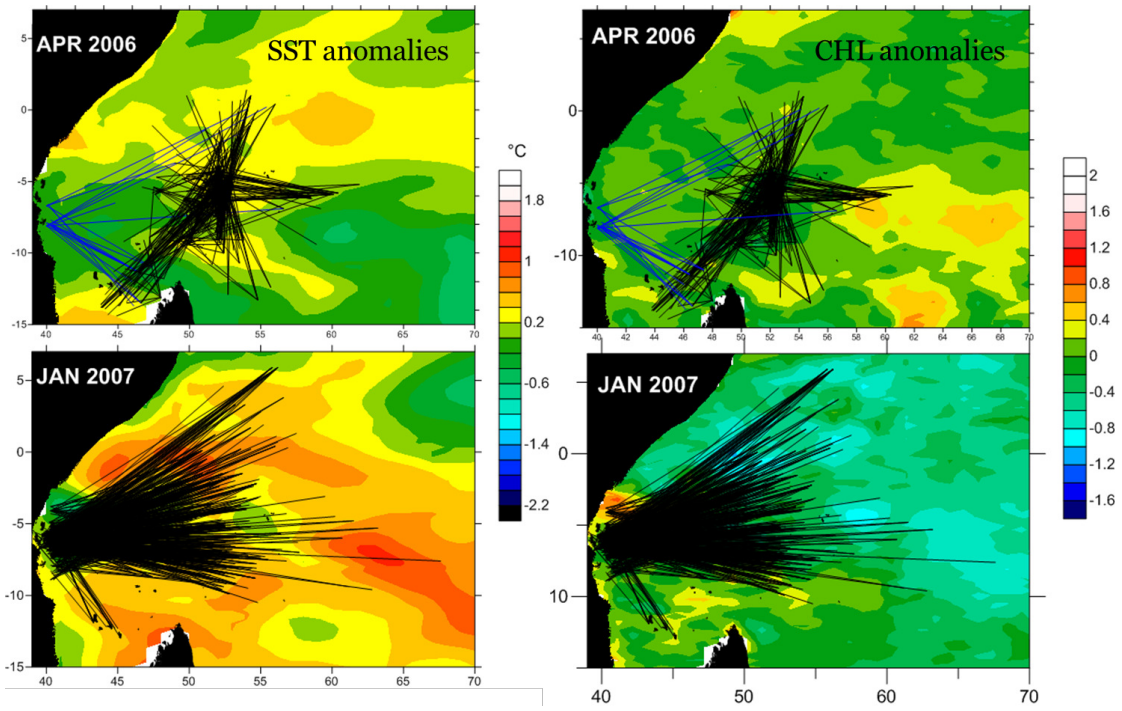

(a) Movement pattern of tuna superposed on SST and Chl-a anomalies for April 2006 and January 2007.

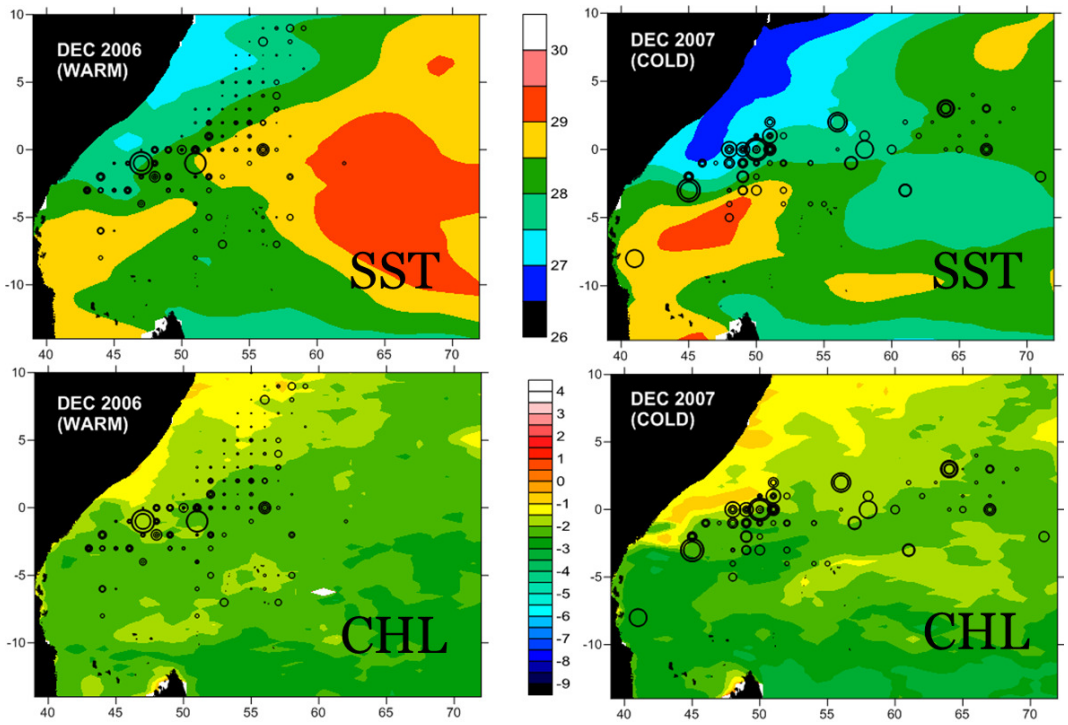

(b) Distribution density of recoveries in warm and cold phases.

Figure 5.9: Movement pattern (a) and distribution density (b) of recoveries in warm and cold phases.

Distance travelled with regard to (1) temperature difference between tagging and recapture, season, year and school effect as well as (2) chlorophyll difference and season, year and school effect was analysed statistically with a GAM. In a cold productive situation, movements are oriented along a continuous temp-Chl gradient, whereas in the warm and Chl-*a* depleted phase, movements are more wide spread, not following a given gradient (Fig. 5.10).

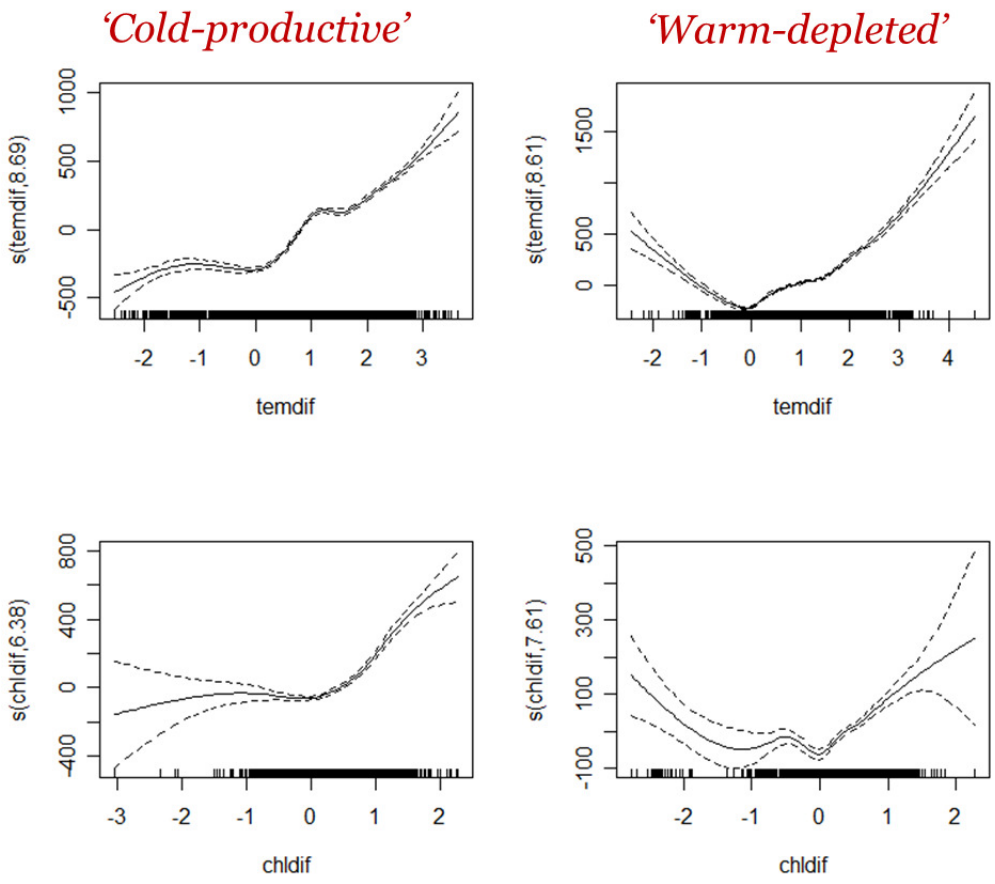

Figure 5.10: GAMs of distance travelled against SST and Chlorophyll difference between tagging and recapture with the combined effects of season, year and school. Dotted lines show 95% confidence interval.

5.4 Discussion

Preliminary results demonstrate that the distance travelled by the three species differ significantly. It was shown that skipjack tuna consistently undertakes shorter distances as opposed to both yellowfin and bigeye. For the latter two species, the

proportion of individuals that travelled shorter distance were smaller. At larger distances, the proportion of bigeye tuna exceeds both skipjack and yellowfin (Fig. 5.6).

With respect to school fishing mode, distance travelled for those caught in FS and those caught under FADs, there was a significant difference in distance travelled between the two school types. Most of the individuals caught in FS tend to travel shorter distances compared to those caught under FADs; however, the mean distance of individuals caught under FADs was lower than tuna in FS. The mean distances travelled varied between the two years analysed (i.e., in 2006 the mean distance travelled was lower than that in 2007). FS formations are associated to be a 'natural process' compared to FADs. FADs reduce the spread of the natural dispersion of movements observed in natural conditions in FS, hence a narrower angular spread is seen under FAD. It is suggested that tuna in FS explore in all directions for potential forage-rich areas. Marsac et al. (2000) stated that tuna under FAD were likely to be trapped and drift along, which might be the case for the tuna recaptured under FAD drifting in a restricted particular direction. Tuna that were tagged in the Seychelles region, moved with an angular spread that was very restricted towards Somalian waters. Following the events of piracy in Somalian waters, by the year 2008 catch efforts in this region were substantially reduced. This has also been reported in the IOTC (2013) report where catches have dropped due to expansion of piracy but catch efforts for the year 2006 were still considerable at that time (IOTC, 2012). Hence, the reduced angular spread towards Somalia is unlikely to be only the effect of piracy. The large distances moved under FADs might be related to the potential effect of FADs drifting the north-flowing east African and Somali currents.

As mentioned in the Results section, the angular movement of tuna tagged in Tanzanian waters during NEM and IM2 seasons and caught under FADs, were primarily heading towards the Seychelles. During the IM1 and SWM seasons, tuna movement was mainly towards Somalian waters and this is consistent with the surface current circulation for those seasons (Ménard et al., 2007b).

Tuna tagged and released in the Tanzanian region with respect to the species and size class, showed great stability in their movement patterns. Tuna moved as one unit irrespective of species and size class. Schooling fish often adopt common

orientation and swimming directions during migration (Stöcker, 1999). Of the tuna tagged in the Seychelles region, adults skipjack and pre-adults bigeye moved towards Tanzanian and Somalian waters which were relatively warm, as can be observed from the Hovmöller diagrams. Skipjacks are known to spawn mostly in equatorial regions throughout the year (Collette et al., 1983). In their study, Stéquert and Marsac (1989) showed the distribution of skipjack larvae to be in the region of Tanzania while juveniles' distribution was shown to be in the region of the Seychelles and the Mozambique Channel.

In the cold-productive regime, the distribution of tuna seemed to be more structured with directed movement of fish, while in the warm depleted regime the distribution seems to be more dispersed. This might be as result of fish prospecting for forage in all directions. The year 2007 was characterised by a warm El Niño phase with low productivity and the year 2006 had a cold phase of high productivity. It was shown that during 2006 tuna movements were oriented in a north-east direction and the distribution density of recoveries not so dispersed. In contrast to year 2007, when movements were spread out and distribution densities of recoveries more widely dispersed (Fig. 5.9). Similar variability in migratory pattern due to large-scale environmental phenomena was observed in the Pacific Ocean. Lehodey (2000) analysed tuna catches in the Pacific Ocean during the 1981 (Niña81), 1982 (Niño82) and 1997 (Niño97). During the Niña81, catches were confined to the west of the Pacific while during periods of EL-Niño, catches spread out. This can also be seen by the distance travelled by the three species of tropical tuna that were shorter in 2006 compared to 2007. Our findings suggest that 2006, being a cold and high productivity phase, tuna do not have to move large distances to find appropriate foraging areas compared to that of 2007 when they dispersed.

The effects of SST and Chl-a on tuna displacements showed different patterns during cold, productive regimes and warm, depleted regimes. In the cold phase, tuna movements from cold to warmer regions increased and similarly, there was movement to relatively more productive zones richer in Chl-a. The pattern is different during the warm depleted regime; large distances were covered by tuna towards both positive and negative gradients of water temperature. The same pattern is seen for in the case of Chl-a, displacements increased towards both relatively rich

and depleted regions. During the cold, productive phase, the response of tuna to SST and Chl-a is seen to be structured movements, moving to warmer and more productive waters in contrast to the warm, depleted phase where there was no apparent directed movement to particular environmental conditions, as fish searched for forage.

5.5 Conclusions

Spatial movements and distribution of tuna are affected by the environmental conditions causing them to change their behaviour. Although it is difficult to know the precise duration tuna are attached to a particular school-type (FS or FAD) from the dataset (as only the date at recapture and the associated fishing mode are known), it was shown that the schooling mode is among the factors that dictate movements of tuna, along with seasonal changes in different locations of the Indian Ocean. Considering the tuna behaviour and the school mode (FAD or FS), it was assumed that the tuna caught in a particular school mode spent most of their time in that mode. Hence, the interpretation of these results should be taken with some caution.

The angular spread of tuna tagged in the Tanzanian region with regard to FADs is not as widespread as for tuna in FS. Displacements of tuna tagged in the Tanzanian region are independent of their size-class or species or school mode. These tuna move together as a unit as compared to those that were tagged in the Seychelles. Tuna tagged around the Seychelles showed different movements in different size categories.

The scientific community dealing with stock assessment is well aware of the uncertainties of stock assessment models. The difficulty is to maintain a sustainable stock while having a fair exploitation rate. Possible ways are to change and adapt fishing practices, establish targeted fishing zones and exploitation of fishing schools. Having information relating tuna behaviour and movement to the environment, can aid estimating the abundance of stocks. Tuna individuals are known to cover distances far larger than the exclusive economic zones (EEZ) of countries. Hence, there is a need for cooperation and coordination between countries having sovereignty over tuna resources and countries exploiting the resource.

Chapter 6

Environmental patterns of tag recovery locations.

6.1 Introduction

The tag-recovery grounds and retention areas of tuna, their variability and dependence on environmental conditions are key components for understanding the stock structure of tuna fisheries. The three species of tuna (bigeye, skipjack and yellowfin) are known to live in a range of habitats and specific, environmental conditions characterise their distribution. The IOTC data consist of mainly purse-seine recovery and are categorised by school-types (FADs or FS). Based on the current stock estimates from the IOTC (IOTC, 2014), exploitation levels of tuna in the Indian Ocean are not alarming nonetheless stock assessment is complex and dynamic. The processes that control or dictate the spatio-temporal variability in these stocks are not thoroughly understood. Among the several issues to be solved, identification of tuna nursery grounds and the movement patterns are difficult to tackle as tuna are very active species. Tag and recapture data are very useful for the purpose of understanding tuna population dynamics. A number of studies have investigated the tuna migratory patterns and behaviour in connection to the environment and the interaction with tuna school-type (Marsac et al., 2000; Ménard et al., 2000a; Fonteneau et al., 2008; Hallier and Gaertner, 2008). It is known that tagging has been used to evaluate different aspects of tuna behaviour such as growth, movement, natural mortality and distribution (Sedberry and Loefer, 2001; Block et al.,

2002; Gaertner and Hallier, 2003). The ocean environment is important in influencing tuna distribution and catchability. Oceanographic features and events such as thermocline depth, oxygen levels, eddy formations, thermal fronts, among others; influence tuna behaviour and movement (Sund et al., 1981; Ramos et al., 1996).

Understanding the underlying structures of tuna population dynamics in the Indian Ocean would aid in the proper evaluation of stocks; seasonal variability is one important aspect among others, when considering the mobility of tuna and development of management strategies for the stock. The Indian Ocean is influenced by the monsoon seasons altering the ocean currents, temperature and the Chl-*a* distribution (Ramage, 1969; Fréon, 1983; Rajapaksha et al., 2010; Marsac et al., 2014). Nakamura (1969) defined two types of migratory movement for tuna, the first type of movement behaviour is related to the feeding and reproduction; while the second type, is related to movement within habitats with respect to different components that is, the environmental cues. On that account, understanding the influences of seasons and inter-annual variability on tuna movement patterns to recovery locations is important. This chapter assesses the effect of environment on movement and recapture locations of tuna from their tag and release regions, while also addressing the effect of school-type.

6.2 Methodology

6.2.1 Data

The same dataset from the RTTP-IO used in Chapter 5 was used in this chapter. The difference from the previous chapter is that, here the study is focused on the directions (tagging regions) from which tuna aggregated in the zones rather than to which zones tuna went after tag and release. Bigeye (*Thunnus obesus*), skipjack (*Katsuwonus pelamis*) and yellowfin tuna (*Thunnus albacares*), which were tagged using conventional tagging method of dart tags (Hallier, 2006), were studied based on similar size-class, seasonal behaviour, school type and environmental conditions. In brief, the dataset has over 31,000 recaptures, implying that the individual destination from tag and release point of each fish to recapture point could be estimated. Depending on the analysis, data filtering was effected for good and reliable length

recordings, species, good records of GPS positions and lastly, limiting the time-at-liberty from 30 to 180 days. The number of tuna varied in each of the investigation carried out in order to have the largest sample number; it roughly varied from 8,000 to 10,000 tuna. Tuna from the five tuna tagging regions were taken into consideration (Tanzania, Madagascar, Seychelles, Oman and Maldives (Fig. 2.3)).

As presented in Chapter 2, the dataset used was standardised through four main steps: calculation of shedding rates, reporting rate, correction of actual recoveries and finally standardization of the recoveries based on purse seine catch at size extrapolated for the three species by five degree area-year-quarter and school-type. In the previous chapter, the two fishing modes or school types were considered, free schools (FS) and fish aggregating devices (FADs). In this chapter, the same school associations were taken into account under the assumption that tuna caught in a particular school-type, spent most of its time under that school-type. A time-at-liberty of at least 30 days was chosen to allow population mixing after the individuals were tagged and released (IOTC, 2008*a*; Hallier and Million, 2009) as it was the case in the previous chapter. Finally, seasonal migratory patterns may exist with individuals returning to the same sub regions, either for feeding or spawning; therefore, we only retained in the dataset the individuals with a time-at-liberty not exceeding 180 days.

6.2.2 Calculation of angular movement towards the recapture zones

Movement patterns of tuna were calculated from the GPS (Global Positioning System) locations of tag and recapture. Calculation of azimuth angle at tagging and recapture and their linear apparent distance travelled (hereafter termed as distance travelled) in nautical miles (nmi, note in the figures the nautical miles have been denoted by M) were done using Vincenty's formula (Vincenty, 1975), as in the previous chapter. Consequently, based on these information tuna angular movements were analysed and categorized by size-class, year, season, school-type and zone. The seasonal spatial stratification was based on the mean Chl-a distribution from Zones A to H, as explained in Chapter 2 (Fig. 2.13). This figure is repeated here to make its access easier for the reader (Fig. 6.1). The Indian Ocean was spatially

and temporally demarcated in several zones as described in Chapter 2 based on the seasons.

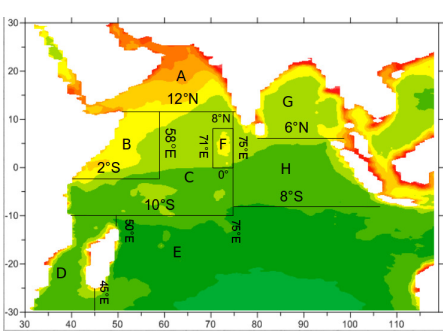

(a) Season 1: North East Monsoon season, Dec-Mar

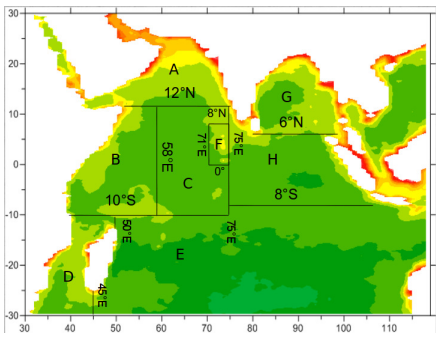

(b) Season 2: Inter-Monsoon season, Apr-May

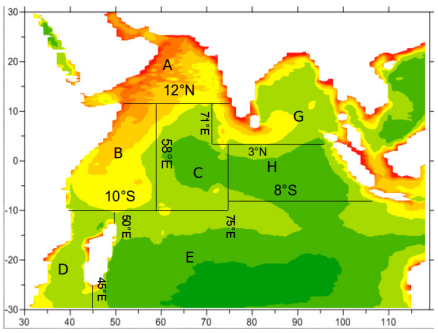

(c) Season 3: South West Monsoon season, Jun-Sep

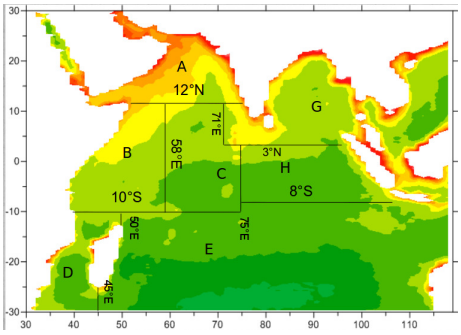

(d) Season 4: Inter-Monsoon, Oct-Nov

Figure 6.1: Zone demarcation based on mean Chl-*a* distribution in the Indian Ocean over the year. Four seasons were established. Season1: North East Monsson (Dec-Mar), season 2: Inter-monsoon (Apr-May), season 3: South West Inter-monsoon (Jun-Sep) and season 4: Inter-monsoon (Oct-Nov)

6.3 Analysis and results

In contrast to the previous chapter, here the aim is to see how the seasonally demarcated zones were populated with tuna from their initial tagging regions. This would allow us to understand directions from which tuna are immigrating to and factors driving the movements to places of recapture. Standardised recapture counts and rose plots of tuna movement arriving in the eight demarcated zones were done on a seasonal basis over the recovery years. Here, the years 2006 and 2007 are presented because these two years were most significant based on the criteria used. In addition

to this, focus was made on Zone B, as it was the zone with most tuna immigration. Finally, tagging regions indicate regions where the tuna was tagged and released; recovery zones are those areas demarcated by Chl-*a* spatial stratifications where the tagged tuna were recovered.

6.3.1 Seasonal and spatial distribution of recoveries

Most tuna tagged in 2006 in the Tanzanian region were recovered during the NE monsoon (season 1) and the Jun-Sep SW monsoon (season 3), while the recoveries in the inter-monsoon (Oct-Nov, season 4) were relatively lower (Table 6.1). The Apr-May inter-monsoon season (season 2) showed fewer recoveries. Similar trends can be observed for the year 2007 with reference to tuna tagged in the Tanzania region. Concerning Seychelles-tagged tuna in 2006, the first and second seasons made up most of the recoveries followed by the a reduced third season. The fourth season showed very low recoveries. In 2007, Seychelles recaptures were fewer than those recorded in 2006. It is noteworthy that very few tuna from Oman and Maldives were recaptured through all the seasons.

Table 6.1: Standardised recoveries (nearest integer) by seasons related to tagging regions for 2006 and 2007. A colour shading is used to highlight the range of number of recoveries (except for sums) in the table, from green to red representing the lowest and highest ranges, respectively..

Table 6.1: Standardised recoveries (nearest integer) by seasons related to tagging regions for 2006 and 2007. A colour shading is used to highlight the range of number of recoveries (except for sums) in the table, from green to red representing the lowest and highest ranges, respectively. The top row shows recoveries coming from the tagging regions: Tanzania, Madagascar, Seychelles, Oman and Maldives.

Recovery 2006	Tanzania	Madagascar	Seychelles	Oman	Maldives	Sum
Season 1	1005	36	506	0	0	1547
Season 2	49	41	586	0	0	676
Season 3	1397	23	167	0	0	1587
Season 4	826	0	6	0	0	833
sum	3277	100	1265	0	0	4642

Recovery 2007	Tanzania	Madagascar	Seychelles	Oman	Maldives	Sum
Season 1	2011	0	5	0	2	2018
Season 2	350	0	4	17	0	371
Season 3	1601	0	12	4	0	1617
Season 4	1360	0	0	0	1	1361
sum	5322	0	21	21	3	5367

Table. 6.2 shows the standardised number of recoveries by species in the seasons of 2006 and 2007. Recoveries of skipjack were mainly in the first season (Dec- Mar monsoon) for both years. The year 2006 showed a gradual decrease in skipjack recaptures over the seasons while in 2007, seasons 3 (SW monsoon) and 4 (inter-monsoon Oct-Nov) showed higher recaptures and the Apr-May inter-monsoon (season 2) was the lowest. It is interesting to note that for yellowfin, the recaptures were the highest in the third and first seasons in 2006 and 2007 respectively. Recovery of bigeye tuna was relatively low in 2006 compared to 2007 and season 1 of 2006 was the highest. In 2007, the Oct-Nov inter-monsoon (season 4) recorded the highest bigeye recoveries followed by the first season. The Apr-May inter-monsoon season records the lowest recaptures for both years.

Table 6.2: Standardised species recoveries (nearest integer) by seasons for 2006 and 2007, all the tagging regions were considered. A colour shading is used to highlight the range of number of recoveries (except for sums) in the table, from green to red representing the lowest and highest ranges, respectively. Top row show recoveries of the three species.

Recovery 2006	Bigeye	Skipjack	Yellowfin	Sum
Season 1	304	778	503	1585
Season 2	16	642	41	699
Season 3	124	405	911	1440
Season 4	87	471	542	1099
Sum	531	2295	1997	4824

Recovery 2007	Bigeye	Skipjack	Yellowfin	Sum
Season 1	547	1041	897	2485
Season 2	151	292	161	604
Season 3	223	901	459	1584
Season 4	679	597	326	1602
sum	1600	2831	1843	6275

In 2006, recoveries showed that Zones B and C were mostly populated in comparison to the other zones (Table 6.3). Skipjack and yellowfin were the most abundant in those 2 zones and interestingly, yellowfin migration was higher. Bigeye fish were likely to be confined to Zones B, C and D with a few in Zone E for both 2006 and 2007. No recoveries were recorded in Zone F in 2006 which is demarcated only during the NE monsoon (S1, Dec-mar) and the first inter-monsoon period (S2, Apr-may). Although skipjack tuna are small in size, they are able to cover large distances with recaptures in Zones G and H. With respect to 2007, the Zones B, C and D were populated by the three species although Zone B is the most favoured zone. Skipjack recaptures were higher than the other two species.

Table 6.3: Standardised species recoveries (nearest integer) by recapture zones for 2006 and 2007. A colour shading is used to highlight the range of number of recoveries (except for sums) in the table, from green to red representing the lowest and highest ranges, respectively. Top row show recapture zones demarcated in Fig. 6.1 for the three species

Recovery 2006	Zone A	Zone B	Zone C	Zone D	Zone E	Zone F	Zone G	Zone H	Sum
Bigeye	0	390	157	17	2	0	0	0	567
Skipjack	16	1483	1118	95	31	0	1	6	2750
Yellowfin	22	1814	558	8	6	0	0	12	2421
Sum	38	3687	1834	120	40	0	1	18	5738

Recovery 2007	Zone A	Zone B	Zone C	Zone D	Zone E	Zone F	Zone G	Zone H	Sum
Bigeye	6	924	619	46	1	0	0	0	1596
Skipjack	37	1606	1155	315	13	0	1	0	3126
Yellowfin	17	854	717	99	10	1	1	18	1716
Sum	59	3384	2491	460	24	1	2	18	6439

Table (6.4) shows the recoveries of tuna by tagging regions and recovery zones. Tagging regions (first column) have been given the zone code of the appropriate tagging regions. Instances where two zone codes are given in first column are because of zone demarcations change by seasons. The first row denotes the recoveries with respect to the zones. Most of tuna tagged in the Tanzanian region were recovered in Zones B and C for both 2006 and 2007, although Zones D and E showed fewer recoveries. A few tuna from Tanzania covered long distances to be recaptured in Zones G and H. Tanzania-tagged fish mostly stayed in the same regions. For the year 2006, fish tagged in the Seychelles region were mostly recovered in the Zones B and C. Tuna tagged in the region of Madagascar moved north and they were evenly distributed in Zones B, C and D with a few in Zone E. Oman tagged tuna in 2007, were quite localised (remaining in Zone A); a small fraction moved southwards to Zones B and C. Maldives, the recoveries were insufficient to analyse.

Table 6.4: Standardised recoveries (nearest integer) from tagging regions by recapture zones.A colour shading is used to highlight the range of number of recoveries (except for sums) in the table, from green to red representing the lowest and highest ranges, respectively. Top row show recapture zones demarcated in Fig. 6.1 and the first column, shows the tagging regions.

Recovery 2006									
Tagging region (zone)	Zone A	Zone B	Zone C	Zone D	Zone E	Zone F	Zone G	Zone H	Sum
Tanzania (B & C)	38	2850	881	52	3	0	1	16	3841
Madagascar (D)	0	76	50	31	2	0	0	0	159
Seychelles (C & B)	0	661	762	37	35	0	0	0	1495
Oman (A)	0	0	0	0	0	0	0	0	0
Maldives (F & G)	0	0	0	0	0	0	0	0	0
Sum	38	3587	1693	120	40	0	1	16	5495

Recovery 2007									
Tagging region (zone)	Zone A	Zone B	Zone C	Zone D	Zone E	Zone F	Zone G	Zone H	Sum
Tanzania (B & C)	21	3053	2052	293	15	0	1	18	5453
Madagascar (D)	0	0	0	0	0	0	0	0	0
Seychelles (C & B)	0	8	14	3	0	0	0	0	26
Oman (A)	10	4	7	0	0	0	0	0	22
Maldives (F & G)	0	0	2	0	0	1	0	0	3
Sum	31	3066	2076	297	15	1	1	18	5504

6.3.2 Sea surface temperature and Chl-*a* distribution at recovery for 2006

The sea surface temperature (SST) and chlorophyll-a (Chl-*a*) distribution were analysed with respect to recapture positions over all the areas. Box-plots over seasons for the year 2006 for SST and Chl-*a* are shown in Figure 6.2. The SST ranges from around 24 °C to a little more than 30 °C. The NE monsoon (S1) and the Oct-Nov inter-monsoon (S4) do not differ so much in terms of variability. However, the Apr-May inter-monsoon (S2) and the SW monsoon (S3) were quite different: higher SST (from 28 - 30 °C) with a narrow range during season S2 while S3 shows reduced and highly variable SST (23.8 - 28.8 °C). Figure 6.2 shows Chl-*a* over the seasons on log scale. Comparing the figures, show that S1 (NE monsoon) and S4 (Oct-Nov inter-monsoon) are close for SST while for Chl-*a* they differ. Seasons S2 (Apr-May inter-monsoon) and S3 (Jun-Sep monsoon), high SST correspond to low

Chl-a whereas S1 and S4 are more specific. Tables 6.5 and 6.6 show the ANOVA table for SST and Chl-a over the seasons. The seasons are significantly different for both parameters. An Empirical Cumulative Distribution Function (ECDF) can be used to compare closeness of the sample distributions, and is shown for both SST and Chl-a (Fig. 6.3). It shows S1 and S4 were close and high temperature seasons correspond to low Chl-a distributions. Seasons 1 and 3 (Dec-Mar and Jun-Sept monsoon seasons) were the most productive.

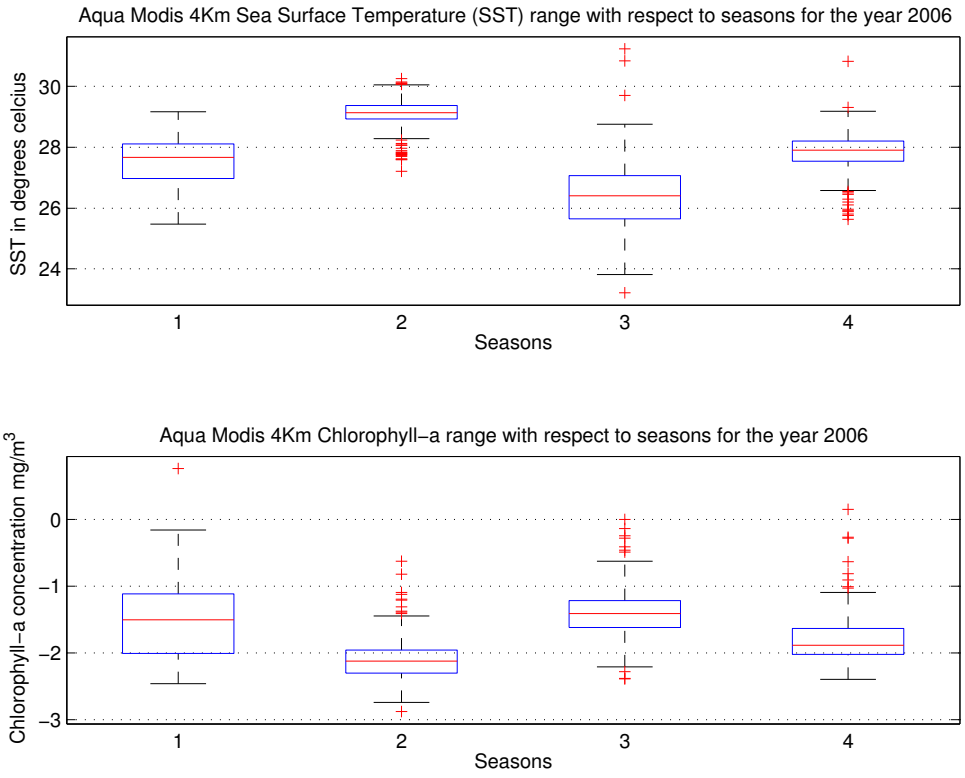

Figure 6.2: Box-plot of SST (upper panel) and Chl-a concentration (log scale, bottom panel with respect to seasons for the year 2006, corresponding to recovery positions of tuna. Where Season 1 = NEM, Season 2 = IM1, Season 3 = SWM and Season 4 = IM2. The central mark of the box-plot is the median, the edges of the box are the 25^{th} and 75^{th} percentiles. Whiskers extend to most extreme data points and outliers are plotted individually.

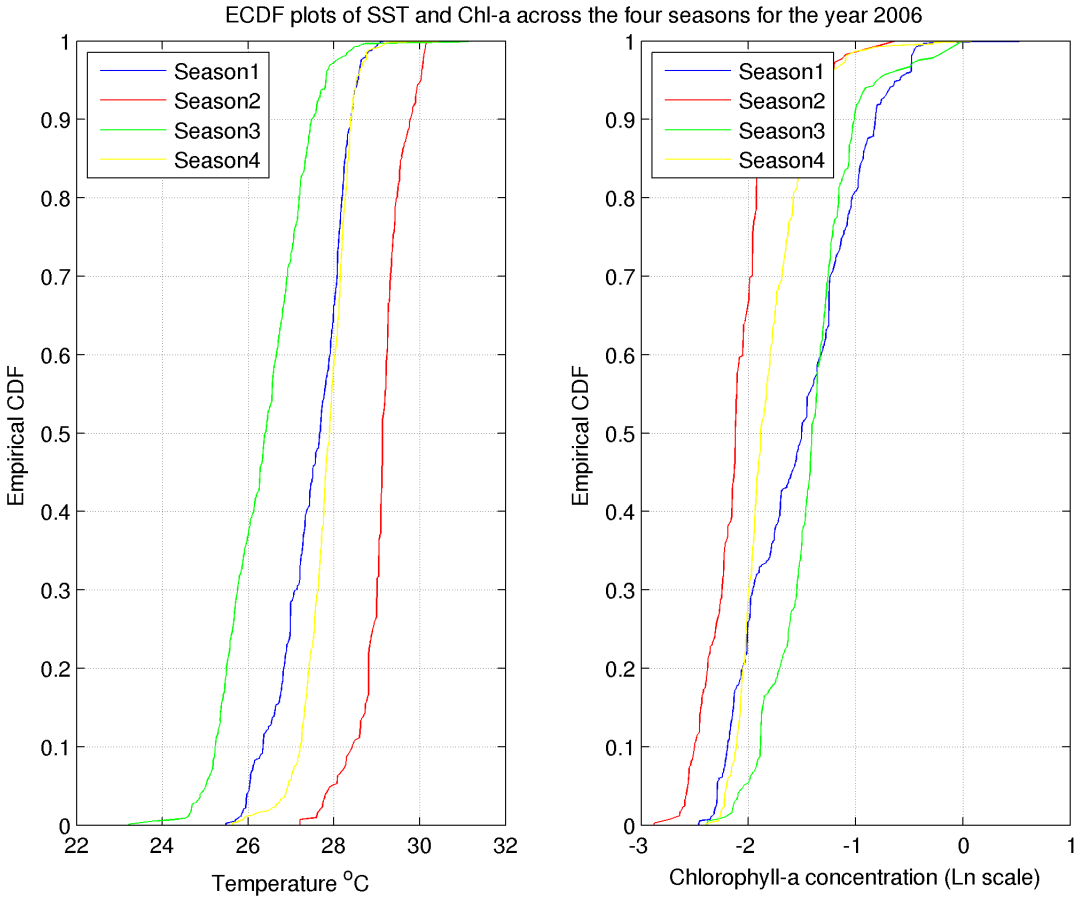

Figure 6.3: EDCF plots of SST and Chl-a variability across the seasons in 2006, corresponding to recovery positions of tuna.

Table 6.5: 2006: Kruskal-Wallis ANOVA table of season and SST

Kruskal-Wallis ANOVA Table

Source	SS	df	MS	Chi-sq	Prob>Chi-sq
Groups	4.89962e+09	3	1633205903.7	2600.97	0
Error	4.05394e+09	4750	853460.1		
Total	8.95355e+09	4753			

Table 6.6: 2006: Kruskal-Wallis ANOVA table of season and Chl-*a*

Kruskal-Wallis ANOVA Table

Source	SS	df	MS	Chi-sq	Prob>Chi-sq
Groups	5.33033e+08	3	177677807.9	677.13	1.91075e-146
Error	1.88523e+09	3069	614282.6		
Total	2.41827e+09	3072			

6.3.3 Sea surface temperature and Chl-*a* distribution at recovery for 2007

Sea surface temperature and Chl-*a* concentration variability with the seasons are shown in Fig. 6.4. Looking at the 'preferred' temperature range (top plot) of tuna recoveries over the seasons in 2007, there are marked differences and similarities to be observed. The SW monsoon (S3) and Oct-Nov inter-monsoon (S4), show a strong variability in temperatures where the tuna were recovered while Seasons 1 and 2 showed little variability. With regard to Chl-*a* concentration, it can be observed that S1, S3 and S4 do not differ in concentrations, with a high variability in 2007, nonetheless the lowest Chl-*a* concentrations at recovery were during the second season (Apr-May inter-monsoon). The correlation of SST between 2006 and 2007 shows an R value of 0.0164 and a P-value of 0.25 (2 d.p), implying that the correlation is not significant. We see similar trends to 2006, where S1 and S4 for 2007 are similar for SST, while for Chl-*a* they differ. In seasons S2 and S3, high SST correspond to low Chl-*a*. Tables 6.7 and 6.8 show the ANOVA table for SST and Chl-*a* over the seasons. The seasons are significantly different for both parameters. It is noteworthy that Chl-*a* concentration was lower in the first and second seasons for 2007 as compared to 2006; this corresponds to a positive dipole effect associated with the El Niño.

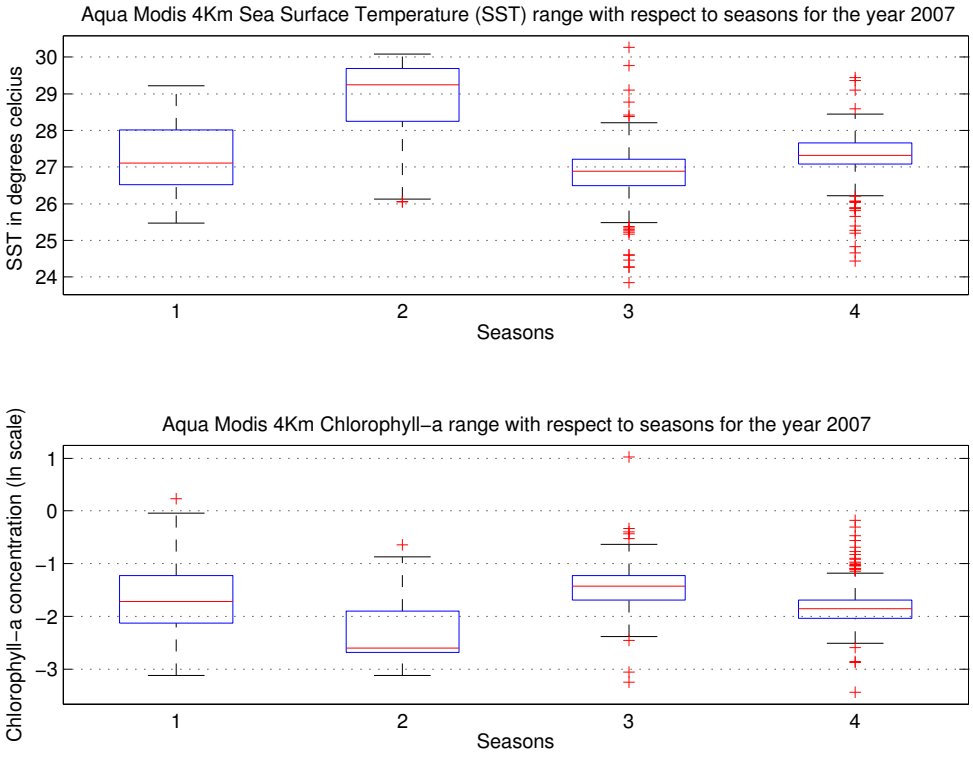

Figure 6.4: Box-plot of SST (upper panel) and Chl-a concentration (log scale, lower panel) with respect to seasons for the year 2007 corresponding to recovery positions of tuna. Where season 1 = NEM, season 2 = IM1, season 3 = SWM and season 4 = IM2. Central mark of the box-plot is the median, the edges of the box are the 25^{th} and 75^{th} percentiles. Whiskers extend to most extreme data points and outliers are plotted individually.

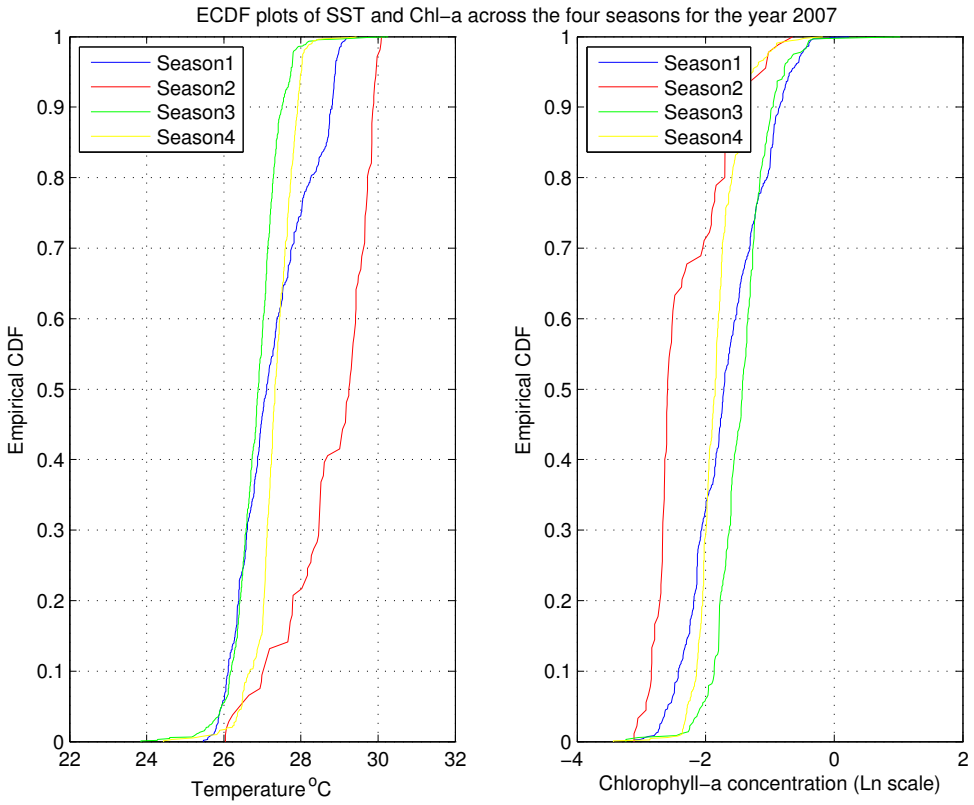

Figure 6.5: EDCF plots of SST and Chl-a variability across the seasons in 2007, corresponding to recovery positions of tuna.

Table 6.7: 2007: Kruskal-Wallis ANOVA table of season and SST

Kruskal-Wallis ANOVA Table

Source	SS	df	MS	Chi-sq	Prob>Chi-sq
Groups	1.26025e+10	3	4.20083e+09	2352.08	0
Error	3.03528e+10	8014	3.78747e+06		
Total	4.29553e+10	8017			

Table 6.8: 2007: Kruskal-Wallis ANOVA table of season and Chl-a

Kruskal-Wallis ANOVA Table

Source	SS	df	MS	Chi-sq	Prob>Chi-sq
Groups	1.70083e+09	3	5.66943e+08	788.56	1.31079e-170
Error	9.26907e+09	5083	1.82354e+06		
Total	1.09699e+10	5086			

6.3.4 Tuna recoveries in Zone B

The following describes tuna movements into Zone B (where recoveries were the most numerous) through the four seasons of year 2006 (Fig. 6.6). The overall observations are that the directional movements for three seasons are similar and from south west. The rose plots for the NEM, SWM and IM2 seasons shows that tuna movements have been from the Tanzanian tagging region; covering distances over 1000 - 1200 nmi. In general, the number of recaptures making up that region varied from 400 - 1400 fish across the seasons. The Apr-May inter-monsoon season of 2006 was different from the rest of the seasons. Immigration was observed not only from tuna tagged in Tanzanian waters but coming from all directions as the larger proportion of fish originate from the North to North-East quadrant. However, the large distances represent tuna coming from Tanzanian waters.

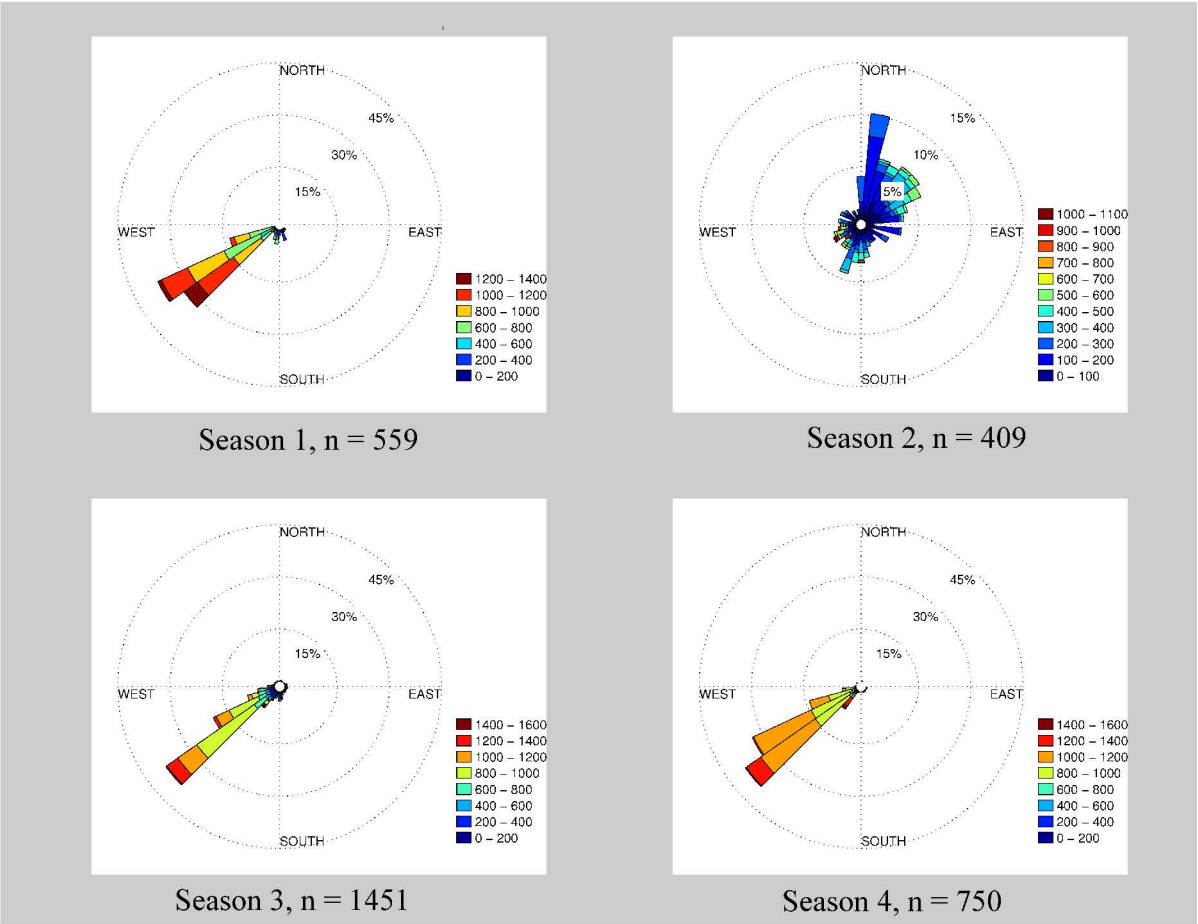

Figure 6.6: 2006: Rose diagrams of angular motion of tuna in recapture Zone B over the seasons. The letter n denotes the number of standardised recaptures to the closest integer. Each of the stripes represent the percentage of tuna that arrived from that particular direction. The colour code is apparent distance (nautical miles, nmi) covered.

It is important to understand the interactions between the angular immigrations in Zone B with the seasons, species type and tagging region. Figure 6.7 shows two box-plots with these interactions for the year 2006. Considering the top plot of the figure, it shows angular movements with seasons and species populating the zone. All three species came from the same direction with the exception of the S2 (Apr-May inter-monsoon) and S3 (SW monsoon) seasons which show a wide variability. It can be noticed that SW monsoon season (Jun-Sept), yellowfin tuna populated the Zone B through the whole angular spectrum and yellowfin also show the largest variability through all seasons except S1 (Dec-Mar monsoon) in comparison to the two other species. It is only in season S2 that major differences of angles among the

three species are observed. The bottom panel (Fig. 6.7), shows that Seasons S1 and S4 have a limited angular dispersion showing that tunas move into the zone from a particular direction (directionally channelled). Zone B shows that tuna arrivals accumulate from all directions but mostly coming from tuna tagged in the Tanzanian region, especially during the SW monsoon (S3). This is also observed to a lesser degree in Seasons S2 and S4.

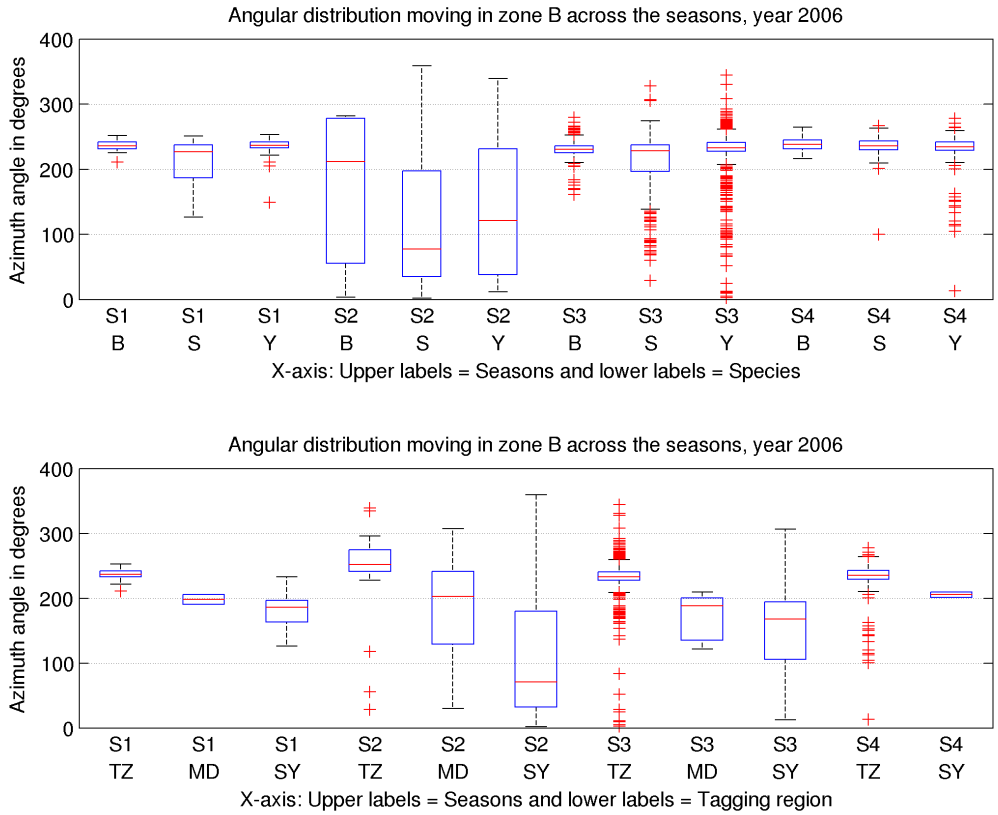

Figure 6.7: 2006: Box-plot of angular migrations to Zone B with respect to seasons, species and tagging region. Where S1= Season 1, S2= Season 2, S3= Season 3 and S4= Season 4; Tz = Tanzania, MD = Madagascar, SY = Seychelles; B = bigeye, S = skipjack and Y = yellowfin. The central mark of the box-plot is the median, the edges of the box are the 25^{th} and 75^{th} percentiles. Whiskers extend to most extreme data points and outliers are plotted individually.

Similar analyses were conducted for the year 2007 for angular movements of tagged tuna in Zone B (Fig. 6.8). With the exception of the Apr-May inter-monsoon (S2), all the three seasons were characterised by similar angular immigrations. Those

three seasons were also characterised by distances of over 800 nmi covered and by angular immigrations which are channelled in one direction. In contrast, the Apr-May season was marked by widespread immigrations in the zone but still directed from the African coast. It is also noted that this season is quite different from what was observed in 2006, whereas the other seasons are similar to the previous year. The direction of immigrations in Zone B over the seasons showed that tuna tagged in the Tanzanian region contributed significantly to immigration to this zone. The Seychelles and Oman region also played an important role in populating Zone B (Fig.6.9, bottom plot).

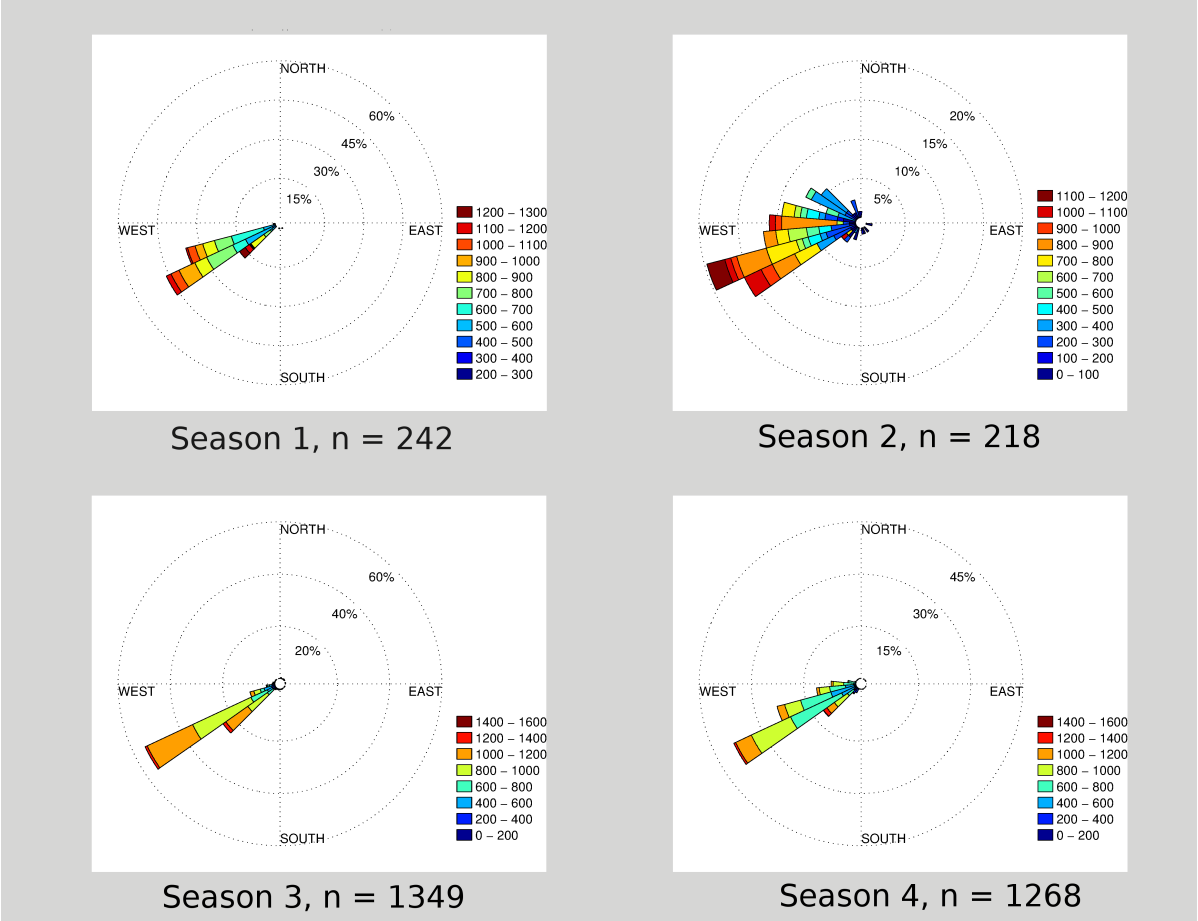

Figure 6.8: 2007: Rose diagrams of angular motion of tuna in recapture Zone B over the seasons. The letter n denotes the number of standardised recaptures to the closest integer. Each of the stripes represent the percentage of tuna that arrived from that particular direction. The colour code is apparent distance (nautical miles) covered.

The top plot of Fig. 6.9, shows the impact of the seasons in relation to species

populating Zone B in 2007. The first season shows similar observation to 2006 where the angular spread was restricted. For Seasons S2 and S4 in 2007, the angular spread was not as large as 2006, only Season 3 (SW monsoon) showed wide angular dispersion with tuna originating from the different tagging regions.

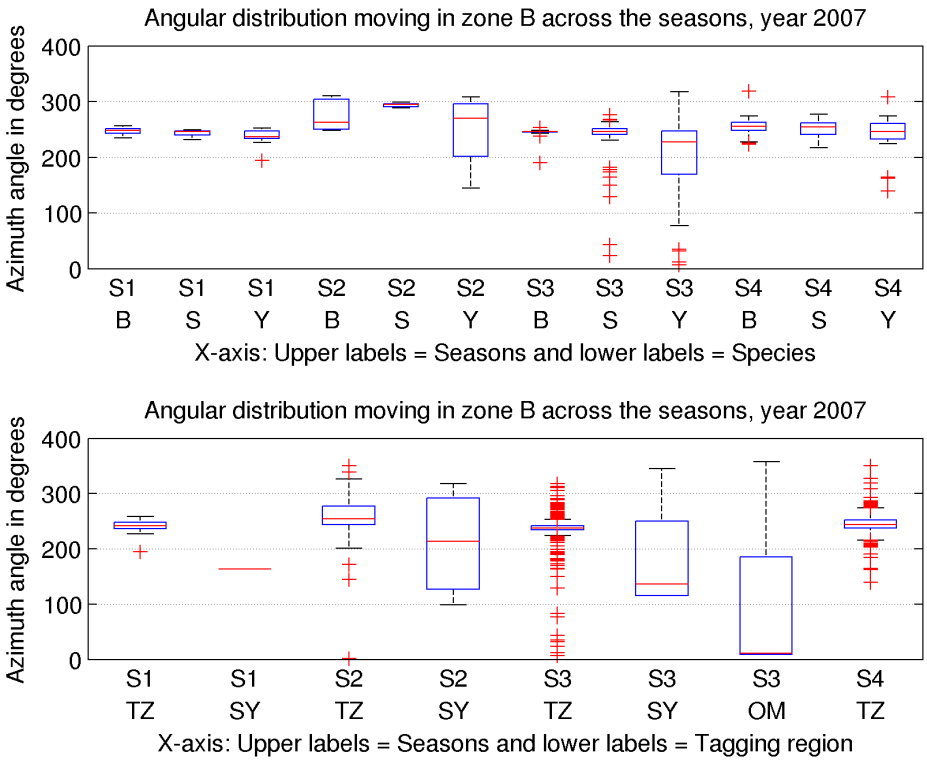

Figure 6.9: 2007: Box-plot of angular migrations to Zone B with respect to seasons, species and tagging region. Where S1= Season 1, S2= Season 2, S3= Season 3 and S4= Season 4; Tz = Tanzania, MD = Madagascar, SY = Seychelles; B = Bigeye, S = skipjack and Y = yellowfin. Central mark of the box-plot is the median, the edges of the box are the 25^{th} and 75^{th} percentiles. Whiskers extend to most extreme data points and outliers are plotted individually.

6.3.5 Sea surface temperature and Chl-*a* distribution at recovery for all years

We compared the environmental conditions (SST and Chl-a) to which tuna moved according to their tagging location. The ANOVA table presented with Fig. 6.10 shows that differences exist. In FS, tuna tagged in Tanzanian and Madagascar

waters were recaptured in similar Chl-a concentrations, whereas tuna tagged in the Seychelles moved to less productive areas. Under FADs, fish tagged in Tanzania, Madagascar and the Seychelles were recovered in similar chlorophyll concentrations. The same observation applies to FADs for tuna tagged in Maldives, Madagascar, Tanzania and the Seychelles, whereas those from Oman moved to lesser productive areas (however, those fish are far fewer). Overall, it is noted that tuna in FS moved to more productive zones than those recaptured under FADs. The SST where fish were recovered under FADs varied between 27 - 28 ^{o}C (median values) except for tuna coming from the Oman tagging region which have a smaller temperature range. SST showed greater variability for tuna recaptured in FS.

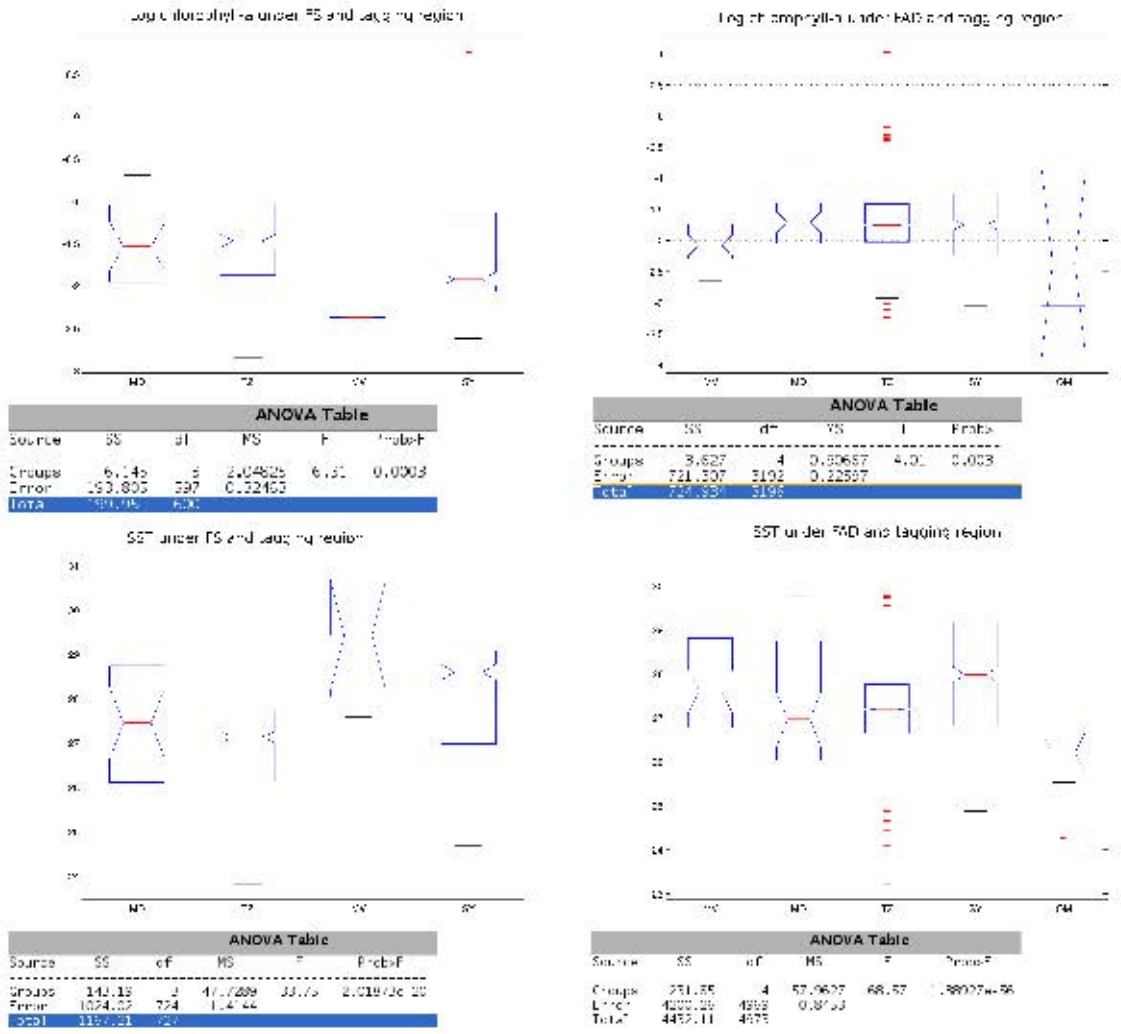

Figure 6.10: ANOVA plot of Chlorophyll (top panels) and SST (bottom panels) with respect to tagging regions in FS (left) and FADs (right). Where Tz = Tanzania, MD = Madagascar, SY = Seychelles, OM = Oman and MV = Maldives. Central mark of the box-plot is the median, the edges of the box are the 25^{th} and 75^{th} percentiles. Whiskers extend to most extreme data points and outliers are plotted individually.

6.3.6 Angular immigration by school type and size of species

Plots of tuna angular immigrations, comparing the school-type at recapture against species size-class at tagging are shown in Fig. 6.11. Under FADs, most tuna came from a similar angular direction (200° to 300°) irrespective of species and size class (Fig. 6.11, upper panel). It should be noted that for juvenile bigeye (Bj), adult skipjack (Sa) and juvenile yellowfin (Yj), there were a large number of outliers showing the direction of immigration from smaller angles or different regions.

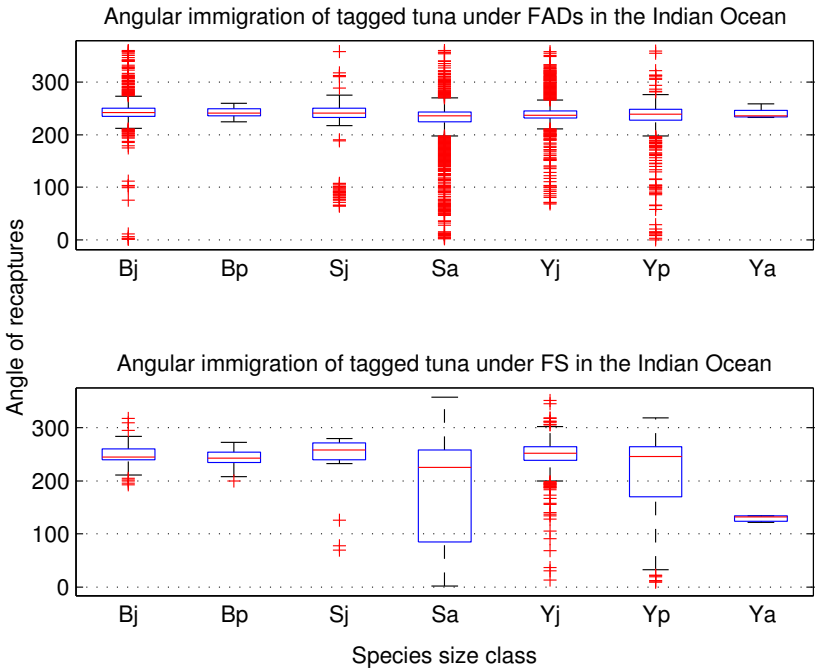

Figure 6.11: Box-plot of angular recaptures (degrees) by size class of species under Free School (FS) and Fish Aggregating Devices (FADs). Where Bj = bigeye juveniles, Bp = bigeye pre-adults, Ba = bigeye adults, Sj = skipjack juveniles, Sa = skipjack adults, Yj = yellowfin juveniles, Yp = yellowfin pre-adults and Ya = yellowfin adults. Central mark of the box-plot is the median, the edges of the box are the 25^{th} and 75^{th} percentiles.

Table 6.9: ANOVA result of angle with respect to tagging regions. Where Tz = Tanzania, MD = Madagascar, SY = Seychelles, OM = Oman and MV = Maldives.

Angular arrivals FS					
	MD	TZ	MV	SY	
means:	160.41	272.25	188.21	130.29	
df:	1032.00				
s:	76.98				
'Source'	'SS'	'df'	'MS'	'F'	'Prob>F'
'Groups'	4909808.51	3.00	1636602.84	276.19	0.00
'Error'	6115168.83	1032.00	5925.55		
'Total'	11024977.34	1035.00			
Angular arrivals FAD					
	MD	TZ	MV	SY	OM
means:	198.02	247.32	136.40	173.90	192.63
df:	5824.00				
s:	35.68				
'Source'	'SS'	'df'	'MS'	'F'	'Prob>F'
'Groups'	2868819.17	4.00	717204.79	563.45	0.00
'Error'	7413221.21	5824.00	1272.87		
'Total'	10282040.38	5828.00			

The species in FS (Fig. 6.11, lower panel) show more angular variations in comparison to fish under FADs. Juvenile and pre-adults of bigeye, juvenile yellowfin and juvenile skipjack have similar directions of immigration with small variations while adults of skipjack, yellowfin and pre-adults yellowfin show a larger span of arrival directions. Table 6.9 shows one-way analysis of variance (ANOVA) output for both school-types. Figure 6.12 depicts the ANOVA plot of angular immigrations with respect to tagging regions in FS and Fig. 6.13 represents the same under FADs. The P values were both 0.00 for FS and FADs, implying that the direction travelled differ significantly across the tagging regions. However, directions travelled show larger variability in FS (Fig. 6.12) than under FADs (Fig. 6.13). Free school tuna tagged near Tanzania which were mostly recaptured in Zone B, show a restricted migration pattern in comparison to those in Madagascar, Maldives and the Seychelles. Tanzanian tagged tuna cannot move in all directions because of the African coast, whilst from the Seychelles or Maldives, they can move in all directions. Under FADs, the mean angular immigrations from the Maldives, Madagascar, the Seychelles and Tanzania show more oriented movements compared to FS, with the exception of tuna tagged in Oman, although they were in reduced numbers, not directly comparable with tuna tagged in other regions.

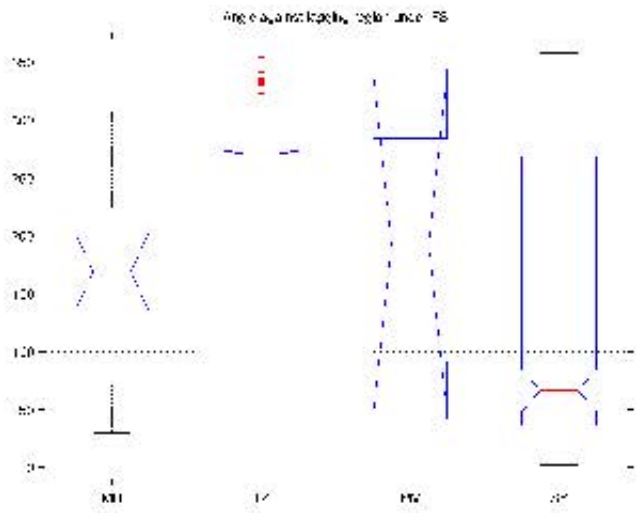

Figure 6.12: ANOVA plot of angle with respect to tagging regions in FS. Where Tz = Tanzania, MD = Madagascar, SY = Seychelles and MV = Maldives. Whiskers denote most extreme data point but not outliers. Central mark of the box-plot is the median, the edges of the box are the 25^{th} and 75^{th} percentiles. Whiskers extend to most extreme data points and outliers are plotted individually.

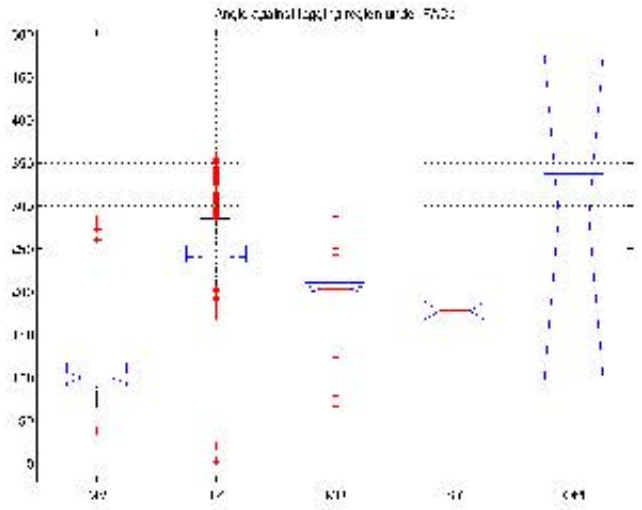

Figure 6.13: ANOVA plot of angle with respect to tagging regions under FADs. Where Tz = Tanzania, MD = Madagascar, SY = Seychelles, OM = Oman and MV = Maldives. Central mark of the box-plot is the median, the edges of the box are the 25^{th} and 75^{th} percentiles. Whiskers extend to most extreme data points and outliers are plotted individually.

To confirm that the angular immigration of the tuna differs according to the school type, a one-way ANOVA analysis was conducted (Fig. 6.14). Tuna in FS and their angular immigrations were sorted and similarly for tuna under FADs. The ANOVA table and the box plots are given below. The boxplots give the comparison interval of the tuna under FADs (labelled 1) and FS (labelled 2) for mean angular immigrations. The table below the figure gives the P value (¡ 0.001) showing that the school types are significantly different. The angular immigrations of the tuna in free schools cover the whole angular spectrum, implying that a mix in the tuna of different origins move together. Tuna under FADs show angular distributions coming from large angular directions with a few outliers at narrow angles.

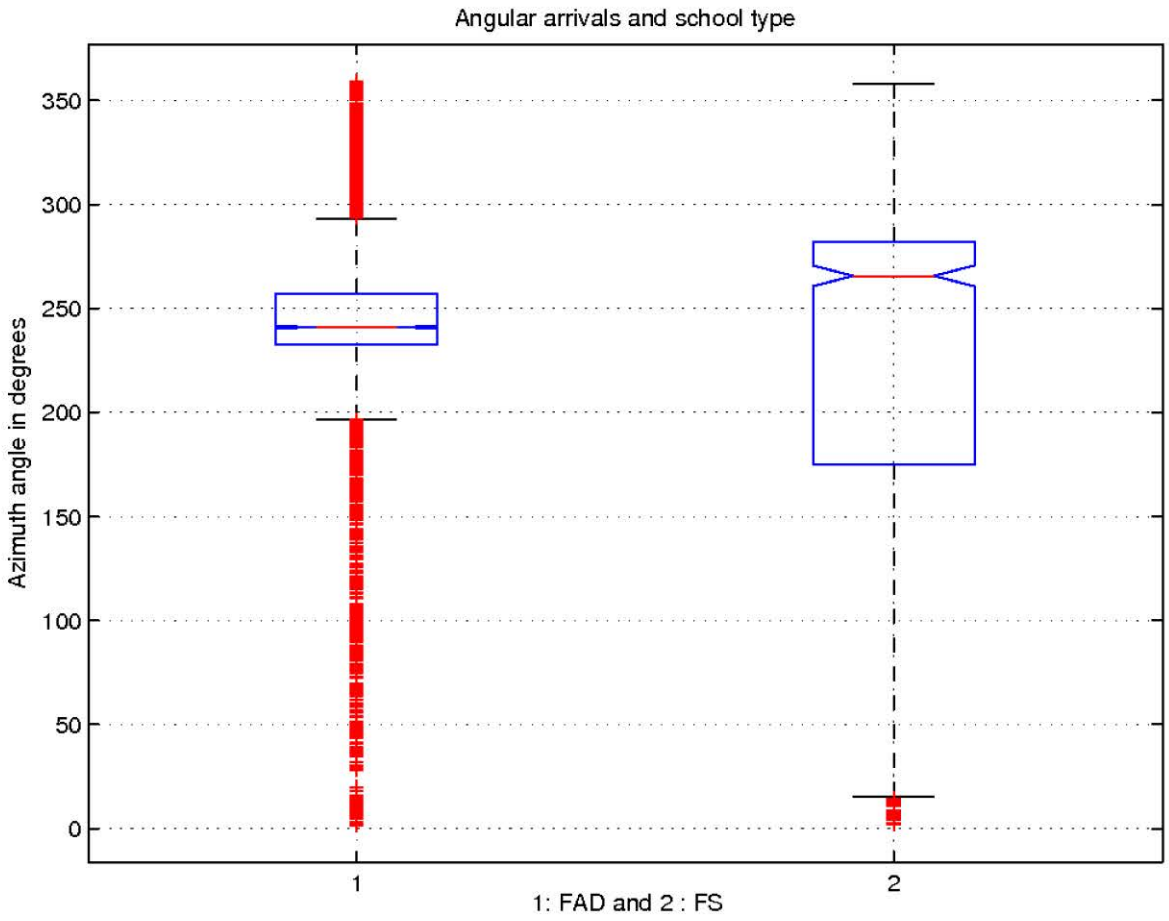

ANOVA Table

Source	SS	df	MS	F	Prob>F
Groups	455087.1	1	455087.1	143.2572	1.02E-32
Error	23920662	7530	3176.715		
Total	24375749	7531			

Figure 6.14: ANOVA plot of school-type and angular immigrations. Central mark of the box-plot is the median, the edges of the box are the 25^{th} and 75^{th} percentiles. Whiskers extend to most extreme data points and outliers are plotted individually.

6.3.7 GAM Analysis

GAMs were used to explore the relationships between the size of fish recaptured and the following variables: distance covered (nautical miles), location of recapture, school-type and environmental variables like SST and Chl-a (log scale). Before exploring different models, a correlation matrix was applied to see dependence among the variables and to select non-correlated variables in the model. Fig. 6.15 shows

the correlation matrix among the variables. The numbered colour codes show the magnitude of correlation and the circled numbers give the p-values, while the size of the circles gives the correlation magnitude. It is observed that there is a good positive correlation between recapture positions and the distance covered by tuna and SST and chlorophyll are inversely correlated (p-value: 0.008, significant). The correlations between for tuna fork length (FL) and the other variables are relatively weak.

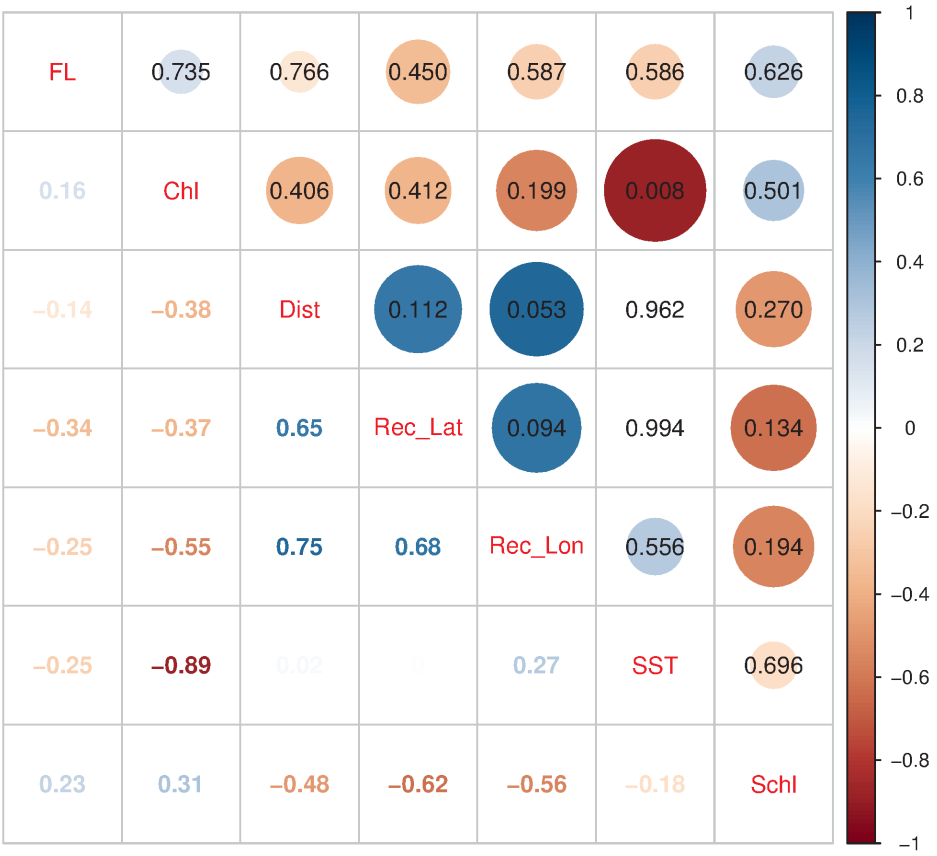

Figure 6.15: Correlation matrix of variables (correlation values are shown). The colour codes show magnitude of correlation and circled numbers gives p-values. 'Rec': recovery, Fl: Fork Length, Schl: school. Note the that empty boxes do not show any colour as their correlation values are near zero (-0.08 and -0.11, left and right)

Based on the correlation diagram above, the influence of the poorly correlated variables to recapture fork length were investigated for 3 types of data (1: complete data (Models 1 and 2), 2: data filtered by FAD (Models 3 and 4) and data filtered by FS: (Models 5 and 6). Their ANOVA results are given in Appendix C. GAM

assesses the impact of predictive variables based on the underlying patterns of the data which most of time have a non-linear relationship. The fitted GAM generated is plotted through the smooth functions which makes up variables. In Appendix C, variables treated as parametric coefficients and approximate significance of smooth terms are shown for each of the models. The algorithm used in this case, plots only approximate significance of smooth terms while considering the interaction of parametric coefficients (species and school). Each of the datasets had 2 scenarios, where the first scenario investigated the effect of Chl-*a*, SST, school, distance and species (Sp) and the second, where distance was replaced with the interaction between recovery longitude and latitude. The deviances explained for Models 1 and 2 were 19.1% and 23.5% when the complete data was considered. For FADs, Models 3 and 4; the deviances explained were 14.1% and 16.9%, respectively. Finally, for FS; Models 5 and 6, the deviances explained were 43.3% and 47.1%, respectively.

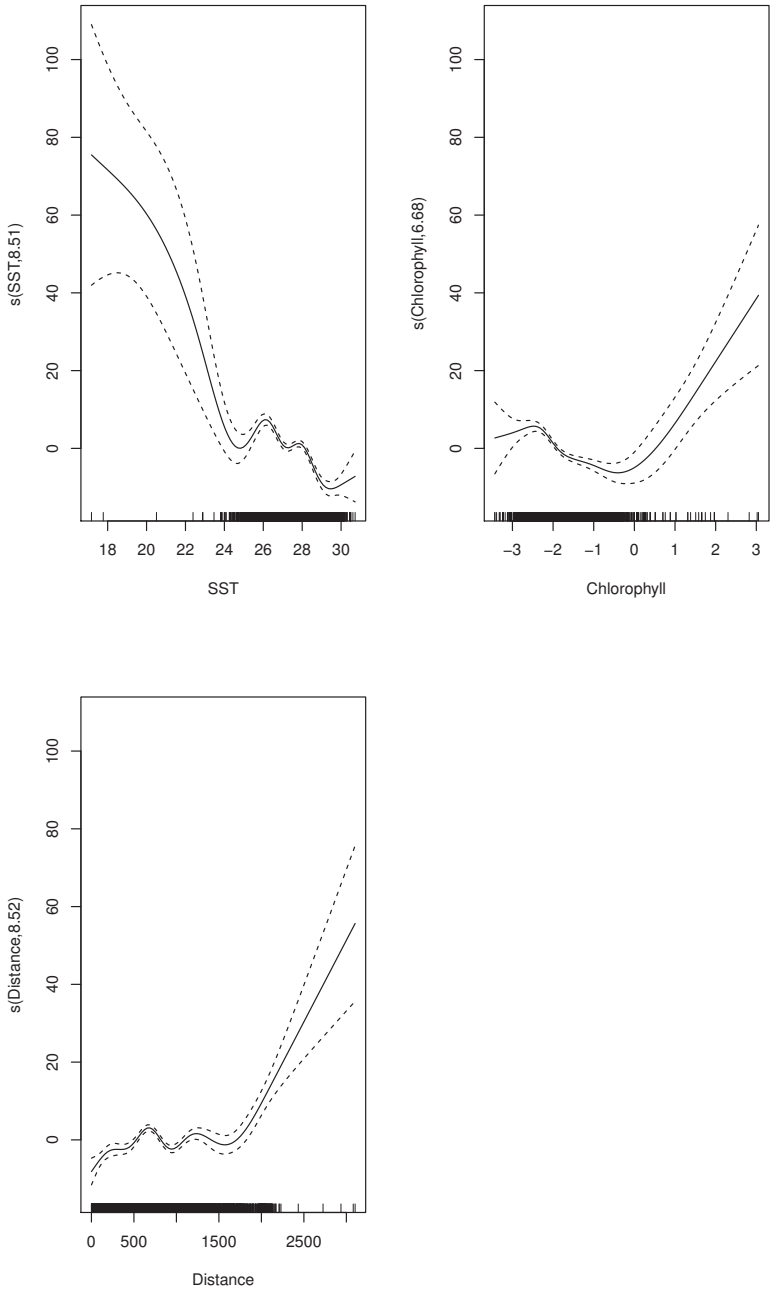

Figure 6.16: GAM Model 1: complete dataset describing relationship of size at recovery with distance, school, species and smoothed terms of Chl-*a* concentration and SST. Density of data is shown on the x-axis.

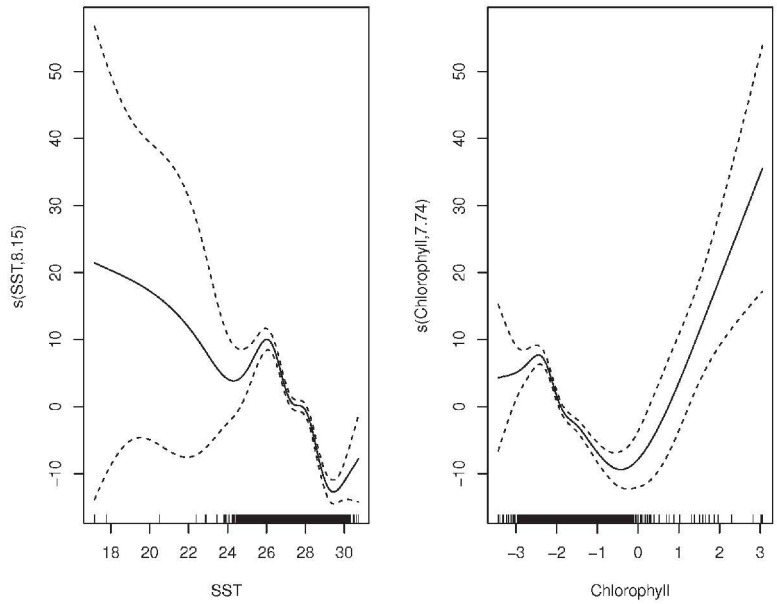

Figure 6.17: GAM Model 2: complete dataset describing relationship of size at recovery with recovery longitude and latitude interaction (Fig. 6.18), school, species and smoothed terms of Chl-a concentration and SST. Density of data is shown on the x-axis.

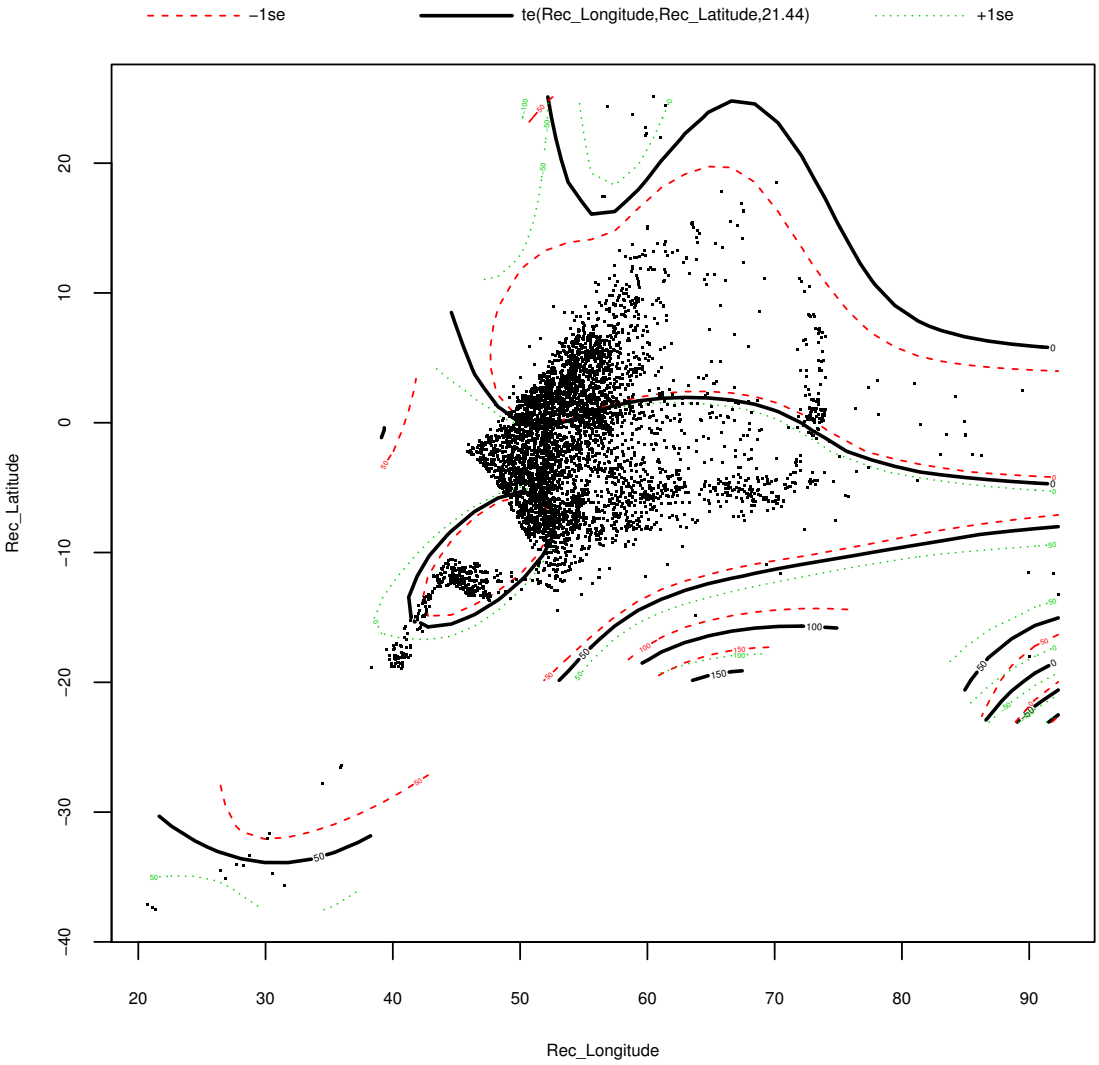

Figure 6.18: Enlarged view of Latitude and longitude interaction of GAM Model 2. The black lines represent the non-linear relationship between size at recovery and the interaction of latitude and longitude.

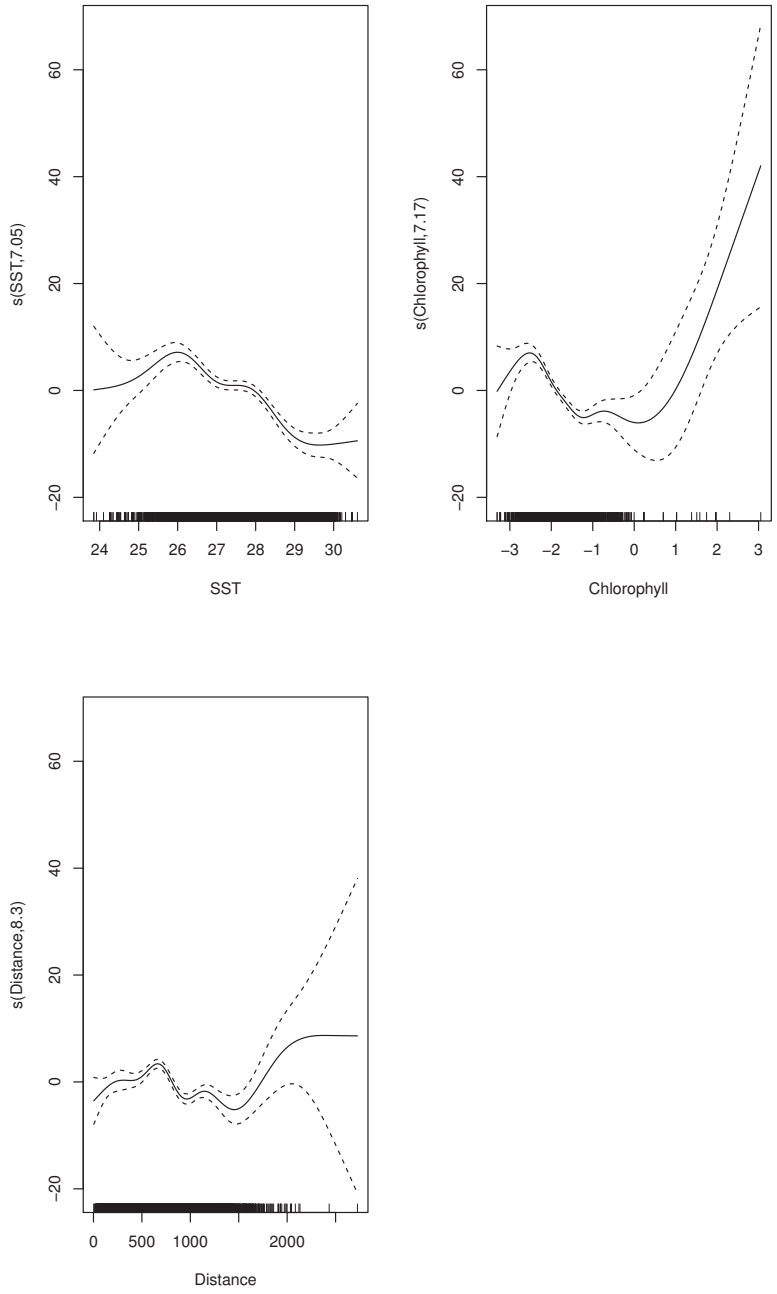

Figure 6.19: GAM Model 3: FADs recoveries describing relationship of size at recovery with distance, school, species and smoothed terms of Chl-a concentration and SST. Density of data is shown on the x-axis

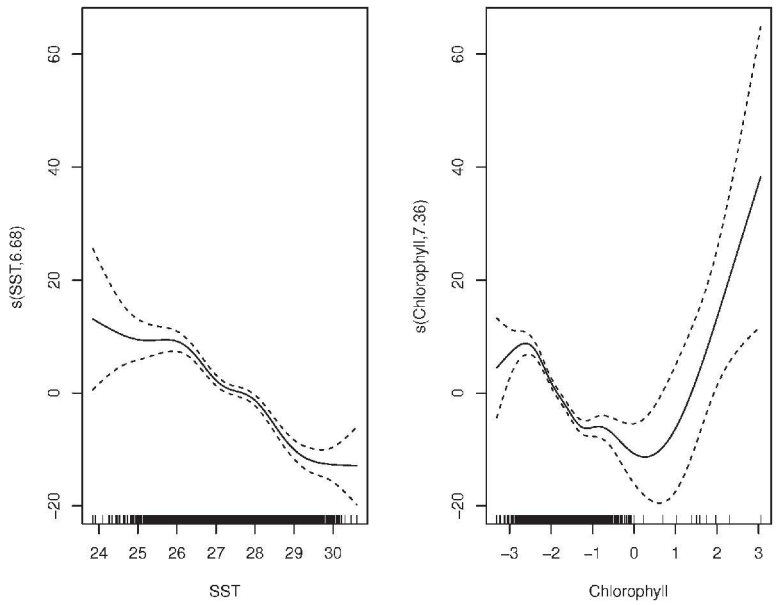

Figure 6.20: GAM Model 4: FADs recoveries describing relationship size at recovery with recovery longitude and latitude interaction (Fig. 6.21), school, species and smoothed terms of Chl-*a* concentration and SST. Density of data is shown on the x-axis.

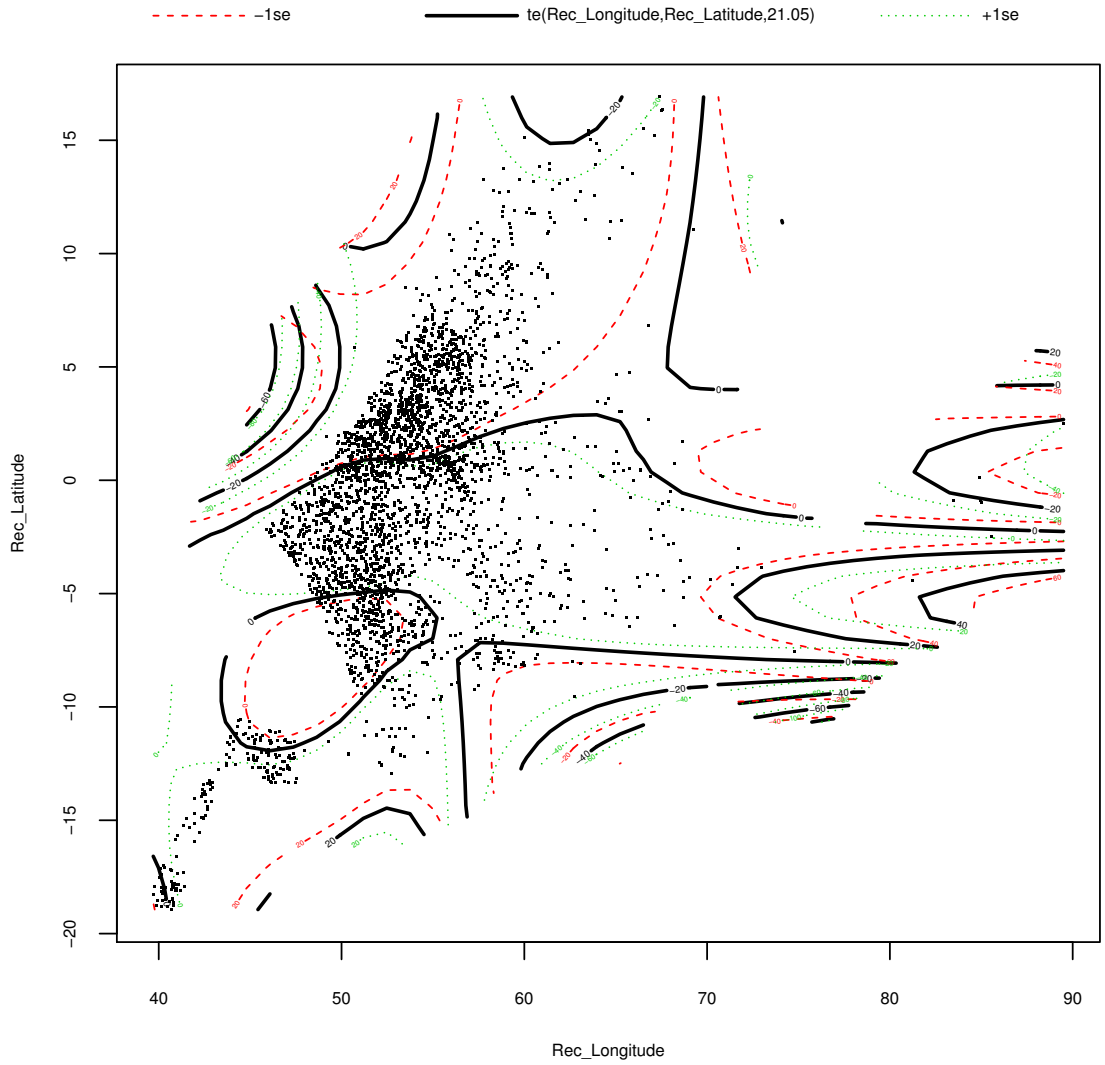

Figure 6.21: Enlarged view of Latitude and longitude interaction of GAM Model 4. The black lines represent the non-linear relationship between size at recovery and the interaction of latitude and longitude.

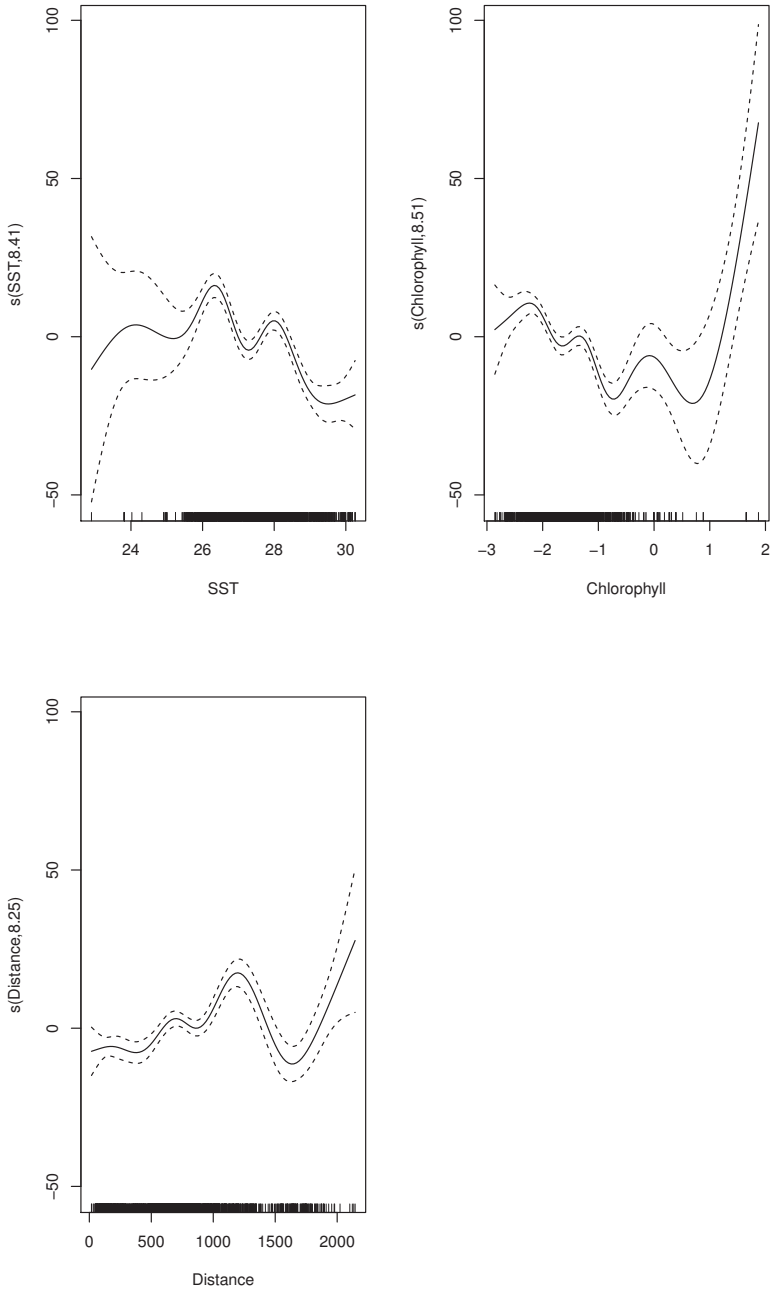

Figure 6.22: GAM Model 5: FS recoveries describing relationship of size at recovery with distance, school, species and smoothed terms of Chl-*a* concentration and SST. Density of data is shown on the x-axis.

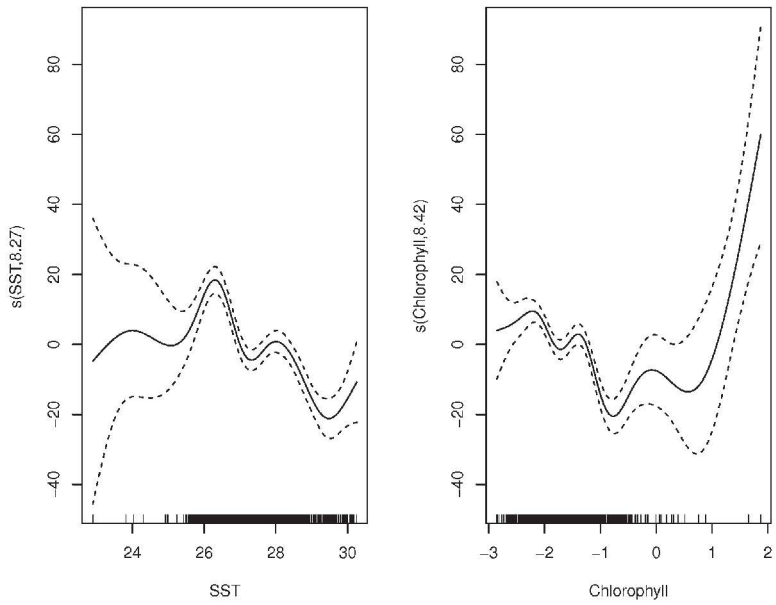

Figure 6.23: GAM Model 6: FS recoveries describing relationship of size at recovery with recovery longitude and latitude interaction (Fig. 6.24), school, species and smoothed terms of Chl-*a* concentration and SST. Density of data is shown on the x-axis.

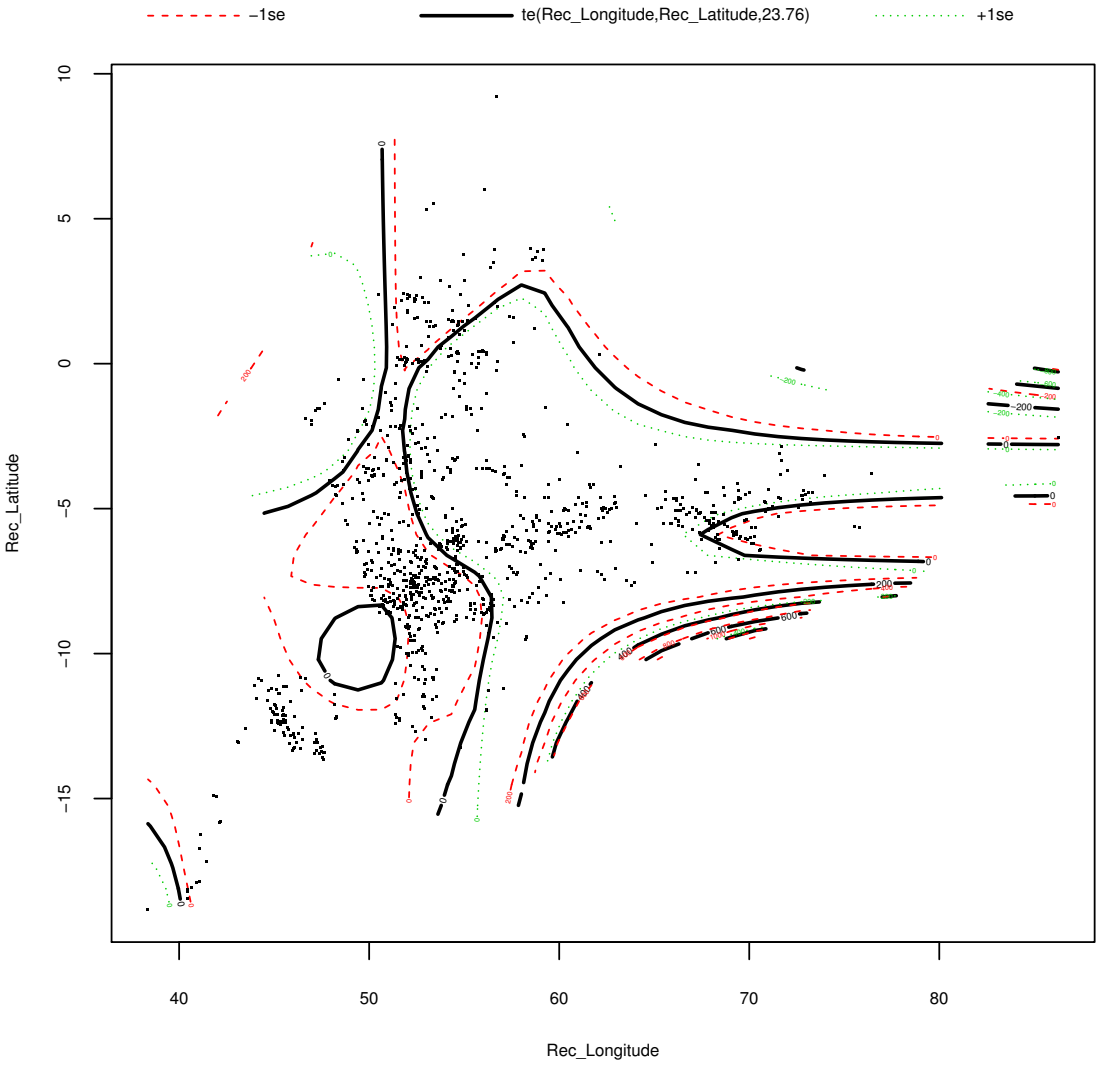

Figure 6.24: Enlarged view of Latitude and longitude interaction of GAM Model 6. The black lines represent the non-linear relationship between size at recovery and the interaction of latitude and longitude.

The Fig. 6.16 shows that small tuna are recovered in relatively warm waters and large tuna in cooler waters while, the chlorophyll plots show small tuna were recaptured in relatively rich chlorophyll zones and as the size increases, they tend to oligotrophic areas. The black ticks on the x axis show the number of observations, Chl-a concentrations of up to 2 (log scale) can be considered in the analysis, but moving along the right of the plot there are fewer observations. Larger tuna move freely towards oligotrophic regions and also to richer Chl-a areas, whereas small

tuna are in moderately Chl-a enhanced waters (Log 0 is for Chl-a = 1 mg.m^{-3}, which is fairly rich). McClain et al. (2004) pointed out that although the biological productivity in oligotrophic regions of gyres is low, the spatial extent of the biological productivity of those regions make the overall region significant. The author defines oligotrophic waters as those with chlorophyll concentrations below 0.07 mg.m^{-3} or a natural log value of -2.65. The distance graph (Fig. 6.16, lower panel) shows that small size tuna move relatively large distances, as there is not much difference until about 1700 nmi (curve is more or less flat) then there is a dramatic change above 2000 miles, with larger tuna moving further. Looking at the latitude and longitude interaction Model 2 (Fig. 6.17), SST and chlorophyll show similar trends as in Model 1. The smoothing curve with respect to temperature shows that warm water preference for small fish (up to 30 ^{o}C) shifts to slightly lower temperatures (25-26 ^{o}C) for larger fishes. With regard to recapture locations (Fig. 6.18), combining latitude and longitude, the area 10^o N - 10^o S and 45^o - 60^o E corresponds to the most favourable region where fish aggregate.

Filtering the dataset for FADs tuna showed similar temperature and chlorophyll trend as described above (Fig. 6.19). The distance plot though, showed more distinction in terms of distance covered where small tuna were recovered quite far from their tagging locations (1500 - 2000 nmi). The latitude and longitude interaction showed that more recoveries were in the western Indian Ocean (Fig. 6.21). The region 5^o N - 5^o S and around 45^o - 55^o E, makes up the area of most recoveries.

The data pertaining to FS only, showed distinctive responses to the variables (Fig. 6.22). Two peak temperatures were observed, where large tuna prefer lower temperatures of (25 - 26 ^{o}C) and smaller tuna in the 28 ^{o}C range. Similarly, peaking trends for Chl-a values are observed, large tuna in low Chl-a regions and smaller tuna found in richer conditions: large tuna in the range of -2.5 - -1.5 (log scale) and on the other extreme, small tuna in Chl-a concentrations of 0 (log scale). In Fig. 6.22, the distance variable shows that distance increases as the size of tuna increase but eventually reaches a maximum while small tuna tend to move even further. The core of the recoveries in FS is likely to be situated in the region of 0^o N and above 10^o S (Fig. 6.24). FS recoveries are more widespread than FAD catches. Although the region 50^o - 60^o E showed considerable recoveries, it is noted that it also stretches

further east to 70^o E.

6.4 Discussion

6.4.1 Tuna dispersion in 2006 and 2007

The recovery seasons of fish in 2006 were dependent on tagging regions. For instance, tuna tagged in Tanzania were recovered across the seasons with the exception of the Apr-May inter-monsoon. The Apr-May inter-monsoon was characterised by tuna tagged from the Seychelles region. The recoveries in 2007 were essentially tuna tagged from the Tanzanian region, which makes sense as most of the tagging effort was deployed there. Although skipjack is commonly known to be the most abundant species compared to yellowfin or bigeye, the South West monsoon showed higher input of yellowfins in 2006. Just like bigeye, few yellowfin were recovered during the Apr-May inter-monsoon of 2006 whereas skipjack were fairly well distributed across the seasons. The bigeye recoveries were more abundant in the NE monsoon in 2006. During 2007, yellowfin and bigeye recoveries were more evenly distributed over the seasons than in 2006. There was an opposite situation for skipjack where the variability of recoveries differed more substantially over the seasons. The fish tagged in the Tanzanian and Seychelles regions were mostly recovered in Zones B and C in both years, noting that Tanzania and the Seychelles also belong to Zones B and C and are also tagging areas. Bigeye abundance in Zones B and C were lower in 2006 while in 2007, their input was considerable. Zone B is mostly characterized by high primary productivity because of upwellings along the coast of Somalia in the SW monsoon. Such high productivity generates energy transfer throughout the trophic pathways and can explain a rather high retention level in the region of fast-growing fish in the region, such as tuna.

Seckel (1972) developed a model of skipjack movement in the North Equatorial Current of the Pacific Ocean and concluded that ocean currents are a possible factor in tuna immigrations. During the NE monsoon, the ocean currents flow southward along the Somalian and Tanzanian coasts, meeting the north-flowing East African current to form the South Equatorial Counter Current (SECC) (Schott and McCreary, 2001). The SECC flows to the East towards and beyond the Seychelles.

During the Apr-May inter-monsoon, the transition period from the northern winter monsoon to the summer monsoon season, the east-flowing SECC eventually merges into the South Equatorial Current (SEC) going westward. This flow causes water masses to flow back to Zone B which may contribute to migration of tuna tagged in the Seychelles to the Zone. During the Apr-May inter-monsoon until the SW monsoon, the flow is observed to go predominantly eastwards (near 15^oS - 0^o and 40^o - 60 ^oE) in the Indian Ocean explaining the eastward movements of tuna from Tanzania. Surprisingly, although the Seychelles region's geographical location would allow access to Zones A, F, H and even G, tuna movements have been restricted to the south west towards Tanzania and the Mozambique Channel. Indeed, we considered time at liberty of less than 6 months, but even tuna from the Maldives have moved down to the south west and Mozambique Channel which has been identified as a potential tuna nursery ground, like the Seychelles (Fraile et al., 2013). Visualising geostrophic currents for NEM season over the years, there are indeed flows leading to the Mozambique Channel, although it is difficult to predict the exact pathway the tuna might have taken, as the dart tagging technique gives only two tuna locations: tagging and recapture.

6.4.2 Effect of the environment and the school type of recaptured tuna movement

Angular immigrations of tagged tuna under FADs showed no difference irrespective of size-class and species as they are potentially attached to FADs with limited ability to move because in a natural situation (i.e. FADs acting as an ecological trap; Marsac et al. (2000), Hallier and Gaertner (2008)). By contrast, there is an observed grouping by size-class and species for recoveries made in FS. Rajapaksha et al. (2010) investigated sea surface temperature, chlorophyll and sea surface height in relation to yellowfin tuna in the north-west Indian Ocean. They found that there was a significant association between the oceanographic variables and yellowfin tuna catch. They reported that high catch rates were linked to areas where the SST was 28 - 30 °C and Chl-a 0.1 - 0.4 mgm^{-3}. It is noted that the Apr-May inter-monsoon registered high temperatures and lower Chl-a concentration. Zagaglia et al. (2004) suggested that migratory movements of yellowfin observed to be associated with SST

above 28 °C which is concurrent with the temperature in our findings but inclusive of bigeye and skipjack tuna.

The differences in the temperatures at recovery in FS and FADs would suggest that tuna in FS have a greater liberty to move from one environment to another than tuna associated with FADs. The temperature range was wider in FS tuna recoveries as compared to those under FADs and FS tuna were recovered in more productive waters. These observations would suggest that tuna in FS move freely and look for optimum conditions for breeding, especially for yellowfin whose spawning grounds are located in the equatorial counter current in the Dec-Mar monsoon season (IOTC, 2014). During their movements, tuna in FS can visit different water masses (with different properties) whereas FAD associated tuna would be retained in the same water mass (with smaller SST and chlorophyll gradients), as they drift along with the FADs.

Zones D and E correspond to the Mozambique Channel and the tropical gyre, respectively. Tuna visit these regions during the austral summer and inter-monsoon, and thus, recaptures below 26 °C were not observed. Zone F (Maldives) shows a Chl-a pattern distinct from the surrounding regions only during the first semester. However, no recaptures were made in this zone although tagging operations took place there. Despite the low in Chl-a concentration in Zone B during the Apr-May inter-monsoon, warm temperatures seem to be a factor enhancing tuna movements. Tables 6.5 - 6.8, further confirms the marked seasonal difference between the inter-monsoon Apr-May and the other seasons which have contributed to movement of tuna from the Seychelles and Madagascar.

6.4.3 Movements towards Zone B

The rose plots of tuna movements for the year 2006 show similar movement patterns across the seasons except for the Apr-May inter-monsoon. Considering Zone B (off the African coast 12^o N - 10^o S and 58^o E, see Fig. 2.13) for this season, movements of tuna were found to be coming from all tagging directions to the zone in comparison to the remaining seasons where the tuna came mainly from Tanzania in the south. This can be explained by the Chl-a distribution. During the same season, the surface boundaries with regard to Zone B enlarge in terms of Chl-a distribution. Hence,

tuna from the Seychelles and Madagascar were not restricted by the chlorophyll distribution. With respect to the year 2007, the widespread of angles of tuna arriving in the Zone B during the Apr-May inter-monsoon season can be explained by the fact the tuna tagged in Seychelles contribute to the overall angular distribution. Although tuna were tagged in Oman in the SW monsoon season, very few tuna arrived in Zone B from Oman. It should also be noted that during the SW monsoon (Jun-Sep) season, the northern region shows peaks in Chl-a blooms and tuna are likely to move to higher latitudes than going to Zone B. Another factor is the IOD, the central Indian Ocean and the region not so far from Tanzanian coast experiences a positive SST anomaly while the northern part is cooler during the months of July to August (Saji et al., 1999).

6.4.4 Variations in the size of recaptured fish

A number of variables have direct impact on the behaviour of tuna as well as indirect and complex effects that should not be interpreted linearly. For regression, additive models offer an adaptable modelling capability. Using GAMs, the idea was to see conceptually how the size of recaptured tuna was influenced by chlorophyll concentration, distance covered (or locations of recovery), SST and the school-type in a parsimonious way along with the species criteria. These variables are known to be key properties that will determine the aggregation of fish in a particular area of the ocean. Montero et al. (2016) studied the interactions of these variables for the Olive Ridley turtles which are a by-catch of tuna fishing. Although the study was directed towards the Olive Ridley but related to tuna catch, it is interesting to note the variable range they considered as predictor for the probability of a capture event. They found that water temperatures (SST) 26 - 30 ^{o}C and chlorophyll concentration of less than 0.36 mg^{-3} were associated with the highest probability of an incidental catch. These temperature ranges correspond to the temperatures predicted for tuna using GAMs. Moreover, the school-type plays a distinct role for the environment and area in which tuna are likely to be found. In addition to be sparsely dispersed from north to south, the FS tuna are likely to be dispersed along the South Equatorial Counter Current. There is no purse-seine fishing in the South Equatorial Current. All purse-seining is within the Somali current, the East African

Coastal Current and the Equatorial Counter Current. FAD associated tuna move shorter distances than FS tuna, as shown the latitude and longitude interaction plots. The plots have shown that there are distinct environmental ranges which can be quantified based on the school-type that tuna are associated with. The environmental cues characterise the behaviour and movement of the tuna and considerably influence their spatial distribution.

6.5 Conclusion

The results of the analyses carried out have given indications of the effects of the environment on short-term tuna movements, putting emphasis on locations of recovery. It is seen that the inter-monsoon period April-May changes the general movement pattern of tuna. Although immigration to Zone B (east of the Somalian coast) comes predominantly from the Tanzanian tagging region during the NE monsoon, the SW monsoon and Oct-Nov inter-monsoon, the Apr-May seasons do not conform to this pattern when most of tuna come from the Seychelles and Madagascar. This observation applies to both years 2006 and 2007. Tuna tagged in Tanzanian waters contribute significantly to the overall distribution of recoveries but the seasonal effect on tuna from regions of Seychelles, Madagascar and Oman can be seen too. Oman's tagged tuna showed limited movement to Zone B during the SW monsoon season along with the IOD impact.

Tuna swimming in schools under FADs come from similar angular directions irrespective of the species and size-class. FS tuna showed marked differences by species and size-class over the seasons. There is a clear distinction between recaptures of tuna under FADs and in FS, fish from FS are likely to have a higher diversity in regions of origin. The GAM analysis shows how SST, chlorophyll, type of school and species have specific responses in terms of size of fish at recovery. However, the effect of such analysis is limited as fish of very large sizes were seldom among the fish recaptured. Large tuna tend to move to areas with environmental and geographical conditions in terms of Chl-a (-2.5 - -1.5 log scale or 0.08 - 0.22 mg^{-3}) and SST (26 - 29 ^{o}C); from oligotrophic to moderately chlorophyll rich waters. The core of recovery positions is school dependent, focused on the western part of the Indian

Ocean for tuna under FADs while for FS tuna there is a more widespread dispersion from south to north but stretching eastwards along the 5^o S latitude.

Chapter 7

Indian Ocean currents and tuna migrations

7.1 Introduction

The environment is known to be a key driver affecting marine species and our understanding is largely reliant on our capacity to observe large-scale spatio-temporal dynamics (Alvarez et al., 2013). Our understanding of the availability and especially the sustainability of tuna is therefore linked to our ability to forecast the dynamics of the marine environment. With the present know-how and technology, forecasts of the marine environment have improved rapidly but we are far from understanding all the underlying factors influencing the marine environment; nonetheless the estimates are improving. It is commonly admitted that in development of sound management strategies for marine resources, the influence of the ocean environment should be understood, especially with climate change threats to marine ecosystems increasing (Parmesan and Yohe, 2003). Furthermore, in the context of climate change, it is relevant to accurately identify oceanic regions inhabited by marine species and how they evolve with time, to implement proper management strategies to ensure its sustainability of the marine resources. For all of these reasons, predicting the movement of the main marine species is a priority (Gaspar et al., 2006).

Previous studies of skipjack movements conducted in the Pacific Ocean showed that the ocean currents are a possible factor for tuna travel (Seckel, 1972). In this chapter, an attempt is made to understand tuna displacements in the Indian Ocean

by comparing five main factors, with respect to the ocean surface hydrodynamics. Satellite altimeter data (i.e., absolute dynamic topography) give the possibility of computing geostrophic velocities through geostrophic balance equations, which are essential parameters for many ocean properties. Those data of medium to high resolution over the world are useful for studying the ocean dynamics over long temporal and large spatial scales. To this end, geostrophic current coupled with maps of absolute dynamic topography (MADT) data from satellite sensors on a daily basis were used to investigate the degree to which tuna displacement is affected by ocean surface currents in the Indian Ocean from their initial tagging locations.

Using the dataset available from the RTTP-IO programme, the influence of ocean currents on the three species of tuna was investigated. The strategy adopted was to look into the displacement of tuna as a mass movement where the movement is likely to be influenced by the ocean surface currents. Here, we shall use different configurations combining ocean current and tuna speed in order to assess their potential in predicting recovery locations.

7.2 Methodology

Tuna distribution in the ocean can be seen as a combination of their own swimming effort and the effect of ocean currents (Seckel, 1972; Gaspar et al., 2006). The tagging dataset set contains the latitude and longitude at release, and an estimated latitude and longitude at the recapture by fishing vessels (primarily purse-seiners). The period between release and recapture, defined as the time-at-liberty, is known but tracks of the tuna between the locations of release and recapture, are impossible to acquire using dart tags (i.e., 'spaghetti' tag). Theoretically, this implies that only the effect of the ocean current from tagging to recovery locations can be investigated whereas the real trajectory followed by the tuna cannot be determined. However, a few assumptions of the swimming vector of the tuna can be stipulated. The study was limited to tuna with time-at-liberty longer than one month but less 181 days.

At the first stage, the tuna were considered as a passive particle drifting over the ocean surface, that is having no means of propulsion. The second stage is that the fish were attributed with an average speed of 0.5 body length per second

(bl.s^{-1}, recapture fork length (FL)) for tuna under FADs and 1 bl.s^{-1} for tuna in FS. Finally, the analysis was carried out with the tuna attributed with a swimming speed (maximum speed) and again depending on the school-type they are associated with, based on literature (discussed below). Therefore, considering species, individual swimming speed and school-type factors, the following scenarios tuna drift due to surface ocean current were simulated:

- species as passive particles,
- species attributed with an average speed (0.5 bl.s^{-1} for FADs and 1 bl.s^{-1} for FS),
- species attributed maximum speeds,
- two size groups (small, FL: $<$ 70 cm and large, FL: $\geq$ 70 cm) with maximum speeds,
- school type with maximum speeds.

The cut off value of 70 cm (maximum size for small size category) has been chosen because juvenile bigeye was considered to be below 70 cm. This value would include skipjacks and juvenile yellowfin.

7.2.1 Ocean current versus swimming depth of tuna

The swimming depth of tuna is an important factor to be considered because of the Earth's rotation, the magnitude and direction of the current varies from layer to layer (Ekman, 1905). Considering a steady wind direction, the surface current moves at 45^o to the right in the northern hemisphere and left in the southern hemisphere with the deflection increasing to 90^o, due to Coriolis force. It is assumed that the Ekman layer rangers from 60 to 120 m depth in winter and from 30 to 60 m during summer (Rio and Hernandez, 2003). Furthermore, Ekman assumed that the bathymetry of the ocean is homogeneous, steady and linear. It would be desirable to consider the range of depth where a tuna can potentially patrol, but as we do not have such information, we shall only consider movements in the mixed layer. Moreover, since most of the data were composed of near surface purse-seine catches and data are

based on dart tags that give no indication of depth, it is justified to assume that the tagged tuna were mostly caught as surface schools (Sabatié et al., 2004).

7.2.2 Altimetry data in the Indian Ocean

We used altimeter products of absolute geostrophic velocities and Maps of Absolute Dynamic Topography (MADT) produced by Ssalto/Duacs and distributed by Aviso, with support from Cnes (http://www.aviso.altimetry.fr/duacs/). The altimeter products were downloaded from January 2005 to November 2007. Taking into account the average distances covered by the tuna of the order of 400 - 600 nmi, the spatial (1/3° x 1/3° on a Mercator grid) and the temporal resolution (daily basis) may provide a good estimate on this spatio-temporal scale.

7.2.3 Simulating tuna drift

Any object in the ocean without any means of propulsion will be subject to drift, as a result of forces from ocean currents, winds and waves. Consequently, considering ocean surface current only, a school of tuna will theoretically have a total displacement (S_{to}) expressed as the sum of resultant displacement (S_{oc}) due to ocean currents and displacement (S_{ts}) of the tuna school relative to ocean current.

$$S_{to} = S_{oc} + S_{ts} \tag{7.1}$$

Considering the above equation, displacement as a result of ocean currents and the individual tuna can be calculated separately. Therefore, over the long term, the net displacement can be calculated as the resultant of the ocean current (S_{oc}) and the individual movement of the tuna. Hence, the overall displacements (S_{to}) would be a summation of the change in velocities from one point to another by each time step, due to ocean current and individual tuna. A number of studies have documented swimming speeds for tropical tuna, which is expressed either relatively to the fish size (body length per second, $bl.s^{-1}$) or in absolute speed ($m.s^{-1}$). Dewar and Graham (1994) found the mean swimming speed for a group of yellowfin to be 2.1 $bl.s^{-1}$ about the size of 51 cm, while Holland (1990) found speeds of 1.24 to 2.01 $m.s^{-1}$. Marsac and Cayré (1998) looked into the swimming speeds of yellowfin in

relation to their school-type and, found speeds of 1.24 m/s (for FS) and 0.87 m/s (for FAD associated). They observed the median swimming speed of the offshore yellowfin to be 1.20 m.s^{-1} at night and ranges from 0.70 to 1.90 m.s^{-1} during the day. For instance, on average for the different fish tracked in 1995-97, the speeds were converted into body lengths which ranged from 1.2 to 2.2 bl.s^{-1} for free school tuna and 0.5 to 0.9 bl.s^{-1} for FADs tuna (Marsac and Cayré, 1998). Although, these speeds were for yellowfin, as tuna of the same size class are considered here (skipjack and juveniles yellowfin and bigeye), it can be assumed that their speeds are close. Hence, we used tuna speeds corresponding to the school-type tuna were associated with. A tuna under FS was given a minimum speed of 1.2 bl.s^{-1} and a maximum speed of 2.2 bl.s^{-1}. For tuna swimming under FADs, a minimum speed of 0.5 bl.s^{-1} and a maximum speed of 0.9 bl.s^{-1} were attributed. The displacement S is expressed as a product of change in velocity ($\triangle$V) over time (t) to move from one point to another expressed by the following equation:

$$S = \triangle V \times t \tag{7.2}$$

The above equation can be further translated into Eqn. 7.3, a summation of the product at each time step (t_i), the final velocity (V_{i+1}) and the initial velocity (V_i).

$$S = \sum_{i=1}^{n} (V_{i+1} - V_i) t_i \tag{7.3}$$

To evaluate the ocean current from one point to another in a two-dimensional coordinate system, the geostrophic equations to calculate velocities are given by the following equations published by Cushman-Roisin and Beckers (2011) and Robinson (2010).

$$f = 2\Omega Sin\varphi \tag{7.4}$$

$$\Omega = \frac{2\pi}{86160} \tag{7.5}$$

$$v = \frac{g\delta ADT}{f\delta x} \tag{7.6}$$

$$u = \frac{-g\delta ADT}{f\delta y} \tag{7.7}$$

In such a formulation, u and v are the horizontal (zonal) and meridional components of the geostrophic velocity, respectively; f is the Coriolis parameter (equation 7.4); g (9.80663 m/s^2) is the acceleration due to gravity; φ is the latitude and x and y are the zonal and meridional distances. These simplified equations of motion apply to homogeneous, frictionless and rapidly rotating fluids. The term Ω is the Earth's rotation rate or angular velocity in rad/s (equation 7.5).

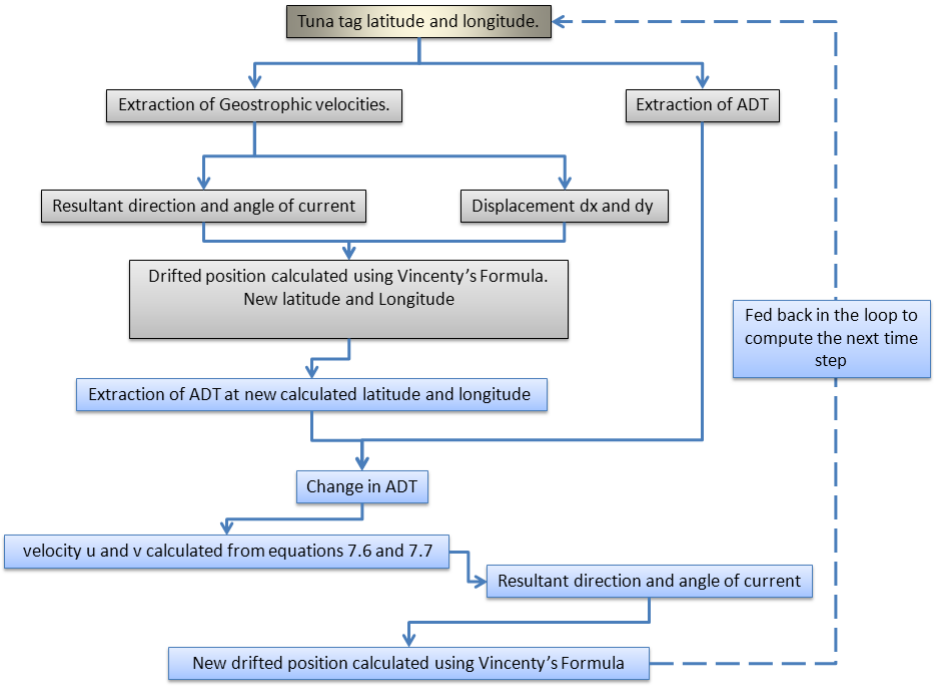

Figure 7.1: Algorithm work flow simulating tuna drift. Grey boxes represent initial conditions required for simulating drift.

Fig. 7.1 shows the algorithm flow-chart tuna drift simulation. Therefore, for a particular tuna tagged, the first step was to extract geostrophic velocities using AVISO data corresponding to the tag position and date. Using the extracted geostrophic velocities u and v, the angle of drift and the displacement are calculated as the initial conditions. The initial angle, displacement, latitude and longitude positions are used to calculate an approximate drifted position by applying Vincenty's formula (Vincenty, 1975) for one time step (1 day). Absolute dynamic topography

(ADT) is then extracted for the calculated drifted and the tag positions. These extracted values are then entered into equations (7.6) and (7.7) to obtain the v and u components and angle of drift from the surface gradient. Finally, a new drift position is calculated for the same time step based on the surface gradient. The newly calculated coordinates now become the initial conditions for the next time steps (day 2). The algorithm runs until the number of time steps has been computed to the date of recapture, which is equivalent to the time-at-liberty of the tuna. This process is repeated for each tuna through the whole dataset.

7.3 Analysis and Results

7.3.1 Tuna drift: passive and active case

The distribution of the three species were plotted to assess the geographic representation of simulated distribution (in blue) to actual recapture positions (in green) in Fig. 7.2. Note that a few red marks (visible on the map) depict the tagging positions. On the left, the simulation was carried without any forcing speed attributed to the tuna, which meant that they were similar to a drifting object (passive case). On the right panels, the tuna were moving at an average speed of 0.5 bl.s^{-1} under FADs and 1 bl.s^{-1} in FS at each time step of the calculation (active case). In this figure, dispersion shows that a better match between simulated and actual recaptures is obtained when considering swimming speed compared to a passive drift case. However, simulated recaptures were still not very close to the actual positions as seen from the ECDF plots (Fig. 7.3).

Figure 7.3 depicts ECDF plots of the simulated drift (in red) latitudes and longitudes with actual recovery positions (in blue) of the three tuna species. It is noted that the simulated drift positions were underestimated in both passive and active cases. The discrepancy between actual and simulated positions is larger for tuna with passive drift only.

The percentage error in simulated and actual recapture positions was calculated as shown in Fig. 7.4. Errors with large magnitudes are shown by the peaks, but if emphasis is laid on reduced error magnitudes (the lower peaks), it is observed that tuna with a swimming speed showed a lower percentage error than the passive ones.

The calculation in latitude points (in blue) deviate more than longitude points (in red) in relation to the actual recapture positions.

Considering the plots species wise, it is difficult to contrast among them. Comparing the three species in the active case, it can be observed that geographically skipjack tuna were slightly better distributed than bigeye and yellowfin, which is confirmed by the ECDF and percentage error plots. Looking at the ECDF plots, yellowfin tuna were slightly closer to actual recovery relative to bigeye but the percentage errors plots does not show much difference.

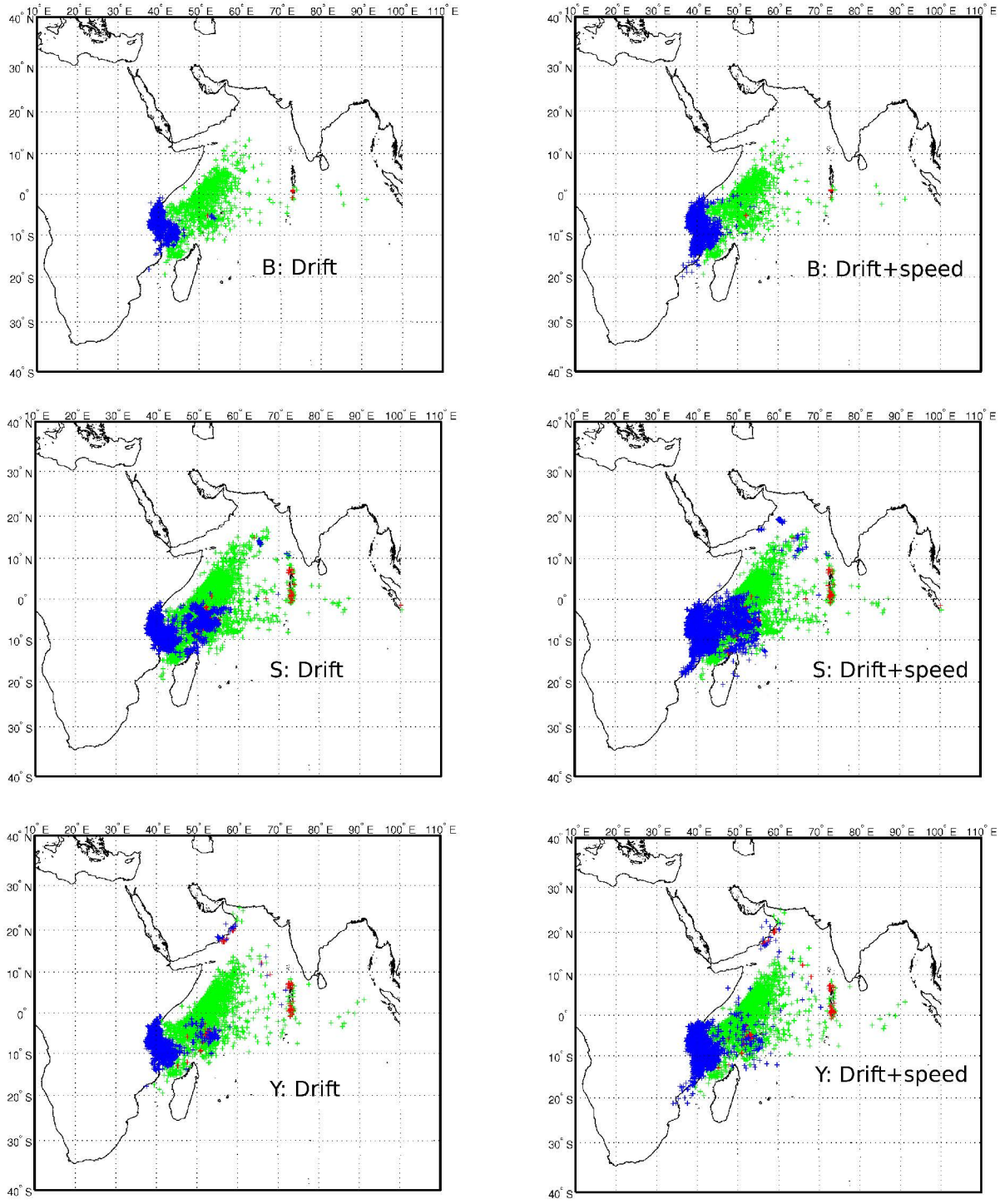

Figure 7.2: Bigeye (S), skipjack (S) and yellowfin (Y) distribution from simulated drift, passive (left column) and active (right column) cases. Passive refers to tuna without swimming and active refers to tuna with swimming speeds of 0.5 bl.s-1 bl.s^{-1} under FADs and 1 bl.s^{-1} in free schools. Simulated distribution (in blue), actual recapture positions (in green) and visible red marks are the tagging positions.

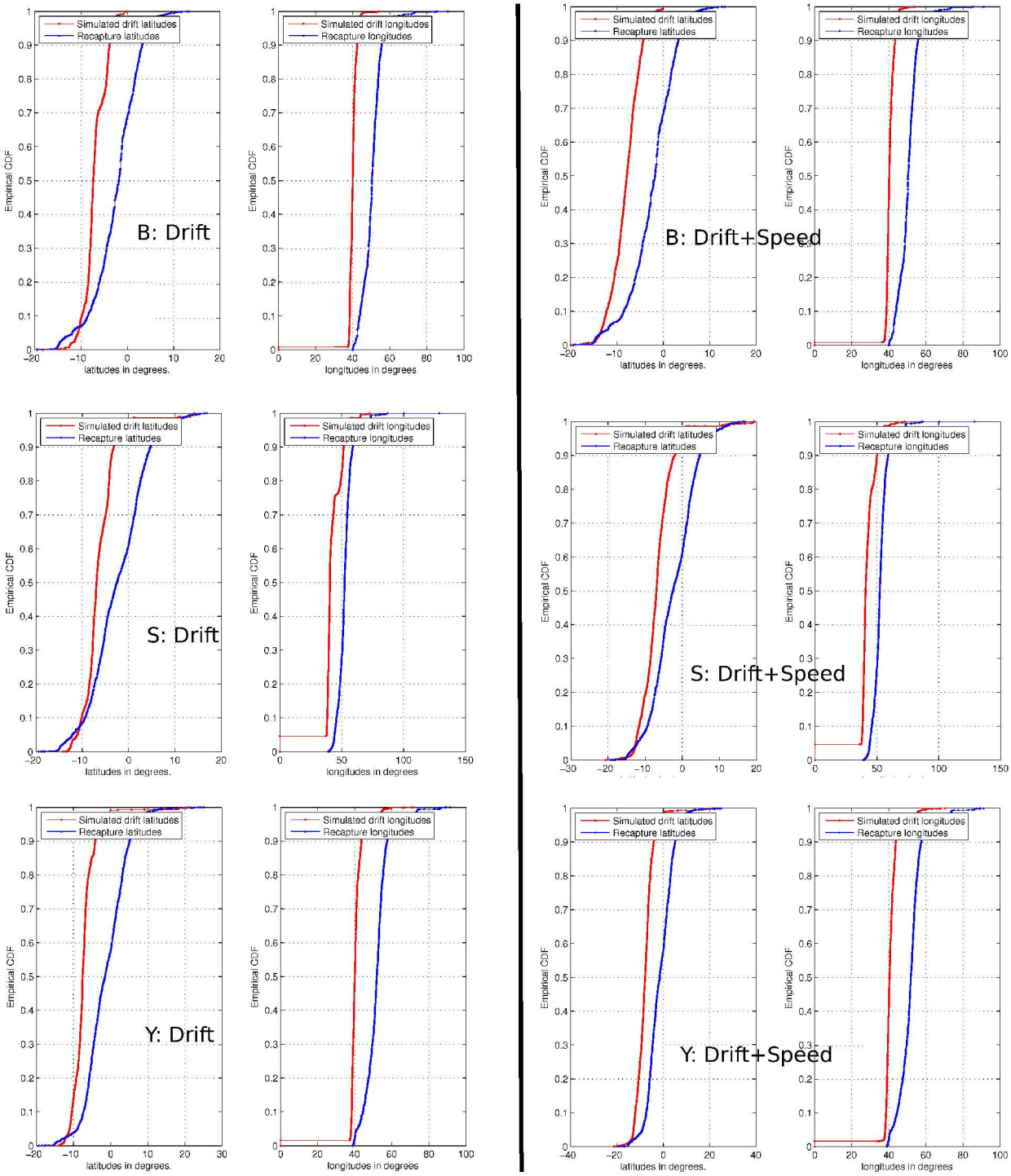

Figure 7.3: ECDF plots of bigeye (B), skipjack (S) and yellowfin (Y) distribution from simulated drift, passive (left column) and active swimming (right column) cases. Passive refers to tuna simulated without swimming and active refers to tuna with swimming speeds of 0.5 bl.s-1 bl.s^{-1} under FADs and 1 bl.s^{-1} in free schools.

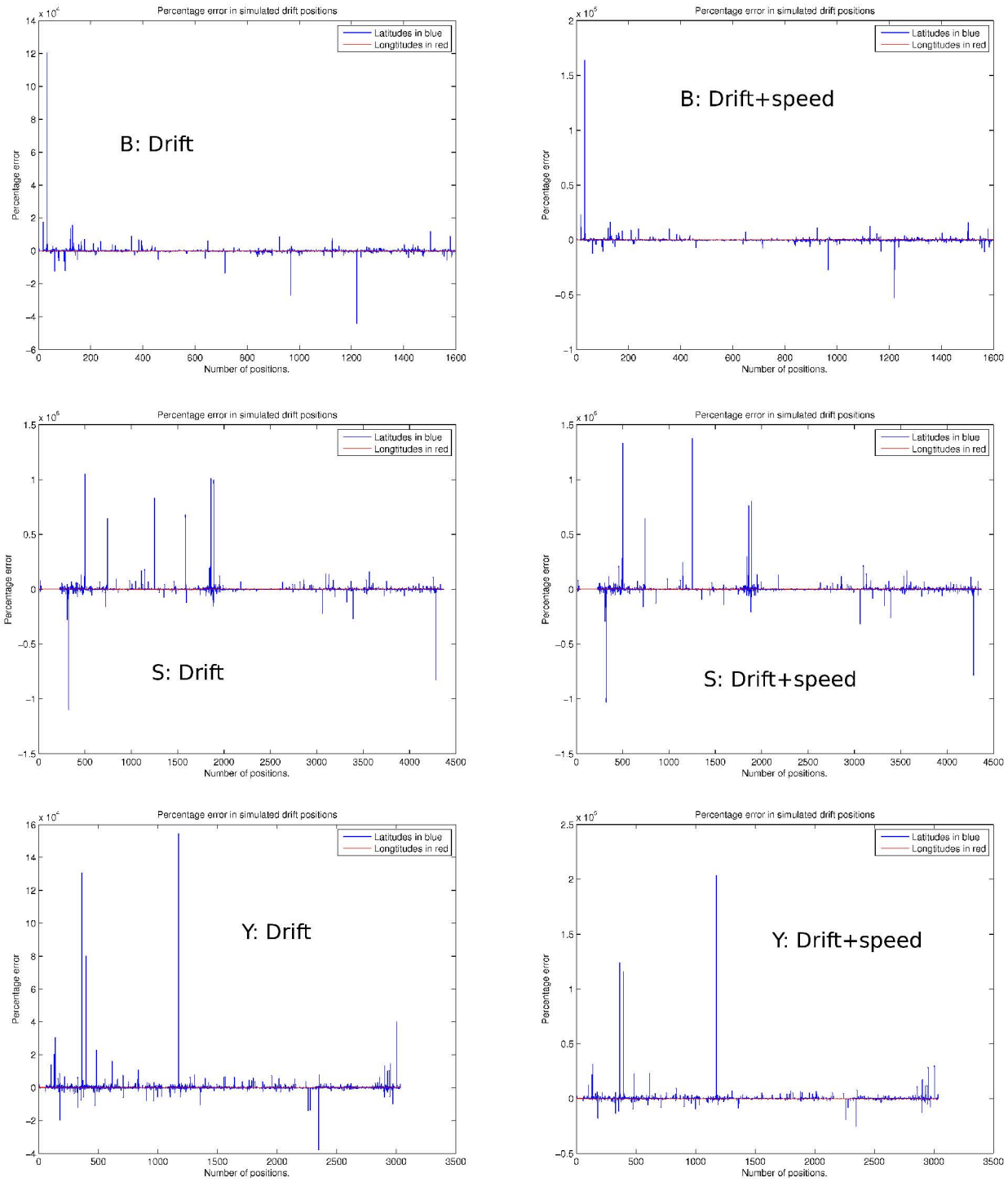

Figure 7.4: Percentage error of calculated longitudes and latitudes, passive (left column) and active (right column) cases. Bigeye (B), skipjack (S) and yellowfin (Y). Passive refers to tuna without swimming and active refers to tuna with swimming speeds of 0.5 bl.s-1 bl.s^{-1} under FADs and 1 bl.s^{-1} in free schools.

7.3.2 Comparison of simulated versus actual recapture locations by species: active case using maximum speeds

In this section and onwards, simulation has been carried out considering maximum speeds (Fig. 7.5 - 7.7) only. The reason to simulate tuna drift with maximum speeds only was because average speed simulation from above analysis were still far from actual recapture locations with average speed, hence considering minimum speeds will not improve the estimate of simulated positions. Maps of actual and simulated locations are shown in the top plots of Fig. 7.5 - 7.7. Simulated distribution is shown (in blue), actual recapture positions (in green) and red marks visible on the map depict the tagging positions. The ECDF plots (middle plots) are used to compare the distribution of simulated versus actual recovery positions. Discrepancies in the simulated drift and actual positions are given by percentage error plots (bottom plots). The simulated recapture positions did not still match actual recapture distribution (green points) perfectly. Comparing the species with each other, the estimates were not very different in terms of closeness of simulated drift positions to actual recovery positions, but simulated drift positions of skipjack matched the actual recovery positions better.

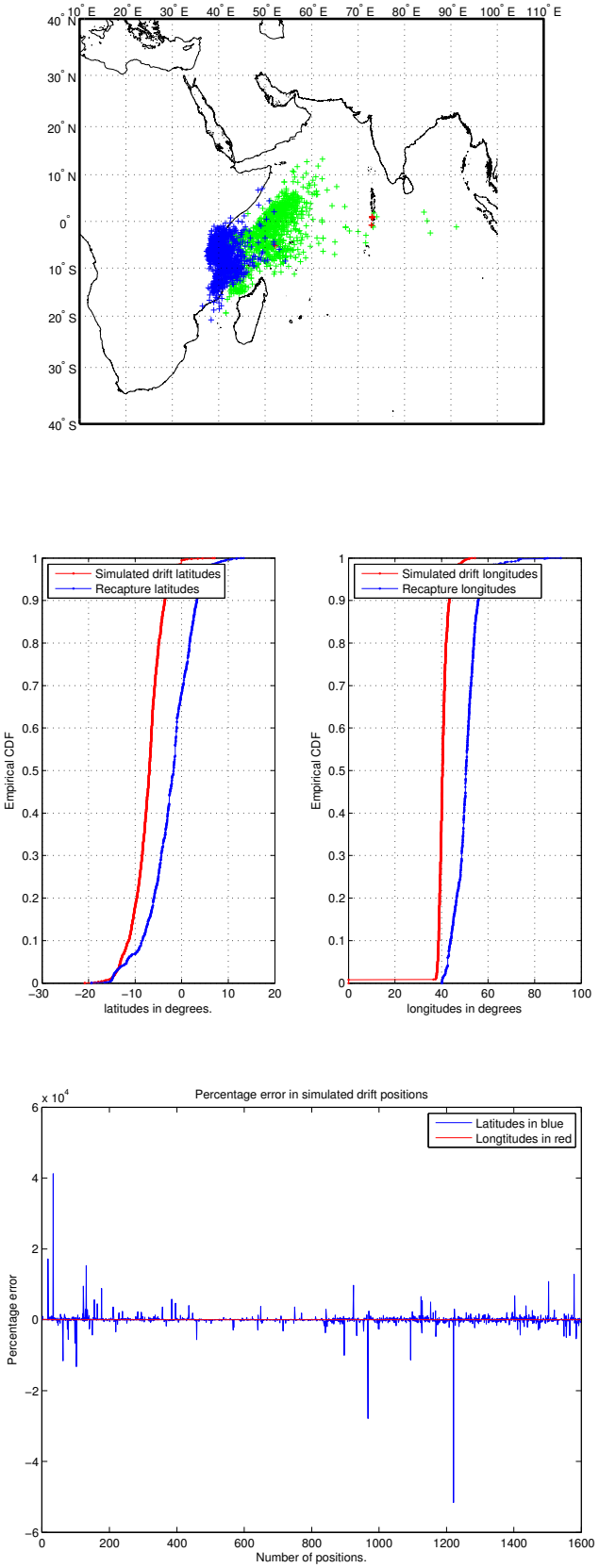

Figure 7.5: Bigeye distribution based on simulated drift attributed with maximum speeds. In FS a maximum speed of 2.2 bl.s^{-1} was assumed and under FADs this was 0.9 bl.s^{-1}.

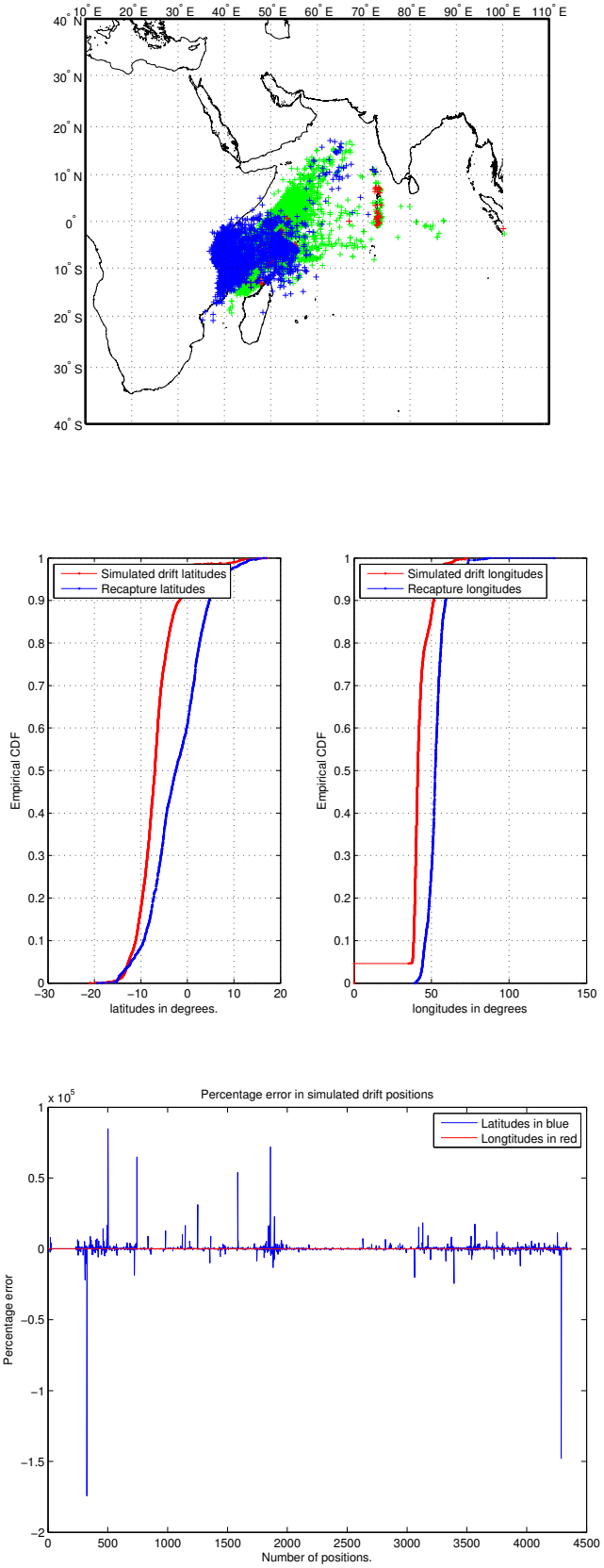

Figure 7.6: Skipjack distribution based on simulated drift attributed with maximum speeds. In FS a maximum speed of 2.2 bl.s^{-1} was assumed and under FADs this was 0.9 bl.s^{-1}.

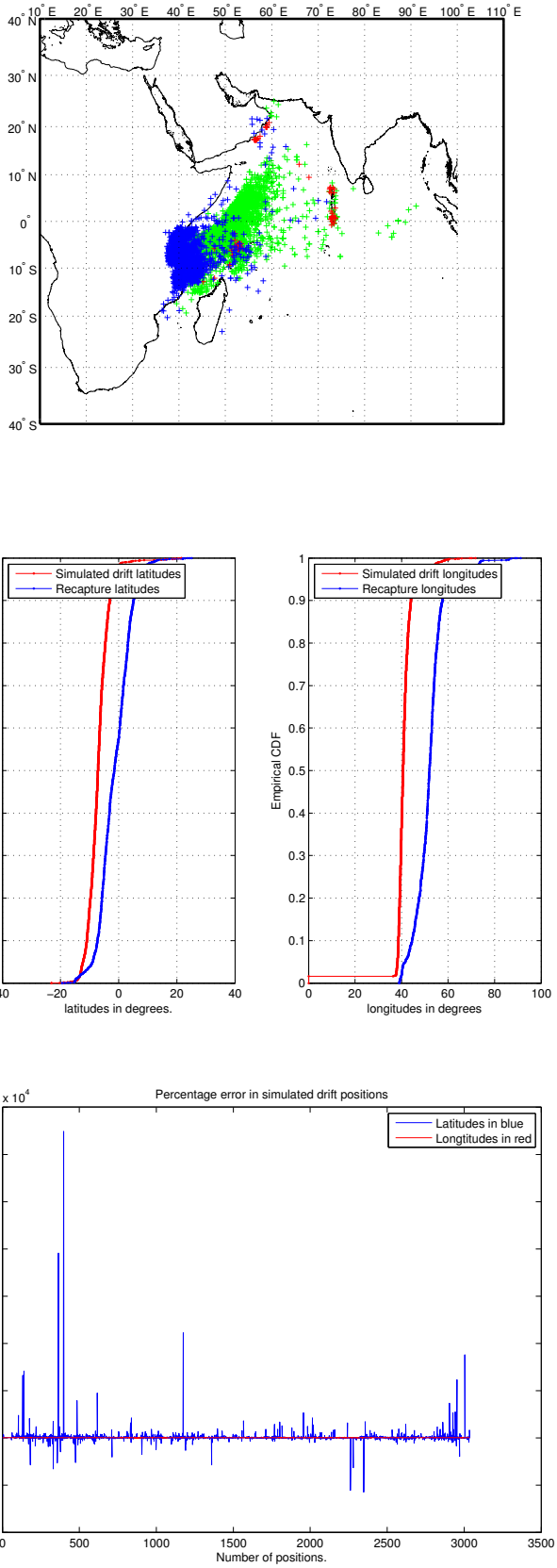

Figure 7.7: Yellowfin distribution based on simulated drift attributed with maximum speeds. In FS a maximum speed of 2.2 bl.s^{-1} was assumed and under FADs this was 0.9 bl.s^{-1}.

7.3.3 Comparison of simulated versus actual recapture locations by size group

The plots below show simulated and actual recapture locations carried out with respect to the two size categories of tuna based on their recapture fork lengths. Simulated movements are calculated using the maximum swimming speeds mentioned above. It should be noted that skipjack tuna fall in the small size category as both juvenile and adult individuals are generally under 70 cm. Comparing the plots of small against large category tuna, the dispersion of simulated positions appears to be more representative of actual recapture positions for large tuna (Fig. 7.8). For small tuna (7.9), dispersion of the simulated drifted positions diverges from actual the recovery positions. The ECDF plot (middle plots) shows the discrepancies and also the calculated percentage error where the order of magnitude is higher for small tuna relative to large tuna.

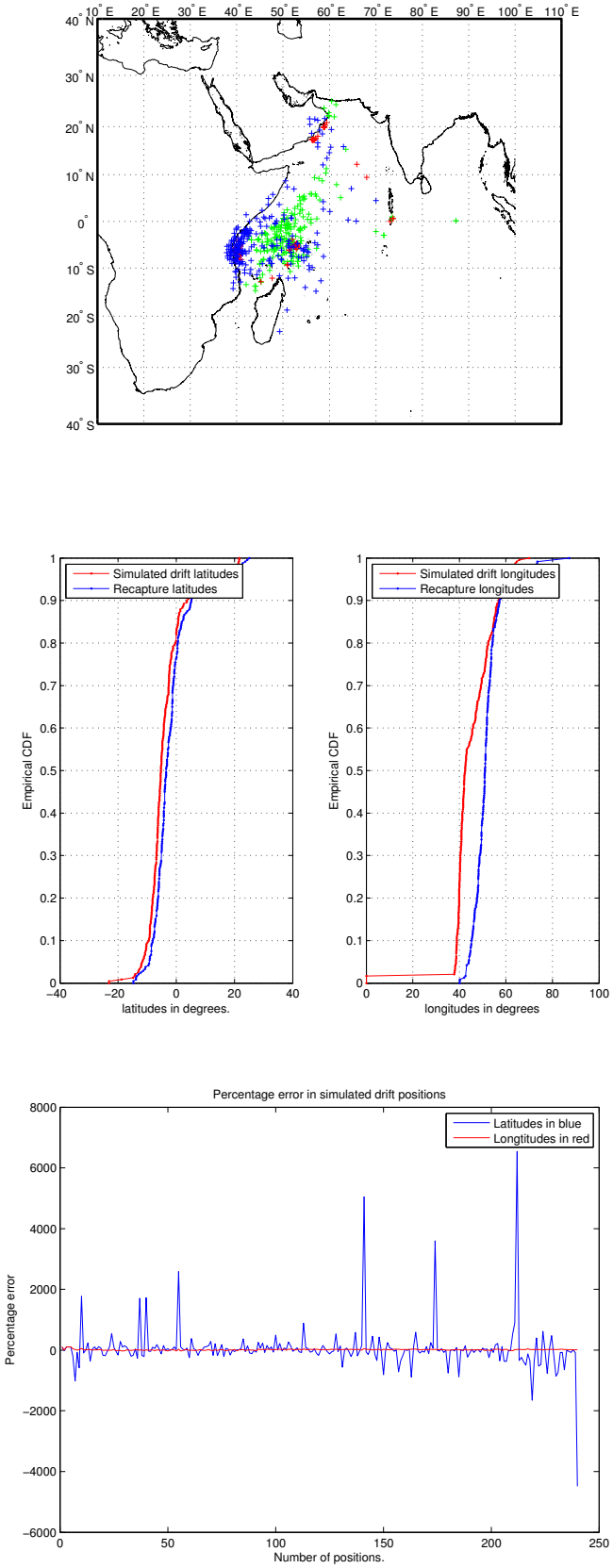

Figure 7.8: Large tuna distribution based on simulated drift. Large tuna, FL: $\geq$ 70 cm. In FS a maximum speed of 2.2 bl.s^{-1} was assumed and under FADs this was 0.9 bl.s^{-1}.

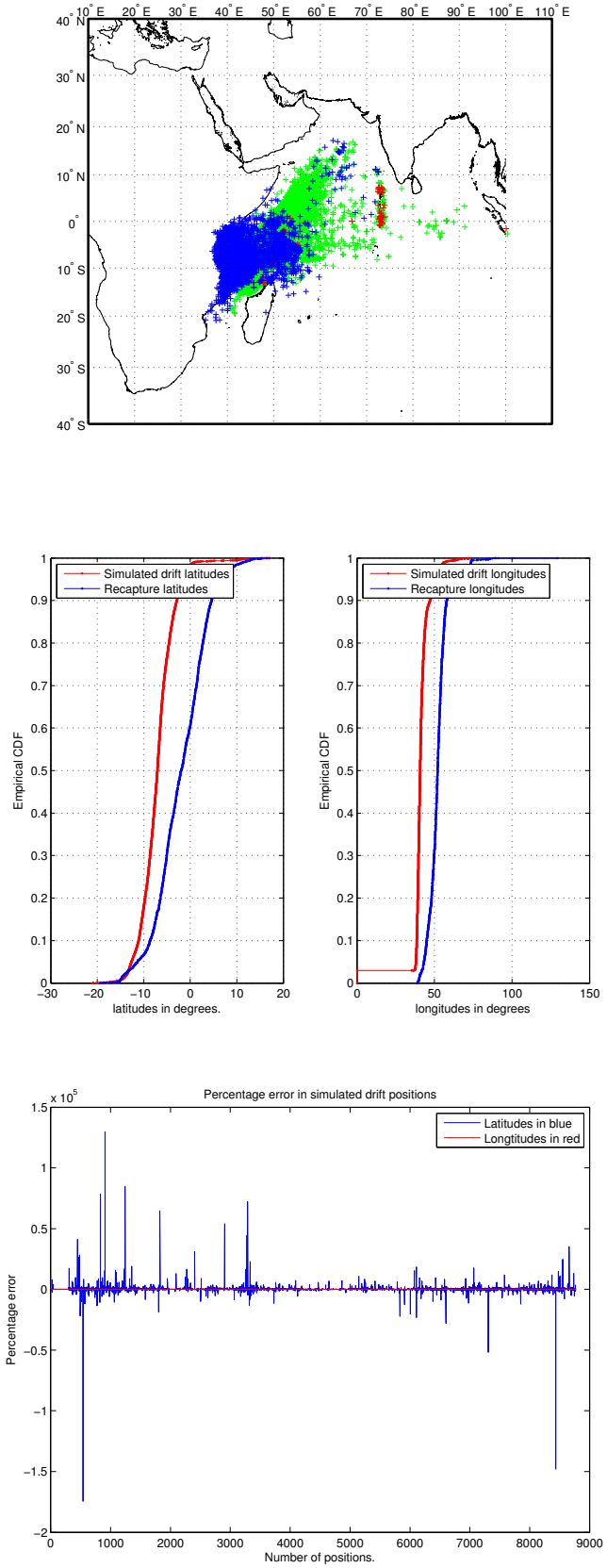

Figure 7.9: Small tuna distribution based on simulated drift. Small tuna, FL: < 70 cm. In FS a maximum speed of 2.2 bl.s^{-1} was assumed and under FADs this was 0.9 bl.s^{-1}.

7.3.4 Comparison of simulated versus actual recapture locations by school-type

The analysis was carried further by filtering the data for tuna caught under FADs from those in FS. Tuna under FADs with maximum speed showed that the simulated positions and actual positions of recovery were not close (Fig. 7.10). The magnitude of the error is larger for tuna simulated under FADs than those in FS. In FS tuna simulated positions were observed to be close to actual recovery positions, particularly in latitude (Fig. 7.11). The top plot for FS tuna show a good geographical distribution, the middle plot shows the simulated and actual recovery positions to be close and the percentage error graph (bottom plot), show a reduced magnitude in comparison to FADs tuna. Therefore, considering the two school-type, FS tuna simulation conforms better to the actual recovery positions than tuna under FADs.

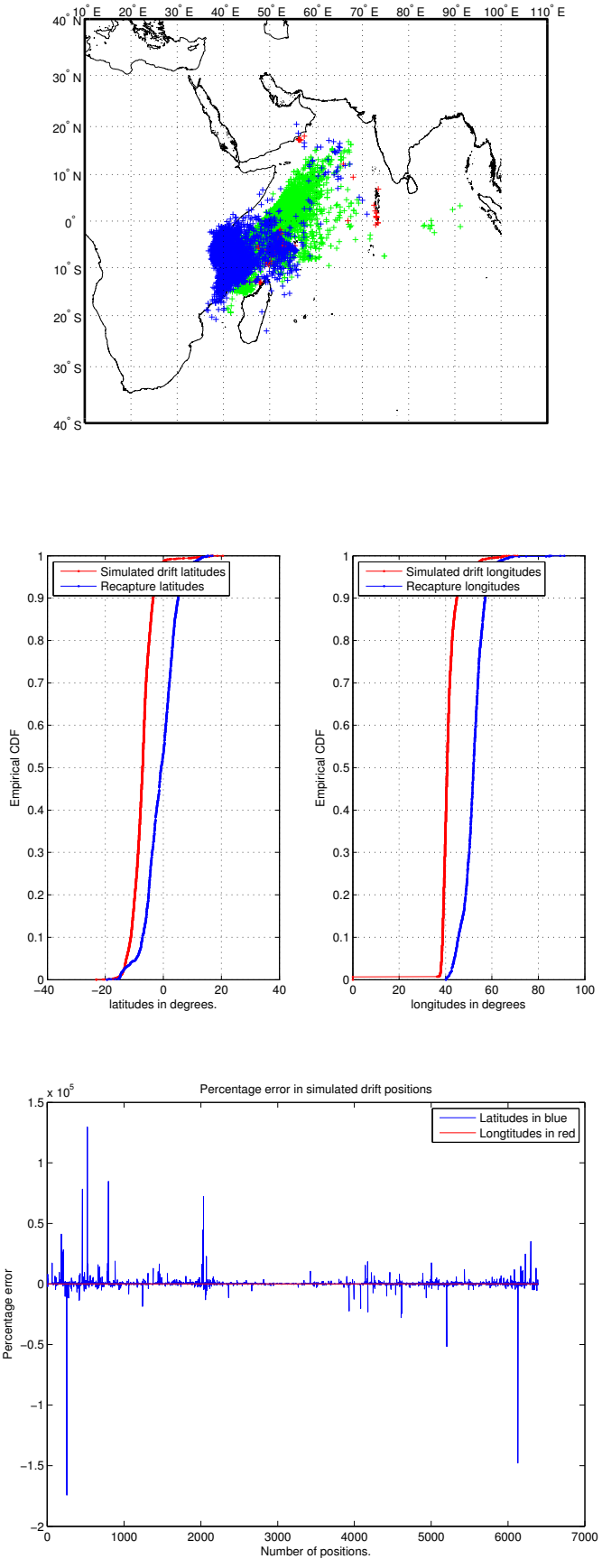

Figure 7.10: FADs tuna distribution based on simulated drift.

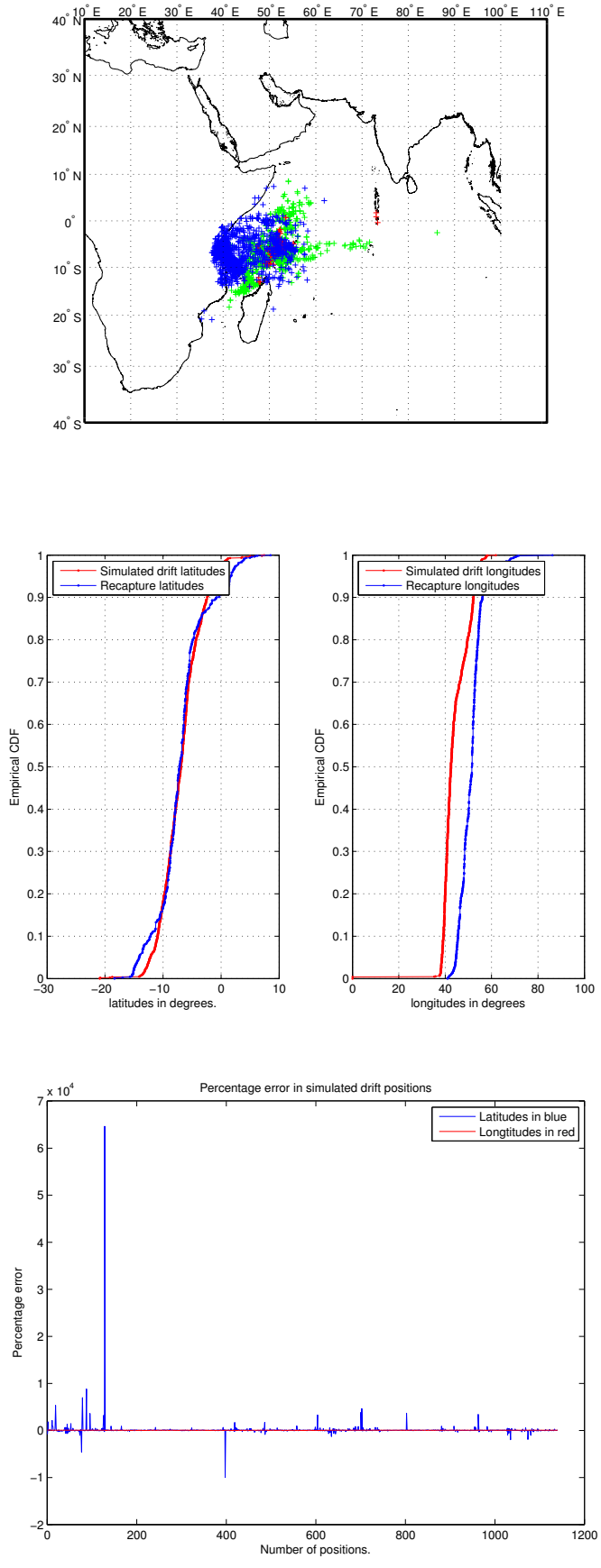

Figure 7.11: FS tuna distribution based on simulated drift.

7.4 Discussion

Eddy circulations often create convergence zones and consequently retention areas for plankton, larvae and fish. Alemany et al. (2010) pointed out that Atlantic bluefin, albacore and bullet tuna spawning could be associated to certain extent with frontal borders of eddies indicated by the concentration of larvae with high geostrophic velocities but also argued that it was not a significant property in any of their analyses. Furthermore, distributions of albacore larvae and three year-old fish were found to be influenced by wind stress moving them from spawning areas near the north-eastern coast in the Pacific to the west along the equator where surface layer showed side by side convergence and downwelling along with divergence and upwelling (Bakun, 2006, 1996). Guyomard et al. (2004) in their study of operational and environmental factors affecting swordfish catch and catch per unit effort (CPUE) of the longline fishery in the Indian Ocean, found that geostrophic currents among other factors such as temperature and chlorophyll, to be significant factor influencing distribution. Gaspar et al. (2006) noted that half of observed displacement is due to current drift in the case of leatherback turtles. The author suggested that for marine animals faster than leatherback turtles, the impact of ocean currents would be less. With the simulations using passive particles, large discrepancies were found between expected and actual recovery.

Categorisation by species showed that the estimates are faintly related to the species type. From the results obtained, this would imply that tuna schools are comprised of a mixture of the species moving together. Skipjack are the most abundant species, therefore there were sufficient returns for the algorithm to estimate simulated positions and thereby reducing the magnitude of the overall calculated error. Hence, simulated skipjack gave a slightly closer match than simulated bigeye and yellowfin. Fonteneau et al. (2013) stated that tuna school composition in terms both size category and species varies depending upon the school-type with which the tuna are associated. They also suggested that drifting FADs follow surface ocean currents or accumulate in frontal and convergence zones but, our results gave enough evidence that large tuna and particularly FS tuna, are influenced by ocean currents.

Calculated latitudes and longitudes shown in the ECDF plots were close to the actual recapture positions when considering FS and large tuna. The observed dis-

crepancies may be accounted for by the equations used in this study. They give an idea of surface water movement in relation to the Earth's rotation or rather the Coriolis effect and gravity. Furthermore, the geostrophic equations have limitations with respect to:

- water current movement is not dictated only by geostrophic balance,
- the geostrophic current may not be time constrained as the balance does not take into account acceleration flow,
- the geostrophic current does not apply within 2^o of equator; Coriolis force tends to zero as Sinφ tends to zero,
- it ignores the influence of friction.

Furthermore, the effect of Ekman's transport has not been considered in the equations along with wind driven flows. Transition periods between monsoons, are usually subjected to strong westerly winds driving the surface east equatorial jet (Wyrtki, 1973*a*). This factor has not been integrated in the equations to calculate the drift. Among the factors, the resolution of the altimetry data used is important. At one-third degree resolution, the discrepancies would be quite large compared to actual recapture positions. Secondly, in the calculation of the drifted positions, average speeds (and even maximum speeds) considered for individual tuna were an estimate. The variability in speed can be quite large (speeds bursts reaching 27 bl.s^{-1} have been reported by Dewar and Graham (1994), and this can explain a great part of the discrepancies between simulated and actual recoveries. The concept that the individual movement of the tuna is negligible with respect to the whole movement of the mass is therefore simplistic.

Predicting tuna migration locations using the above approach does not take into account the influence of environmental factors. For instance, from an environmental point of view, Bakun (2006) argued that surface fronts and mesoscale eddies can considerably alter patterns in the habitats of marine organisms. While there are plausible concurrences of effects of ocean currents, tuna are also influenced by the spatial forage distribution (Sund et al., 1981; Bertrand et al., 2002). Hence, depending on the probability of a particular tuna school encountering an area rich

in biomass of marine species, their duration of stay in that area will be extended to make most of the high prey density. Therefore, the present physical algorithm cannot capture all environmental influences.

In 2007, the mean temperature during the positive Indian Ocean Dipole (IOD) event was above 29 °C extending to the northern part of the Indian Ocean and potential fishing grounds of yellowfin were more focused on the western Madagascar region by longliners (Lan et al., 2013). IOD events have been observed to change fishing patterns in terms of distribution and catch rates (Marsac and Le Blanc, 2000; Ménard et al., 2007a). In 2007, the ocean environment showed noticeable changes in the spatial distribution of chlorophyll and deep thermocline anomaly compared to 2006, making forage availability scattered (Marsac, 2008) and consequently affecting tuna movement patterns.

The results by size category showed that simulated large tuna have a closer match to actual recovery positions than small tuna. The reason for this better match of the large tuna is that the body length per second for large fish is much faster than one body length per second for a small fish. So relative to the same currents, big fish swimming at the same maximum speed in terms of body lengths as small fish, will be swimming much faster relative to the current. Due to faster speed, the simulated drift gets closer to the actual drift for large fish. Gaspar et al. (2006) suggested that impact of ocean currents would be less on faster swimming species than the leatherback turtle. The present results are thus in agreement with Gaspar et al. (2006). Considering the case of tuna swimming under FADs, there was a low calculated drift match relative to FS. A number of papers have highlighted the bio-physical behaviour of tuna under FADS (Marsac et al., 2000; Ménard et al., 2000a; Fonteneau and Gascuel, 2008; Hallier and Gaertner, 2008). Considering the above arguments concerning tuna dispersion, ocean currents are an important variable to account for when analysing tuna movements.

In this chapter, simulating tuna in the passive mode showed that it was not enough to predict their movement and further including tuna swimming speeds improved the estimate but still did not exhibit a perfect match with actual recapture locations. Attributing maximum speeds to the fish further improved the estimates, depending on the school-type with which they were associated. It is important to

get the speeds as close as possible to reality. The percentage error plots show discrepancies at a number of positions when we consider estimated and actual recovery positions of individual tuna. The results have shown that swimming speed is an important criterion and also that surface ocean currents play a key role in tuna movement. In general, including speeds and currents in spaghetti tag experiments can provide quite good estimates of migration locations from tagging to recovery.

Sibert et al. (1999) used an advection-diffusion-reaction model to estimate tuna movement and mortality of tagged skipjack tuna in a closed domain. They reckoned that the spatial model provided a better fit to the data while the spatially aggregated model allowed estimates of natural mortality rate independent of movement. In the present study, fish mortality as such was not taken into consideration, as the dataset was comprised of all tuna that were tagged and recaptured. The spatial and temporal resolutions is an important factor determining the model fit. Sibert et al. (1999) have used large time steps and the finite difference method was solved on a regular grid with a spatial resolution of 60 nmi (111.12 km). In this study, spatial resolution of the ocean currents used to estimate probable movement directions was $1/3^{o}$ (about 37 km) and the time step was one day. Hence, the accuracy of the results in our case is higher but the error estimate would be larger compared to those of Sibert et al. (1999) as a finer grid was used. Moreover, the domain of the simulation in this study is an open domain (the whole Indian Ocean) where the boundary conditions are similar to that of the surface ocean currents.

7.5 Conclusion

Absolute geostrophic velocities and Maps of Absolute Dynamic Topography on a daily basis from January 2005 to November 2007 for the Indian Ocean were combined with RTTP-IO tagging dataset to evaluate the influence of currents on the movement of surface tuna schools. The methodology proposed is based on a recursive calculation of the geographic location due to the effect of geostrophic currents and change in surface slope of the sea topography. Although the results do not show a perfect match between simulated and actual recapture positions, ocean currents can be considered as essential information to interpret tuna migration behaviour.

The use of satellite altimetry data might help to track tuna species and with the improvement of a better resolution of satellite data, this will be a new factor to incorporate in future studies on movement of marine species.

The geostrophic flow does influence the movement of large and free school tuna. It is obvious that in addition to the geostrophic flows, the swimming speed of tuna is an essential variable to consider to obtain a better match between simulated and actual recapture locations. The disadvantage of conventional dart-tagging experiments is that only date and location of release and recapture are known, what happens during the time-at-liberty is not available which would have been crucial piece of information to improve and validate the algorithm. This should be further investigated using satellite tracking tags, capable of providing positions during their time-at-liberty along with depth profiles to give an enhanced appreciation of tuna movement and behaviour in relation to ocean currents (Schick and Lutcavage, 2009; Block et al., 2005, 2011). Records resulting from pop-up or sonic tagging would shed more light on the relationship between tuna movement and ocean currents, as continuous positioning would give a more precise time step of actual tuna positions along with depth information which could be accounted for in the algorithm.

For instance, it would be possible to test the effect of varying Ekman velocities in the water column. In the event that continuous positioning was possible and having an extended time-at-liberty of the tuna, this could give better estimates of their drift as better estimate of speeds would be possible. However, this study has only focused on ocean surface currents, a better approach might be to incorporate the influence of other parameters such as temperature and chlorophyll-a to see the link with those factors as well. This could possibly be included in the following way. Upon the calculation of displacement (the distance and the direction) of a fish to each new positions at each time step, temperature and chlorophyll-a can be evaluated at those locations. Depending on the conditions prevailing, a weighted average could be implemented where the duration of stay could increase or decrease based on the temperature and chlorophyll conditions. Furthermore, tuna residency periods and regions could add to understanding their movement dynamics and aid in regional management of tuna stocks. Although each individual tuna has its own swimming speed and they are independent of one another, they are likely to

move in multispecies groups (notably when juveniles) and water mass movement can therefore contribute to give an overall movement direction of the multispecies schools.

This study shows that it is possible to successfully model the migration patterns of tuna, using estimated swimming speeds and geostrophic currents, in spite of the assumptions involved in estimating swimming speeds and the limitations of modelling geostrophic currents. In particular, large tuna migrations were simulated more successfully than smaller tuna and FS tuna were better modelled than tuna under FADs.

Chapter 8

General conclusions

8.1 Context of research

Common practices to assess fish biomass by direct methods are trawl surveys or echo integration techniques performed during acoustic surveys. However, such methods cannot be applied to large pelagic species. Tagging is another widespread technique applied to many taxa (birds, fish, marine turtles, mammals) to study movements, to assess the abundance of stocks and to determine biological parameters (growth, mortality or survival rates). Tropical tuna resources have been the focus of tagging programmes that were developed in the Pacific and Atlantic Oceans since the 1960s, whereas such activities were virtually absent in the Indian Ocean. Owing to the rapid increase of tropical tuna catches in the Indian Ocean since the 1990s, there was a pressing need for effective stock assessment of tuna stocks. It was agreed that a large scale tagging programme would be the best approach to provide additional and crucial information on estimates pertaining to tuna biology in terms of growth, movements, behaviour, interaction with the ocean environment, and harvest rate of the stock (Murua et al., 2015).This programme (Indian Ocean Tuna Tagging Programme) was developed under the auspices of the Indian Ocean Tuna Commission, with two components: the Regional Tuna Tagging Programme (RTTP-IO) from 2005 to 2009 and a series of small-scale projects from 2002 to 2009. It targeted three main species of tuna (yellowfin, skipjack and bigeye) commercially exploited by various fishing gear types (Hallier, 2008). While taking into account size-class and school type of tuna the objectives of this thesis were to:

- Understand the effects of season, year, school-type and the ocean environment on tuna migrations using a multivariate approach.
- Estimate survival probabilities of the three species.
- Understand movements of tuna based on oceanographic conditions prevailing in the Indian Ocean.
- Demarcate tagging and recapture zones with regard to migration patterns.
- Understand spatial dynamics of tuna schools and its interaction with the ocean environment.
- How ocean surface currents contribute to migration of tuna.

8.1.1 Constraints

The dataset generated from the RTTP-IO programme itself is huge. This was merged with results of small-scale tagging activities that were carried out in parallel, making a database of 219,149 tuna tagged and 34,294 tuna recaptured. Depending on the investigation, selection criteria were applied in order to generate the dataset used for the analysis. Prior to any processing, the data had to be verified and corrected whenever possible. One important step was to standardize the recoveries, to obtain recapture probabilities that are comparable over the whole geographic area of the recoveries. Given that the dataset was large, processing was a time-consuming exercise. Moreover, oceanographic data of chlorophyll concentration, sea surface temperature and altimeter from satellite were incorporated which added to processing requirements. It should be emphasised that some software used to carry out analyses with respect to particular hypotheses, were not able to handle the whole dataset. Thus, in some cases the data had to be truncated in order to process the data. These instances are detailed in the relevant sections of the dissertation.

8.2 Multivariate approach

Patterns in the assemblage of species were analysed with respect to school type (free swimming or associated with fish aggregating devices), fish size and environmental

factors (sea surface temperature and chlorophyll-a concentration) which may influence fish movements. Using a multivariate approach, it was difficult to show the correlation between biotic and abiotic variables because of the nature of the tagging survey. Using this approach, a diversity of species is needed for a better response. Nonetheless, the multivariate approach showed the links between the eight categories of tuna size-class and factors investigated (Chapter 3). Adult skipjack contributed heavily to overall abundance during the years 2005 to 2007 (77.45%). Adult yellowfin were the main contributors to overall abundance in the years 2008-2011, followed by bigeye adults, as the skipjack abundance in the tag returns declined due to their shorter lifespan relative to the two other species. Through the multivariate analysis, it has been demonstrated that year and geographic zone are significant factors influencing behaviour whereas the school and season factors were not significant. Cluster analysis also showed the complexity of the factors of species/size class with the year, zone, school (FS vs FAD) and season factors. The SIMPER analysis showed skipjack adults in Zone A were abundant with yellowfin adults moving towards Seychelles (Zones B and C). The multivariate approach showed some limitations in terms of the paucity of variables in the present study, but nonetheless provided useful insight into understanding tuna migrations.

8.3 Survival estimation

The objectives of Chapter 4 were to estimate the survival and recovery probabilities of tuna tagged through the RTTP-IO programme. The MARK software was deemed to be a promising approach to look into the survival and recovery estimates for the three species of tagged and released tuna. Depending on the tagging approach used, the dataset was fitted with appropriate robust models fitting the tagging and recovery processes. The Brownie and Seber models were applied. We found two major constraints in the dataset: (1) for logistical reasons the tagging was done on an irregular temporal basis; (2) more reporting was expected from a variety of fishing gears in the Indian Ocean (longline, gill net, small scale fishing gears). In the end, only purse seine returns were sufficient to be analysed. As a consequence, irregularity in both sampling and recovery caused huge inconsistencies in the estimates.

Both Brownie and Seber approaches resulted in a combination of different forms of Brownie and Seber models, where permutation of time varying parameters and time independent parameters for survival and recovery were assessed. The lowest AIC value provided the most parsimonious model. Using Brownie parameterisations, the parsimonious model showed that survival stabilises to around 1 (an unrealistic value) as the recovery to tagging ratio was not sufficient for the model to give a proper estimate. Seber (S and r) parameterisations gave a better estimate of survival than the Brownie parameterisations.

Because of the lack of consistent results, the whole dataset of large scale and small scale tagging was then studied using the Kaplan-Meier approach. The Kaplan-Meier estimate enabled us to re-estimate the longevity of the three species. Based on the survival curves, the total mortality (z) was 0.4, 0.8 and 0.5 for bigeye, skipjack and yellowfin, respectively. It was estimated that the cohorts (99%) vanished at 12, 5.8 and 10 years, respectively. The Kaplan-Meier estimate also showed that tuna swimming in free schools have a higher probability of survival while showing that the three species are different in terms of vulnerability. Exploitation of tuna under FADs impacts abundance more than exploitation of tuna in FS.

8.4 Tuna migration

8.4.1 Migration of tagged and released tuna

Considering migration patterns of tuna tagged in the Tanzanian region, tuna headed in a north easterly direction towards the Seychelles, particularly Zone B for both years 2006 and 2007 when high abundance was recorded. However, movements have also been observed down to the Mozambique Channel identified as a nursery ground for tuna (Fraile et al., 2013). Migrations have also been observed heading to the north, towards the Arabian Sea. Seasonal changes were another factor observed to influence movement patterns, with exploration pathways of tuna changing from one season to another. Seasonal spatial stratification of surface water allows wider or narrower access to productive areas or regions. Temperature and chlorophyll, are indeed significant parameters which affect the mobility of tuna. Warmer temperatures allow wider exploration space for tuna to find forage-rich areas as compared to

colder waters. It is to be noted that 2006 was a cold and productive year in the west Indian Ocean, whilst 2007 had warm and chlorophyll-depleted conditions associated with an El Niño event (Chapter 5).

The apparent distance travelled was analysed with respect to fish size category (Chapter 5). Tuna associated with FADs moved in the same direction irrespective of their size-class. The findings of this study also showed that long distances were covered by adult tuna as well as juveniles. It was observed that the overall distances travelled in 2007 for the three species were longer for both FADs and FS compared to 2006. Since 2006 was a cold and productive phase, distances covered to find forage-rich areas were shorter and in 2007 (warm and chlorophyll depleted phase) tuna travelled further.

The Tanzanian region tagging represented the majority of the tagging, along with the Seychelles. For fish tagged in Tanzanian waters, it was observed that those under FADs moved predominantly towards Somalia and the Seychelles, while those in free schools moved mainly to the Seychelles and Mozambique. There is no distinction in terms of size-class and species for both school-types tagged in Tanzanian waters. For tuna tagged in the Seychelles regions, FAD tuna did not move out of the Seychelles region, while FS tuna headed in all directions. The Seychelles region showed grouping by species and size-class.

Warm ocean events (2007) showed that tuna dispersed in all directions in contrast to cold ocean phases when structured movements can be observed. Warm events coincided with less productive waters and the likelihood of tuna disbursing in all directions for forage but productive cold waters (e.g. 2006), showed limited movement of tuna.

8.4.2 Recapture zones

The whole area was partitioned into zones reflecting chlorophyll variability across seasons (Chapter 6). The recapture of tuna in Zone B (East African coast and Somalian Basin) by seasons showed a significant difference between the first inter-monsoon season (IM1, from April-May) compared to other seasons. During this period, the Chl-*a* surface boundary distribution in Zone B of the Indian Ocean enlarged, allowing tuna from the Seychelles and Madagascar to explore this zone.

Temperature variation was wider for tuna in FS school than under FADs. This indicates that tuna in FS are able to explore in more diverse directions than tuna under FADs.

Large scale movements of tuna tagged in the Tanzanian region were observed going to Zones A (Arabian Sea) and H (East Indian Ocean). The Mozambique Channel along with the Seychelles, are seen as potential nursery grounds (Fraile et al., 2013); the abundance of yellowfin was significant in those regions. The school-type showed differences in recapture by species. FS tuna were mostly adult yellowfin, while skipjack tuna formed the main catches under FADs. Seasonal differences were also observed. Even though skipjack contributed heavily to the overall abundance, yellowfin were most abundant in the North-East Monsoon season.

The GAM-based approach clarified the spatial distribution and environment (SST and Chl-a) to which tuna migrate. The geographical area between 5^o N - 5^o S and 45^o - 55^o E is the core of tuna recoveries under FADs, while in FS, the core recovery region is between 0^o N - 10^o S and 50^o - 60^o E with some extension to 70^o E. The area 0^o - 5^o S and 60^o - 70^o E corresponds to major spawning area. We found that the preferred range of temperatures was between 25 - 29 ^{o}C. Concerning Chl-a concentration, the preferred range was found to be 0.082 mg.m^{-3} - 7.39 mg.m^{-3}.

8.5 Tuna drift and ocean currents

In order to understand the role of ocean surface currents in the migration behaviour of tuna, geostrophic balance equations were used to model the influence of surface ocean currents on tuna. Tagging locations and altimeter data from satellites were used as initial conditions and fed into the geostrophic balance equations (Chapter 7). Here, five scenarios were investigated:

- species as passive particles,
- species attributed with an average speed (0.5 bl.s^{-1} for FADs and 1 bl.s^{-1} for FS),
- species attributed maximum speeds (FS: maximum speed of 2.2 bl.s^{-1} and FADs: maximum speed of 0.9 bl.s^{-1}),

- two size groups (small, FL: < 70 cm and large, FL: ≥ 70 cm) with maximum speeds,
- school type with maximum speeds.

The results showed that considering tuna as passive objects (such as physical particles) did not work, as simulated recapture positions and actual recapture positions were very different. When tuna were attributed with average speeds in the equations along with the calculated surface ocean currents, results of simulated recapture locations improved relative to actual positions, but still did not match with them. Thereafter the tuna were given maximum swimming speeds based on literature. As expected, this case study further improved the closeness of simulated recapture locations to real recapture positions. Considering species-wise calculations, the simulated positions did not show noticeable improvement except for the case of skipjack which provided a slightly closer match than bigeye and yellowfin. Size-class categorisation of tuna (rather than species-wise), gave a better match for large tuna than small tuna and both of the size groups that were also modelled using maximum swimming speeds. Finally, the school-group categorisation showed that the simulated drift and recovery positions were closer for tuna in free schools than those under FADs. We have attributed the tuna with maximum speeds that are school-type and body length (fork length) dependent. Small and large tuna were processed separately as tuna of small or of large size. Large fish were found to have a closer match because large tuna swim faster and are more likely to migrate further and also to be found in FS than FADs, hence the closer match relative to small tuna and FADs.

8.6 Way forward

The RTTIP-IO programme produced an enormous amount of diverse data. In this study, we have concentrated on short term recoveries, so have focused on an appropriate subset of the data for this purpose, it would have been desirable to have the whole dataset processed. Limitations related to processing capacity restricted the processing to a subset of the data. Analysing the diversity of information on appropriate spatial and temporal scales is deemed to be important. Relating the

tuna recaptures to plankton biomass distribution using an ecosystem approach can help to better understand their movement patterns. Another aspect that needs to be explored is relating the tuna distribution with other kinds of oceanic features such as sea mounts, eddy formations, upwelling and downwelling zones. But the nature of dart tagging does not allow such studies, whereas tracking techniques using electronic tags would be the most appropriate approach to better understand tuna interactions with the ocean environment.

Appendix A

Real Function Parameters

A.1 Brownie parameterization

BSY_TZA2012tg_rc

Real Function Parameters of S(g*t) f(g*t) PIM

Parameter	Estimate	Standard Error	95% Confidence Interval Lower	Upper
1:S	0.5003095	0.0000000	0.5003095	0.5003095
2:S	0.5672407	0.0000000	0.5672407	0.5672407
3:S	1.0000000	0.1446322E-006	0.9999997	1.0000003
4:S	1.0000000	0.1064832E-006	0.9999998	1.0000002
5:S	1.0000000	0.1732641E-006	0.9999997	1.0000003
6:S	1.0000000	0.5793920E-007	0.9999999	1.0000001
7:S	1.0000000	0.1500300E-008	1.0000000	1.0000000
8:S	1.0000000	0.0000000	1.0000000	1.0000000
9:S	1.0000000	0.2558755E-008	1.0000000	1.0000000
10:S	1.0000000	0.2401724E-007	1.0000000	1.0000000
11:S	1.0000000	0.6078310E-009	1.0000000	1.0000000
12:S	1.0000000	0.5727307E-008	1.0000000	1.0000000
13:S	1.0000000	0.2531285E-007	1.0000000	1.0000000
14:S	1.0000000	0.2118245E-006	0.9999996	1.0000004
15:S	1.0000000	0.5387363E-007	0.9999999	1.0000001
16:S	1.0000000	0.2952108E-007	0.9999999	1.0000001
17:S	1.0000000	0.1640123E-006	0.9999997	1.0000003
18:S	1.0000000	0.1381934E-006	0.9999997	1.0000003
19:S	1.0000000	0.1218591E-006	0.9999998	1.0000002
20:S	1.0000000	0.1542464E-006	0.9999997	1.0000003
21:S	1.0000000	0.1124558E-006	0.9999998	1.0000002
22:S	1.0000000	0.7813335E-007	0.9999998	1.0000002
23:S	1.0000000	0.1798800E-006	0.9999996	1.0000004
24:S	1.0000000	0.4691628E-007	0.9999999	1.0000001
25:S	1.0000000	0.2159725E-006	0.9999996	1.0000004
26:S	1.0000000	0.4728914E-006	0.9999991	1.0000009
27:S	1.0000000	0.3089882E-004	0.9835351E-296	1.0000000
28:S	0.9999999	0.1944767E-003	0.8689717E-297	1.0000000
29:S	0.4951880	0.0000000	0.4951880	0.4951880
30:S	0.5093123	13.872773	0.5818565E-047	1.0000000
31:S	0.4553563	0.0000000	0.4553563	0.4553563
32:S	0.4954053	0.0000000	0.4954053	0.4954053
33:S	0.4844152	0.0000000	0.4844152	0.4844152
34:S	1.0000000	0.1481025E-006	0.9999997	1.0000003
35:S	1.0000000	0.4346288E-007	0.9999999	1.0000001
36:S	1.0000000	0.9524615E-007	0.9999998	1.0000002
37:S	1.0000000	0.2452684E-007	1.0000000	1.0000000

38:S	1.0000000	0.1659683E-008	1.0000000	1.0000000
39:S	1.0000000	0.1435318E-008	1.0000000	1.0000000
40:S	1.0000000	0.8291985E-007	0.9999998	1.0000002
41:S	1.0000000	0.8265288E-008	1.0000000	1.0000000
42:S	1.0000000	0.2149164E-007	1.0000000	1.0000000
43:S	1.0000000	0.1177586E-007	1.0000000	1.0000000
44:S	1.0000000	0.1740445E-008	1.0000000	1.0000000
45:S	1.0000000	0.4165815E-009	1.0000000	1.0000000
46:S	1.0000000	0.7214316E-007	0.9999999	1.0000001
47:S	1.0000000	0.5861510E-007	0.9999999	1.0000001
48:S	1.0000000	0.5651263E-007	0.9999999	1.0000001
49:S	1.0000000	0.1524328E-006	0.9999997	1.0000003
50:S	1.0000000	0.2571993E-006	0.9999995	1.0000005
51:S	1.0000000	0.1996351E-007	1.0000000	1.0000000
52:S	1.0000000	0.7581047E-006	0.9999985	1.0000015
53:S	1.0000000	0.2610815E-006	0.9999995	1.0000005
54:S	1.0000000	0.1384211E-005	0.9999973	1.0000027
55:S	1.0000000	0.9585901E-006	0.9999981	1.0000019
56:S	1.0000000	0.2472571E-005	0.9999952	1.0000048
57:S	1.0000000	0.3100248E-005	0.9999939	1.0000061
58:S	1.0000000	0.5278891E-004	0.9998965	1.0001035
59:S	0.9999999	0.1935036E-003	0.1755422E-296	1.0000000
60:S	0.5406232	28.289887	0.1280321E-096	1.0000000
61:S	0.5066232	0.0000000	0.5066232	0.5066232
62:S	0.4761506	0.0000000	0.4761506	0.4761506
63:S	0.4794138	0.0000000	0.4794138	0.4794138
64:S	0.4992756	0.0000000	0.4992756	0.4992756
65:S	1.0000000	0.2140343E-006	0.9999996	1.0000004
66:S	1.0000000	0.6393852E-007	0.9999999	1.0000001
67:S	1.0000000	0.7790910E-007	0.9999998	1.0000002
68:S	1.0000000	0.8509647E-008	1.0000000	1.0000000
69:S	1.0000000	0.4360869E-009	1.0000000	1.0000000
70:S	1.0000000	0.6649108E-008	1.0000000	1.0000000
71:S	1.0000000	0.1610124E-007	1.0000000	1.0000000
72:S	1.0000000	0.3072193E-008	1.0000000	1.0000000
73:S	0.7793380	0.2669462E-007	0.7793379	0.7793380
74:S	0.9237396	0.0000000	0.9237396	0.9237396
75:S	0.8487845	0.0000000	0.8487845	0.8487845
76:S	0.9448449	0.0000000	0.9448449	0.9448449
77:S	0.9451257	0.0000000	0.9451257	0.9451257
78:S	0.8472366	0.0000000	0.8472366	0.8472366
79:S	0.9418703	0.0000000	0.9418703	0.9418703
80:S	0.7888830	0.0000000	0.7888830	0.7888830
81:S	0.8715840	0.0000000	0.8715840	0.8715840
82:S	0.8846411	0.0000000	0.8846411	0.8846411
83:S	0.9143918	0.0000000	0.9143918	0.9143918
84:S	0.9451765	0.0000000	0.9451765	0.9451765
85:S	0.8734734	0.0000000	0.8734734	0.8734734
86:S	0.9973720	0.3535627	0.5730932E-112	1.0000000
87:S	0.9924628	0.6506733	0.1195104E-071	1.0000000
88:S	0.9979920	0.2737584	0.2596297E-113	1.0000000
89:S	0.9843932	0.7216275	0.6564104E-038	1.0000000
90:S	0.9979616	0.3178392	0.4944981E-130	1.0000000
91:S	0.1465028E-003	0.0000000	0.1465028E-003	0.1465028E-003
92:S	0.5168781	0.0000000	0.5168781	0.5168781
93:S	0.5357497	0.0000000	0.5357497	0.5357497
94:f	0.5303074	0.0000000	0.5303074	0.5303074
95:f	0.4906615	0.0000000	0.4906615	0.4906615
96:f	0.4901704	0.0000000	0.4901704	0.4901704
97:f	1.0000000	0.1897712E-003	0.5476061E-296	1.0000000
98:f	1.0000000	0.2524220E-004	0.9999505	1.0000495
99:f	1.0000000	0.5302803E-006	0.9999990	1.0000010
100:f	1.0000000	0.6456570E-006	0.9999987	1.0000013
101:f	1.0000000	0.1996842E-004	0.9999609	1.0000391
102:f	1.0000000	0.1445118E-006	0.9999997	1.0000003
103:f	1.0000000	0.1439518E-006	0.9999997	1.0000003

104:f	1.0000000	0.2544112E-005	0.9999950	1.0000050
105:f	1.0000000	0.5442115E-005	0.9999893	1.0000107
106:f	1.0000000	0.2659181E-006	0.9999995	1.0000005
107:f	1.0000000	0.3655755E-006	0.9999993	1.0000007
108:f	1.0000000	0.6402003E-005	0.9999875	1.0000125
109:f	1.0000000	0.1531755E-005	0.9999970	1.0000030
110:f	1.0000000	0.7174773E-007	0.9999999	1.0000001
111:f	0.9999999	0.8370445E-004	0.1563590E-296	1.0000000
112:f	1.0000000	0.4897020E-007	0.9999999	1.0000001
113:f	1.0000000	0.2542699E-005	0.9999950	1.0000050
114:f	1.0000000	0.6302835E-005	0.9999876	1.0000124
115:f	1.0000000	0.8451431E-006	0.9999983	1.0000017
116:f	1.0000000	0.1898966E-004	0.9999628	1.0000372
117:f	1.0000000	0.6384379E-005	0.9999875	1.0000125
118:f	0.9999996	0.2282196E-003	0.2366279E-297	1.0000000
119:f	1.0000000	0.1298534E-003	0.9997455	1.0002545
120:f	1.0000000	0.9626276E-005	0.9999811	1.0000189
121:f	1.0000000	0.3548382E-004	0.9999304	1.0000695
122:f	1.0000000	0.9206183E-004	0.9998196	1.0001804
123:f	0.4558732	0.0000000	0.4558732	0.4558732
124:f	0.5092969	0.0000000	0.5092969	0.5092969
125:f	0.4631558	0.0000000	0.4631558	0.4631558
126:f	0.4811058	0.0000000	0.4811058	0.4811058
127:f	0.5421891	0.0000000	0.5421891	0.5421891
128:f	1.0000000	0.2020550E-003	0.2415073E-296	1.0000000
129:f	0.9999998	0.1529986E-003	0.6479953E-297	1.0000000
130:f	1.0000000	0.8953102E-007	0.9999998	1.0000002
131:f	1.0000000	0.4099588E-006	0.9999992	1.0000008
132:f	1.0000000	0.2765487E-008	1.0000000	1.0000000
133:f	1.0000000	0.7706196E-008	1.0000000	1.0000000
134:f	1.0000000	0.6084557E-007	0.9999999	1.0000001
135:f	1.0000000	0.2030328E-007	1.0000000	1.0000000
136:f	1.0000000	0.2296787E-007	1.0000000	1.0000000
137:f	1.0000000	0.2792023E-007	0.9999999	1.0000001
138:f	1.0000000	0.2181588E-006	0.9999996	1.0000004
139:f	1.0000000	0.2123547E-006	0.9999996	1.0000004
140:f	1.0000000	0.9564214E-007	0.9999998	1.0000002
141:f	1.0000000	0.9460782E-006	0.9999981	1.0000019
142:f	1.0000000	0.5808344E-006	0.9999989	1.0000011
143:f	1.0000000	0.1137572E-005	0.9999978	1.0000022
144:f	1.0000000	0.2596934E-006	0.9999995	1.0000005
145:f	1.0000000	0.1623508E-004	0.9999682	1.0000318
146:f	1.0000000	0.2633735E-005	0.9999948	1.0000052
147:f	0.9999999	0.9654232E-004	0.1511225E-296	1.0000000
148:f	1.0000000	0.1384971E-005	0.9999973	1.0000027
149:f	0.9999999	0.1503714E-003	0.1744183E-296	1.0000000
150:f	1.0000000	0.6764131E-004	0.3591596E-296	1.0000000
151:f	1.0000000	0.4618295E-004	0.9999095	1.0000905
152:f	0.9999996	0.2610161E-003	0.2412002E-297	1.0000000
153:f	0.5113434	0.0000000	0.5113434	0.5113434
154:f	1.0000000	0.1118124E-003	0.9997808	1.0002191
155:f	0.5272333	0.0000000	0.5272333	0.5272333
156:f	0.4937405	0.0000000	0.4937405	0.4937405
157:f	0.5197838	0.0000000	0.5197838	0.5197838
158:f	0.4833292	0.0000000	0.4833292	0.4833292
159:f	0.4677459	0.0000000	0.4677459	0.4677459
160:f	1.0000000	0.1098249E-003	0.3269787E-296	1.0000000
161:f	1.0000000	0.8872744E-005	0.9999826	1.0000174
162:f	1.0000000	0.1190431E-005	0.9999977	1.0000023
163:f	1.0000000	0.3287274E-006	0.9999994	1.0000006
164:f	1.0000000	0.1950038E-006	0.9999996	1.0000004
165:f	1.0000000	0.2562787E-006	0.9999995	1.0000005
166:f	1.0000000	0.7834981E-007	0.9999998	1.0000002
167:f	1.0000000	0.5112218E-007	0.9999999	1.0000001
168:f	0.2838985	0.0000000	0.2838985	0.2838985
169:f	0.3329615	0.0000000	0.3329615	0.3329615

170:f	0.3055611	0.0000000	0.3055611	0.3055611
171:f	0.8137833	0.0000000	0.8137833	0.8137833
172:f	0.2486825	0.0559027	0.1555017	0.3730356
173:f	0.3053669	0.0383372	0.2357521	0.3851778
174:f	0.5020945	0.0382373	0.4276592	0.5764370
175:f	0.3034953	0.0903666	0.1586109	0.5017958
176:f	0.4388970	0.0551405	0.3352588	0.5481543
177:f	0.3827792	0.0573789	0.2781247	0.4995613
178:f	0.9979932	0.0948368	0.2454869E-037	1.0000000
179:f	0.7232145	0.0000000	0.7232145	0.7232145
180:f	0.4386030	0.0000000	0.4386030	0.4386030
181:f	0.3761180	0.0000000	0.3761180	0.3761180
182:f	0.6320264	0.5993407	0.0108779	0.9962860
183:f	0.5172334	1.1778681	0.1034304E-003	0.9999099
184:f	0.5528408	1.2648919	0.5453548E-004	0.9999643
185:f	0.1022516	0.1457283	0.0050465	0.7189149
186:f	0.9944680	0.9101371	0.2698181E-138	1.0000000
187:f	0.9898518	0.0000000	0.9898518	0.9898518
188:f	0.4966954	0.0000000	0.4966954	0.4966954
189:f	0.5474144	53.057612	0.6153601E-182	1.0000000

A.2 Seber parameterization

BSY_TZA_Schl_TgRcSeber

Real Function Parameters of S(t) r(.) PIM

Parameter	Estimate	Standard Error	95% Confidence Interval Lower	Upper
1:S	0.4500114	0.0000000	0.4500114	0.4500114
2:S	0.4492919	0.0000000	0.4492919	0.4492919
3:S	1.0000000	0.2235175E-007	1.0000000	1.0000000
4:S	0.9933333	0.0066444	0.9542345	0.9990617
5:S	0.9677419	0.0141917	0.9248516	0.9865100
6:S	0.8668885	0.0138565	0.8373124	0.8917827
7:S	0.9637931	0.0054848	0.9513654	0.9731348
8:S	0.9837947	0.0032810	0.9759368	0.9891152
9:S	0.8146877	0.0101793	0.7939021	0.8338158
10:S	0.7142857	0.0126566	0.6888475	0.7384339
11:S	0.8997006	0.0082185	0.8824041	0.9146990
12:S	0.8785358	0.0094222	0.8588263	0.8958274
13:S	0.7121212	0.0139332	0.6840608	0.7386416
14:S	0.7220745	0.0163360	0.6889526	0.7529343
15:S	0.9410681	0.0101061	0.9178485	0.9580250
16:S	0.8160470	0.0171396	0.7800581	0.8472999
17:S	0.7122303	0.0221700	0.6669075	0.7536640
18:S	0.9393939	0.0138453	0.9058679	0.9614870
19:S	0.6594982	0.0283703	0.6019119	0.7127299
20:S	0.7880436	0.0301293	0.7230467	0.8411382
21:S	0.8482759	0.0297928	0.7803032	0.8979682
22:S	0.6422765	0.0432198	0.5539299	0.7219099
23:S	0.9113926	0.0319723	0.8256017	0.9571701
24:S	0.6388892	0.0566066	0.5223960	0.7410530
25:S	0.6521741	0.0702238	0.5054629	0.7747565
26:S	0.9666667	0.0327731	0.7979917	0.9953248
27:S	0.2413796	0.0794628	0.1196581	0.4268804
28:S	0.2857163	0.1707481	0.0720152	0.6733941
29:S	0.1411157E-009	0.1187941E-004	-0.2328350E-004	0.2328378E-004
30:S	0.4501823	0.0000000	0.4501823	0.4501823
31:S	0.4496859	0.0000000	0.4496859	0.4496859
32:S	0.4498176	0.0000000	0.4498176	0.4498176
33:r	1.0000000	0.0000000	1.0000000	1.0000000

Appendix B

PRIMER output

B.1 SIMPER analysis for year and zone

SIMPER
Similarity Percentages - species contributions

Two-Way Analysis

Data worksheet
Name: Data6
Data type: Abundance
Sample selection: All
Variable selection: All

Parameters
Resemblance: S17 Bray Curtis similarity
Cut off for low contributions: 90.00%

Factor Groups
Sample Year Zone
B_S3_FS_05 05 B
B_S4_FS_05 05 B
B_S3_FAD_05 05 B
B_S4_FAD_05 05 B
C_S1_FS_05 05 C
C_S4_FS_05 05 C
C_S1_FAD_05 05 C
C_S4_FAD_05 05 C
D_S2_FAD_05 05 D
B_S1_FS_06 06 B
B_S2_FS_06 06 B
B_S3_FS_06 06 B
B_S4_FS_06 06 B
B_S1_FAD_06 06 B
B_S2_FAD_06 06 B
B_S3_FAD_06 06 B
B_S4_FAD_06 06 B
C_S1_FS_06 06 C
C_S2_FS_06 06 C
C_S4_FS_06 06 C
C_S1_FAD_06 06 C
C_S2_FAD_06 06 C
C_S3_FAD_06 06 C
C_S4_FAD_06 06 C
D_S1_FS_06 06 D
D_S2_FS_06 06 D

D_S2_FAD_06 06 D
E_S1_FS_06 06 E
E_S2_FS_06 06 E
E_S1_FAD_06 06 E
E_S2_FAD_06 06 E
A_S3_FAD_06 06 A
A_S4_FAD_06 06 A
H_S1_FAD_06 06 H
H_S4_FAD_06 06 H
B_S1_FS_07 07 B
B_S2_FS_07 07 B
B_S3_FS_07 07 B
B_S4_FS_07 07 B
B_S1_FAD_07 07 B
B_S2_FAD_07 07 B
B_S3_FAD_07 07 B
B_S4_FAD_07 07 B
C_S1_FS_07 07 C
C_S4_FS_07 07 C
C_S1_FAD_07 07 C
C_S2_FAD_07 07 C
C_S3_FAD_07 07 C
C_S4_FAD_07 07 C
D_S1_FS_07 07 D
D_S2_FS_07 07 D
D_S1_FAD_07 07 D
D_S2_FAD_07 07 D
E_S1_FS_07 07 E
E_S1_FAD_07 07 E
A_S3_FAD_07 07 A
A_S4_FAD_07 07 A
H_S1_FAD_07 07 H
B_S1_FS_08 08 B
B_S2_FS_08 08 B
B_S3_FS_08 08 B
B_S4_FS_08 08 B
B_S1_FAD_08 08 B
B_S2_FAD_08 08 B
B_S3_FAD_08 08 B
B_S4_FAD_08 08 B
C_S1_FS_08 08 C
C_S3_FS_08 08 C
C_S4_FS_08 08 C
C_S1_FAD_08 08 C
C_S2_FAD_08 08 C
C_S3_FAD_08 08 C
C_S4_FAD_08 08 C
D_S1_FS_08 08 D
D_S2_FS_08 08 D
D_S3_FS_08 08 D
D_S1_FAD_08 08 D
D_S2_FAD_08 08 D
D_S3_FAD_08 08 D
E_S1_FS_08 08 E
E_S1_FAD_08 08 E
E_S2_FAD_08 08 E
A_S3_FAD_08 08 A
H_S1_FS_08 08 H
B_S1_FS_09 09 B
B_S3_FS_09 09 B
B_S1_FAD_09 09 B
B_S2_FAD_09 09 B
B_S3_FAD_09 09 B
B_S4_FAD_09 09 B
C_S1_FS_09 09 C
C_S2_FS_09 09 C

C_S3_FS_09 09 C
C_S4_FS_09 09 C
C_S1_FAD_09 09 C
C_S2_FAD_09 09 C
C_S3_FAD_09 09 C
C_S4_FAD_09 09 C
D_S1_FS_09 09 D
D_S2_FS_09 09 D
D_S1_FAD_09 09 D
D_S2_FAD_09 09 D
E_S1_FS_09 09 E
E_S2_FS_09 09 E
E_S3_FS_09 09 E
E_S1_FAD_09 09 E
E_S2_FAD_09 09 E
H_S2_FS_09 09 H
H_S2_FAD_09 09 H
H_S3_FAD_09 09 H
H_S4_FAD_09 09 H
B_S1_FS_10 10 B
B_S2_FS_10 10 B
B_S3_FS_10 10 B
B_S4_FS_10 10 B
B_S1_FAD_10 10 B
B_S2_FAD_10 10 B
B_S3_FAD_10 10 B
B_S4_FAD_10 10 B
C_S1_FS_10 10 C
C_S2_FS_10 10 C
C_S3_FS_10 10 C
C_S4_FS_10 10 C
C_S1_FAD_10 10 C
C_S4_FAD_10 10 C
D_S1_FS_10 10 D
D_S1_FAD_10 10 D
D_S2_FAD_10 10 D
B_S3_FS_11 11 B
B_S1_FAD_11 11 B
B_S3_FAD_11 11 B
C_S1_FS_11 11 C
C_S1_FAD_11 11 C
D_S1_FAD_11 11 D
E_S2_FS_11 11 E
H_S1_FS_11 11 H
H_S1_FAD_11 11 H

Examines Year groups
(across all Zone groups)
Group 05
Average similarity: 38.26

Species	Av.Abund	Av.Sim	Sim/SD	Contrib%	Cum.%
S_Adt	2.54	29.64	1.20	77.45	77.45
B_juv	0.43	3.08	0.54	8.05	85.50
Y_juv	0.50	2.83	0.29	7.41	92.91

Group 06
Average similarity: 49.02

Species	Av.Abund	Av.Sim	Sim/SD	Contrib%	Cum.%
S_Adt	9.09	27.63	1.81	56.37	56.37
Y_pAd	3.23	5.12	1.09	10.44	66.80
B_juv	2.96	4.90	0.90	10.00	76.81
Y_juv	3.72	4.89	0.66	9.98	86.78
Y_Adt	1.91	4.23	0.99	8.63	95.42

```
Group 07
Average similarity: 48.11

Species Av.Abund Av.Sim Sim/SD Contrib% Cum.%
S_Adt    12.66  16.72   1.98    34.76 34.76
Y_pAd     5.85   8.26   1.37    17.17 51.94
B_juv     6.55   6.63   1.47    13.79 65.73
Y_Adt     4.96   6.41   1.08    13.33 79.06
Y_juv     5.47   5.04   1.36    10.47 89.53
B_pAd     3.86   3.90   0.94     8.11 97.64

Group 08
Average similarity: 48.31

Species Av.Abund Av.Sim Sim/SD Contrib% Cum.%
Y_Adt     5.14  15.50   1.34    32.08 32.08
S_Adt     5.19  12.85   1.57    26.61 58.69
B_juv     3.39   5.61   0.84    11.62 70.31
Y_pAd     2.18   5.10   1.00    10.56 80.86
B_pAd     2.93   4.53   0.73     9.38 90.24

Group 09
Average similarity: 30.29

Species Av.Abund Av.Sim Sim/SD Contrib% Cum.%
Y_Adt     2.69  15.61   0.83    51.54 51.54
S_Adt     1.71   5.40   0.61    17.84 69.38
S_juv     0.65   3.30   0.35    10.88 80.26
B_Adt     1.01   2.09   0.41     6.89 87.15
B_pAd     1.10   1.68   0.36     5.56 92.71

Group 10
Average similarity: 31.91

Species Av.Abund Av.Sim Sim/SD Contrib% Cum.%
Y_Adt     2.49  21.35   0.98    66.89 66.89
B_Adt     1.48   6.82   0.72    21.38 88.27
Y_juv     0.47   2.24   0.27     7.03 95.30

Group 11
Average similarity: 61.75

Species Av.Abund Av.Sim Sim/SD Contrib%  Cum.%
Y_Adt     2.53  49.61   1.78    80.34  80.34
B_Adt     1.43  12.14   0.59    19.66 100.00

Groups 05  &  06
Average dissimilarity = 73.23

Group 05 Group 06
Species Av.Abund Av.Abund Av.Diss Diss/SD Contrib% Cum.%
S_Adt     2.54     9.09   29.01    1.85    39.62 39.62
Y_juv     0.50     3.72   12.01    1.12    16.40 56.02
Y_pAd     0.40     3.23   10.80    1.50    14.75 70.77
B_juv     0.43     2.96    8.41    1.46    11.48 82.25
Y_Adt     0.13     1.91    6.41    1.48     8.76 91.01

Groups 05  &  07
Average dissimilarity = 77.53

Group 05 Group 07
Species Av.Abund Av.Abund Av.Diss Diss/SD Contrib% Cum.%
S_Adt     2.54    12.66   21.22    1.91    27.37 27.37
Y_pAd     0.40     5.85   12.05    2.21    15.55 42.91
Y_Adt     0.13     4.96   11.89    1.55    15.33 58.24
B_juv     0.43     6.55   11.13    1.85    14.35 72.60
```

```
Y_juv     0.50     5.47    9.50    1.92    12.25 84.84
B_pAd     0.32     3.86    8.78    1.29    11.32 96.16

Groups 06  &  07
Average dissimilarity = 54.31

Group 06 Group 07
Species Av.Abund Av.Abund Av.Diss Diss/SD Contrib% Cum.%
S_Adt     9.09    12.66   15.23    1.31    28.05 28.05
Y_pAd     3.23     5.85    8.97    1.04    16.52 44.56
Y_juv     3.72     5.47    8.18    1.48    15.05 59.62
B_juv     2.96     6.55    7.55    1.30    13.90 73.51
Y_Adt     1.91     4.96    6.05    1.17    11.14 84.65
B_pAd     0.95     3.86    5.24    1.11     9.65 94.30

Groups 05  &  08
Average dissimilarity = 78.30

Group 05 Group 08
Species Av.Abund Av.Abund Av.Diss Diss/SD Contrib% Cum.%
Y_Adt     0.13     5.14   22.83    1.87    29.16 29.16
S_Adt     2.54     5.19   16.08    1.40    20.53 49.69
B_juv     0.43     3.39   10.52    1.09    13.44 63.13
B_pAd     0.32     2.93    8.40    1.04    10.73 73.86
Y_pAd     0.40     2.18    8.08    1.20    10.31 84.17
B_Adt     0.00     1.15    6.34    0.89     8.10 92.27

Groups 06  &  08
Average dissimilarity = 62.08

Group 06 Group 08
Species Av.Abund Av.Abund Av.Diss Diss/SD Contrib% Cum.%
S_Adt     9.09     5.19   17.90    1.52    28.83 28.83
Y_Adt     1.91     5.14   10.67    0.96    17.19 46.02
B_juv     2.96     3.39    8.23    1.35    13.25 59.27
Y_juv     3.72     1.47    7.36    1.01    11.85 71.12
Y_pAd     3.23     2.18    6.16    1.24     9.92 81.05
B_pAd     0.95     2.93    6.11    0.88     9.84 90.88

Groups 07  &  08
Average dissimilarity = 55.45

Group 07 Group 08
Species Av.Abund Av.Abund Av.Diss Diss/SD Contrib% Cum.%
S_Adt    12.66     5.19   13.86    1.62    25.00 25.00
Y_Adt     4.96     5.14    8.81    0.92    15.89 40.89
B_juv     6.55     3.39    8.17    1.51    14.73 55.62
Y_pAd     5.85     2.18    7.30    1.15    13.17 68.78
Y_juv     5.47     1.47    6.90    1.49    12.45 81.23
B_pAd     3.86     2.93    6.45    1.26    11.64 92.87

Groups 05  &  09
Average dissimilarity = 78.86

Group 05 Group 09
Species Av.Abund Av.Abund Av.Diss Diss/SD Contrib% Cum.%
S_Adt     2.54     1.71   20.59    1.42    26.11 26.11
Y_Adt     0.13     2.69   19.00    1.31    24.10 50.21
S_juv     0.27     0.65    8.46    0.58    10.73 60.93
B_Adt     0.00     1.01    8.07    0.66    10.23 71.16
Y_juv     0.50     0.45    7.56    0.58     9.59 80.75
B_pAd     0.32     1.10    6.18    0.77     7.84 88.59
Y_pAd     0.40     0.57    5.32    0.90     6.75 95.34

Groups 06  &  09
Average dissimilarity = 78.60
```

```
Group 06 Group 09
Species Av.Abund Av.Abund Av.Diss Diss/SD Contrib% Cum.%
S_Adt      9.09     1.71   27.56    1.79    35.07 35.07
Y_Adt      1.91     2.69   13.55    0.94    17.24 52.31
Y_juv      3.72     0.45    7.87    1.01    10.01 62.32
B_juv      2.96     0.27    7.72    1.14     9.83 72.14
Y_pAd      3.23     0.57    7.35    1.09     9.35 81.49
S_juv      1.10     0.65    6.21    0.67     7.90 89.39
B_pAd      0.95     1.10    4.25    0.59     5.41 94.80

Groups 07  &  09
Average dissimilarity = 76.92

Group 07 Group 09
Species Av.Abund Av.Abund Av.Diss Diss/SD Contrib% Cum.%
S_Adt     12.66     1.71   20.59    1.92    26.77 26.77
Y_pAd      5.85     0.57   11.54    1.38    15.00 41.77
Y_Adt      4.96     2.69   11.20    1.30    14.56 56.32
B_juv      6.55     0.27   10.36    1.71    13.47 69.79
Y_juv      5.47     0.45    9.06    1.48    11.78 81.57
B_pAd      3.86     1.10    7.04    1.14     9.15 90.72

Groups 08  &  09
Average dissimilarity = 66.68

Group 08 Group 09
Species Av.Abund Av.Abund Av.Diss Diss/SD Contrib% Cum.%
Y_Adt      5.14     2.69   16.86    1.15    25.29 25.29
S_Adt      5.19     1.71   13.89    1.29    20.84 46.13
B_juv      3.39     0.27    9.15    1.08    13.72 59.86
B_pAd      2.93     1.10    8.29    0.99    12.43 72.28
Y_pAd      2.18     0.57    6.18    1.10     9.27 81.56
B_Adt      1.15     1.01    5.54    0.81     8.31 89.86
Y_juv      1.47     0.45    3.98    0.86     5.97 95.83

Groups 05  &  10
Average dissimilarity = 84.09

Group 05 Group 10
Species Av.Abund Av.Abund Av.Diss Diss/SD Contrib% Cum.%
S_Adt      2.54     0.81   25.97    1.57    30.89 30.89
Y_Adt      0.13     2.49   22.13    1.35    26.32 57.21
B_Adt      0.00     1.48   13.35    0.85    15.87 73.08
Y_juv      0.50     0.47    8.30    0.59     9.86 82.95
B_juv      0.43     0.30    4.28    0.80     5.10 88.04
Y_pAd      0.40     0.18    3.69    0.81     4.38 92.42

Groups 06  &  10
Average dissimilarity = 83.90

Group 06 Group 10
Species Av.Abund Av.Abund Av.Diss Diss/SD Contrib% Cum.%
S_Adt      9.09     0.81   32.25    2.32    38.44 38.44
Y_pAd      3.23     0.18   10.59    1.71    12.63 51.07
Y_juv      3.72     0.47   10.46    1.25    12.46 63.53
B_juv      2.96     0.30    9.36    1.52    11.16 74.69
Y_Adt      1.91     2.49    9.15    0.90    10.91 85.60
B_Adt      0.07     1.48    5.67    0.60     6.76 92.36

Groups 07  &  10
Average dissimilarity = 84.12

Group 07 Group 10
Species Av.Abund Av.Abund Av.Diss Diss/SD Contrib% Cum.%
S_Adt     12.66     0.81   24.63    2.68    29.28 29.28
```

```
B_juv     6.55     0.30   12.04    2.07    14.31 43.58
Y_pAd     5.85     0.18   11.98    2.69    14.24 57.83
Y_Adt     4.96     2.49   11.19    1.30    13.30 71.13
Y_juv     5.47     0.47    9.77    1.96    11.61 82.74
B_pAd     3.86     0.13    8.29    1.30     9.85 92.59

Groups 08  &  10
Average dissimilarity = 72.88

Group 08 Group 10
Species Av.Abund Av.Abund Av.Diss Diss/SD Contrib% Cum.%
Y_Adt     5.14     2.49   16.76    1.44    23.00 23.00
S_Adt     5.19     0.81   16.09    1.62    22.08 45.08
B_juv     3.39     0.30    9.98    1.12    13.70 58.78
B_pAd     2.93     0.13    9.08    1.08    12.46 71.24
Y_pAd     2.18     0.18    8.64    1.33    11.86 83.10
B_Adt     1.15     1.48    7.12    0.87     9.78 92.87

Groups 09  &  10
Average dissimilarity = 72.34

Group 09 Group 10
Species Av.Abund Av.Abund Av.Diss Diss/SD Contrib% Cum.%
Y_Adt     2.69     2.49   21.59    1.61    29.85 29.85
S_Adt     1.71     0.81   14.62    1.06    20.21 50.05
B_Adt     1.01     1.48   13.10    0.94    18.11 68.16
B_pAd     1.10     0.13    6.27    0.81     8.66 76.83
Y_pAd     0.57     0.18    5.19    0.67     7.18 84.01
Y_juv     0.45     0.47    4.54    0.73     6.28 90.28

Groups 05  &  11
Average dissimilarity = 93.03

Group 05 Group 11
Species Av.Abund Av.Abund Av.Diss Diss/SD Contrib% Cum.%
Y_Adt     0.13     2.53   33.53    1.56    36.04 36.04
S_Adt     2.54     0.19   25.03    1.67    26.90 62.94
B_Adt     0.00     1.43   18.66    1.43    20.06 83.00
B_juv     0.43     0.00    3.95    0.79     4.24 87.25
Y_juv     0.50     0.00    3.77    0.64     4.05 91.30

Groups 06  &  11
Average dissimilarity = 89.80

Group 06 Group 11
Species Av.Abund Av.Abund Av.Diss Diss/SD Contrib% Cum.%
S_Adt     9.09     0.19   36.11    2.16    40.21 40.21
Y_Adt     1.91     2.53   12.55    0.84    13.98 54.19
B_juv     2.96     0.00   10.23    1.32    11.40 65.59
Y_juv     3.72     0.00    9.18    1.03    10.23 75.81
Y_pAd     3.23     0.00    8.81    1.36     9.82 85.63
B_Adt     0.07     1.43    6.48    0.82     7.22 92.85

Groups 07  &  11
Average dissimilarity = 85.65

Group 07 Group 11
Species Av.Abund Av.Abund Av.Diss Diss/SD Contrib% Cum.%
S_Adt    12.66     0.19   23.73    2.47    27.71 27.71
Y_Adt     4.96     2.53   12.87    1.11    15.03 42.74
Y_pAd     5.85     0.00   12.83    1.55    14.98 57.72
B_juv     6.55     0.00   11.67    2.03    13.63 71.35
Y_juv     5.47     0.00    9.99    1.84    11.67 83.02
B_pAd     3.86     0.00    7.56    1.25     8.83 91.84

Groups 08  &  11
```

Average dissimilarity = 68.95

Group 08 Group 11

Species	Av.Abund	Av.Abund	Av.Diss	Diss/SD	Contrib%	Cum.%
Y_Adt	5.14	2.53	15.80	1.15	22.91	22.91
S_Adt	5.19	0.19	15.61	1.58	22.64	45.55
B_pAd	2.93	0.00	9.38	0.98	13.61	59.16
B_juv	3.39	0.00	9.38	1.08	13.60	72.76
Y_pAd	2.18	0.00	8.05	1.26	11.68	84.44
B_Adt	1.15	1.43	6.45	0.82	9.36	93.80

Groups 09 & 11

Average dissimilarity = 75.85

Group 09 Group 11

Species	Av.Abund	Av.Abund	Av.Diss	Diss/SD	Contrib%	Cum.%
Y_Adt	2.69	2.53	29.54	1.47	38.95	38.95
B_Adt	1.01	1.43	12.69	0.98	16.73	55.68
S_Adt	1.71	0.19	12.64	0.95	16.66	72.34
S_juv	0.65	0.00	7.11	0.50	9.38	81.72
B_pAd	1.10	0.00	5.57	0.56	7.34	89.06
Y_juv	0.45	0.00	3.59	0.45	4.73	93.79

Groups 10 & 11

Average dissimilarity = 56.08

Group 10 Group 11

Species	Av.Abund	Av.Abund	Av.Diss	Diss/SD	Contrib%	Cum.%
Y_Adt	2.49	2.53	24.39	1.51	43.49	43.49
B_Adt	1.48	1.43	17.77	1.12	31.69	75.18
S_Adt	0.81	0.19	5.59	0.68	9.97	85.15
Y_juv	0.47	0.00	4.11	0.41	7.34	92.49

Examines Zone groups

(across all Year groups)

Group B

Average similarity: 45.72

Species	Av.Abund	Av.Sim	Sim/SD	Contrib%	Cum.%
Y_Adt	5.00	14.95	0.98	32.70	32.70
S_Adt	7.27	12.83	1.06	28.06	60.76
Y_pAd	3.23	4.61	0.99	10.08	70.84
B_juv	3.31	3.92	0.82	8.58	79.42
B_Adt	1.54	3.48	0.48	7.61	87.03
Y_juv	3.18	2.94	0.63	6.43	93.45

Group C

Average similarity: 32.72

Species	Av.Abund	Av.Sim	Sim/SD	Contrib%	Cum.%
S_Adt	5.61	12.71	0.90	38.84	38.84
Y_Adt	3.62	8.69	0.74	26.55	65.39
Y_pAd	2.49	2.99	0.64	9.13	74.52
B_juv	2.24	2.33	0.55	7.13	81.65
B_Adt	1.03	2.16	0.39	6.60	88.25
Y_juv	1.92	1.78	0.41	5.43	93.68

Group D

Average similarity: 49.27

Species	Av.Abund	Av.Sim	Sim/SD	Contrib%	Cum.%
S_Adt	6.63	16.22	1.44	32.93	32.93
B_juv	3.82	7.63	0.95	15.48	48.41
Y_Adt	1.77	7.47	0.71	15.16	63.57
B_pAd	1.84	6.36	0.94	12.91	76.49
Y_juv	2.33	6.09	0.62	12.36	88.85

```
Y_pAd     1.76   4.67   0.98     9.49 98.33

Group E
Average similarity: 54.14

Species Av.Abund Av.Sim Sim/SD Contrib% Cum.%
Y_Adt     1.22  27.63   1.06    51.04 51.04
S_Adt     1.36  19.46   0.72    35.95 86.98
Y_pAd     0.67   2.28   0.25     4.22 91.20

Group A
Average similarity: 60.27

Species Av.Abund Av.Sim Sim/SD Contrib% Cum.%
S_Adt     3.84  32.24   2.10    53.50 53.50
Y_juv     1.59  19.69   0.71    32.68 86.18
Y_Adt     0.59   4.31   0.71     7.15 93.33

Group H
Average similarity: 36.03

Species Av.Abund Av.Sim Sim/SD Contrib% Cum.%
S_juv     0.51  14.19   0.66    39.39 39.39
Y_Adt     0.61  11.68   0.35    32.42 71.81
S_Adt     0.99   4.25   0.50    11.79 83.60
Y_juv     0.26   2.99   0.35     8.31 91.91

Groups B  &  C
Average dissimilarity = 59.10

 Group B  Group C
Species Av.Abund Av.Abund Av.Diss Diss/SD Contrib% Cum.%
S_Adt     7.27     5.61   13.87    1.06    23.48 23.48
Y_Adt     5.00     3.62   13.10    1.07    22.17 45.65
B_Adt     1.54     1.03    6.88    0.63    11.64 57.28
B_juv     3.31     2.24    5.78    1.04     9.78 67.06
Y_pAd     3.23     2.49    5.71    0.96     9.67 76.73
Y_juv     3.18     1.92    5.67    0.92     9.59 86.33
B_pAd     2.56     1.44    5.16    0.89     8.73 95.05

Groups B  &  D
Average dissimilarity = 58.92

 Group B  Group D
Species Av.Abund Av.Abund Av.Diss Diss/SD Contrib% Cum.%
Y_Adt     5.00     1.77   13.89    1.09    23.57 23.57
S_Adt     7.27     6.63   12.50    1.16    21.21 44.79
Y_juv     3.18     2.33    7.84    0.81    13.30 58.09
B_juv     3.31     3.82    6.66    1.06    11.30 69.38
B_Adt     1.54     0.17    6.01    0.68    10.20 79.58
B_pAd     2.56     1.84    5.89    0.94    10.00 89.58
Y_pAd     3.23     1.76    4.67    0.99     7.93 97.51

Groups C  &  D
Average dissimilarity = 61.32

 Group C  Group D
Species Av.Abund Av.Abund Av.Diss Diss/SD Contrib% Cum.%
S_Adt     5.61     6.63   14.70    1.36    23.97 23.97
Y_Adt     3.62     1.77   12.22    0.95    19.93 43.90
Y_juv     1.92     2.33    7.40    0.78    12.07 55.96
B_juv     2.24     3.82    6.88    1.04    11.22 67.18
B_pAd     1.44     1.84    6.67    0.94    10.88 78.06
B_Adt     1.03     0.17    5.20    0.49     8.48 86.54
Y_pAd     2.49     1.76    5.00    1.08     8.15 94.69
```

```
Groups B  &  E
Average dissimilarity = 73.77

 Group B  Group E
Species Av.Abund Av.Abund Av.Diss Diss/SD Contrib% Cum.%
S_Adt      7.27     1.36   18.52    1.31    25.11 25.11
Y_Adt      5.00     1.22   17.50    1.45    23.72 48.83
Y_pAd      3.23     0.67    8.62    1.25    11.69 60.51
B_pAd      2.56     0.69    7.21    0.90     9.77 70.29
B_juv      3.31     0.44    7.01    1.04     9.50 79.79
Y_juv      3.18     0.23    6.81    0.86     9.23 89.02
B_Adt      1.54     0.13    6.36    0.66     8.62 97.64

Groups C  &  E
Average dissimilarity = 70.97

 Group C  Group E
Species Av.Abund Av.Abund Av.Diss Diss/SD Contrib% Cum.%
S_Adt      5.61     1.36   18.84    1.41    26.55 26.55
Y_Adt      3.62     1.22   16.98    0.99    23.93 50.49
Y_pAd      2.49     0.67    7.29    1.07    10.28 60.76
B_pAd      1.44     0.69    6.23    0.67     8.78 69.54
S_juv      0.69     0.13    5.74    0.58     8.08 77.63
B_juv      2.24     0.44    5.59    0.90     7.87 85.50
B_Adt      1.03     0.13    5.40    0.56     7.61 93.10

Groups D  &  E
Average dissimilarity = 60.96

 Group D  Group E
Species Av.Abund Av.Abund Av.Diss Diss/SD Contrib% Cum.%
S_Adt      6.63     1.36   21.17    1.79    34.73 34.73
B_pAd      1.84     0.69    9.53    1.05    15.64 50.37
B_juv      3.82     0.44    9.48    1.14    15.55 65.92
Y_Adt      1.77     1.22    6.57    0.72    10.78 76.70
Y_pAd      1.76     0.67    5.50    1.05     9.01 85.71
Y_juv      2.33     0.23    5.02    0.91     8.23 93.94

Groups B  &  A
Average dissimilarity = 73.53

 Group B  Group A
Species Av.Abund Av.Abund Av.Diss Diss/SD Contrib% Cum.%
S_Adt      7.27     3.84   19.13    1.41    26.02 26.02
Y_Adt      5.00     0.59   14.20    1.49    19.31 45.33
B_juv      3.31     0.00   10.60    1.91    14.42 59.75
Y_pAd      3.23     0.75    9.28    1.84    12.62 72.38
Y_juv      3.18     1.59    8.82    1.29    12.00 84.37
B_pAd      2.56     0.15    6.78    0.99     9.22 93.59

Groups C  &  A
Average dissimilarity = 66.56

 Group C  Group A
Species Av.Abund Av.Abund Av.Diss Diss/SD Contrib% Cum.%
S_Adt      5.61     3.84   21.03    2.13    31.59 31.59
Y_juv      1.92     1.59   11.05    0.78    16.60 48.19
Y_Adt      3.62     0.59    9.49    0.89    14.26 62.45
Y_pAd      2.49     0.75    9.27    1.50    13.92 76.37
B_juv      2.24     0.00    8.44    1.23    12.68 89.05
B_pAd      1.44     0.15    3.87    0.76     5.82 94.86

Groups D  &  A
Average dissimilarity = 66.36

 Group D  Group A
```

```
Species Av.Abund Av.Abund Av.Diss Diss/SD Contrib% Cum.%
S_Adt     6.63     3.84   19.57    1.79    29.49 29.49
B_juv     3.82     0.00   15.48    2.16    23.32 52.81
Y_juv     2.33     1.59   10.14    1.39    15.27 68.09
Y_pAd     1.76     0.75    6.62    1.24     9.97 78.06
B_pAd     1.84     0.15    6.16    1.06     9.28 87.34
Y_Adt     1.77     0.59    4.56    1.01     6.87 94.21

Groups E  &  A
Average dissimilarity = 60.12

 Group E  Group A
Species Av.Abund Av.Abund Av.Diss Diss/SD Contrib% Cum.%
Y_juv     0.23     1.59   21.66    1.06    36.03 36.03
S_Adt     1.36     3.84   15.52    0.84    25.82 61.85
Y_pAd     0.67     0.75    6.96    1.18    11.58 73.44
Y_Adt     1.22     0.59    5.34    0.72     8.88 82.31
B_juv     0.44     0.00    3.57    0.71     5.93 88.24
S_juv     0.13     0.00    3.55    0.57     5.91 94.15

Groups B  &  H
Average dissimilarity = 82.04

 Group B  Group H
Species Av.Abund Av.Abund Av.Diss Diss/SD Contrib% Cum.%
S_Adt     7.27     0.99   19.52    1.32    23.80 23.80
Y_Adt     5.00     0.61   17.05    1.41    20.79 44.58
B_Adt     1.54     0.00    9.41    0.71    11.47 56.05
Y_pAd     3.23     0.00    9.15    1.02    11.15 67.20
Y_juv     3.18     0.26    8.40    0.97    10.24 77.44
S_juv     0.71     0.51    6.49    0.64     7.91 85.35
B_pAd     2.56     0.00    6.04    0.85     7.36 92.71

Groups C  &  H
Average dissimilarity = 77.83

 Group C  Group H
Species Av.Abund Av.Abund Av.Diss Diss/SD Contrib% Cum.%
S_Adt     5.61     0.99   21.79    1.45    27.99 27.99
Y_Adt     3.62     0.61   16.14    1.04    20.73 48.73
S_juv     0.69     0.51    9.63    0.60    12.38 61.10
Y_juv     1.92     0.26    6.99    0.76     8.98 70.08
Y_pAd     2.49     0.00    6.95    0.93     8.93 79.01
B_juv     2.24     0.25    6.58    0.90     8.46 87.47
B_Adt     1.03     0.00    6.07    0.50     7.80 95.28

Groups D  &  H
Average dissimilarity = 79.20

 Group D  Group H
Species Av.Abund Av.Abund Av.Diss Diss/SD Contrib% Cum.%
S_Adt     6.63     0.99   23.26    1.72    29.37 29.37
Y_Adt     1.77     0.61   13.53    0.98    17.08 46.45
B_pAd     1.84     0.00   12.24    1.21    15.46 61.91
S_juv     0.63     0.51    7.98    0.81    10.07 71.99
B_juv     3.82     0.25    7.95    0.87    10.04 82.03
Y_juv     2.33     0.26    6.66    0.94     8.41 90.44

Groups E  &  H
Average dissimilarity = 82.91

 Group E  Group H
Species Av.Abund Av.Abund Av.Diss Diss/SD Contrib% Cum.%
Y_Adt     1.22     0.61   29.41    1.16    35.47 35.47
S_Adt     1.36     0.99   16.31    1.09    19.67 55.15
S_juv     0.13     0.51   12.41    0.89    14.97 70.12
```

```
Y_juv      0.23      0.26     6.16     0.68      7.43 77.55
B_juv      0.44      0.25     5.72     0.76      6.90 84.46
B_pAd      0.69      0.00     5.62     0.43      6.78 91.24

Groups A  &  H
Average dissimilarity = 81.98

 Group A  Group H
Species Av.Abund Av.Abund Av.Diss Diss/SD Contrib% Cum.%
S_Adt      3.84      0.99    35.27     1.67     43.03 43.03
Y_juv      1.59      0.26    21.86     1.11     26.67 69.70
Y_Adt      0.59      0.61     9.88     0.52     12.06 81.75
Y_pAd      0.75      0.00     7.23     0.80      8.82 90.57
```

B.2 SIMPER analysis for season and school-type

SIMPER
Similarity Percentages - species contributions

Two-Way Analysis

Data worksheet
Name: AllRecapture
Data type: Abundance
Sample selection: All
Variable selection: All

Parameters
Resemblance: S17 Bray Curtis similarity
Cut off for low contributions: 90.00%

Factor Groups
Sample School Season
B_S3_FS_05 FS S3
B_S3_FS_06 FS S3
B_S3_FS_07 FS S3
B_S3_FS_08 FS S3
C_S3_FS_08 FS S3
D_S3_FS_08 FS S3
B_S3_FS_09 FS S3
C_S3_FS_09 FS S3
E_S3_FS_09 FS S3
B_S3_FS_10 FS S3
C_S3_FS_10 FS S3
B_S3_FS_11 FS S3
B_S4_FS_05 FS S4
C_S4_FS_05 FS S4
B_S4_FS_06 FS S4
C_S4_FS_06 FS S4
B_S4_FS_07 FS S4
C_S4_FS_07 FS S4
B_S4_FS_08 FS S4
C_S4_FS_08 FS S4
C_S4_FS_09 FS S4
B_S4_FS_10 FS S4
C_S4_FS_10 FS S4
C_S1_FS_05 FS S1
B_S1_FS_06 FS S1
C_S1_FS_06 FS S1
D_S1_FS_06 FS S1
E_S1_FS_06 FS S1
B_S1_FS_07 FS S1
C_S1_FS_07 FS S1
D_S1_FS_07 FS S1
E_S1_FS_07 FS S1
B_S1_FS_08 FS S1
C_S1_FS_08 FS S1
D_S1_FS_08 FS S1
E_S1_FS_08 FS S1
H_S1_FS_08 FS S1
B_S1_FS_09 FS S1
C_S1_FS_09 FS S1
D_S1_FS_09 FS S1
E_S1_FS_09 FS S1
B_S1_FS_10 FS S1
C_S1_FS_10 FS S1
D_S1_FS_10 FS S1
C_S1_FS_11 FS S1
H_S1_FS_11 FS S1
B_S2_FS_06 FS S2
C_S2_FS_06 FS S2

D_S2_FS_06 FS S2
E_S2_FS_06 FS S2
B_S2_FS_07 FS S2
D_S2_FS_07 FS S2
B_S2_FS_08 FS S2
D_S2_FS_08 FS S2
C_S2_FS_09 FS S2
D_S2_FS_09 FS S2
E_S2_FS_09 FS S2
H_S2_FS_09 FS S2
B_S2_FS_10 FS S2
C_S2_FS_10 FS S2
E_S2_FS_11 FS S2
B_S3_FAD_05 FAD S3
A_S3_FAD_06 FAD S3
B_S3_FAD_06 FAD S3
C_S3_FAD_06 FAD S3
A_S3_FAD_07 FAD S3
B_S3_FAD_07 FAD S3
C_S3_FAD_07 FAD S3
A_S3_FAD_08 FAD S3
B_S3_FAD_08 FAD S3
C_S3_FAD_08 FAD S3
D_S3_FAD_08 FAD S3
B_S3_FAD_09 FAD S3
C_S3_FAD_09 FAD S3
H_S3_FAD_09 FAD S3
B_S3_FAD_10 FAD S3
B_S3_FAD_11 FAD S3
B_S4_FAD_05 FAD S4
C_S4_FAD_05 FAD S4
A_S4_FAD_06 FAD S4
B_S4_FAD_06 FAD S4
C_S4_FAD_06 FAD S4
H_S4_FAD_06 FAD S4
A_S4_FAD_07 FAD S4
B_S4_FAD_07 FAD S4
C_S4_FAD_07 FAD S4
B_S4_FAD_08 FAD S4
C_S4_FAD_08 FAD S4
B_S4_FAD_09 FAD S4
C_S4_FAD_09 FAD S4
H_S4_FAD_09 FAD S4
B_S4_FAD_10 FAD S4
C_S4_FAD_10 FAD S4
C_S1_FAD_05 FAD S1
B_S1_FAD_06 FAD S1
C_S1_FAD_06 FAD S1
E_S1_FAD_06 FAD S1
H_S1_FAD_06 FAD S1
B_S1_FAD_07 FAD S1
C_S1_FAD_07 FAD S1
D_S1_FAD_07 FAD S1
E_S1_FAD_07 FAD S1
H_S1_FAD_07 FAD S1
B_S1_FAD_08 FAD S1
C_S1_FAD_08 FAD S1
D_S1_FAD_08 FAD S1
E_S1_FAD_08 FAD S1
B_S1_FAD_09 FAD S1
C_S1_FAD_09 FAD S1
D_S1_FAD_09 FAD S1
E_S1_FAD_09 FAD S1
B_S1_FAD_10 FAD S1
C_S1_FAD_10 FAD S1
D_S1_FAD_10 FAD S1

```
B_S1_FAD_11 FAD S1
C_S1_FAD_11 FAD S1
D_S1_FAD_11 FAD S1
H_S1_FAD_11 FAD S1
D_S2_FAD_05 FAD S2
B_S2_FAD_06 FAD S2
C_S2_FAD_06 FAD S2
D_S2_FAD_06 FAD S2
E_S2_FAD_06 FAD S2
B_S2_FAD_07 FAD S2
C_S2_FAD_07 FAD S2
D_S2_FAD_07 FAD S2
B_S2_FAD_08 FAD S2
C_S2_FAD_08 FAD S2
D_S2_FAD_08 FAD S2
E_S2_FAD_08 FAD S2
B_S2_FAD_09 FAD S2
C_S2_FAD_09 FAD S2
D_S2_FAD_09 FAD S2
E_S2_FAD_09 FAD S2
H_S2_FAD_09 FAD S2
B_S2_FAD_10 FAD S2
D_S2_FAD_10 FAD S2

Examines School groups
(across all Season groups)
Group FS
Average similarity: 28.38

Species Av.Abund Av.Sim Sim/SD Contrib% Cum.%
Y_Adt     3.28  11.69   0.72    41.21 41.21
S_Adt     3.70   8.12   0.69    28.61 69.82
Y_pAd     1.35   2.49   0.47     8.79 78.61
Y_juv     1.19   1.72   0.37     6.08 84.68
B_Adt     0.94   1.62   0.26     5.72 90.40

Group FAD
Average similarity: 26.08

Species Av.Abund Av.Sim Sim/SD Contrib% Cum.%
S_Adt     6.86  11.27   0.83    43.21 43.21
Y_Adt     3.11   5.93   0.49    22.73 65.94
B_juv     3.34   2.30   0.50     8.83 74.77
Y_pAd     2.83   2.14   0.53     8.22 82.99
Y_juv     2.80   1.81   0.44     6.93 89.92
B_pAd     2.20   1.51   0.39     5.77 95.69

Groups FS  &  FAD
Average dissimilarity = 73.43

Group FS Group FAD
Species Av.Abund  Av.Abund Av.Diss Diss/SD Contrib% Cum.%
S_Adt     3.70      6.86   20.29    1.37    27.63 27.63
Y_Adt     3.28      3.11   14.79    1.05    20.15 47.78
B_juv     1.29      3.34    8.12    1.08    11.05 58.83
Y_pAd     1.35      2.83    8.08    1.04    11.00 69.83
Y_juv     1.19      2.80    7.42    0.87    10.10 79.93
B_pAd     0.93      2.20    6.60    0.85     8.99 88.92
B_Adt     0.94      0.78    5.08    0.60     6.91 95.83

Examines Season groups
(across all School groups)
Group S3
Average similarity: 31.01

Species Av.Abund Av.Sim Sim/SD Contrib% Cum.%
```

```
S_Adt     6.35  10.82   0.87    34.88 34.88
Y_Adt     4.75   9.22   0.81    29.74 64.62
B_Adt     1.78   2.96   0.34     9.56 74.17
Y_pAd     2.22   2.32   0.60     7.49 81.66
B_juv     2.73   2.30   0.58     7.42 89.08
Y_juv     2.99   1.92   0.50     6.19 95.27

Group S4
Average similarity: 27.89

Species Av.Abund Av.Sim Sim/SD Contrib% Cum.%
S_Adt     5.14  13.55   0.86    48.59 48.59
Y_Adt     2.76   7.82   0.58    28.03 76.62
Y_juv     1.67   2.27   0.38     8.15 84.78
Y_pAd     1.83   1.66   0.48     5.94 90.71

Group S1
Average similarity: 27.46

Species Av.Abund Av.Sim Sim/SD Contrib% Cum.%
Y_Adt     3.19   9.23   0.59    33.60 33.60
S_Adt     4.87   8.38   0.79    30.52 64.12
Y_pAd     2.68   2.89   0.54    10.52 74.63
B_juv     2.56   2.29   0.51     8.33 82.96
Y_juv     1.86   1.95   0.44     7.11 90.08

Group S2
Average similarity: 22.83

Species Av.Abund Av.Sim Sim/SD Contrib% Cum.%
S_Adt     5.79  10.45   0.70    45.76 45.76
Y_Adt     2.22   5.91   0.46    25.89 71.65
B_juv     2.77   1.54   0.36     6.75 78.40
Y_pAd     1.67   1.45   0.40     6.34 84.75
B_pAd     1.58   1.37   0.42     5.99 90.73

Groups S3  &  S4
Average dissimilarity = 69.79

Group S3 Group S4
Species Av.Abund Av.Abund Av.Diss Diss/SD Contrib% Cum.%
S_Adt     6.35     5.14   18.85    1.43    27.01 27.01
Y_Adt     4.75     2.76   13.80    1.15    19.78 46.79
Y_juv     2.99     1.67    7.74    0.81    11.09 57.87
B_Adt     1.78     0.63    7.46    0.65    10.69 68.57
B_juv     2.73     1.43    6.79    1.09     9.74 78.30
Y_pAd     2.22     1.83    6.60    1.18     9.46 87.76
B_pAd     1.25     1.34    4.45    0.79     6.38 94.14

Groups S3  &  S1
Average dissimilarity = 71.74

Group S3 Group S1
Species Av.Abund Av.Abund Av.Diss Diss/SD Contrib% Cum.%
S_Adt     6.35     4.87   17.34    1.30    24.17 24.17
Y_Adt     4.75     3.19   14.07    1.19    19.61 43.78
B_juv     2.73     2.56    7.77    1.17    10.82 54.61
Y_pAd     2.22     2.68    7.75    1.13    10.80 65.41
Y_juv     2.99     1.86    7.58    0.82    10.57 75.98
B_Adt     1.78     0.82    7.39    0.66    10.30 86.28
B_pAd     1.25     2.07    5.77    0.86     8.04 94.32

Groups S4  &  S1
Average dissimilarity = 72.08

Group S4 Group S1
```

```
Species Av.Abund Av.Abund Av.Diss Diss/SD Contrib% Cum.%
S_Adt      5.14     4.87   20.07    1.43    27.85 27.85
Y_Adt      2.76     3.19   15.15    0.99    21.02 48.86
Y_pAd      1.83     2.68    8.38    1.07    11.63 60.49
Y_juv      1.67     1.86    7.61    0.84    10.56 71.05
B_juv      1.43     2.56    7.48    1.03    10.37 81.42
B_pAd      1.34     2.07    6.58    0.89     9.13 90.55

Groups S3  &  S2
Average dissimilarity = 74.83

Group S3 Group S2
Species Av.Abund Av.Abund Av.Diss Diss/SD Contrib% Cum.%
S_Adt      6.35     5.79   20.43    1.38    27.30 27.30
Y_Adt      4.75     2.22   13.90    1.14    18.58 45.88
B_juv      2.73     2.77    8.38    1.15    11.20 57.08
Y_juv      2.99     1.97    7.99    0.82    10.68 67.76
B_Adt      1.78     0.29    7.49    0.61    10.01 77.77
Y_pAd      2.22     1.67    6.51    1.12     8.70 86.47
B_pAd      1.25     1.58    5.21    0.79     6.97 93.43

Groups S4  &  S2
Average dissimilarity = 74.78

Group S4 Group S2
Species Av.Abund Av.Abund Av.Diss Diss/SD Contrib% Cum.%
S_Adt      5.14     5.79   24.51    1.54    32.77 32.77
Y_Adt      2.76     2.22   14.41    0.95    19.27 52.04
Y_juv      1.67     1.97    8.09    0.87    10.81 62.85
B_juv      1.43     2.77    7.78    0.97    10.40 73.26
Y_pAd      1.83     1.67    6.83    1.13     9.13 82.39
B_pAd      1.34     1.58    6.09    0.83     8.14 90.53

Groups S1  &  S2
Average dissimilarity = 74.54

Group S1 Group S2
Species Av.Abund Av.Abund Av.Diss Diss/SD Contrib% Cum.%
S_Adt      4.87     5.79   21.35    1.36    28.64 28.64
Y_Adt      3.19     2.22   14.32    0.99    19.21 47.85
B_juv      2.56     2.77    9.05    1.11    12.15 59.99
Y_pAd      2.68     1.67    8.41    0.99    11.28 71.27
B_pAd      2.07     1.58    7.31    0.88     9.80 81.07
Y_juv      1.86     1.97    7.20    0.92     9.66 90.74
```

B.3 BEST analysis

```
BEST
Biota and/or Environment matching

Data worksheet
Name: Nrm_trnf_envt_sub
Data type: Environmental
Sample selection: All
Variable selection: All

Resemblance worksheet
Name: Resem1
Data type: Similarity
Selection: All

Parameters
Rank correlation method: Spearman
Method: BIOENV
Maximum number of variables: 5
Resemblance:
Analyse between: Samples
Resemblance measure: D1 Euclidean distance

Variables
  1 Temp/oc
  2 lg_Chl/mg-3

Global Test
Sample statistic (Rho): 0.018
Significance level of sample statistic: 35.1%
Number of permutations: 999 (Random sample)
Number of permuted statistics greater than or equal to Rho: 350

Best results
No.Vars    Corr. Selections
      1    0.018 1
      2    0.015 All
      1    0.012 2

Outputs
Plot: Graph6
```

Appendix C

GAM Results

```
Model 1

Family: gaussian
Link function: identity

Formula:
Fork_length ~ +s(SST) + s(Chlorophyll) + s(Distance) + (School) +
    Sp

Parametric coefficients:
            Estimate Std. Error t value Pr(>|t|)
(Intercept)  36.1811     0.7699   46.99   <2e-16 ***
School        6.5600     0.3934   16.68   <2e-16 ***
Sp           12.3815     0.3059   40.47   <2e-16 ***
---
Signif. codes:  0 '***' 0.001 '**' 0.01 '*' 0.05 '.' 0.1 ' ' 1

Approximate significance of smooth terms:
                edf Ref.df     F p-value
s(SST)         8.509  8.930 30.00  <2e-16 ***
s(Chlorophyll) 6.678  7.830 17.45  <2e-16 ***
s(Distance)    8.516  8.933 18.32  <2e-16 ***
---
Signif. codes:  0 '***' 0.001 '**' 0.01 '*' 0.05 '.' 0.1 ' ' 1

R-sq.(adj) =  0.189   Deviance explained = 19.1%
GCV = 504.63  Scale est. = 503.39    n = 10865

=====================================================================

Model 2

Family: gaussian
Link function: identity

Formula:
Fork_length ~ +s(Chlorophyll) + s(SST) + (School) + te(Rec_Longitude,
    Rec_Latitude, bs = c("cs", "cs")) + Sp

Parametric coefficients:
            Estimate Std. Error t value Pr(>|t|)
(Intercept)  36.8592     0.7742   47.61   <2e-16 ***
School        5.5240     0.4143   13.33   <2e-16 ***
Sp           12.5636     0.3003   41.84   <2e-16 ***
---
Signif. codes:  0 '***' 0.001 '**' 0.01 '*' 0.05 '.' 0.1 ' ' 1
```

```
Approximate significance of smooth terms:
                                edf Ref.df     F p-value
s(Chlorophyll)                7.737  8.598 24.91  <2e-16 ***
s(SST)                        8.145  8.799 38.48  <2e-16 ***
te(Rec_Longitude,Rec_Latitude) 21.442 24.000 33.34  <2e-16 ***
---
Signif. codes:  0 '***' 0.001 '**' 0.01 '*' 0.05 '.' 0.1 ' ' 1

R-sq.(adj) =  0.232   Deviance explained = 23.5%
GCV = 478.14  Scale est. = 476.36    n = 10865


======================================================================

Model 3

Family: gaussian
Link function: identity

Formula:
Fork_length ~ +s(SST) + s(Chlorophyll) + s(Distance) +  Sp

Parametric coefficients:
            Estimate Std. Error t value Pr(>|t|)
(Intercept)  22.9688     0.3506   65.51   <2e-16 ***
School       22.9688     0.3506   65.51   <2e-16 ***
Sp            9.7512     0.3160   30.85   <2e-16 ***
---
Signif. codes:  0 '***' 0.001 '**' 0.01 '*' 0.05 '.' 0.1 ' ' 1

Approximate significance of smooth terms:
                edf Ref.df     F p-value
s(SST)         7.053  8.136 20.79  <2e-16 ***
s(Chlorophyll) 7.175  8.245 17.06  <2e-16 ***
s(Distance)    8.298  8.870 12.48  <2e-16 ***
---
Signif. codes:  0 '***' 0.001 '**' 0.01 '*' 0.05 '.' 0.1 ' ' 1

Rank: 29/30
R-sq.(adj) =  0.139   Deviance explained = 14.1%
GCV = 378.67  Scale est. = 377.41    n = 7390

======================================================================

Model 4

Family: gaussian
Link function: identity

Formula:
Fork_length ~ +s(Chlorophyll) + s(SST) + te(Rec_Longitude,
    Rec_Latitude, bs = c("cs", "cs")) + Sp

Parametric coefficients:
            Estimate Std. Error t value Pr(>|t|)
(Intercept)  22.6759     0.3483   65.11   <2e-16 ***
School       22.6759     0.3483   65.11   <2e-16 ***
Sp           10.0301     0.3143   31.91   <2e-16 ***
---
Signif. codes:  0 '***' 0.001 '**' 0.01 '*' 0.05 '.' 0.1 ' ' 1

Approximate significance of smooth terms:
                                edf Ref.df     F p-value
s(Chlorophyll)                7.362  8.378 21.53  <2e-16 ***
s(SST)                        6.682  7.842 28.06  <2e-16 ***
```

```
te(Rec_Longitude,Rec_Latitude) 21.054 24.000 14.76  <2e-16 ***
---
Signif. codes:  0 '***' 0.001 '**' 0.01 '*' 0.05 '.' 0.1 ' ' 1

Rank: 44/45
R-sq.(adj) =  0.165   Deviance explained = 16.9%
GCV = 367.66  Scale est. = 365.81    n = 7390

=========================================================================

Model 5

Family: gaussian
Link function: identity

Formula:
Fork_length ~ +s(SST) + s(Chlorophyll) + s(Distance) +    Sp

Parametric coefficients:
            Estimate Std. Error t value Pr(>|t|)
(Intercept)   4.7035     0.4429   10.62   <2e-16 ***
School        9.4071     0.8859   10.62   <2e-16 ***
Sp           25.2058     0.9227   27.32   <2e-16 ***
---
Signif. codes:  0 '***' 0.001 '**' 0.01 '*' 0.05 '.' 0.1 ' ' 1

Approximate significance of smooth terms:
                edf Ref.df     F p-value
s(SST)         8.414  8.903 16.23  <2e-16 ***
s(Chlorophyll) 8.506  8.926 11.83  <2e-16 ***
s(Distance)    8.251  8.848 12.51  <2e-16 ***
---
Signif. codes:  0 '***' 0.001 '**' 0.01 '*' 0.05 '.' 0.1 ' ' 1

Rank: 29/30
R-sq.(adj) =  0.425   Deviance explained = 43.3%
GCV = 678.62  Scale est. = 668.91    n = 1900

=========================================================================

Model 6

Family: gaussian
Link function: identity

Formula:
Fork_length ~ +s(Chlorophyll) + s(SST) + te(Rec_Longitude,
    Rec_Latitude, bs = c("cs", "cs")) + Sp

Parametric coefficients:
            Estimate Std. Error t value Pr(>|t|)
(Intercept)   4.7865     0.4346   11.01   <2e-16 ***
School        9.5729     0.8692   11.01   <2e-16 ***
Sp           25.0265     0.9060   27.62   <2e-16 ***
---
Signif. codes:  0 '***' 0.001 '**' 0.01 '*' 0.05 '.' 0.1 ' ' 1

Approximate significance of smooth terms:
                                  edf Ref.df     F p-value
s(Chlorophyll)                  8.421  8.901 12.71  <2e-16 ***
s(SST)                          8.270  8.854 15.86  <2e-16 ***
te(Rec_Longitude,Rec_Latitude) 23.759 24.000 10.70  <2e-16 ***
---
Signif. codes:  0 '***' 0.001 '**' 0.01 '*' 0.05 '.' 0.1 ' ' 1

Rank: 44/45
```

```
R-sq.(adj) =  0.459   Deviance explained = 47.1%
GCV = 643.44  Scale est. = 629.06    n = 1900
```

Bibliography

Alemany, F., Quintanilla, L., Velez-Belchi, P., Garcia, A., Cortés, D., Rodriguez, J., Fernández de Puelles, M., González-Pola, C. and López-Jurado, J. (2010), 'Characterization of the spawning habitat of atlantic bluefin tuna and related species in the balearic sea (western mediterranean)', *Progress in Oceanography* **86**(1), 21–38.

Altman, P. L., Dittmer, D. S. et al. (1962), 'Growth, including reproduction and morphological development.', *Growth, including reproduction and morphological development.* .

Alvarez, A., Chiggiato, J. and Schroeder, K. (2013), 'Mapping sub-surface geostrophic currents from altimetry and a fleet of gliders', *Deep Sea Research Part I: Oceanographic Research Papers* **74**, 115–129.

Anderson, M., Gorley, R. and Clarke, K. (2008), 'Permanova1 for primer: guide to software and statistical methods.', *Plymouth: PRIMER-E* p. 214.

Arreguín-Sánchez, F. (1996), 'Catchability: a key parameter for fish stock assessment', *Reviews in Fish Biology and Fisheries* **6**(2), 221–242.

Bain, C. A. (1982), 'Local wind forcing and small scale upwelling', *Coastal Engineering Proceedings* **1**(18).

Bakun, A. (1996), 'Patterns in the ocean: ocean processes and marine population dynamics'.

Bakun, A. (2006), 'Fronts and eddies as key structures in the habitat of marine fish larvae: opportunity, adaptive response and competitive advantage', *Scientia Marina* **70**(S2), 105–122.

Bayliff, W. H. (1979), 'Migrations of yellowfin tuna in the eastern pacific ocean as determined from tagging experiments initiated during 1968-1974', *Inter-American Tropical Tuna Commission Bulletin* **17**(6), 445–506.

Bertrand, A., Bard, F.-X. and Josse, E. (2002), 'Tuna food habits related to the micronekton distribution in french polynesia', *Marine Biology* **140**(5), 1023–1037.

Bjornsson, H. and Venegas, S. (1997), 'A manual for eof and svd analyses of climatic data', *CCGCR Report* **97**(1), 112–134.

Block, B. A., Costa, D. P., Boehlert, G. W. and Kochevar, R. E. (2002), 'Revealing pelagic habitat use: the tagging of pacific pelagics program', *Oceanologica Acta* **25**(5), 255–266.

Block, B. A., Jonsen, I., Jorgensen, S., Winship, A., Shaffer, S. A., Bograd, S., Hazen, E., Foley, D., Breed, G., Harrison, A.-L. et al. (2011), 'Tracking apex marine predator movements in a dynamic ocean', *Nature* **475**(7354), 86–90.

Block, B. A., Teo, S. L., Walli, A., Boustany, A., Stokesbury, M. J., Farwell, C. J., Weng, K. C., Dewar, H. and Williams, T. D. (2005), 'Electronic tagging and population structure of atlantic bluefin tuna', *Nature* **434**(7037), 1121–1127.

Bray, J. and Curtis, J. (1957), 'An ordination of the upland forest communities of southern wisconsin', *Ecological Monographs* **27**, 325–349.

Brownie, C., Anderson, D., Burnham, K. and Robson, D. (1985), *Statistical inference from band recovery data – a handbook*, second edition edn, U.S. Fish and Wildlife Service, Resource Publication 156, Washington, D.C., USA.

Capello, M., Soria, M., Cotel, P., Potin, G., Dagorn, L. and Fréon, P. (2012), 'The heterogeneous spatial and temporal patterns of behavior of small pelagic fish in an array of fish aggregating devices (fads)', *Journal of Experimental Marine Biology and Ecology* **430**, 56–62.

Carruthers, T., Fonteneau, A. and Hallier, J.-P. (2014), 'Estimating tag reporting rates for tropical tuna fleets of the indian ocean', *Fisheries Research* **155**, 20–32.

Cayré, P. and Farrugio, H. (1986), 'Biologie de la reproduction du listao (katsuwonus pelamis) de l'océan atlantique', *Proc. ICCAT Intl* pp. 252–272.

Cayré, P. and Marsac, F. (1993), 'Modelling the yellowfin tuna (thunnus albacares) vertical distribution using sonic tagging results and local environmental parameters', *Aquatic Living Resources* **6**(01), 1–14.

Chapman, D. G., Fink, B. D. and Bennett, E. B. (1965), 'A method for estimating the rate of shedding of tags from yellowfin tuna', *Inter-American Tropical Tuna Commission Bulletin* **10**(5), 333–352.

Chassot, E., Dubroca, L., Delgado de Molina, A., Assan, C., Soto, M., Floch, L. and Fonteneau, A. (2012), Decomposing purse seine cpues to estimate an abundance index for yellowfin free-swimming schools in the indian ocean during 1981–2011, Technical report, IOTC-2012-WPTT-14-33.

Clarke, K. and Ainsworth, M. (1993), 'A method of linking multivariate community structure to environmental variables', *Marine Ecology-Progress Series* **92**, 205–205.

Clarke, K. and Gorley, R. (2006), *PRIMER v6: User Manual/Tutorial*, PRIMER-E, Plymouth.

Collette, B. B., Nauen, C. E. et al. (1983), *FAO species catalogue. Volume 2. Scombrids of the world. An annotated and illustrated catalogue of tunas, mackerels, bonitos and related species known to date.*, number 125.

Commins, M., Ansorge, I. and Ryan, P. (2013), 'Multi-scale factors influencing seabird assemblages in the african sector of the southern ocean.', *Antarctic Science* pp. 1–11.

Cooch, E. and White, G. (2006), 'Program mark: a gentle introduction', *available online with the MARK programme* **7**.

Cushman-Roisin, B. and Beckers, J.-M. (2011), *Introduction to geophysical fluid dynamics: physical and numerical aspects*, Vol. 101, Academic Press.

DeMaster, D. and Drevenak, J. (1988), 'Survivorship patterns in three species of captive cetaceans.', *Marine mammals* **4**(4), 297–311.

Dewar, H. and Graham, J. (1994), 'Studies of tropical tuna swimming performance in a large water tunnel-energetics', *The Journal of experimental biology* **192**(1), 13–31.

Ekman, V. W. (1905), 'On the influence of the earth\'s rotation on ocean currents', *Ark. Mat. Astron. Fys.* **2**, 1–53.

ESRI (2009), *Environmental Systems Resource Institute*, ArcMap 9.2. ESRI. Redlands, California, Vienna, Austria.

ETOPO2v2 (2006), 'Global gridded 2-minute database, national geophysical data center, national oceanic and atmospheric administration', *U.S. Dept. of Commerce* .
http://www.ngdc.noaa.gov/mgg/global/etopo2.html

FAO (1968), 'Report of the first session of the indain ocean fishery commission', *Food and Agriculture Organization of the United Nations* (60).

FAO (2013), Tuna a global perspective, Technical report, Food and Agriculture Organization of the United Nations, FAO Rome, Italy.

FAO (2016), Fishing gear types, purse seines, Technical report, Food and Agriculture Organization of the United Nations.
http://www.fao.org/fishery/geartype/249/en

Field, J. ., Clarke, K., Warwick, R. et al. (1982), 'A practical strategy for analysing multispecies distribution patterns', *Marine ecology progress series* **8**(1).

Fonteneau, A. (2008), Tuna movement patterns presently shown in the indian ocean by tag recoveries from the iottp tagging program, Technical report, The Indian Ocean Tuna Commission (IOTC).
http://www.iotc.org/files/proceedings/2008/wptda/
IOTC-2008-WPTDA-05.pdf

Fonteneau, A., Chassot, E. and Bodin, N. (2013), 'Global spatio-temporal patterns in tropical tuna purse seine fisheries on drifting fish aggregating devices (dfads): Taking a historical perspective to inform current challenges', *Aquatic Living Resources* **26**(01), 37–48.

Fonteneau, A. and Gascuel, D. (2008), 'Growth rates and apparent growth curves, for yellowfin, skipjack and bigeye tagged and recovered in the indian ocean during the iottp', *The Indain Ocean Tuna Commission* .

Fonteneau, A., Lucas, V., Tewkai, E., Delgado, A. and Demarcq, H. (2008), 'Mesoscale exploitation of a major tuna concentration in the indian ocean', *Aquatic Living Resources* **21**(02), 109–121.

Fonteneau, A., Pallares, P. and Renaud, P. (2000), 'A worldwide review of purse seine fisheries on fads', *Pêche thonière et dispositifs de concentration de poissons, Caribbean-Martinique* .
http://archimer.ifremer.fr/doc/00042/15278/

Fraile, I., H.Murua, Zudaire, I., Arrizabalaga, H. and Rooker, J. (2013), Discrimination of yellowfin tuna from the putative nurseries of the western indian ocean., Technical report, The Indian Ocean Tuna Commission (IOTC).

Fréon, P. (1983), 'Production models as applied to sub-stocks depending on upwelling fluctuations', *FAO Fish. Report* **291**(3), 1047–1064.

Gaertner, D. and Hallier, J. (2009), An updated analysis of tag-shedding by tropical tunas in the indian ocean, Technical report, The Indian Ocean Tuna Commission.
http://www.iotc.org/files/proceedings/2009/wptt/IOTC-2009-WPTT-34.pdf

Gaertner, D. and Hallier, J.-P. (2003), 'Estimate of natural mortality of bigeye tuna (thunnus obesus) in the eastern atlantic from tag attrition model', *Collect. Vol. Sci. Pap, ICCAT* **55**(5), 1868–1879.

Gaspar, P., Georges, J.-Y., Fossette, S., Lenoble, A., Ferraroli, S. and Le Maho, Y. (2006), 'Marine animal behaviour: neglecting ocean currents can lead us

up the wrong track', *Proceedings of the Royal Society B: Biological Sciences* **273**(1602), 2697–2702.

Guyomard, D., Desruisseaux, M., Poisson, F., Taqueta, M. and Petit, M. (2004), 'Gam analysis of operational and environmental factors affecting swordfish (xiphias gladius) catch and cpue of the reunion island longline fishery, in the south western indian ocean', *IOTC-2004-WPB-08, IOTC* **7**.

Hall, M. A., Garcia, M., Lennert-Cody, C., Arenas, P. and Miller, F. (1992), 'The association of tunas with floating objects and dolpmns in the eastern pacific ocean: A review of the current purse-seine fishery', *INTER· AMERICAN TROPICAL TUNA COMMISSION COMISION INTERAMERICANA DEL ATUN TROPICAL* p. 87.

Hallier, J. (2006), Field manual for tropical tuna tagging, technical report, Technical report, The Indian Ocean Tuna Commission.

Hallier, J. and Gaertner, D. (2008), 'Drifting fish aggregation devices could act as an ecological trap for tropical tuna species', *Marine Ecology Progress Series* **353**, 255–264.

Hallier, J. and Million, J. (2009), The contribution of the regional tuna tagging project – indian ocean to iotc-stock assessment, technical report, Technical report, The Indian Ocean Tuna Commission.

Hallier, J. P. (2008), Status of the indian ocean tuna tagging programme - rttp-io, Technical report, The Indian Ocean Tuna Commission (IOTC).

Hassani, S. and Stequert, B. (1991), 'Sexual maturity, spawning and fecundity of the yellowfin tuna (thunnus albacares) of the western indian ocean', *Food and Agriculture Organization of the United Nations* **4**.

Hastie, T. J. and Tibshirani, R. J. (1990), *Generalized additive models*, Vol. 43, CRC Press.

Hazin, H., Hazin, F., Amorim, C., Travassos, P., Freduo, T., Mourato, B. and Carvalho, F. (2012), 'Standardization of a cpue series of yelowfin tuna, thun-

nus albacares, caught by brazilian longliners in the southwestern atlantic ocean', *ICCAT* **68**(3), 995–1001.

Hillary, R. and Areso, J. (2008), Reporting rate analyses for recaptures from seychelles port for yellowfin, bigeye and skipjack tuna, Technical report, The Indian Ocean Tuna Commission, IOTC-2008-WPTT-18.

Holland, K. N. (1990), 'Horizontal and vertical movements of yellowfin and bigeye tuna associated with fish aggregating devices', *Fish. Bull.* **88**, 493–507.

Hovmöller, E. (1949), 'The trough-and-ridge diagram', *Tellus* **1**(2), 62–66.

Hutchinson, M. R., Itano, D. G., Muir, J. A. and Holland, K. N. (2015), 'Post-release survival of juvenile silky sharks captured in a tropical tuna purse seine fishery', *Mar Ecol Prog Ser* **521**, 143–154.

Hynd, J. S. (1969), 'Isotherm maps for tuna fisherman', *Australian Fisheries* .

ICCAT (2009), Iccat manual, Technical report, International Commission for the Conservation of Atlantic Tuna.
http://www.iccat.int/en/ICCATManual.htm

IHO (1953), 'Limits of oceans and seas', *International Hydrograhic Organization* **23**.

IOTC (1996), Agreement for the establishment of the indian ocean tuna commission, technical report, Technical report, The Indian Ocean Tuna Commission.
http://www.iotc.org/files/proceedings/misc/ComReportsTexts/IOTC%20Agreement.pdf

IOTC (2000*a*), A proposal for an indian ocean tropical tuna tagging programme (iottp), Technical report, The Indian Ocean Tuna Commission.
http://www.iotc.org/files/proceedings/misc/TagProg/English/TPSummE.pdf

IOTC (2000*b*), Report of the second session of the iotc working party on tagging, Technical report, The Indian Ocean Tuna Commission (IOTC), IOTC-2000-WPT-R[EN], Victoria, Seychelles.

IOTC (2008*a*), Report of the first session of the iotc. working party on tagging data analysis, Technical report, The Indian Ocean Tuna Commission (IOTC).

IOTC (2008*b*), Report of the tenth session of the iotc working party on tropical tunas, Technical report, The Indian Ocean Tuna Commission (IOTC), Bangkok, Thailand.

IOTC (2010), Report of the twelfth session of the iotc, working party on tropical tunas, Technical report, The Indian Ocean Tuna Commission (IOTC),IOTC-2010-WPTT-R[E], Victoria, Seychelles.

IOTC (2011), Report of the thirteenth session of the iotc working party on tropical tunas, Technical report, The Indian Ocean Tuna Commission (IOTC), Lankanfinolhu, North Malé Atoll, Republic of Maldives.

IOTC (2012), Report of the fifteenth session of the iotc, Technical report, The Indian Ocean Tuna Commission (IOTC).

IOTC (2013), Report of the sixteenth session of the iotc scientific committee, Technical report, IOTC–2013–SC16–R[E].

IOTC (2014), Report of the seventeenth session of the iotc scientific committee, Technical report, IOTC–2014–SC17–R[E].

Kingsford, M. (1999), 'Fish attracting devices (fad)s and experimental designs', *Science Marine* **63(3-4)**, 181–190.

Kolasinski, J., KaehlerJ, S. and Jaquemet, S. (2012), 'Distribution and sources of particulate organic matter in a mesoscale eddy dipole in the mozambique channel (south-western indian ocean): Insight from c and n stable isotopes.', *Journal of Marine Systems* **96–97**, 122–131.

Lan, K.-W., Evans, K. and Lee, M.-A. (2013), 'Effects of climate variability on the distribution and fishing conditions of yellowfin tuna (thunnus albacares) in the western indian ocean', *Climatic Change* **119**(1), 63–77.

Le Gall, J.-Y. and Bergès, J.-C. (1989), *Télédétection satellitaire et pêcheries thonières océaniques*, Vol. 302, Food & Agriculture Org.

Lehodey, P. (2000), 'Impacts of the el niño southern oscillation on tuna populations and fisheries in the tropical pacific ocean', *Secretariat of the Pacific Community No. RG-1* .

Lehodey, P., Bertignac, M., Hampton, J., Lewis, A. and Picaut, J. (1997), 'El nino southern oscillation and tuna in the western pacific', *NATURE* **389**, 715.

Lezama-Ochoa, A., Boyra, G., Goñi, N., Arrizabalaga, H. and Bertrand, A. (2010), 'Investigating relationships between albacore tuna (thunnus alalunga) {CPUE} and prey distribution in the bay of biscay', *Progress in Oceanography* **86**(1–2), 105 – 114.
http://www.sciencedirect.com/science/article/pii/S0079661110000406

Lutjeharms, J. and Machu, E. (2000), 'An upwelling cell inshore of the east madagascar current', *Deep Sea Research Part I: Oceanographic Research Papers* **47**(12), 2405–2411.

Maindonald, J. (2010), 'Smoothing terms in gam models'.

Mansor, S., Tan, C., Ibrahim, H. and R.M.S.Abdul (2001), 'Satellite fish forecasting in south china', *22nd Asian Conference in Remote Sensing* p. 5–9.

Maravelias, C. and Reid, D. (1997), 'Identifying the effects of oceanographic features and zooplankton on prespawning herring abundance using generalized additive models', *Oceanographic Literature Review* **44**(8).

Marçalo, A., Marques, T. A., Araújo, J., Pousão-Ferreira, P., Erzini, K. and Stratoudakis, Y. (2010), 'Fishing simulation experiments for predicting the effects of purse-seine capture on sardine (sardina pilchardus)', *ICES Journal of Marine Science: Journal du Conseil* **67**(2), 334–344.

Marsac, F. (2008), 'Outlook of ocean climate variability in the west tropical indian ocean, 1997-2008', *IOTC-2008 WPTT-27* pp. 1–9.

Marsac, F. (2011), Indian ocean seasonal stratification.

Marsac, F. (2012), 'Outline of climate and oceanographic conditions in the indian ocean over the the period 2002-2012', *14th session of the IOTC Working Party on Tropical Tunas, Mauritius* pp. 24–29.

Marsac, F. (2013), 'Outline of climate and oceanographic conditions in the indian ocean: an update to august 2013', *15th Session of the Working Party on Tropical Tuna, IOTC-2013-WPTT15-09* p. 14.

Marsac, F. and Blanc, J. L. (1998), 'Interannual and enso-associated variability of the coupled ocean-atmosphere system with possible impacts on the yellowfin tuna fisheries of the indian and atlantic oceans.', *COLLECTIVE VOLUME OF SCIENTIFIC PAPERS-INTERNATIONAL COMMISSION FOR THE CONSERVATION OF ATLANTIC TUNAS* **50**, 345–377.

Marsac, F. and Cayré, P. (1998), Telemetry applied to behaviour analysis of yellowfin tuna (thunnus albacares, bonnaterre, 1788) movements in a network of fish aggregating devices, *in* 'Advances in Invertebrates and Fish Telemetry', Springer, pp. 155–171.

Marsac, F., Fonteneau, A. and Ménard, F. (2000), 'Drifting fads used in tuna fisheries: an ecological trap?', *Proceedings of the International Symposium on tuna fishing and fish aggregating devices* .

Marsac, F., Fonteneau, A., Michaud, P. and Michel, J. (2014), 'L'or bleu des seychelles: histoire de la pêche industrielle au thon dans l'océan indien'.

Marsac, F. and Le Blanc, J.-L. (2000), 'Enso cycle and purse seine tuna fisheries in the indian ocean with emphasis on the 1998–1999 la niña', *IOTC Proc* **3**, 354–363.

MATLAB (2011), *version 7.13.0.564 (R2011b)*, The MathWorks Inc.

Maury, O. (2010), 'An overview of apecosm, a spatialized mass balanced "apex predators ecosystem model" to study physiologically structured tuna population dynamics in their ecosystem', *Progress in Oceanography* **84**(1), 113–117.

Maury, O., Faugeras, B., Shin, Y.-J., Poggiale, J.-C., Ari, T. B. and Marsac, F. (2007), 'Modeling environmental effects on the size-structured energy flow through marine ecosystems. part 1: The model', *Progress in Oceanography* **74**(4), 479–499.

McClain, C. R., Signorini, S. R. and Christian, J. R. (2004), 'Subtropical gyre variability observed by ocean-color satellites', *Deep Sea Research Part II: Topical Studies in Oceanography* **51**(1), 281–301.

Ménard, F., Fonteneau, A., Gaertner, D., Nordstrom, V., Stéquert, B. and Marchal, E. (2000b), 'Exploitation of small tunas by a purse-seine fishery with fish aggregating devices and their feeding ecology in an eastern tropical atlantic ecosystem', *ICES Journal of Marine Science: Journal du Conseil* **57**(3), 525–530.

Ménard, F., Lorrain, A., Potier, M. and Marsac, F. (2007b), 'Isotopic evidence of distinct feeding ecologies and movement patterns in two migratory predators (yellowfin tuna and swordfish) of the western indian ocean', *Marine Biology* **153**(2), 141–152.

Ménard, F., Marsac, F., Bellier, E. and Cazelles, B. (2007a), 'Climatic oscillations and tuna catch rates in the indian ocean: a wavelet approach to time series analysis', *Fisheries Oceanography* **16**(1), 95–104.

Ménard, F., Stéquert, B., Rubin, A., Herrera, M. and Marchal, É. (2000a), 'Food consumption of tuna in the equatorial atlantic ocean: Fad-associated versus unassociated schools', *Aquatic Living Resources* **13**(4), 233–240.

Microsoft (2010), *Microsoft Office Professional Plus 2010*, Microsoft Office.

Miyabe, N. and Nakano, H. (2004), *Historical trends of tuna catches in the world*, Vol. 467, FAO.

Miyake, M., Guillotreau, P., Sun, C.-H. and Ishimura, G. (2010), *Recent developments in the tuna industry: stocks, fisheries, management, processing, trade and markets*, Food and Agriculture Organization of the United Nations.

Montero, J. T., Martinez-Rincon, R. O., Heppell, S. S., Hall, M. and Ewal, M. (2016), 'Characterizing environmental and spatial variables associated with the incidental catch of olive ridley (lepidochelys olivacea) in the eastern tropical pacific purse-seine fishery', *Fisheries Oceanography* **25**(1), 1–14.

Murua, H., Eveson, J. P. and Marsac, F. (2015), 'The indian ocean tuna tagging programme: Building better science for more sustainability', *Fisheries Research* (163), 1–6.

Nakamura, H. (1969), 'Tuna: distribution and migration'.

Parmesan, C. and Yohe, G. (2003), 'A globally coherent fingerprint of climate change impacts across natural systems', *Nature* **421**(6918), 37–42.

Pereira, J. (2005), 'Behavior of bigeye tuna a baitboat fishery', *International Commission for the Conservation of Atlantic Tuna* **57(1)**, 116–128.

Polacheck, T., Paige Eveson, J. and Laslett, G. M. (2010), 'Classifying tagging experiments for commercial fisheries into three fundamental types based on design, data requirements and estimable population parameters', *Fish and fisheries* **11**(2), 133–148.

Pollock, K. H., Winterstein, S. R., Bunck, C. M. and Curtis, P. D. (1989), 'Survival analysis in telemetry studies: the staggered entry design', *The Journal of Wildlife Management* pp. 7–15.

Praulai, N. (2004), 'Reproductive biology of bigeye tuna in the eastern indian ocean', *WPTT04-05, IOTC Proceedings* **7**, 1–5.

R Development Core Team (2008), *R: A Language and Environment for Statistical Computing*, R Foundation for Statistical Computing, Vienna, Austria. ISBN 3-900051-07-0.
http://www.R-project.org

Rajapaksha, J., Nishida, T. and Samarakoon, L. (2010), Environmental preferences of yellowfin tuna (thunnus albacores) in the northeast indian ocean: an application of remote sensing data to longline catches, Technical report, The Indian Ocean Tuna Commission.
http://www.iotc.org/files/proceedings/2010/wptt/IOTC-2010-WPTT-43.pdf

Ramage, C. S. (1969), 'Indian ocean surface meteorology and oceanography', *Mar. Biol* **7**, 11–30.

Ramos, A., Santiago, J., Sangra, P. and Canton, M. (1996), 'An application of satellite-derived sea surface temperature data to the skipjack (katsuwonus pelamis linnaeus, 1758) and albacore tuna (thunnus alalunga bonaterre, 1788) fisheries in the north-east atlantic', *International Journal of Remote Sensing* **17**(4), 749–759.

Riggs, F. (1981), Status report: Tunas in the indian ocean, technical report, Technical report, NOAA-TECH. MEMO-National-Marine-Fisheries.

Rio, M.-H. and Hernandez, F. (2003), 'High-frequency response of wind-driven currents measured by drifting buoys and altimetry over the world ocean', *Journal of Geophysical Research: Oceans (1978-2012)* **108**(C8).

Robinson, I. S. (2010), *Discovering the Ocean from Space: The unique applications of satellite oceanography*, Vol. 4110, Springer.

Romanov, E. V. (2002), 'Bycatch in the tuna purse-seine fisheries of the western indian ocean', *Fishery Bulletin* **100**(1), 90–105.

Sabatié, R., Marsac, F., Hallier, J., Potier, M., Lucas, V. and Ménard, F. (2004), 'Feeding partitioning among tuna taken in surface and mid-water layers: the case of yellowfin (thunnus albacares) and bigeye (t. obesus) in the western tropical indian ocean'.

Saji, N., Goswami, B. N., Vinayachandran, P. and Yamagata, T. (1999), 'A dipole mode in the tropical indian ocean', *Nature* **401**(6751), 360–363.

Schaefer, K. M., Fuller, D. W. and Block, B. A. (2007), 'Movements, behavior, and habitat utilization of yellowfin tuna (thunnus albacares) in the northeastern pacific ocean, ascertained through archival tag data', *Marine Biology* **152**, 503–525.

Schick, R. and Lutcavage, M. (2009), 'Inclusion of prey data improves prediction of bluefin tuna (thunnus thynnus) distribution', *Fisheries Oceanography* **18**(1), 77–81.

Schott, F. A. and Fischer, J. (2000), 'Winter monsoon circulation of the northern arabian sea and somali current', *Journal of Geophysical Research: Oceans (1978–2012)* **105**(C3), 6359–6376.

Schott, F. A. and McCreary, J. P. J. (2001), 'The monsoon circulation of the indian ocean', *Progress in Oceanography* **51**, 1–123.

Seber, G. A. F. (1970), 'Estimating time-specific survival and reporting rates for adult birds from band returns', *Biometrika* **57**(2), pp. 313–318.
http://www.jstor.org/stable/2334838

Seckel, G. R. (1972), 'Hawaiian-caught skipjack tuna and their physical environment', *Fish. Bull* **72**(3), 763–787.

Sedberry, G. and Loefer, J. (2001), 'Satellite telemetry tracking of swordfish, xiphias gladius, off the eastern united states', *Marine Biology* **139**(2), 355–360.

Sharp, G. and Dizon, A. (1978), *The physiological ecology of tunas*, Academic Press.

Sibert, J. R., Hampton, J., Fournier, D. A. and Bills, P. J. (1999), 'An advection–diffusion–reaction model for the estimation of fish movement parameters from tagging data, with application to skipjack tuna (katsuwonus pelamis)', *Canadian journal of fisheries and aquatic sciences* **56**(6), 925–938.

Solovieff, B. (1970), 'Distribution and biology of bigeye tuna in the indian ocean', *Rybn. Khoz* .

Stéquert, B. and Marsac, F. (1989), *Tropical tuna: surface fisheries in the Indian Ocean*, number 282, Food & Agriculture Org.

Stöcker, S. (1999), 'Models for tuna school formation', *Mathematical Biosciences* **156**(1), 167–190.

Sugathadasa, N. and Hallier, J. (2010), Regional tuna tagging project-indian ocean: It consultant documentation, Technical report, The Indian Ocean Tuna Commission (IOTC), Victoria, Seychelles.

Sund, P., Blackburn, M. and Williams, F. (1981), 'Tunas and their environment in the pacific ocean: A review', *Oceanogr. Mar. Biol. Ann. Rev.* **19**, 443–512.

Swartzman, G., Huang, C. and Kaluzny, S. (1992), 'Spatial analysis of bering sea groundfish survey data using generalized additive models', *Canadian Journal of Fisheries and Aquatic Sciences* **49**(7), 1366–1378.

Team, R. C. (2015), *R: A Language and Environment for Statistical Computing*, R Foundation for Statistical Computing, Vienna, Austria.
http://www.R-project.org

Tewkai, E. and Marsac, F. (2010), 'Influence of mesoscale eddies on spatial structuring of top predators' communities in the mozambique channel.', *Progr. Oceanogr.* **86**, 214–223.

van der Toorn, J. (1997), 'Survival guide to survival rates', *Marine mammals: Pub. Disp. Res.* pp. 27–38.

Vincenty, T. (1975), 'Direct and inverse solutions of geodesics on the ellipsoid with application of nested equations', *Survey review* **23**(176), 88–93.

Walther, G.-R., Post, E., Convey, P., Menzel, A., Parmesan, C., Beebee, T. J., Fromentin, J.-M., Hoegh-Guldberg, O. and Bairlein, F. (2002), 'Ecological responses to recent climate change', *Nature* **416**(6879), 389–395.

Warren, B. A. (1981*a*), 'The shallow oxygen minimum of the south indian ocean', *Deep Sea Research Part A. Oceanographic Research Papers* **28**(8), 859–864.

Warren, B. A. (1981*b*), 'Transindian hydrographic section at lat. 18 s: Property distributions and circulation in the south indian ocean', *Deep Sea Research Part A. Oceanographic Research Papers* **28**(8), 759–788.

Webster, P. J., Moore, A. M., Loschnigg, J. P. and Leben, R. R. (1999), 'Coupled ocean–atmosphere dynamics in the indian ocean during 1997–98', *Nature* **401**(6751), 356–360.

White, G. and Burnham, K. (1999), *Program MARK: Survival estimation from populations of marked animals.*, Bird Study 46 Supplement, Plymouth.

Wiggert, J., Hood, R., S.W.A. Naqvi, K. H. B. and Smith, S. (2009), *Indian Ocean Biogeochemical Processes and Ecological Variability*, Vol. 185, Geophys. Monogr. Ser.

Wyrtki, K. (1971), 'Oceanographic atlas of the international indian ocean expedition'.

Wyrtki, K. (1973*a*), Physical oceanography of the indian ocean, *in* B. Zeitzschel and S. Gerlach, eds, 'The Biology of the Indian Ocean', Vol. 3 of *Ecological Studies*,

Springer Berlin Heidelberg, pp. 18–36.
http://dx.doi.org/10.1007/978-3-642-65468-8_3

Wyrtki, K. (1973*b*), Physical oceanography of the indian ocean, *in* 'The biology of the Indian Ocean', Springer, pp. 18–36.

Wyrtki, K. (1975), 'El niño-the dynamic response of the equatorial pacific oceanto atmospheric forcing', *Journal of Physical Oceanography* **5**(4), 572–584.

Zagaglia, C. R., Lorenzzetti, J. A. and Stech, J. L. (2004), 'Remote sensing data and longline catches of yellowfin tuna (*Thunnus albacares*) in the equatorial atlantic', *Remote Sensing of Environment* **93**(1), 267–281.

Zainuddin, M., Katsuya, S. and Sei-Ichi, S. (2008), 'Albacore (thunnus alalunga) fishing ground in relation to oceanographic conditions in the western north pacific ocean using remotely sensed satellite data', *Fisheries Oceanography* **17**, 61–73.